CHARACTERIZATION AND GENETIC ANALYSIS OF THE RESISTANCE OF NONOBESE DIABETIC MICE TO TUMOR NECROSIS FACTOR-ALPHA-MEDIATED HEPATOCYTE APOPTOSIS AND LETHALITY

By

FRANCES RENA BAHJAT

A DISSERTATION PRESENTED TO THE GRADUATE SCHOOL
OF THE UNIVERSITY OF FLORIDA IN PARTIAL FULFILLMENT
OF THE REQUIREMENTS FOR THE DEGREE OF
DOCTOR OF PHILOSOPHY

UNIVERSITY OF FLORIDA

2002

ACKNOWLEDGMENTS

I would first like to thank my mentors Lyle L. Moldawer Ph.D. and Michael J. Clare-Salzler, M.D for their exceptional generosity, motivating insight, and gentle yet persistent guidance. These two men have been inspirational mentors who have taught me a great many things over the years, both personally and professionally. I honestly feel that I will never be able to justly compensate them for their countless efforts. I also would like to thank the other members of my committee, Drs. James Crawford, Laurence Morel, Margaret Wallace, and Naohiro Terada for their efforts over the past four years. I appreciate them for their constant encouragement and for generously sharing their scientific expertise.

Also, I would like to acknowledge the many people in both the Moldawer and Clare-Salzler laboratories who lent their expertise to this work. I would above all like to thank Justin DeBernardis for his diligent work, as well as for his tolerance, encouragement, and friendship. He may never truly understand how much of a contribution he has made to this work. I will miss working with such a remarkable individual. I must also thank Angela Avery for making my life easier over the past few years. She has never complained no matter how horrible the task and I appreciate her continued friendship and support. Also, Amer Abouhamze, Cindy Tannahill, and Ricardo Ungaro deserve many thanks. I appreciate them for making sure that I always had the reagents and lab materials that I needed, for making sure the equipment was working, for doing just about anything I have ever asked of them, but most of all for the many intelligent conversations over the past years. I would also like to thank the many residents that I have had the pleasure of working with in the past for their friendship and support. I would also like to thank Dr. Sally MacKay for her words of wisdom and for helping me with all of the molecular

techniques I never had the chance to learn. A special thanks goes to Jen Lanz, who has been my style guru and a tremendous source of strength for me in this last year. I will be forever thankful for her friendship and technical assistance in the laboratory.

My scholastic journey has indeed been a long and difficult one, traversed only with the aide of many influential teachers, friends and family. I am so very thankful to have been inspired by one of my undergraduate professors from Benedictine University, Donald Taylor, Ph.D., to make the decision to pursue a graduate degree. He was, and still remains, one of my best teachers and I truly appreciate and admire his commitment to science and education. I thank my parents for their unconditional love and support, and especially for raising me to believe that there are no limits to what one can accomplish with a little hard work. I would like to thank my brother, Shawn, for making me laugh and always being supportive. Finally, I thank my husband, Keith Bahjat, for his never-ending confidence in me and his constant encouragement. I would also like to thank him for lending me his scientific expertise on occasion, though this required a fair amount of coercion. I thank him for his valuable contribution to this work and to my life.

TABLE OF CONTENTS

page

ACKNOWLEDGMENTS ii

ABSTRACT vii

CHAPTER

1 INTRODUCTION 1

Tumor Necrosis Factor-alpha Biology and Signal Transduction 1
Role of Tumor Necrosis Factor-alpha in Disease 5
Murine Model of TNFα-mediated Hepatocyte Apoptosis and Lethality 8
Quantitative Trait Locus Analysis 11
Nonobese Diabetic Mouse Model of Human Diabetes 15
Specific Aims 17

2 REDUCED SUSCEPTIBILITY OF NONOBESE DIABETIC MICE TO TNF-ALPHA D-GALACTOSAMINE MEDIATED LIVER INJURY AND LETHALITY 19

Introduction 19
Materials and Methods 20
  Reagents 21
  Animal Experimental Protocols 22
  Preparation of Cell Homogenates for Caspase-3Activity Assay 22
  Caspase-3-like Activity Determination 22
  Cytokine Measurements and Serum Transaminase Determinations 23
  In situ TUNEL Assays on Liver Tissue Sections 23
  Flow Cytometric Analysis for Detection of p55 TNF Receptor 24
  Hepatocyte Isolation and Culture 25
  In vitro Hepatocyte Assays 25
  MTT Cytotoxicity Assay 26
Results 26
  LPS/D-galactosamine-induced Lethality and TNFα Production 26
  Apoptosis and Liver Toxicity in LPS/D-galactosamine Treated NOD and B6 Mice 28

rhTNFα and D-galactosamine Toxicity in NOD and B6 Mice....29
Liver Injury and Apoptosis in rhTNFα and D-galactosamine-Treated Mice....30
Flow Cytometric Analysis of p55 TNF Receptor in NOD and B6 Mice....30
Jo-2-induced Hepatic Injury and Lethality in B6 and NOD Mice....31
In vitro Hepatocyte Response to rhTNFα and D-galactosamine Treatment....34
In vitro Hepatocyte Response to Jo-2 Treatment....35
Discussion....36

3 GENETIC ANALYSIS OF NOD RESISTANCE TO TNF-MEDIATED LIVER INJURY AND LETHALITY....42

Introduction....42
Materials and Methods....43
Animal Experimental Protocols....43
IL-6 ELISA....44
Caspase-3 Activity Determination and the Use of DNA Quantitation....44
Genotypic Analyses....45
Data Analyses....45
TRADD Sequencing....48
Results....49
Mortality, Liver Injury and Apoptosis in rhTNFα and D-GalN Treated (NODxB6) F1 Mice....49
IL-6 Response in NOD, B6 and F1 Mice after rhTNFα and D-GalN Treatment....51
D-Galactosamine and TNFα-induced Lethality in B6.NOD Congenic Mice....51
Initial QTL Mapping of Mortality Trait....53
Sequencing of the NOD and B6 TRADD Gene....58
Final QTL Mapping of Mortality Trait....59
QTL Mapping of Additional Traits....65
Analysis of Control Animals from Individual Mapping Experiments....74
Discussion....75

4 SUMMARY AND CONCLUSIONS....88

APPENDIX

A MAP MANAGER QTX LINKS AND INTERVAL MAPPING (IM) REPORTS....105

QT Links Report for Initial Mortality Analysis of 149 recombinant mice....105
IM Reports for Initial Mortality Analysis....107
QT Links Report for Final Mortality Analysis of 294 Recombinant Mice....
IM Reports for Final Mortality Analysis....113
QT Links Reports for AST, IL-6, Caspase-3 (DNA), and Caspase-3 (Protein) Data .129
IM Reports for for AST, IL-6, Caspase-3 (DNA), and Caspase-3 (Protein)....136

B TRADD SEQUENCING DATA....187

LIST OF REFERENCES 190

BIOGRAPHICAL SKETCH 203

Abstract of Dissertation Presented to the Graduate School
of the University of Florida in Partial Fulfillment of the
Requirements for the Degree of Doctor of Philosophy

CHARACTERIZATION AND GENETIC ANALYSIS OF THE RESISTANCE OF NONOBESE DIABETIC MICE TO TUMOR NECROSIS FACTOR-ALPHA-MEDIATED HEPATOCYTE APOPTOSIS AND LETHALITY

By
Frances Rena Bahjat
August 2002

Chair: Michael J. Clare-Salzler, M.D.
Department: Immunology, Pathology, and Laboratory Medicine

Tumor necrosis factor-alpha (TNFα) is a proinflammatory cytokine produced primarily by activated macrophages during inflammation. TNFα is one of several proximal cytokines involved in both the activation of innate immunity, as well as in the initiation and polarization of the acquired immune response. TNFα is also capable of inducing hepatocyte apoptosis and irreversible liver injury, especially in the presence of transcriptional inhibition by D-galactosamine (D-GalN). Although many strains of mice are highly sensitive to the lethal effects of TNFα and D-GalN, we have demonstrated that the nonobese diabetic (NOD) mouse is highly resistant to LPS or recombinant human TNFα (rhTNFα) and D-GalN induced hepatocyte apoptosis, liver injury, and lethality. Therefore, the overall aim of this study was to more fully characterize the decreased responsiveness of NOD mice to TNFα and D-GalN induced lethality and liver injury, as well as to employ a genetic approach to identify potential loci involved in TNFα-mediated liver injury. By mating NOD and C57BL/6 (B6) strains, we demonstrated that

(B6xNOD) F1 mice remained sensitive to both LPS or TNFα and D-GalN induced lethality, but exhibited intermediate hepatic apoptosis and injury responses when compared to parental strains, indicating that multiple genes may be involved in this phenotype. Quantitative trait locus (QTL) analysis was performed for mortality in female progeny from a backcross of (B6xNOD)F1 and NOD mice using a traditional genome-wide scan, revealing several significant loci on chromosomes 8, 11, and 13. In addition, caspase-3 activity, plasma IL-6, and plasma AST concentrations were also mapped in a separate QTL analysis, revealing suggestive loci on chromosomes 1, 5, and 16, with the chromosome 5 locus approaching significance. Candidate genes in these regions include several TNF receptor-associated signaling molecules, as well as diabetes susceptibility loci. Based on these findings, we can conclude that resistance to TNFα and D-GalN induced lethality and liver injury is a polygenic trait with at least three, and potentially up to six distinct contributing loci. Further analysis of candidate genes may provide a powerful tool for the study of related genes in humans.

CHAPTER 1

INTRODUCTION

Tumor Necrosis Factor-alpha Biology and Signal Transduction

Although initially recognized for its anti-tumor activity (Carswell et al. 1975), tumor necrosis factor-alpha (TNFα) is a cytokine, which has been shown in recent decades to elicit a wide range of biological responses. Since its identification, TNFα has been found to play an integral role in innate and adaptive immunity; however, exaggerated production of TNFα has been implicated in the pathogenesis of various diseases. In particular, increased TNFα-mediated cellular apoptosis contributes to a number of pathologic disorders including hepatocyte injury, lymphocyte apoptosis, and endothelial cell dysfunction (Larrea et al. 1996). Therefore, considerable effort has been directed toward the elucidation of the biological actions of TNFα, as well as the structure and function of TNF receptor signal transduction pathways.

TNFα belongs to the TNF superfamily of related ligands and is expressed initially as a 26-kDa transmembrane protein, which is further processed by a family of metalloproteases yielding a soluble 17-kDa soluble form (see figure 1-1) (Bjornberg et al. 1995). Both the cell-associated and secreted forms of TNFα elicit responses by binding to at least two different receptors, the p55 (CD120a) and the p75 (CD120b) TNF receptors, belonging to the TNF/nerve growth factor family (Wallach et al. 1999). Interestingly, current studies reveal that TNFα binding to its receptors simultaneously invokes signaling pathways that both induce and antagonize apoptosis (Hsu et al. 1996). The two opposing responses initiated by TNFα suggest that multiple distinct signaling pathways are present, and a balance within and between these pathways determines the outcome of signaling. In fact, recent studies indicate that not only do multiple pathways exist for

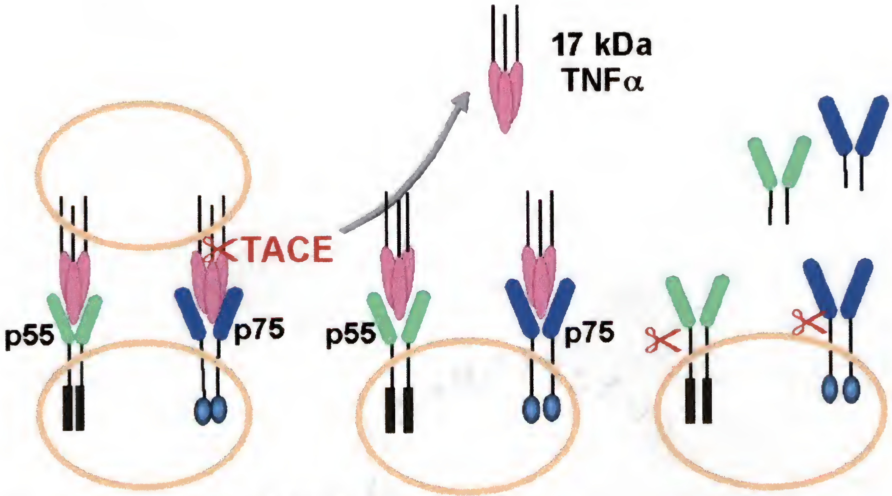

Figure 1-1: TNFα and TNF receptors

a single receptor, but many signaling molecules are promiscuous allowing for cross-talk between pathways initiated by different receptors (Wallach et al. 1996).

Most members of the TNF superfamily exist as homotrimers, TNFα included. Binding of a single homotrimer of TNFα to either of its two known receptors results in aggregation of the receptor allowing juxtaposition of intracellular domains, which are required for the recruitment of additional signaling molecules (Wallach et al. 1999). Adaptor proteins containing death domains and other shared sequence motifs bind to the intracellular domain of the ligated receptors, to each other, or to both (Wallach et al. 1999). Unlike the p75 receptor, the p55 TNF receptor contains an intracellular death domain allowing the recruitment of death effector molecules and execution of the apoptotic cascade (Wallach et al. 1999). In this regard, the p55 TNF receptor shares greater homology with another related family member, the Fas death receptor (CD95). For example, ligation of the Fas receptor allows recruitment of FADD (Fas-associated protein with death domain) (Wallach et al. 1999), which, in turn, recruits caspase-8 to the death-induced signaling complex (DISC- composed of Fas/FADD/caspase-8) formed on the intracellular domain of the receptor (Siegel and Fleisher 1999). Recruitment and enzymatic modification of caspase-8 initiates a proteolytic cascade of other downstream caspases and death effector molecules initiating apoptotic cell death (Wallach et al. 1999). In addition, FADD can also bind TRADD (TNF-receptor associated protein with death domain), a proximal mediator in the TNF p55 receptor signaling pathway, resulting in initiation of the same FADD/caspase-8-dependent apoptotic cascade (Luo et al. 1998; Faubion and Gores 1999). Therefore, the adaptor protein FADD represents a convergence point of Fas and p55 TNF receptor pathways (see figure 1-2). In addition, the p55 TNF receptor also initiates apoptosis via the RIP/RAIDD/caspase-2 cascade (Wallach et al. 1999).

In addition to the death pathways described above, both TNF receptors initiate pathways that promote cell survival, which appears to be integral to its proinflammatory response. TNF receptor associated factors (TRAFs) are adaptor proteins that participate in activation of transcription factors and protein kinases (Wallach et al. 1999). Both

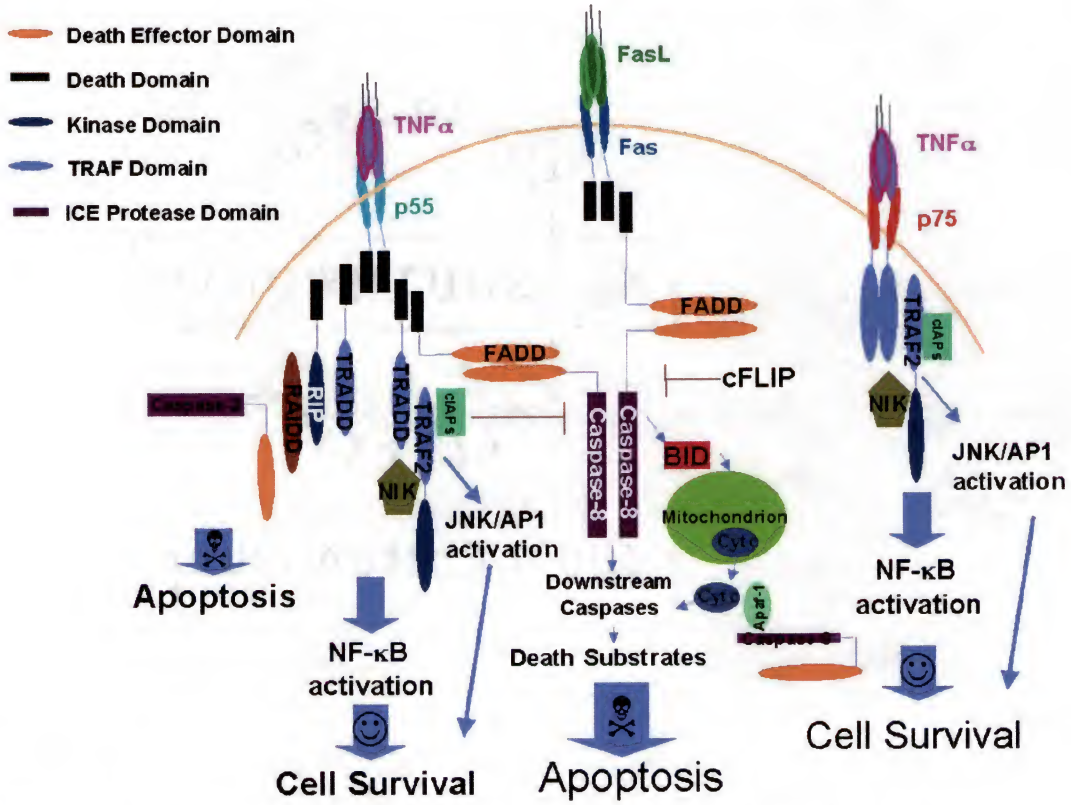
Death Effector Domain
Death Domain
Kinase Domain
TRAF Domain
ICE Protease Domain
FasL
TNFα
Fas
TNFα
p55
p75
FADD
FADD
cFLIP
Caspase-2
RAIDD
RIP
TRADD
TRADD
TRAF2
cIAPs
Caspase-8
Caspase-8
TRAF2
cIAPs
NIK
BID
NIK
JNK/AP1 activation
Mitochondrion
Cyt c
JNK/AP1 activation
Apoptosis
Downstream Caspases
Cyt c
Apaf-1
NF-κB activation
Caspase-9
NF-κB activation
Death Substrates
Cell Survival
Apoptosis
Cell Survival

Figure 1-2: Proposed interactions of signaling complexes in the TNF and Fas receptor signaling pathways.

the p55 and p75 TNF receptors bind TRAF2 and initiate signaling pathways involved in activation of the transcription factor nuclear factor kappa B (NF-κB) (Rensing Ehl et al. 1995; Ponton et al. 1996; Wallach et al. 1999). NF-κB is a family of hetero or homodimers comprised of a combination of any two of the following subunits: p50, p52, RelA, RelB, and c-Rel. The most common heterodimer is Rel-A/p50, which is often referred to as NF-κB. However, dimer composition is cell-type specific, and functionally diverse, suggesting that NF-κB regulation, activation and function are complex and depend upon cell type and stimulus. In fact, some homodimeric forms of NF-κB (p50 homodimers, in particular) are considered to be anti-inflammatory since they bind to the kB region on the promoter of early activation and inflammatory genes, but do not induce transcription. NF-κB is primarily regulated by a family of I-κB proteins that may form complexes with NF-κB in the cytosol. Upon phosphorylation and degradation of I-κB, NF-κB is translocated to the nucleus allowing for transcriptional regulation of various genes (Ghosh et al. 1998). The proinflammatory properties of TNFα are induced in part through activation of NF-κB-dependent survival genes (Baker and Reddy 1996). Additionally, NF-κB activation appears to directly inhibit TNFα-induced apoptosis (Baker and Reddy 1996) by initiating the synthesis of anti-apoptotic proteins, such as cellular inhibitors of apoptosis (cIAPs) (Chu et al. 1997). These NF-κB-induced survival proteins act by potentiating the NF-κB pathway and/or by inhibiting specific portions of the apoptotic cascade.

Nevertheless, such generalizations may represent an oversimplification of the actual physiological properties of these molecules. Data that conflict with this simplified TNFα signal transduction model (presented in figure 1-2) are often reported. Despite the absence of a death domain, the p75 receptor has been shown in T lymphocytes to initiate apoptosis independent of p55 TNF receptor signaling (Zheng et al. 1995; Alexander-Miller et al. 1998; Herbein et al. 1998). In fact, TNFα appears to play a dual role in activated T cells, which predominantly express the p75 receptor (Ware et al. 1991; Zheng et al. 1995). TNFα promotes proliferation in naïve T cells (Yokota et al. 1988) through the actions of the p75 receptor (Gehr et al. 1992; Tartaglia et al. 1993; Grell et al. 1998). Conversely, TNFα promotes p75-induced cell death in activated CD8+ T-cells (Zheng et al. 1995; Alexander-Miller et al. 1998; Herbein et al. 1998).

The differential response by T-cells may depend upon the availability of cell signaling intermediates to determine whether TNFα is either proapoptotic or proliferative for T-cells or fibroblasts. For example, Pimentel-Muinos et al. demonstrated that induction of the adaptor molecule RIP (receptor interacting protein) following IL-2-driven T cell activation initiates the death pathway in p75 expressing Jurkat T cells (Pimentel-Muinos and Seed 1999). Contrarily, RIP expression induced NF-κB activation in a fibroblast cell line (Pimentel-Muinos and Seed 1999). Similar cell-type specific results have been reported by other groups (Medvedev et al. 1994). These data revealed that addition of an anti-p75 TNFR polyclonal antiserum or anti-p75 monoclonal antibody (mAb) plus anti-immunoglobulin (Ig) to crosslink the receptors led to cytotoxic response of human rhabdomyosarcoma cells (KYM-1) but no toxicity in U937 cells, further demonstrating the cell-specific nature of TNF receptor signaling.

These data indicate that a single pathway may not function in all cell types and circumstances, thus signaling pathways need to be examined in a cell-specific context. Unfortunately, this may confound interpretation of previous data concerning the role of specific TNFα signaling pathways (Pimentel-Muinos and Seed 1999). In addition, although specific functions have been assigned to the adaptor molecules in these pathways based on the observed cellular responses, the physiological importance of each molecule in the context of the different ligands and receptors must await further confirmation.

Role of Tumor Necrosis Factor-alpha in Disease

Given the significant role of TNFα in innate and adaptive immunity, it is not surprising that the biosynthesis and action of this cytokine and its receptors are highly regulated. Produced primarily by activated monocytes/macrophages, but also by a surprisingly diverse cell lineage, TNFα synthesis and release is frequently episodic and controlled at both transcriptional and translational levels (Cavaillon and Haeffner 1993). Moreover, to limit the response to TNFα, both TNF receptors can be cleaved yielding soluble forms of their extracellular domains, which are also thought to function as antagonists of TNFα bioactivity (Van Zee et al. 1992; Ulich et al. 1993; Hale et al. 1995).

Despite this regulation, inappropriate production of TNFα is often seen and is associated with significant pathology. In fact, many human diseases can be explained by inappropriate activation of the host's own immune system. For instance, TNFα is known to promote remodeling of target tissues in response to injury or inflammation by initiating the apoptotic cascade in some tissues while simultaneously inducing the proliferation of others. In particular, increased TNFα-mediated cellular apoptosis contributes to a number of pathologic disorders including hepatocyte injury, lymphocyte apoptosis, endothelial cell dysfunction and neuronal cell death (Larrea et al. 1996). In a recent editorial, Kowdley hypothesized that host-driven inflammation and TNFα-mediated hepatocyte injury might be the 'smoking gun' in the pathogenesis of chronic hepatitis C (Kowdley 1999). However, liver injury is not the only disorder in which TNFα-mediated apoptosis is alleged to participate. TNFα-mediated apoptosis is also thought to contribute to the lymphopenia and endothelial cell dysfunction associated with sepsis, synovial changes in rheumatoid arthritis, progression of multiple sclerosis, acute renal failure, and in the killing or control of some neoplastic growths (Denekamp 1993; Brynskov et al. 1994; Raine 1995; Feldmann et al. 1996).

It is clear that proinflammatory cytokines like TNFα play a fundamental role in the regulation, initiation, maintenance, and termination of the inflammatory response. More than 50 different cytokines have been identified and much is known about the signal transduction pathways involved. However, TNFα continues to be regarded as one of the proximal cytokines in the proinflammatory response and thus remains a potential target for therapy. Many clinical studies aimed at controlling the transcription and effects of TNFα have been initiated. Studies aimed at blocking LPS, a classic TNFα-inducing stimulus, were successful in vitro and in rodent models of endotoxic shock, but failed to suppress the inflammatory response in in vivo human studies (Lynn and Golenbock 1992). Animal studies involving anti-TNFα therapies for sepsis and multi-organ failure led many to expect comparable benefits in humans. However, controlled clinical studies in sepsis have failed to show a survival benefit (Fisher et al. 1993; Abraham et al. 1995). In contrast, more beneficial results with anti-TNFα therapies (Elliott and Maini 1994; Elliott et al. 1994a; Elliott et al. 1994b) have been seen in chronic inflammatory or noninfectious diseases like rheumatoid arthritis and inflammatory bowel disease. The failure of TNFα antagonists in some, but not all, clinical trials is evidence that we have yet to fully understand the potential roles of TNFα in acute and chronic inflammatory disease.

Although TNFα-mediated apoptosis participates in several disease processes, the most relevant to these studies is the observation that TNFα and cellular apoptosis likely contribute to hepatocyte injury in chronic hepatitis C. In addition to the role of TNFα in chronic hepatits C, TNFα-mediated apoptosis has been implicated in hepatocellular death following injury as a result of ischemia/reperfusion and hepatotoxins (Bradham et al. 1998). Increased TNFα expression has been detected in liver biopsies from patients with hepatitis C infections and is presumed to be localized to infiltrating inflammatory cells (Gonzalez-Amaro et al. 1994; Fukuda et al. 1995; Larrea et al. 1996). Also, increased hepatocyte apoptosis has been detected in livers from patients with chronic hepatitis C

(Lau et al. 1995). Therefore, a better understanding of the gene products and pathways involved in TNFα-mediated hepatocellular apoptosis would be useful for future studies not only in liver disease, but also in other experimental models of TNFα-mediated apoptosis.

Murine Model of TNF-mediated Hepatocyte Apoptosis and Lethality

The role of TNFα in the pathophysiology resulting from hepatitis C infection has been investigated using a murine model of hepatocellular apoptosis and lethality. However, hepatocytes are typically resistant to TNFα-mediated death (Leist et al. 1994; Xu et al. 1998). Current studies reveal that NF-κB activation is necessary for prevention of TNFα-mediated hepatocellular totoxicity (Xu et al. 1998). In hepatocytes, particularly, TNFα-mediated apoptosis requires simultaneous inhibition of either DNA or RNA synthesis (Leist et al. 1994). Xu and colleagues noted that blocking NF-κB in RALA hepatocytes also resulted in increased TNFα-mediated apoptosis (Xu et al. 1998).

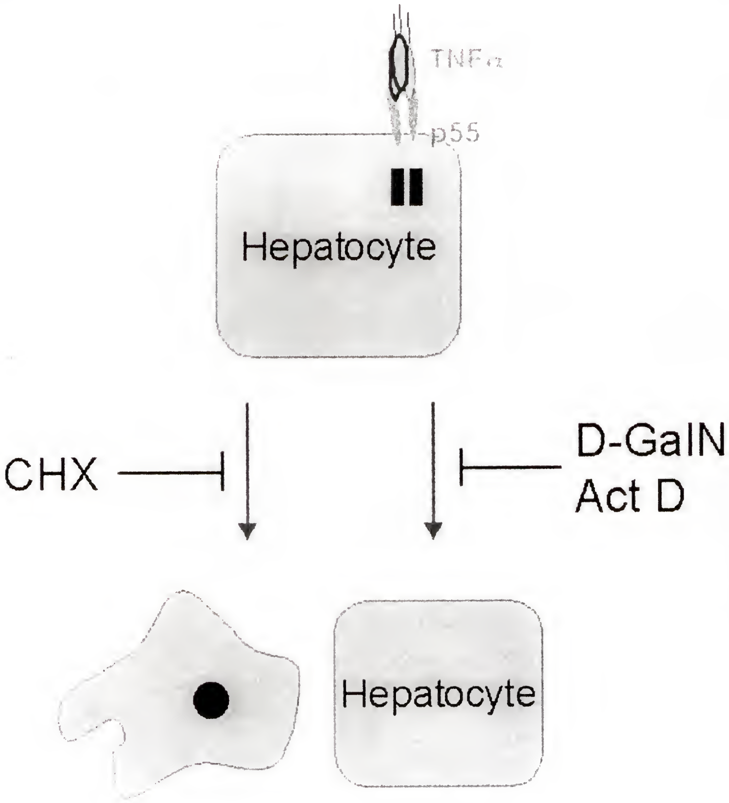

Figure 1-3: The effect of transcriptional (D-GalN and Actinomycin D) and translational inhibitors (cyclohexamide (CHX)) on TNFα-mediated apoptosis in hepatocytes.

Pretreatment of the same cells with the transcriptional inhibitor, actinomycin D (ActD), promoted TNFα-mediated apoptosis but did not prevent NF-κB translocation. Rather, ActD pretreatment prevented the transcription of NF-κB-induced genes in response to TNFα. In addition, hepatic regeneration induces TNFα (Taub 1996), and inhibition of NF-κB by forced over-expression of an I-kB (inhibitor of NF-κB) dominant negative in the livers of mice after hepatic resection produces massive apoptosis (Iimuro et al. 1998). Taken together, these findings suggest that blockade of NF-κB dependent transcription of 'survival genes' by either D-GalN or ActD in hepatocytes results in TNFα-mediated apoptosis (see figure 1-3). Interestingly, studies using translational inhibitors reveal that TNFα and D-GalN-mediated hepatocyte toxicity was also dependent upon functional translation, as well as transcription (see figure 1-3) (Leist et al. 1994). These data suggest that hepatocyte apoptosis depends upon the synthesis of constitutive proteins, as well as constitutively expressed mRNA transcripts.

Several decades ago, Galanos and Freudenberg demonstrated that treatment of mice with D-GalN increased by several thousand-fold their sensitivity to the lethal effects of LPS or TNFα (Galanos et al. 1979; Freudenberg et al. 1986). These data provided researchers with a unique model for the study of TNFα-dependent hepatocellular apoptosis. D-galactosamine is metabolized by the liver and selectively blocks transcription in hepatocytes by depleting uridine nucleotides necessary for the production of new mRNA transcripts (Leist et al. 1995). LPS, when administered along with D-GalN, produces a primarily TNFα-dependent model of fulminant hepatocellular apoptotic injury and lethality, unlike the shock and necrotic liver injury found in high dose LPS models (Tiegs et al. 1989; Galanos and Freudenberg 1993; Bohlinger et al. 1996). In fact, high dose LPS-induced lethality has been shown to be mechanistically distinct from models using sensitization with transcriptional inhibitors (Mignon et al. 1999). Lethality from LPS and D-GalN treatment is secondary to caspase-3-mediated apoptotic liver injury, as demonstrated by the ability of synthetic caspase inhibitors to block the apoptosis and lethality seen in treated mice (Bohlinger et al. 1996; Mignon et al. 1999). However, these inhibitors do not prevent lethality to high dose LPS, nor do they block the early inflammatory responses to LPS and D-GalN treatment, indicating that toxicity in this model is independent of the systemic inflammatory response (Jaeschke et al. 1998; Mignon et al. 1999).

The role of apoptosis in this model has been well described by Mignon et al (1999). These studies reveal that caspase inhibitors can prevent and overcome hepatic injury induced by TNFα. In the absence of apoptosis, therefore, neutrophil transmigration, subsequent hepatic necrosis, and death do not occur in this model. In addition, SCID mice are not protected from lethality, suggesting that T and B cells are not required for hepatocyte apoptosis and lethality in this model (Miethke et al. 1992). This model of liver injury and lethality is mediated by TNFα signaling through the p55 TNF receptor specifically, resulting in activation of caspases and subsequent hepatocyte apoptosis (Lesslauer et al. 1991; Leist et al. 1995). Moreover, the use of recombinant human TNFα, as opposed to murine TNFα, in this model along with D-GalN promotes the specific targeting of the p55 TNF receptor due to species specificity of human versus murine TNFα (Smith et al. 1986; Brouckaert et al. 1992).

The dual effects of TNFα on pathways that both promote and antagonize cellular apoptosis have complicated efforts to dissect the role played by this cytokine in models of acute inflammation and liver injury. Therefore, in order to identify the multiple properties of TNFα in the murine D-GalN/LPS model of hepatocellular apoptosis and lethality, investigators have frequently employed various knockout and transgenic mice. Rothe et al. (1993) demonstrated that mice lacking a functional p55 TNF receptor were resistant to LPS induced lethalityonly when sensitized with D-GalN, while Peschon et al. (1998) demonstrated that mice lacking the p75 receptor were not protected (also see Nowak et al. 2000). Conversely, Morikawa et al. (1996), as well as our laboratory, observed that lpr mice lacking a functional CD95/Fas were not protected from LPS and D-GalN induced injury or lethality, indicating that the presence of Fas/FasL signaling is not required (also see Josephs et al. 2000). Also, mice deficient in proteases necessary for cleavage of membrane bound TNFα to the soluble form are also resistant to LPS/D-GalN-induced mortality suggesting that it is the secreted 17 kD form of the protein responsible for the liver injury and mortality (Nowak et al. 2000). Therefore, the summation of prior work with this model suggests that this model of liver injury and lethality is mediated by soluble TNFα signaling predominantly through the p55 TNF receptor, resulting in activation of caspases and subsequent hepatocyte apoptosis (Lesslauer et al. 1991; Leist et al. 1995).

Quantitative Trait Locus Analysis

The genetics of disease is often complex and polygenic in nature. Typically, no one gene is found to be necessary or sufficient for disease onset. Disease susceptibility, onset, progression, and prognosis are often determined by the additive or epistatic effects of inherited alleles. Due to the polygenic nature of many disease phenotypes, classical single-gene/protein based genetic analyses inevitably fail to identify all of the genes involved. Fortunately, whole genome searches genes contributing to a complex phenotype or quantitative trait can be conducted without any knowledge of the genes involved, and can identify chromosomal regions controlling various aspects of a complex disease phenotype. Through repeated sibling matings, researchers have established panels of well-defined inbred mouse strains. This rigid inbreeding process has essentially fixed many medically relevant traits in these strains creating disease models for study.

Inbred strains are in theory genetically identical and homozygous at every locus across their genome. Even though they are kept under identical environmental conditions, many strains of mice differ in their responsiveness to various stimuli or insults indicating that genetic factors are responsible for these differences. The genes responsible for these differences may be identified by performing a series of crosses of parental strains having divergent phenotypes. The simplest cross is called a backcross where parental strains are mated producing an F1 progeny that is heterozygous at every locus. This heterozygote is then backcrossed to one of the parental strains yielding progeny having one of only two possible genotypes at any given locus due to recombination during meiosis. The progeny of the cross are observed for the trait of interest. This type of genetic approach is referred to as quantitative trait locus (QTL) analysis, which is a method that makes use of linkage maps allowing for the identification of specific genetic loci influencing a particular trait of interest (Fisler and Warden 1997). In QTL mapping, trait values are tested for statistical association with genotypes of the marker loci in the progeny of a cross. This technique requires genetically and phenotypically divergent strains and a linkage map covering the entire genome. The steps involved in QTL mapping are illustrated in figure 1-4. The backcross progeny (typically about 100 to 150 animals) are then phenotyped for the trait of interest. The animals are also genotyped at various markers across the genome (typically at 20 centimorgans (cM)

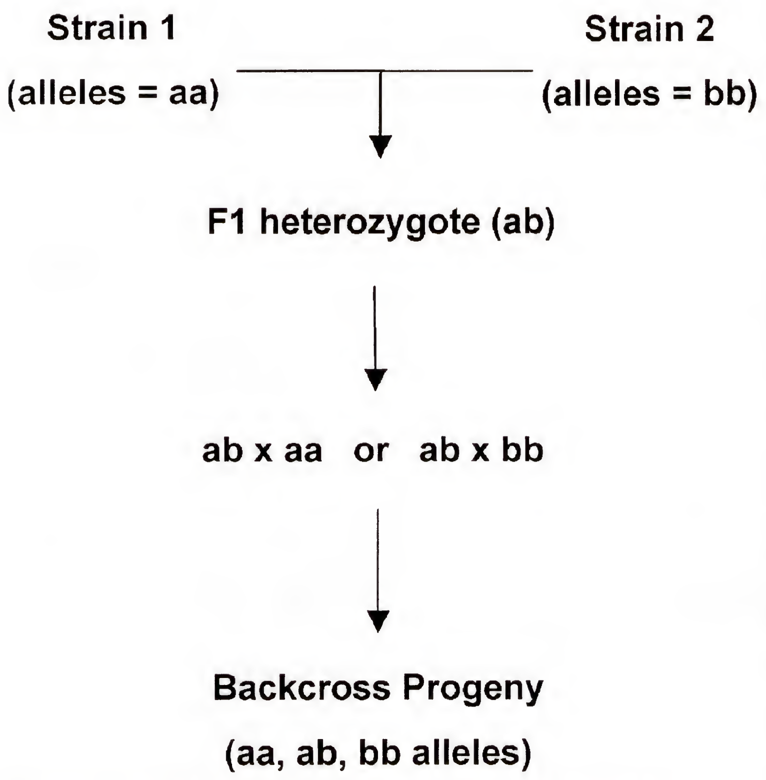

Figure 1-4: QTL Mapping Strategy . The first step is to cross phenotypically divergent strains producing an F1 heterozygote. Next, the F1 is backcrossed to one of the parent strains yielding the BC1 progeny and the phenotypes of all are recorded. The progeny are also genotyped at markers spread across the genome. Lastly, statistical associations of markers and phenotypes are performed to identify loci responsible for the trait.

intervals). The genotypes and phenotypes are then tested for association and the genomic regions affecting the trait or traits of interest are identified.

QTL mapping has played an important role in the agricultural sciences. Knowledge of loci contributing to variations among plant traits has been used to design crosses leading to improved agricultural products and thus increased crop yields. These genetic techniques have also been utilized successfully in various animal models of disease (Fisler and Warden 1997). In the past decade, QTL mapping has been utilized for the mapping of genes involved in a variety of traits in mice including obesity, atherosclerosis, diabetes susceptibility, systemic lupus erythematosis (SLE), collagen-induced arthritis and susceptibility to cancer (Yui et al. 1996; Mahler et al. 1998; Griffiths et al. 1999; McIndoe et al. 1999; Todd 1999).

There are obvious advantages for the use of rodent models for genetic mapping. These types of genetic studies in animals are relatively rapid compared to human studies and may allow for a more detailed description of the genes contributing to a specific phenotype. Evidence indicates that QTLs identified in rodent models of disease are often homologous to QTLs identified in large-scale human genetic mapping studies. Thus, results from animal studies may yield invaluable information for the identification of human susceptibility alleles, and possibly allow the diagnosis and treatment of these diseases to become gene-based (Fisler and Warden 1997). In addition, there are several other important advantages of conducting these studies in well-defined murine strains. For example, the phenotypic differences among inbred strains are generally quite large compared to those seen in human populations. Also, the genetic background is relatively stable and well described, and statistical power becomes less problematic.

Following the completion of the QTL analysis, an additional genetic strategy can be employed to confirm the role of a candidate gene(s) or loci involved in a disease phenotype. A common experimental strategy for the identification of susceptibility genes and determination of their functions is to create a series of consomic or congenic mouse strains, each carrying one of the genomic intervals or chromosomes associated with the trait on the background of the control strain. The use of breeding strategies to transfer genetic loci from one strain to another is a classic genetic approach that has been used since its development by Nobel Prize winner George Snell (Graff et al. 1966). The technique is to repeatedly backcross the donor and recipient mice while also selecting progeny carrying the gene of interest in each generation. This required about 12 generations of backcrosses and an additional intercross to obtain mice homozygous for the desired gene.

With the increasing availability of polymorphic markers and the development of rapid PCR techniques, a new genetic strategy has been developed. This strategy, called marker-assisted selection protocols (MASPs), uses a selection process at each generation of breeding of donor and recipient mice in order to select for the gene or interval of interest and the absence of contaminating genes from the donor (Wakeland et al. 1997). Selection is possible due to the presence of simple sequence length polymorphisms (SSLPs) in the mouse genome characterized by short repetitive sequences that vary among strains of mice based on the inaccurate replication of this repetitive DNA (Wakeland et al. 1997). Inbred mouse strains have been well characterized and many polymorphic markers are available allowing for the distinction between donor and recipient alleles across the mouse genome. This strategy significantly lessens the number of generations necessary for the generation of congenic mice. There are additional advantages to this approach. Congenic mouse strains carrying genomic intervals with unidentified genes can serve to facilitate the investigation into the contribution of each gene, alone and in combination, to the phenotype of the complex trait. Even prior to identification of the specific gene in the identified genetic interval, it becomes possible to identify its function. Once a phenotype is associated with the genetic interval, the position of the gene can be successively fine mapped via congenic recombinant analysis, thereby excluding false candidate genes and providing for the initiation of positional cloning.

Identification of QTLs in disease models is crucial for understanding the molecular basis of complex traits and the subsequent identification of potential therapeutic targets. These genetic studies in rodent models are beginning to uncover a host of candidate genes and genetic intervals associated with various diseases, which can now be examined for homology to human sequences and eventually to related human genes.

Nonobese Diabetic Mouse Model of Human Diabetes

The nonobese diabetic (NOD) mouse is a well-characterized autoimmune model that has a disease phenotype analogous to human type I diabetes (Leiter and Atkinson 1998). NOD mice spontaneously develop autoimmune diabetes characterized by leukocytic infiltration of the pancreatic islets at 3-5 weeks of age, and eventual destruction of insulin secreting pancreatic beta cells resulting in hyperglycemia (Leiter and Atkinson 1998). Although insulin-dependent diabetes (IDD) in the NOD mouse is a complex polygenic trait, the primary genetic element underlying diabetes susceptibility in the NOD mouse appears to be the major histocompatibility complex (MHC). The unusual H-2^{g7} (K^d, I-A^{g7}, I-E^{null}, D^b) possessed by the NOD mouse along with other non-MHC susceptibility loci have been identified as primary mediators of disease development (Quartey-Papafio et al. 1995; McDevitt 1998). The MHC class II molecules of diabetes-prone humans and mice share a homozygous lack of aspartic acid at position 57 in the MHC class II chain. Substitution of aspartic acid at position 57 protects NOD mice from diabetes, indicating the pivotal role that presentation of peptides via class II plays in defining the peripheral T cell repertoire (Quartey-Papafio et al. 1995; McDevitt 1998).

Although the importance of the inflammatory response in the generation of autoimmunity has been appreciated for some time, the underlying molecular mechanisms have remained elusive. Recent studies have stimulated interest in the role of TNFα in the development of diabetes in the NOD mouse. Studies by Held et al. (1990) revealed the presence of TNFα mRNA in the inflamed islets of NOD mice. Additional studies by Yang et al. demonstrated that treatment of neonatal NOD mice with recombinant TNFα accelerated diabetes, while treatment with anti-TNFα antibodies protected mice from disease (Yang et al. 1994). Moreover, Green et al. (1998) have demonstrated that forced expression of TNFα in islets of neonatal NOD mice accelerated the onset and progression of diabetes.

Conversely, the disease promoting properties of TNFα were not observed in adult NOD mice. In fact, Yang et al. (1994) determined that NOD mice treated with recombinant TNFα were actually protected against diabetes, while treatment with anti-TNFα antibodies exacerbated disease. Additionally, Grewal et al. (1996) established that NOD mice expressing TNFα under control of the rat insulin promoter were protected from diabetes when transgene expression was initiated in adulthood.

The role of the p55 TNF receptor signaling in diabetes in the NOD mouse has also been investigated. NOD chimeric mice having islets deficient in the p55 TNF receptor were protected from diabetes, implying that TNFα signaling via the p55 TNF receptor is critical in islet cell destruction (Pakala et al. 1999). Systemic administration of TNFα and its inhibitors resulted in varying outcomes depending upon the age of the mice and the frequency, duration and dose of this cytokine. An explanation for the differential effects of TNFα is unknown; however, it suggests TNFα obviously plays an important but still undefined role in diabetes in the NOD mouse.

Other studies have compared endogenous TNFα production in NOD and nondiabetic control strains. For example, Chosich et al. compared LPS/IFN-g-stimulated TNFα production in two lines of NOD mice, NOD/Lt (high diabetes incidence) and NOD/WEHI (low diabetes incidence). Data revealed that NOD/Lt mice demonstrated higher levels of biologically active TNFα compared to NOD/WEHI and control BALB/c mice (Chosich et al. 1994). In fact, the mean plasma TNFα levels produced after mice were primed intravenously (i.v.) with 1000 units of murine interferon gamma (IFN-g) and stimulated after 3 hours with 5 micrograms of LPS (administered i.v) were significantly higher in the mice that developed diabetes than in all non-diabetic mice. In contrast, Setoguchi et al. demonstrated that NOD mice producing lower amounts of TNFα when stimulated with Streptococcal preparations had higher diabetes incidence (Setoguchi et al. 1992). In fact, none of the mice producing increased amounts of TNFα became diabetic.

Furthermore, Strassmann and Jacob reported that peritoneal macrophages from NOD mice have markedly reduced TNFα production in response to LPS and interferon-gamma (IFN-g) stimulation. Of the 24 mouse strains tested, in vitro TNFα production by peritoneal macrophages stimulated with LPS and IFN-g was lowest in NZW and NOD strains (Jacob et al. 1996). Additional studies by Bazzoni and Beutler (1995) reported that TNFα mRNA levels from peritoneal macrophages of NOD mice were equivalent to macrophages from BALB/c indicating no differences in expression of the TNFα gene following LPS-induced activation. In addition, Alleva et al. (2000) have recently shown that levels of TNFα produced by endotoxin-activated macrophages were within the range produced by macrophages from a panel of normal strains including B6, BALB/c and C57BL/10 (B10) mice.

Specific Aims

Apparently, there is no consensus regarding the ability of NOD mice to synthesize or respond to TNFα. Studies to clarify the signaling pathways activated and the responses elicited by TNFα treatment in NOD mice may prove critical in the understanding of the role of TNFα in diabetes. Data from our laboratory suggest that NOD mice are resistant to TNF-mediated liver injury and lethality in the D-GalN model. Also, the availability of various B6.NOD congenic strains allows for the examination of the contribution of known diabetes-associated loci to this resistance. Therefore, the specific aims of the studies in the following chapters were to characterize the responsiveness of NOD mice to TNFα and D-GalN treatment and to employ a genetic approach to dissect the p55 TNF receptor signaling pathways involved in TNFα-mediated liver toxicity in

D-GalN sensitized NOD and B6 mice. Specifically, the aims were to fully characterize the phenotypic differences in hepatocellular apoptosis and lethality observed between NOD and B6 mice in response to treatment with LPS or recombinant human TNFα (rhTNFα) and D-GalN or to a Fas-agonist (Jo-2) antibody, to demonstrate that decreased responsiveness to TNFα/D-GalN treatment in NOD mice can be explained by differences in TNFα signaling in NOD primary hepatocytes when compared to B6 primary hepatocytes, to make use of the divergent phenotypes present in NOD and B6 mice in order to identify by quantitative trait loci analysis regions in the mouse genome that contribute to p55 TNF receptor-mediated liver apoptotic injury and lethality and finally to examine the contribution of known Idd regions from NOD mice using available B6.NOD congenic strains.

A more complete understanding of intracellular signaling pathways leading to apoptosis or inflammation is essential for an in vivo understanding of how TNFα mediates acute inflammatory diseases. It is clear that in order to modulate selected biological actions of this cytokine, it is necessary to dissect and understand the signaling pathways involved. This information may provide the basis for a rational pharmacological approach aimed at abrogating the undesirable effects of TNFα, while maintaining the necessary effects for resolution of inflammation and repair processes.

CHAPTER 2
REDUCED SUSCEPTIBILITY OF NONOBESE DIABETIC MICE TO TNFα AND D-GALACTOSAMINE MEDIATED LIVER INJURY AND LETHALITY

Introduction

The nonobese diabetic (NOD) mouse is a well-characterized model that is both pathologically and genetically analogous to human type I diabetes (Leiter and Atkinson 1998). The genetic defects present in the NOD mouse which promote the loss of either central or peripheral tolerance to self-antigen are unknown. However, studies by Serreze and Leiter et al. indicate that defects in antigen-presenting cell differentiation and function may contribute to the lack of tolerance to pancreatic cell self-antigens (Leiter and Serreze 1992; Serreze 1993; Serreze et al. 1993a; Serreze et al. 1993b; Serreze and Leiter 1994; Leiter and Atkinson 1998).

Recent studies have suggested that TNFα expression is increased in the pancreatic cells of NOD mice, and this localized TNFα production plays a critical role in both the initiation of insulitis and the subsequent progression to cell destruction (Held et al. 1990). NOD mice deficient in the p55 TNF receptor develop insulitis similar to that of wild-type NOD mice; however, progression to diabetes is not observed (Kagi et al. 1999), indicating that beta cell destruction may occur via a p55-TNF receptor dependent mechanism.

Although TNFα contributes to the autoimmune predisposition of NOD mice, little is known about their ability to synthesize or respond to TNFα. Therefore, the purpose of the studies in this chapter was to evaluate whether NOD mice synthesize TNFα and respond to endogenously produced and exogenously administered TNFα in a manner similar to that seen for B6 mice. Identifying differences in TNFα production and responsiveness of NOD mice can provide the basis for not only a better understanding of TNFα-dependent disease progression in autoimmune diabetes, but also in endotoxin-induced shock and liver injury.

Transcriptional inhibition in the liver with D-GalN increases by several thousand-fold the sensitivity of mice to the lethal effects of LPS and TNFα (Galanos et al. 1979). D-Galactosamine selectively blocks transcription in hepatocytes by depleting uridine nucleotides necessary for the production of mRNA transcripts (Leist et al. 1995). Treatment of animals with LPS or TNFα in conjunction with D-GalN results in acute hepatocyte apoptosis and liver failure (Morikawa et al. 1996; Mignon et al. 1999). This model of liver injury and lethality is mediated by TNFα signaling through the p55 TNF receptor, resulting in activation of caspases and subsequent hepatocyte apoptosis [Leist, 1995 #6722; (Lesslauer et al. 1991).

We first examined the responsiveness of NOD and B6 mice to lethality and hepatic injury secondary to the administration of LPS and D-GalN. To eliminate the possibility that differences in the responsiveness to LPS could be explained by a reduced production of TNFα, these studies were repeated in both strains of D-GalN-sensitized mice with recombinant human TNFα (rhTNFα), which binds predominantly to the mouse p55 TNF receptor (Brouckaert, P.G. et al. 1989; Brouckaert, P. et al. 1992). Finally, because the p55 TNF receptor signaling pathway converges with the Fas signaling pathways (Ogasawara et al. 1993; Lawson et al. 1999), NOD and B6 mice were also treated with the Fas agonist, Jo-2. Data in this chapter were published in December, 2000 (Bahjat et al. 2000).

Materials and Methods

Reagents

LPS from Escherichia coli 0111:B4 and D-GalN were obtained from Sigma (St. Louis, MO). Jo-2, a purified hamster anti-mouse Fas mAb in no azide/low endotoxin format with agonist properties for Fas (CD95) was obtained from PharMingen (San Diego, CA). Purified hamster IgG, group 2, a monoclonal isotype control Ab (NA/LE)

(APC)-labeled Ab was also obtained from PharMingen. Recombinant human TNFα was the generous gift of Dr. Tadahiko Kohno (Amgen, Thousand Oaks, CA).

Animal Experimental Protocols

Female C57BL//6, SWR and NOD/LtJ mice between five and eight weeks of age were obtained from The Jackson Laboratory (Bar Harbor, ME) or from the Department of Pathology Animal Resource Facility, University of Florida College of Medicine (Gainesville, FL). NOD and B6 mice bred at the University of Florida were derived from breeding stock obtained from The Jackson Laboratory. All animal protocols were approved by the Institutional Animal Care and Use Committee of the University of Florida College of Medicine.

To assess mortality, animals were treated with intraperitoneal (i.p.) injections of 8 mg D-GalN per mouse in combination with LPS or rhTNFα in 200 μl sterile physiologic saline (155 mM NaCl). An anti-Fas monoclonal antibody (mAb, clone Jo-2) diluted in 200 μl sterile physiologic saline vehicle was also administered to some animals. Control groups of mice received either physiologic saline alone or 8 mg D-GalN in physiologic saline. As a control for the anti-Fas-injected animals, an isotype Ab control was injected at the same concentration. Mice were monitored for mortality every 6 hours for the first 24 hours and then twice daily for up to 72 hours. Alternatively, mice were injected and anesthetized with sodium pentobarbital (50 mg/kg body weight), then were bled by retro-orbital puncture at 90 minutes for serum TNFα measurements. At three hours (post Jo-2 injection) or six hours (post LPS or TNFα injection), additional mice were anesthetized with sodium pentobarbital (50 mg/kg body weight) and bled by cardiac puncture for quantitation of serum transaminases. Mice were then sacrificed by cervical dislocation, and the livers were harvested, rinsed in cold PBS, and immediately homogenized for caspase-3-like activity assay. In addition, one lobe of the liver was fixed in 10% buffered formalin for paraffin embedding, and 5-μm sections were cut and affixed to slides. One slide was stained with hematoxylin and eosin, and another was used for in situ 3'-TUNEL staining as described below.

Preparation of Liver or Spleen Cell Homogenates

Tissues were harvested and rinsed in cold sterile PBS and then homogenized in three volumes (v/w) of ice-cold homogenization buffer (25 mM HEPES (pH 7.5), 5 mM MgCl2, 1 mM EDTA, 1 mM PMSF, 1 μg/ml leupeptin, and 1 μg/ml aprotinin). Homogenates were centrifuged at 13,500 rpm in a Beckman J2-HS centrifuge for 15 minutes, and supernatants were assayed for protein content using a Bio-Rad protein assay kit (Bio-Rad Laboratories, Hercules, CA) according to instructions provided.

Caspase-3-like Activity Determination

Protein extracts from either primary hepatocytes or from one lobe of liver or whole spleen were assayed for caspase-3-like activity using protocols previously described (Fukuzuka et al. 1999). Briefly, 40 μg of total protein per sample were incubated with the synthetic substrate benzyloxycarbonyl-Asp-Glu-Val-Asp-7-amino-4-trifluoromethylcoumarin (Z-DEVD-AFC) (Enzyme Systems Products, Livermore, CA). The cleavage of substrate was monitored in a fluorescence reader using 400 nm excitation and 505 nm emission wavelengths. Calibration curves were generated using standard concentrations of AFC and the caspase-3-like activity was calculated from the slope of the recorded relative fluorescence and expressed as relative fluorescence units.

Cytokine Measurements and Serum Transaminase Determinations

TNFα bioactivity was determined using the WEHI 164 clone 13 cell line cytotoxicity assay as previously described (Solorzano et al. 1997). Specificity of the assay was determined by incubating murine serum samples with anti-TNFα Abs to block cytotoxicity (Solorzano et al. 1997).

Transaminase levels (aspartate aminotransferase (AST)) were determined on serum samples using a commercial kit adapted for the small sample volumes obtained from mice (Sigma) as previously described (Solorzano et al. 1997).

In situ TUNEL Assays on Liver Tissue Sections

Livers were fixed in 10% buffered formalin and embedded in paraffin. Sections of 5 μm were affixed to slides and then deparaffinized and rehydrated. Slides were either stained with hematoxylin and eosin for analysis of morphologic changes or further prepared for fluorescent 3'-end labeling of genomic DNA fragments using a commercial Apoptag kit (Promega, Madison, WI). Slides underwent proteinase K digestion for 15 min in buffer (0.5 M EDTA (pH 8.0), 200 mM Tris, 1 mg proteinase K stock per ml buffer). Slides were washed three times for five minutes in PBS and equilibrated with buffer for 15 minutes. Staining solution containing the FITC-labeled nucleotide mix and TdT in equilibration buffer was added to each slide for 80 minutes. The enzymatic reaction was stopped, and slides were counterstained with a propidium iodide/anti-fade DNA intercolating counterstain solution (Oncor, Inc., Gaithersburg, MD). Slides were photographed using a Zeiss Axioskop2 wide-field fluorescence microscope with appropriate filter set (Zeiss, Welwyn Garden City, U.K.).

Flow Cytometric Analysis for Detection of p55 TNF Receptor

Splenocytes were prepared by needle dissection in RPMI 1640 supplemented with 10% FCS and washed once in ice-cold PBS before being re-suspended in 5 ml of ice-cold PBS buffer. One hundred thousand splenocytes were stained with 20 ng biotinylated rhTNFα, biotinylated control protein, or 100 molar excess of unlabeled rhTNFα followed by biotinylated rhTNFα for 1 hour at 4°C, as detailed in the protocol provided in the Fluorokine™ kit (R&D Systems, Minneapolis, MN). Fluoroscene isothiocyanate-conjugated streptavidin was added to all tubes for 30 minutes and then cells were washed twice. In addition, cells were stained with allophycocyanin (APC)-labeled anti-mouse CD3 mAb (PharMingen) for 15 minutes. Cells were then washed once, and samples were stained with the vital dye 7-aminoactinomycin D (7-AAD) (Molecular Probes, Eugene, OR) for 30 min at a concentration of 1 μg/ml. Samples were analyzed using a FACScalibur™ (Becton Dickinson, San Jose, CA). Data were analyzed by gating on CD3-negative and 7-AAD-negative viable cells using CellQuest™ software (Becton Dickinson).

Murine Hepatocyte Isolation and Culture

Murine hepatocytes were isolated using a modification of the method described by Klaunig et al. (24) with viability exceeding 90%, as assessed using trypan blue staining. Briefly, mice were anesthetized with sodium pentobarbital (50 mg/kg body weight) and an incision was made through the skin on the ventral midline. The viscera was displaced to reveal the inferior vena cava and portal vein. A ligature was placed around the vena cava posterior to the renal veins and gently tied after introduction of a 24-gauge catheter into the vena cava distal to the ligature. A perfusion buffer (Krebs Ringer solution containing 20 mM glucose and 0.2 mM EGTA, pH 7.4) was initiated at 2 ml/min. The portal vein was then quickly severed, and the anterior vena cava was clamped between the diaphragm and heart. The perfusion rate was increased gradually to 7 ml/min for a total volume of 50 ml. The perfusion was continued with digestion buffer (Krebs Ringer Solution containing 20 mM glucose, 1.37 mM CaCl2, 0.72% BSA fraction V (Sigma) and 100 U/ml type I collagenase (Sigma), pH 7.4) for another 50 ml total volume. The liver was then excised, and the capsule was ruptured to release cells. The cells were further dispersed by aspiration through a large bore pipet. Hepatocytes were isolated by centrifugation at 50xg for five minutes at 4°C. Cells were washed three times with ice-cold culture medium (DMEM with 10% FBS and 1% penicillin and streptomycin). The cells were then plated at a density of 500,000 cells/ml on culture dishes coated with 20 μg per ml of type III acid soluble calf skin collagen (Sigma) in either 100 μl volume for 96-well plates for MTT toxicity assay or 3 ml volume for six-well plates for caspase-3-like activity determination. After resting for eight hours, cells were treated by replacement of original culture media with new media with or without D-GalN added at various concentrations. Cells were then incubated for 30 minutes before addition of 1 μg/ml rhTNFα. Cells were incubated for six hours for caspase-3-like activity assay or for 20 hours for MTT cytotoxicity assay. Alternatively, some cells were treated with the Fas agonist Ab, Jo-2, or isotype control Ab at a concentration of 1 μg/ml. Cytotoxicity and caspase-3-like activity were determined.

In vitro Hepatocyte Assays

Briefly, hepatocytes were isolated from NOD and B6 mice according to the protocols outlined in the methods above. Briefly, cells are placed into culture, rested six hours prior to treatment, and harvested at defined intervals after exposure to D-GalN and rhTNFα. Cells were harvested following exposure to D-GalN and TNFα, media alone, or media plus D-GalN. Apoptotic cell death was determined by caspase-3 activity using a fluorometric assay on cellular lysates with synthetic substrate. Cell viability was determined by incubating the cells with 0.6 mg/ml of MTT for two hours then lysing the cells with isopropanol and determining the quantity of reduced MTT spectrophotometrically. In addition, cells were alternatively treated with Jo-2 or isotype antibody in order to assess responsiveness of NOD and B6 hepatocytes and confirm in vivo results.

MTT Cytotoxicity Assay

Formazan production from MTT was measured after incubation of cells with 0.6 mg/ml MTT in 100 μl culture media per well in a 96-well plate for 1.5 hours. Medium was then removed, and cells were lysed in 100 μl 2-propanol. Next, 100 μl water were added, and plates were read in an ELISA reader at 560/690 nm.

Results

LPS/D-GalN-induced Lethality and TNFα Production in NOD and B6 Mice

NOD and B6 mice were injected intraperitoneally with D-GalN (8 mg) and increasing doses of LPS (1 ng–100 μg), and blood was obtained at 90 minutes for serum TNFα determinations. Mice were monitored for up to 72 hours, and percent mortality was determined. LPS and D-GalN treatment produced dose-dependent increases in mortality in B6 mice (Figure 2-1). Increasing the dose of LPS from 1 ng to 10 ng and higher produced 100% percent mortality. Mice started to die within 6-8 hours after LPS administration, and mortality generally occurred within 12–24 hours. However, D-GalN-sensitized NOD mice were resistant to at least 100-fold higher concentrations of LPS. Lethality was not seen until doses of LPS approached 1 μg, and even at doses of 100 μg, only 50% mortality was observed. Mortality in NOD mice, when it occurred, followed a similar time course with the majority of animals dying within 24 hours. Physiologic

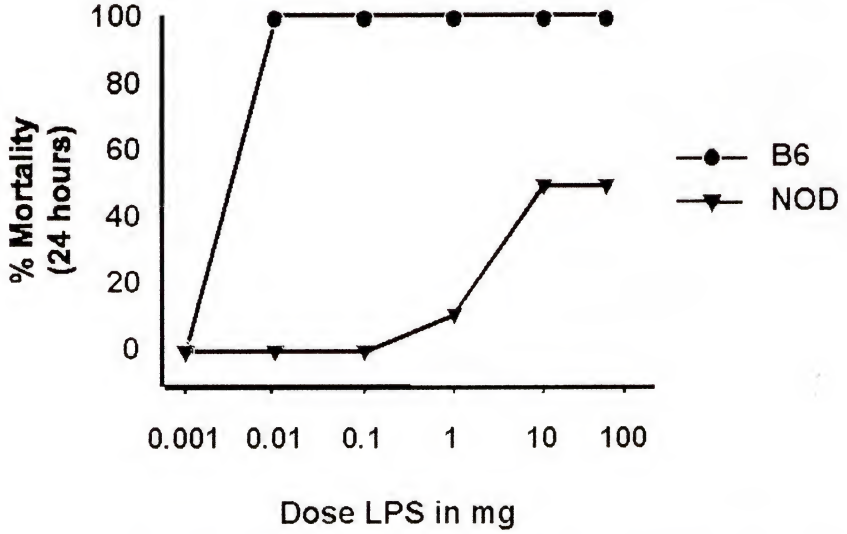

Figure 2-1 - Survival Responses to Increasing Doses of Lipopolysaccharide (LPS) in D-GalN-Sensitized B6 and NOD Mice. Values represent the percent mortality of between 6 and 18 mice per dose of LPS at 24 hours. The differences in survival between NOD and B6 mice were highly significant (p<0.001 by c2 analysis).

saline or D-GalN (8 mg) treatments alone produced no mortality in either strain (data not shown).

Jacob, Lee, and Strassman reported that peritoneal macrophages from NOD mice have a reduced production of TNFα when stimulated with LPS and IFN-gamma (Jacob et al. 1996). Data from their laboratory also revealed that NOD mice produced lower levels of TNFα than did most other strains, even though TNFα gene expression was similar among these strains. To determine whether the differences in survival could be explained by a differential TNFα production, serum TNFα concentrations were determined at 90 minutes, a time period previously shown to represent the peak serum appearance after LPS administration (Josephs et al. 2000). As shown in Figure 2-2, peak serum TNFα concentrations in B6 and NOD mice treated with 100ng or 1μg LPS with D-GalN were not significantly different, although they were modestly reduced in the NOD mouse at the lower dose of LPS.

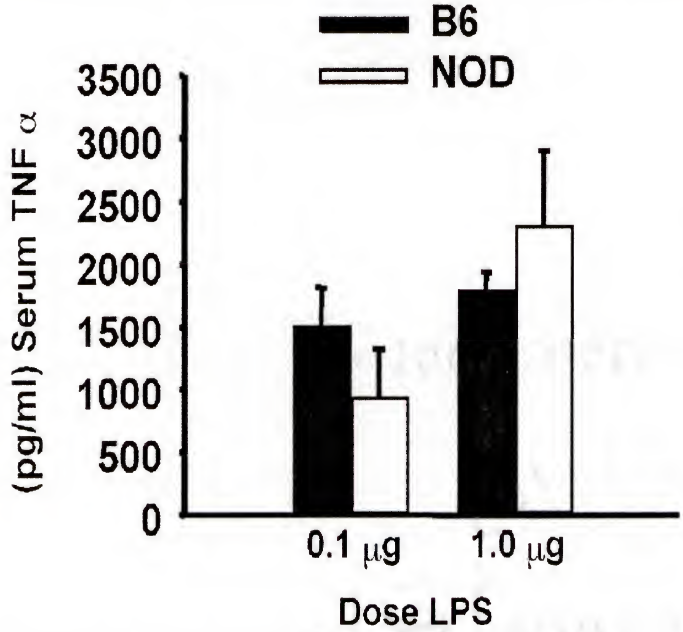

Figure 2-2 - Peak serum TNFα Responses to LPS and D-galactosamine in B6 and NOD mice. Mice were bled at 90 minutes post treatment and serum TNFα bioactivity determined using the WEHI 164 clone 13 cytotoxicity assay. Data represent the mean ± SEM of between 17 and 29 observations per group. Serum TNFα responses did not significantly differ between the two groups of mice at either dose ($p>0.05$ for both), although the reductions in serum TNFα in NOD mice at the lower dose approached significance ($p=0.065$).

Apoptosis and Liver Toxicity in LPS/D-GalN Treated NOD and B6 Mice

Mice injected with 100ng LPS and 8mg D-GalN were sacrificed at 6 hours after blood was collected. This time was chosen, based on our previous work, because it preceded death but was a time period associated with significant liver injury (Josephs et al. 2000; Nowak et al. 2000). Livers were harvested; one lobe was homogenized for caspase-3-like activity, and another lobe was fixed in 10% buffered formalin for sectioning and histological analysis. Liver injury assessed by 6 hour serum transaminase levels revealed 75% less liver-specific enzyme appearance (p<0.05) in the blood of NOD compared with B6 mice (Figure 2-3A). Although caspase-3-like activity at 6 hours was increased in NOD mice, the levels were significantly lower (287 ± 11 vs 194 ± 11 relative fluorescence intensity, p<0.05) than those in livers from B6 mice (Figure 2-3B). D-GalN treatment alone did not increase caspase-3-like activity in the liver. Increased caspase-3-like activity was also not readily observed in spleens from LPS and D-GalN-treated or D-GalN alone-treated animals (data not shown). In situ TUNEL assays also revealed that NOD mice had markedly fewer apoptotic cells in liver sections than were found in livers from B6 mice (Figure

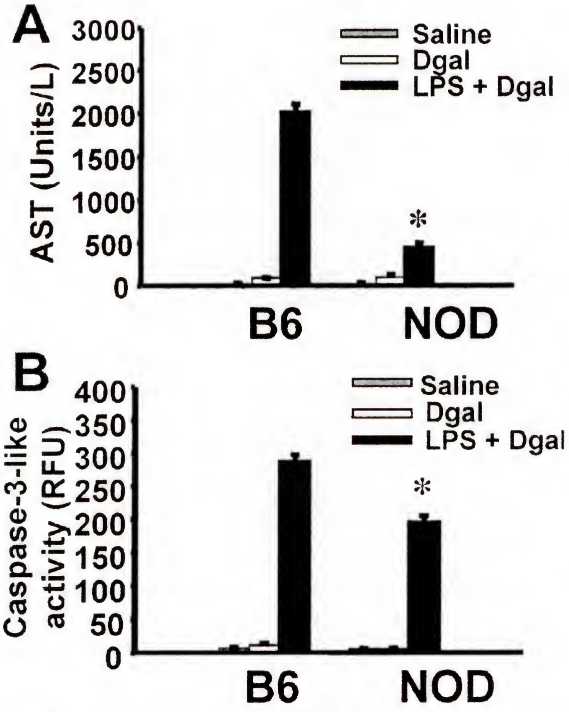

Figure 2-3 - Liver Caspase-3-Like Activity and Serum AST in B6 and NOD Mice Challenged with D-GalN and/or LPS. Animals were bled and sacrificed at six hours post treatment. The following data represents one of three independent experiments. AST (A). Values represent the mean ± SEM of six animals per group for serum transaminase levels p<0.001. Liver caspase-3-like activity assay (B). Values represent the mean ± SEM of five animals per group for caspase-3-like activity assay. p<0.001

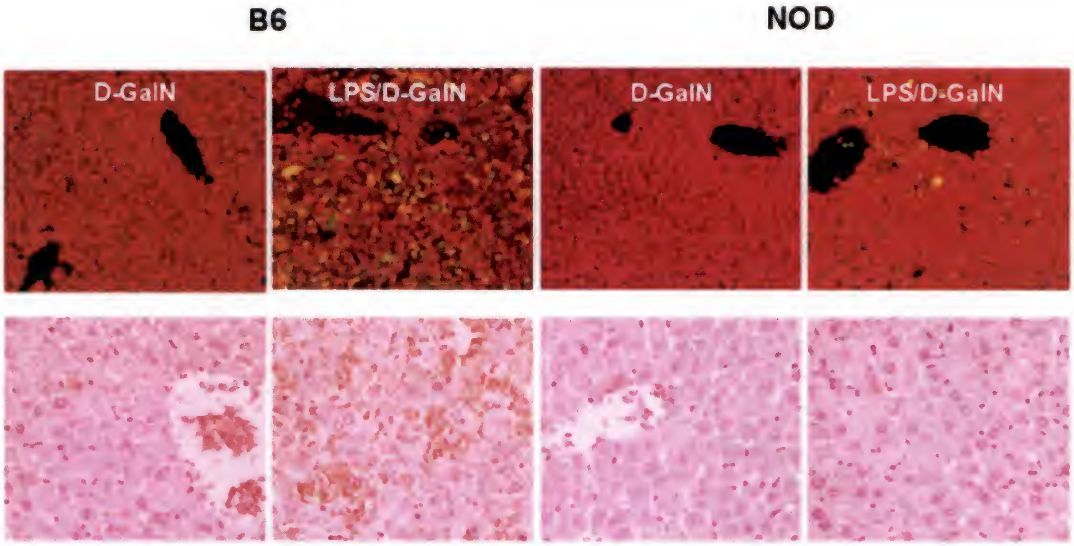

Figure 2-4. Histopathologic Analysis of In situ TUNEL (top row) and Hematoxylin and Eosin stained livers (bottom row) from LPS and D-GalN Treated C57BL/6 and NOD Mice. Data presented are representative of 3 independent experiments.

2-4). Histopathologic analysis of hematoxylin and eosin-stained liver sections from LPS and D-GalN-treated B6 mice revealed pervasive destruction of liver architecture and extensive apoptosis. In contrast, the degree of apoptosis and destruction of liver architecture was reduced, albeit not eliminated, in NOD mice. Livers of D-GalN alone-treated B6 and NOD mice were phenotypically comparable to saline-injected animals.

rhTNFα and D-GalN Toxicity in NOD and B6 Mice

Although peak serum TNFα concentrations did not significantly differ between NOD and B6 mice, the possibility existed that differences in the production of TNFα may have explained the differences in survival and apoptotic liver injury. Furthermore, by taking advantage of the property that human TNFα binds preferentially to the mouse p55 TNF receptor (Brouckaert, P.G. et al. 1989; Brouckaert, P. et al. 1992), administration of human TNFα to D-GalN-sensitized mice offers the opportunity to identify survival responses dependent exclusively on p55 TNF receptor signaling. B6 mice treated with D-GalN were sensitive to rhTNFα with doses as low as 1μg, producing >50% lethality, and 10μg human TNFα, producing 100% lethality (Figure 2-5).

In contrast, NOD mice were resistant to rhTNFα and D-GalN-induced lethality. Doses of rhTNFα as high as 100μg with 8mg D-GalN produced no mortality in NOD mice. Higher doses could not be evaluated due to the large amounts of recombinant protein required.

Liver Injury and Apoptosis in rhTNFα and D-GalN-treated NOD and B6 Mice

Caspase-3-like activity in livers from B6 mice treated for five hours with 10μg rhTNFα and D-GalN was significantly higher than was seen in NOD mice (Figure 2-6B), and serum transaminases were also significantly elevated (both $p < 0.05$) (Figure 2-6A). Apoptotic liver injury was also confirmed histologically (Figure 2-7), and by in situ TUNEL staining. Although NOD mice were protected from mortality to rhTNFα and D-GalN at the doses evaluated, they did exhibit some hepatic injury, hepatocyte apoptosis, and increased caspase-3-like activity.

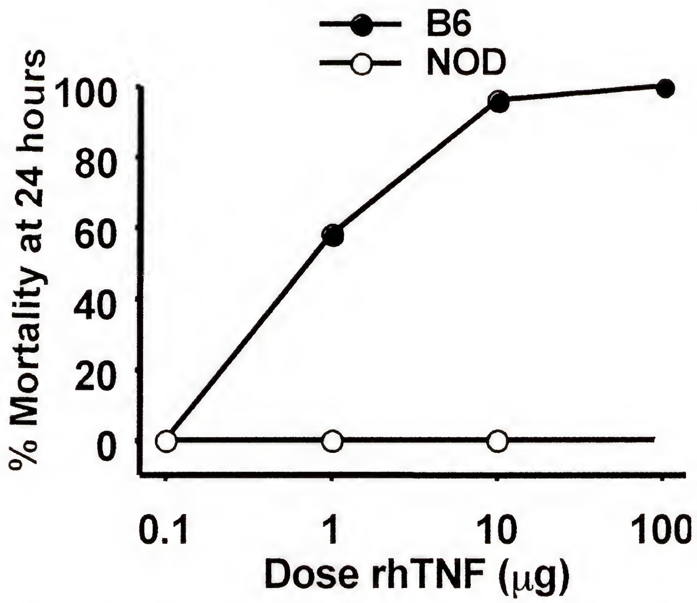

Figure 2-5 -Survival Responses to Increasing Doses of Recombinant Human Tumor Necrosis Factora (rhTNFα) in D-GalN-Sensitized B6 and NOD Mice Values represent the percent mortality of between 11 and 55 mice per dose of rhTNFα at 24 hours. The differences in survival between NOD and B6 mice were highly significant (p<0.001 by c2 analysis.

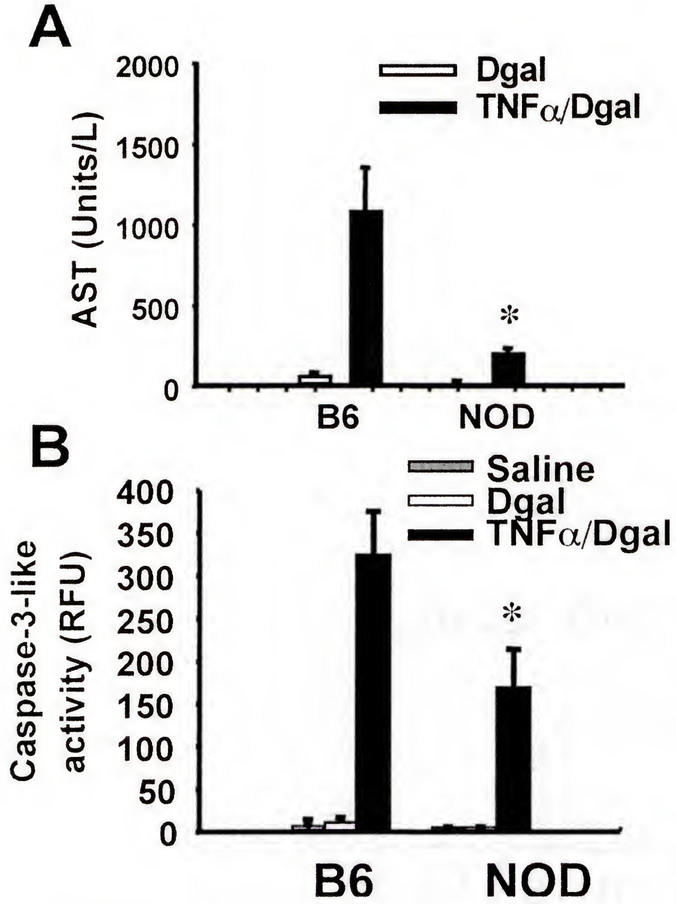

Figure 2-6 - Liver Caspase-3-Like Activity and Serum AST in B6 and NOD Mice Challenged with Saline, D-GalN and/or rhTNFα. Animals were bled and sacrificed at six hours post treatment with 10 mg rhTNFα and 8 mg D-GalN. Serum was evaluated for transaminase levels (AST)(A). Values represent the mean ± SEM of six animals per strain for treated and four animals per strain for D-GalN controls ($p<0.01$). Livers were immediately processed for caspase-3-like activity. Values represent the mean ± SEM of 26 animals per group ($p<0.05$).

Flow Cytometric Analysis of p55 TNF Receptor in NOD and B6 Mice

One possible explanation for the differential response between NOD and B6 mice may be the inability of recombinant human TNFα to bind to the p55 TNF receptor on NOD cells. To directly evaluate this question, binding of biotinylated-rhTNFα to NOD and B6 splenocytes was analyzed using a FITC-conjugated streptavidin secondary label followed by flow cytometric analysis. Figure 2-8 clearly shows comparable binding of rhTNFα to CD3 and 7-AAD double-negative splenocytes from NOD and B6 mice (mean fluorescence intensity (MFI) = 74.99 and MFI = 100.00, respectively). This binding was effectively blocked using a 100 molar excess of unlabeled rhTNFα. No significant differences in binding of biotinylated rhTNFα were seen in various cell populations examined in other studies, including CD4+ splenocytes or peritoneal macrophages (data not shown).

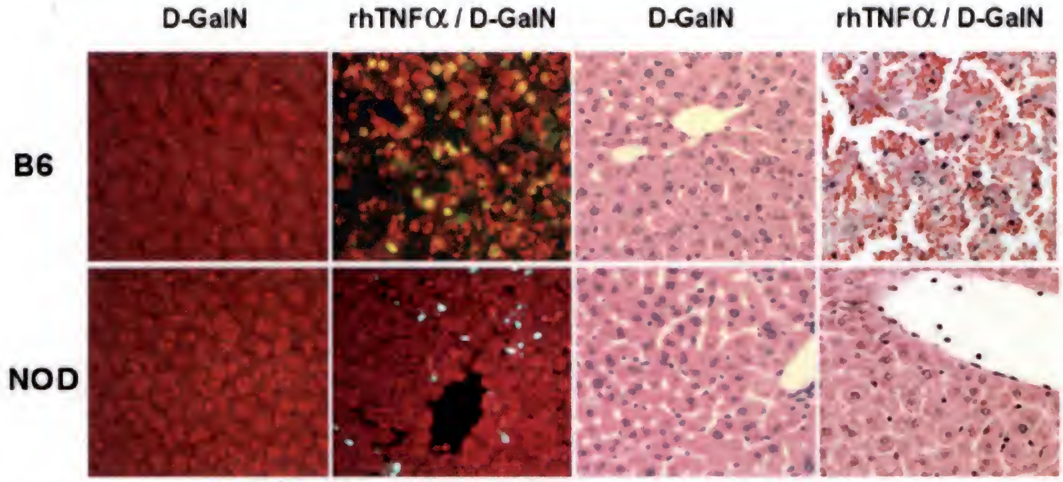

Figure 2-7. Histopathologic Analysis of In situ TUNEL (top row) and Hematoxylin and Eosin stained livers (bottom row) from rhTNFα and D-GalN Treated C57BL/6 and NOD Mice. Data presented are representative of 3 independent experiments.

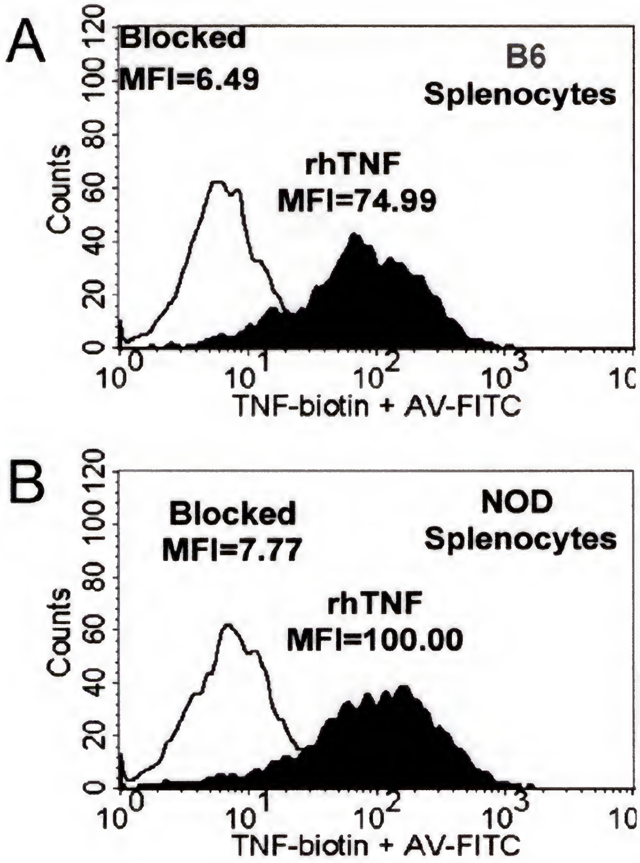

Figure 2-8 Flow Cytometric Determination of Recombinant Human TNFα Binding to B6 and NOD Splenocytes. Binding of recombinant human TNFα to CD3-, 7-aad- splenocytes were performed as described in the Analytical Methods section using flow cytometric analysis. Specific staining of viable (7-aad-), non-CD3+ splenocytes was evaluated on at least 10,000 events. These data are a representative analysis of three independent experiments. The open peak represents the blocked or competed sample (excess unlabeled TNFα added) and the dark peaks represent the labeled sample. Mean channel fluorescence (MFI) for splenocytes from NOD and B6 mice were similar with the NOD always greater than the B6, and could be equivalently competed with excess unlabeled TNFα.

Jo-2-induced Hepatic Injury and Lethality in B6 and NOD Mice

Due to the sensitivity of hepatocytes to Fas-mediated death, another well-described model of liver injury utilizes an agonist antibody, Jo-2. Several investigators have demonstrated that activation of the Fas signaling pathway by the agonist Jo-2 or FasL (Fas ligand) leads to rapid activation of caspase-3 in the liver (Rodriguez et al. 1996), subsequent hepatocyte apoptosis, liver failure and death (Ogasawara et al. 1993; Enari et al. 1995; Kondo et al. 1997). Jo-2 binds the Fas receptor resulting in a cell death pathway similar, but not identical to the TNF receptor death pathway (Hatano et al. 2000). Since the Fas and TNF receptor pathways share both common and uncommon intermediates (Wong and Goeddel 1994; Enari et al. 1996) assessing sensitivity to both rhTNFα and a Fas-agonist would provide information about the functional differences in p55 TNF and Fas/FasL signaling in the NOD mouse. For example, should the Fas pathway be functional in the NOD mouse, then efforts to examine known signaling molecules will be focused on those intermediates specific for the p55 TNF receptor signaling pathway. Because the p55 TNF receptor shares with Fas (Apo1, CD95) an

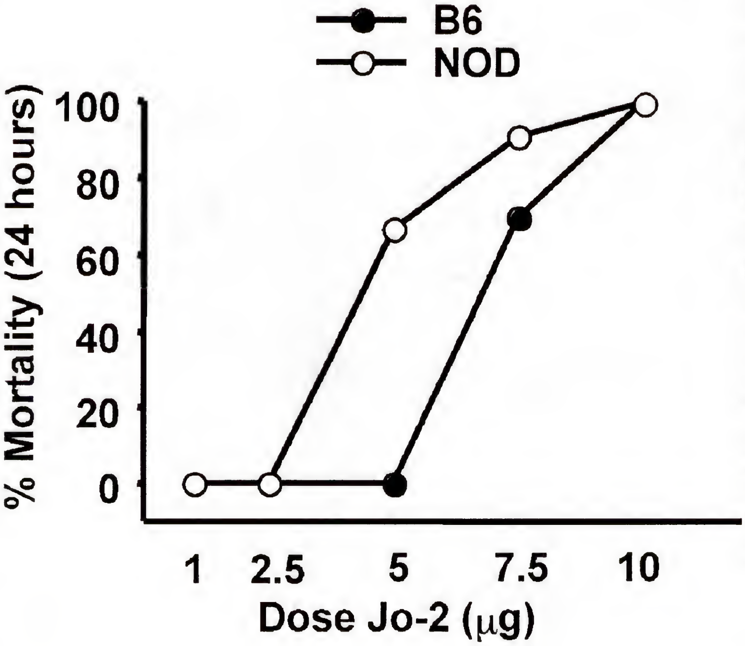

Figure 2-9 - Survival Responses to Increasing Doses of a Fas Agonist (Jo-2) in B6 and NOD Mice. Values represent the percent mortality of between six and 16 mice per group at 24 hours. Although there was no overall differences in survival between B6 and NOD mice, mortality tended to be worse in NOD mice, especially at the intermediate doses (5 μg).

intracellular signaling pathway that converges at the level of Fas-associated protein with death domain (FADD) and caspase-8, the responsiveness of NOD mice to a Fas agonist was examined. NOD and B6 mice were challenged with increasing doses (1–10μg) of the Fas agonist Ab (Jo-2) known to induce hepatocyte apoptosis and death (Ogasawara et al. 1993; Lawson et al. 1999). Both NOD and B6 mice were sensitive to the lethal effects of Jo-2. In fact, NOD mice appeared to be more sensitive to the lethal effects than B6 mice, although this difference did not reach statistical significance (note that the x-axis on Figure 2-9 is a linear scale, whereas the x-axis in Figures 2-1 and 2-5 are logarithmic scales). With a dose of 10μg Jo-2 Ab, mice had to be sacrificed at 3 hours, because death occurred in both groups between four and eight hours. At three hours, serum transaminase levels (Figure 2-10A) capase-3-like activity (Figure 2-10B), and

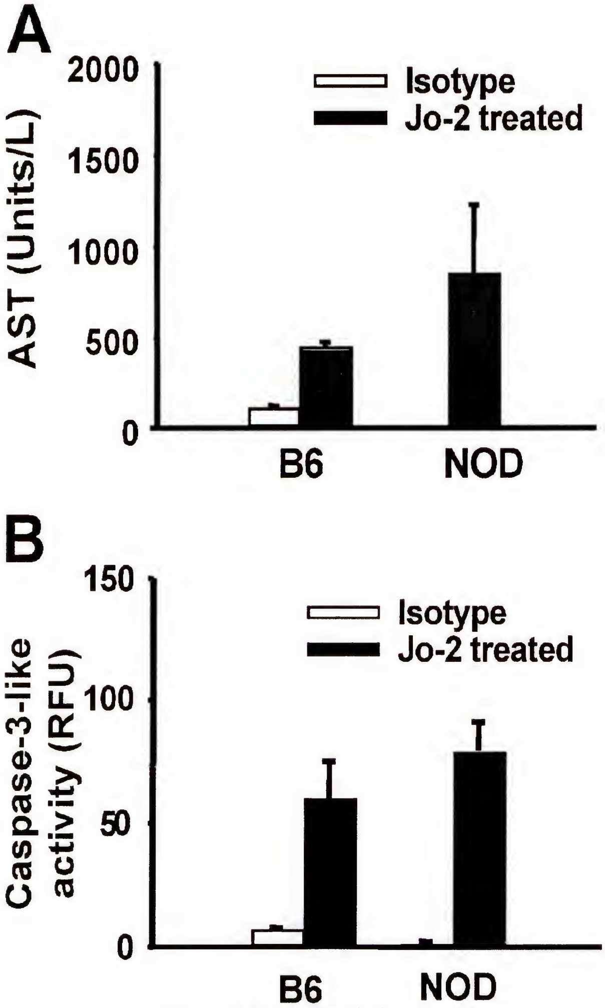

Figure 2-10: Caspase-3-Like Activity and Serum AST levels in B6 and NOD Mice Treated with a Fas Agonist (Jo-2). Animals were bled and sacrificed at 3 hours, just prior to onset of death. Serum was evaluated for transaminase levels (AST)(A). Values represent the mean ± SEM of six animals per strain for treated and four animals per strain for D-GalN controls (p=0.308). Liver caspase-3-like activity was also determined (B). Values represent the mean of twelve animals per group. There was no difference in the caspase-3-like activity between B6 and NOD mice following injection with Jo-2 (p=0.326).

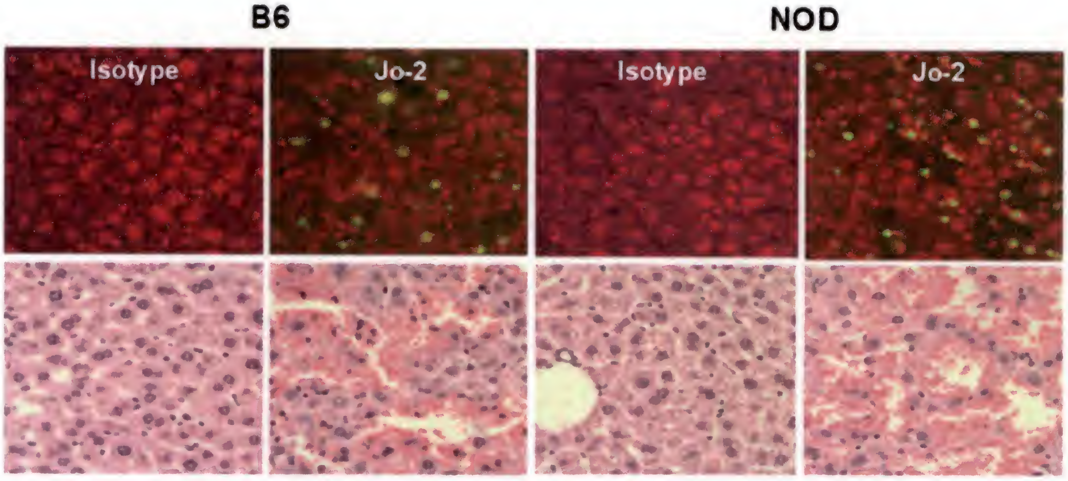

Figure 2-11. Histopathologic Analysis of In situ TUNEL (top row) and Hematoxylin and Eosin stained livers (bottom row) from Anti-Fas (Jo-2) Treated B6 and NOD Mice. Data presented are representative of 3 independent experiments.

histologic evidence of apoptotic liver injury (Figure 2-11) were similar in both NOD and B6 mice.

In vitro Hepatocyte Response to rhTNFα and D-GalN Treatment

To determine whether the differences in sensitivity to rhTNFα/ D-GalN treatment between the B6 and NOD mice were due to differences in hepatocyte responsiveness, primary hepatocytes were isolated and cultured in the presence of rhTNFα and D-GalN. Hepatocytes were examined for survival and caspase-3-like activity. NOD hepatocytes were less sensitive to the toxic effects of rhTNFα/D-GalN when compared with B6 hepatocytes at doses of 1, 2.5 and 5 mM D-GalN with rhTNFα ($p<0.01$). However, no difference was seen between the two strains at a dose of 0.1mM D-GalN with rhTNFα treatment ($p=0.621$). (Figure 2-12A). In addition, caspase-3-like activity was also increased in the B6 hepatocytes and was significantly higher than caspase-3-like activity levels from the NOD mice when incubated at doses of 2.5 and 5mM D-GalN with 1μg per ml of rhTNFα. (Figure 2-12B).

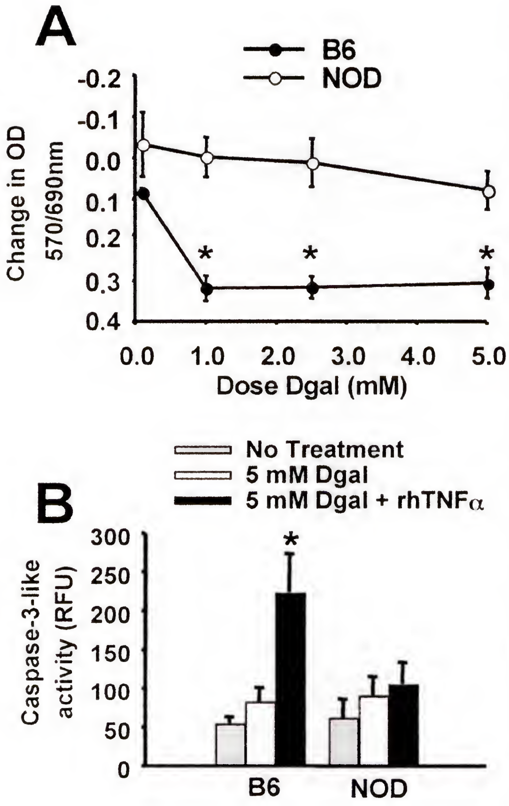

Figure 2-12. Cytotoxicity and Caspase-3-Like Activity in Primary Hepatocytes from B6 and NOD Mice Treated In vitro with D-GalN and/or rhTNFα.. Primary hepatocytes from NOD and B6 mice were left untreated or treated with the indicated doses of D-GalN with or without 1 μg per mL of rhTNFα per 500,000 cells. MTT cytotoxicity assays were performed on cells following a 20 hour incubation (A) Values represent the change in OD measured at 570/690nm between the D-GalN/rhTNFα treated and D-GalN alone treated samples (Change in OD = OD of D-GalN/rhTNFα treated – OD of D-GalN treated). Also the values represent the mean change ± SEM of eight sample wells from a single representative experiment. OD values ranged from 1.1 to 0.6 with the untreated samples not being significantly different from the D-GalN treated samples (data not shown). In addition, caspase-3-like activity assays were performed following a 6 hour incubation in order to determine the degree of apoptosis induced by D-GalN and rhTNFα treatment (B) Values represent the mean ± SEM of three independent experiments per strain per treatment. Hepatocytes were left untreated or treated with 5 mM D-GalN with or without rhTNFα.

In vitro Hepatocyte Response to Jo-2 Treatment

The responsiveness of B6 and NOD hepatocytes to a Fas agonist was also examined. Hepatocytes from NOD and B6 mice were isolated and cultured in the presence of 1 μg/ml Jo-2 Ab or isotype control. As shown in Figure 2-13, no difference in sensitivity to Jo-2 was seen in hepatocytes from either strain of mice treated in vitro determined by cell survival and caspase-3-like activity.

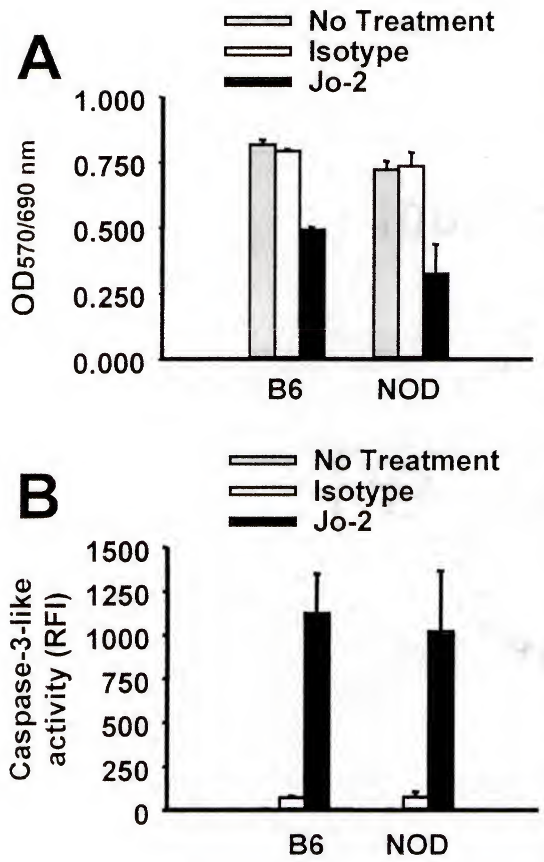

Figure 2-13 Cytotoxicity and Caspase-3-Like Activity Determination in In vitro Primary Hepatocytes from B6 and NOD Mice Treated with a Fas Agonist Antibody (Jo-2). Hepatocytes from NOD and B6 mice were either untreated or treated with isotype control antibody or Jo-2 at a concentration of 1 μg per mL per 500,000. MTT cytotoxicity assays were performed on cells following a 20 hour incubation (A). Values represent the mean ± SEM of eight sample wells per treatment from one representative experiment. No significant difference in Jo-2-induced toxicity was seen between NOD and B6 hepatocytes ($p=0.307$). Caspase-3-like activity assays were performed on cells following a 6 hour incubation (B) Values represent the mean ± SEM of three independent experiments per strain per treatment. No difference was seen in the caspase-3-like activity between B6 and NOD hepatocytes following treatment with Jo-2 ($p=0.992$)

Discussion

The present study documents for the first time the observation that NOD mice sensitized with D-GalN are resistant to the lethal effects of LPS and rhTNFα. This resistance appears to be due to a postreceptor defect in TNFα signaling through the p55 TNF receptor. LPS and D-GalN administration produces a primarily TNFα-dependent model of fulminant hepatocellular apoptotic injury and lethality, unlike the shock and necrotic liver injury found in high dose LPS models (Tiegs et al. 1989; Galanos and Freudenberg 1993; Bohlinger et al. 1996). In fact, high dose LPS-induced lethality was mechanistically different from the models using sensitization with transcriptional inhibitors (Mignon et al. 1999). Lethality from LPS and D-GalN treatment is secondary to caspase-3-mediated apoptotic liver injury, as demonstrated by the ability of synthetic caspase inhibitors to block the apoptosis and lethality seen in mice treated with LPS and D-GalN (Bohlinger et al. 1996; Mignon et al. 1999). However, these inhibitors do not prevent lethality to high dose LPS, nor do they block the early inflammatory responses to LPS and D-GalN treatment, indicating that toxicity in this model is independent of the systemic inflammatory response (Jaeschke et al. 1998; Mignon et al. 1999). Rothe et al. demonstrated that mice lacking a functional p55 TNF receptor were resistant to LPS only when sensitized with a transcriptional inhibitor like D-GalN (Rothe et al. 1993).

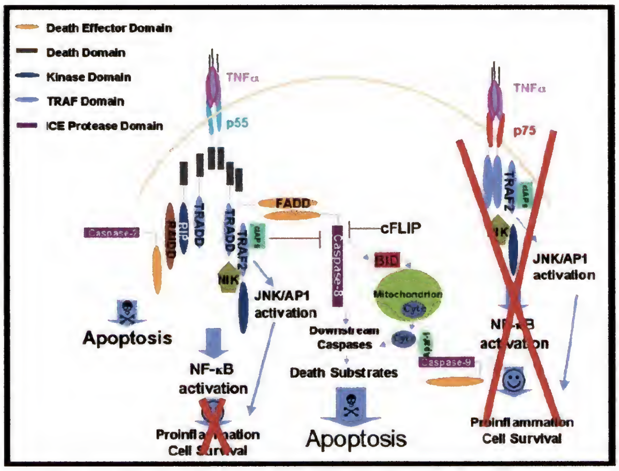
Death Effector Domain
Death Domain
Kinase Domain
TRAF Domain
ICE Protease Domain
TNFα
p55
TNFα
p75
FADD
cFLIP
Caspase-2
RAIDD
RIP
TRADD
TRADD
TRAF2
IAPs
NIK
JNK/AP1 activation
Caspase-8
BID
Mitochondrion
Cyt c
Downstream Caspases
Cyt c
Apaf-1
Caspase-9
Death Substrates
Apoptosis
NF-κB activation
Proinflammation Cell Survival
Apoptosis
TRAF2
IAPs
NIK
JNK/AP1 activation
NF-κB activation
Proinflammation Cell Survival

Figure 2-14: Effect of rhTNFα and D-galactosamine Treatment Upon TNF Signaling in the Murine D-GalN Model of Hepatocellular Apoptosis and Lethality.

It has also been shown that the p55 and not the p75 TNF receptor is necessary and sufficient for TNFα-mediated hepatic apoptotic injury and lethality in this model (Nowak et al. 2000). Conversely, Morikawa et al. observed that lpr mice lacking a functional CD95/Fas were not protected from LPS and D-GalN induced injury or lethality, indicating that the presence of Fas/FasL signaling is not required (Morikawa et al. 1996).

There are several advantages to the model system we have chosen to employ. The use of rhTNFα in this study allows for the specific targeting of the p55 TNF receptor in the mouse, due to the specificity of rhTNFα for the mouse p55 TNF receptor (see figure 2-14) (Smith et al. 1986; Brouckaert, P.G. et al. 1989; Brouckaert, P. et al. 1992). When administered along with D-GalN, rhTNFα binding to the p55 TNF receptor results primarily in activation of the death pathway. The reason for the dominance of the death pathway in this model is due to the partial inhibition of the transcription of NF-kB-dependent 'survival genes', which are necessary for the inhibition of the cell death program in hepatocytes (see figure 2-14) (Xu et al. 1998). In addition, by using rhTNFα, we have eliminated the effects of genetic differences in TNFα produced in response to LPS that may or may not exist between the two strains of mice.

These studies with rhTNFα, however, cannot localize the specific defect or defects in the TNF signal transduction pathway necessary to explain the resistance in NOD mice. The defect appears to be a post-receptor event, because binding of rhTNFα to NOD splenocytes appeared normal. Furthermore, because levels of caspase-3-like activity in the livers of NOD mice treated with LPS or rhTNFα and D-GalN were markedly reduced, but not absent, the findings would be consistent with a defect in apoptosis signaling distal to TNFα binding to the p55 TNF receptor, but perhaps proximal to or at the level of activation of caspase-3. These data indicate that the ability of NOD mice to signal via the p55 TNF receptor is not completely absent, in that some increased caspase-3-like activity is apparent even though the animals survived.

However, an unexpected observation was that although NOD mice were resistant to lethality and hepatocyte injury induced by p55 TNF signaling, the animals were sensitive to Fas-mediated lethality and hepatocyte injury. The onset of injury and lethality in NOD and B6 mice treated with Jo-2 were similar, indicating that the Fas pathway was functional in NOD mice. Fas-induced cell death is thought to occur more directly than p55-induced death due to the simultaneous activation of NF-B and other antiapoptotic proteins that inhibit the p55 TNF receptor death pathway (Hsu et al. 1996).

Additionally, we have shown that primary hepatocytes isolated from NOD mice are less sensitive to in vitro rhTNFα and D-GalN-induced apoptosis and toxicity than are B6 hepatocytes, indicating that hepatocytes from NOD mice are indeed resistant to this treatment. Also, NOD hepatocytes isolated and cultured in vitro were equally sensitive to Jo-2 when compared with B6 mice, confirming the absence of a defect in the Fas signaling pathway in hepatocytes from NOD mice. The differential sensitivity to TNFα and Fas agonists in NOD mice may, however, allow for identification of potential defects in the p55 TNF receptor signaling pathway which explain resistance in NOD mice.

The p55 and Fas death receptors both contain an intracellular death domain allowing for recruitment of death effector molecules and execution of the apoptotic cascade in the signaling cell. For example, the Fas pathway involves binding of the FADD to the death domains of the trimerized Fas receptors. This FADD adaptor protein contains a death effector domain at the N terminus that is responsible for the recruitment of caspase-8 to the death-induced signaling complex (Siegel and Fleisher 1999). Additionally, FADD has also been shown to bind to TNF receptor-associated protein with death domain (TRADD), a proximal mediator in the p55 TNF receptor signaling pathway, resulting in activation of caspases and other death effector molecules culminating in apoptotic cell death (Luo et al. 1998; Faubion and Gores 1999). Therefore, the adaptor protein FADD represents the convergence point of Fas and p55 TNF receptor pathways.

The current data indicate that the Fas pathway is functional in livers of NOD mice. Because FADD binds to both the Fas receptor and TRADD via the same death domain, the defect seen in the p55 TNF receptor signaling pathway of NOD mice is likely to be independent of intermediates common to the Fas pathway, but rather proximal to the convergence at FADD and caspase-8. The experimental data are therefore consistent with a defect in either the signaling capacity of the p55 TNF receptor or the ability of its death domain to form a signaling complex with TRADD, FADD, RIP or other intracellular signaling molecules. An alternative explanation for the reduced apoptotic injury in hepatocytes from NOD mice treated with LPS or rhTNFα and D-GalN is that NF-B activation is increased, resulting in greater expression of NF-B-dependent "survival genes" (Schrum et al. 2000). This appears to be less likely, because preliminary evidence indicates no increase in nuclear NF-kB translocation in livers from NOD mice treated with LPS and D-GalN, as determined by electromobility shift assay (data not shown).

Future investigations need to examine the structure and functional relationships in the p55 TNF death-induced signaling complex as a potential site for the lack of responsiveness in NOD mice. One difficulty in examining these pathways is that although TRADD-FADD and p55-TRADD complexes were found by Hsu et al. to be very stable, the trimer of p55-TRADD-FADD was thought to be only transient and unstable without other proteins such as TNF receptor-associated factors being present (Hsu et al. 1996). In addition, although they are members of the same superfamily of molecules, Fas and p55 TNF receptors have both shared and unshared signaling mechanisms. Historically, the molecular events activated by these receptors are in dispute because the analytical techniques used to acquire this information largely involve artificial systems. Therefore, apoptosis via p55 and Fas receptors occurs through a complex set of molecular events with transient unstable intermediates, making it difficult to determine where the defect, when present, may lie.

The observation, however, that NOD mice are resistant to the hepatocyte injury and lethality associated with p55 TNF receptor signaling has significant implications for other p55 TNF receptor-dependent processes, such as apoptosis of lymphoid cell populations. Further studies are required to determine whether T and B cell populations from NOD mice are resistant to TNFα-mediated apoptosis.

CHAPTER 3
GENETIC ANALYSIS OF NOD RESISTANCE TO TNFα-MEDIATED LIVER INJURY AND LETHALITY

Introduction

A common experimental approach to identify in vivo the key mediators involved in the TNFα signaling pathway has been to create and employ transgenic murine models with a known genotypic alteration. Such an approach has been most commonly employed with transgenic or knockout mice, overexpressing or deficient in a signaling intermediate. Much of what we have learned about the role of TNFα receptor signaling in LPS and TNFα mediated lethality has come from these studies using TNF receptor knockout or transgenic mice, or mice with knockouts in signaling intermediates. This approach has several limitations, the most obvious being that it is based on prior knowledge of the signaling pathway, and it is obviously limited to genes and genetic loci that are already presumed to contribute to the phenotypic response being studied.

Much less frequently, however, inbred strains with varying degrees of responsiveness have been employed to identify potentially new intermediates in the signaling pathway. This approach is much more exploratory, and requires fewer preconceptions regarding the contribution of known signaling intermediates; however, it does require the presence of two inbred strains with widely divergent phenotyptes. Fortunately, we have made the novel observation that the NOD mouse strain when sensitized with D-GalN are highly resistant to both LPS and rhTNFα-induced liver injury compared to B6 mice. These data provided both a model system to investigate dysregulated apoptotic signaling in the liver, and two strains of mice with uniquely divergent phenotypes. Therefore, detailed phenotypic analysis of the NOD, B6, and (NODxB6)F1 mice, as well as a quantitative trait loci analysis of NOD and B6 recombinant mice should provide novel genetic loci or candidate genes involved in rhTNFα and D-GalN-mediated apoptosis and lethality.

In order to perform a QTL analysis of hepatocellular apoptosis and lethality using the resistant NOD and susceptible B6 mouse, it was necessary to extensively characterize the phenotypes of the parental strains. These data provided the reference to which the (NODxB6)F1 heterozygotes, NOD x (NODxB6)F1 backcross progeny, and congenic mice were compared. Since the actions of rhTNFα in this model produce hepatocyte apoptosis followed by wide-spread necrosis, the three phenotypic parameters we chose to characterize were the degree of apoptosis (as assessed by liver caspase-3-like activity assays), the extent of the proinflammatory response (as assessed by serum IL-6 concentration), and serum AST levels (as an indicator of liver injury). In situ TUNEL was also assessed on the parental strains and F1 heterozygotes; however, it was determined to be too labor intensive to utilize as a phenotype for QTL analysis. In addition to these three phenotypes, a separate analysis was conducted using mortality as the trait of interest. Mortality was chosen as a phenotype both because of its clinical significance as well as its statistical power (alive versus dead) which would further increase the likelihood of identifying specific regions in the B6 and NOD mouse genomes conferring sensitivity or resistance to rhTNFα-mediated hepatocellular apoptosis and lethality.

Materials and Methods

Animal Experimental Protocols

Female B6, NOD, (NODxB6)F1 heterozygotes, B6.NOD congenic, and F1xNOD backcross mice between five and eight weeks of age were obtained from The Jackson Laboratory (Bar Harbor, ME) or from the Department of Pathology Animal Facility, University of Florida College of Medicine. NOD and B6 mice bred at the University of Florida were derived from breeding stock obtained from The Jackson Laboratory. All care, housing, and breeding were performed by the Pathology Animal Facility or Animal Resources at the University of Florida. All animal treatment protocols were approved by the Institutional Animal Care and Use Committee of the University of Florida College of Medicine.

Mice were treated with 10 mg rhTNFα and 8 mg D-GalN, a dose that was previously determined to produce uniform lethality in the B6 mouse, while producing no mortality in NOD mice. Individually, mice were phenotyped using mortality as an outcome variable for the first group of backcross progeny. The second group of backcross progeny were treated in the same manner, but sacrificed at 5 hours and serum and tissues collected and measured for caspase-3-like activity, serum IL-6 levels, and serum AST levels as described previously in Chapter 2.

IL-6 ELISA

IL-6 was measured using an ELISA kit and commercial reagents. The murine IL-6 Minikit™ (Endogen, Rockford, IL) was used according to manufacturers instructions. All statistical analyses were performed using a one-way ANOVA with a Tukey post-hoc test.

Serum AST Assays

Serum AST levels were determined using the method described in the Materials and Methods section in chapter 2 of this manuscript.

Caspase-3-like Activity Determination and the Use of DNA Quantitation for Data Adjustment

Caspase-3-like activity was determined as described previously in Chapter 2; however, data were reported following normalization for liver DNA content (referred to as caspase-3 (DNA)). We hypothesized that hepatic congestion and increases in blood infiltrate into the livers of animals following TNFα and D-GalN treatment may lead to an underestimation of caspase-3-like activity levels since these animals have enlarged livers and a larger proportion of protein derived not from parenchymal cells, but from blood congestion. In this case, caspase-3-like activity levels in the whole tissue may underestimate activity present in hepatocytes. . Since the activity was traditionally normalized based on total protein content in the liver, this data (referred to as caspase-3 (protein)) was also used in the subsequent QTL analysis for comparison with the caspase-3-like activity normalized for DNA content. All statistical analyses were performed using a one-way ANOVA with a Tukey post-hoc test.

Genotypic Analyses

Genomic DNA was isolated from tail snips or tissues using a commercial DNeasy™ kit from Qiagen, Inc. Over 70 microsatellite primer pairs polymorphic between NOD and B6 spanning the entire mouse genome (Yui et al. 1996) were purchased as Mappairs™ from Research Genetics, Inc. (Huntsville, Al.) and the experimental procedures employed were standard PCR reactions using commercially available reagents, as described below. Very briefly, genomic DNA (100 ng) was amplified in 20 μL reactions with 200 nM of each primer and appropriate amount of Qiagen Taq PCR Master Mix™ Kit reagent as described by the manufacturer. PCR was performed using a Hybaid PCR Express or a Perkin-Elmer Cetus 9600 thermal cycler. The optimal temperature and times for the primer pairs were outlined in the Mappairs™ instructions. Specifically, the PCR cycling conditions were as follows: Initial denaturation at 95°C for two minutes, 34 cycles of 95°C for 30 seconds , 57°C for 30 seconds, and 72°C for one minute. Final extension was carried out at 72°C for ten minutes. All loci had a predicted size difference between B6 and NOD alleles of greater than 10 bp, thus PCR products were visualized on 5% agarose gels stained with ethidium bromide.

QTL Analysis Strategy and Data Analyses with Map Manager QTX™

The analysis to identify QTL involved in the resistance of NOD mice was divided into stages. At the first stage, an initial mortality analysis was performed using data from 149 NODx(NODxB6)F1 recombinant progeny which were observed for mortality in response to 10 mg rhTNFα and 8 mg D-GalN treatment. These animals were then genotyped at 70 loci spaced across the genome (markers used in the initial genome scan are outlined in figure 3-5) and the segregation patterns of marker loci were analyzed in all female NODx(NODxB6)F1 (or BC1) progeny using Map Manager QTX™ software available at http://mapmgr.roswellpark.org/mmQTX.html (Manly and Olson 1999; Manly et al. 2001). At the second stage, all markers on chromosomes revealing suggestive loci in stage one (chromosomes 11, 8, and 13), along with additional markers on those chromosomes, were used to genotype a second set of animals (marker maps presented in figures 3-5 and 3-7). The final mortality analysis included data from 294 NOD x (NODxB6)F1 recombinant progeny. The third stage of the QTL analysis involved a separate set of mice that were treated with 10 mg rhTNFα and 8 mg D-GalN and sacrificed at 5 hours. The livers from each recombinant mouse were harvested for caspase-3-like activity assays and preparation of genomic DNA for genotyping. In addition, serum was harvested and analyzed for IL-6 and AST levels. Also, control mice (NOD, B6, and F1) were assayed with each independent experiment. Markers used for AST, IL-6 and caspase-3 QTL analysis are also outlined in figure 3-5 and 3-7.

Two different statistical approaches were used in the QTL data analysis- marker regression analysis and interval mapping. Marker regression analysis is convenient and rapid since it only tests the association of trait values with the genotypes of single marker loci, while interval mapping simultaneously tests for the presence of a QTL and estimates the position between two marker loci giving a curve indicative of the predicted LRS scores at all positions (Broman 2001). The probability of linkage of the mortality phenotype with marker genotype in the interval mapping analysis was estimated at 1cM (centiMorgan) intervals for all recombinant mice. Both simple interval mapping and composite interval mapping were performed, the difference being that composite interval mapping allows for the inclusion of background loci. When more than one QTL appear to contribute to a phenotype, they can be evaluated individually by adding the most significant QTL to a trait-specific background list and these background loci control the effects of nearby QTL in subsequent interval mapping analyses (Manly and Olson 1999).

Marker regression and interval mapping were performed using Map Manager QTX™ by scoring all affected mice as zero and all unaffected mice as one. In addition, continuous variables (caspase-3-like activity, IL-6 levels, and AST levels) were also analyzed with Map Manager QTX™ using 138 NOD x (NODxB6)F1 recombinant progeny. The Map Manager QTX™ statistical analysis program is advantageous because it permits the introduction of continuous variables (caspase-3-like activity, IL-6 and AST levels) thus eliminating the statistical difficulties with converting continuous variables to dichotomous measurements, and the loss of information that invariably results.

Given the large number of tests involved in genome-wide analysis, even a highly significant association between phenotypes and genotypes can occur simply by chance; therefore, it is essential to estimate the probabilities of attaining a particular linkage statistic by chance in order to establish threshold values that are indeed likely to be significant. The method used by Map Manager QTX™ to establish a genome-wide significance is called the permutation test and was developed by Doerge and Churchill in 1996 (Doerge and Churchill 1996). A permutation test estimates an empirical genome-wide probability for observing a given LRS score by chance by randomization of the phenotypes while simultaneously keeping the genotypes constant followed by simple interval mapping (Doerge and Churchill 1996). Interval mapping was performed for each chromosome of interest and permutation tests were conducted using at least 1000 permutations to establish critical values for significant associations, according to the guidelines of Lander and Kruglyak (Lander and Kruglyak 1995).

A suggestive LRS score corresponds to a genome-wide Type 1 error probability of 0.63 or that which would result in an average of one false positive per genome scan. A significant LRS score corresponds to a genome-wide Type 1 error probability of 0.05, which is the commonly accepted significance level and permits the detection of QTL with a moderate effect given that the number of animals analyzed is sufficient. The highly significant LRS score corresponds to a $p<0.001$, which would indicate a very strong QTL (meaning that it explains over 20% of the total variance seen in the trait)(Manly and Olson 1999). Also, the Kosambi mapping function was used in all analyses, which is one of the most widely used mapping functions since these equations fit the results observed in various species. Mapping functions act to correct for the nonadditive recombination fractions or crossover interference (Manly and Olson 1999).

TRADD Sequencing

TRADD mRNA sequencing was performed using NOD and B6 liver tissue to isolate total RNA using the RNeasy™ kit (Qiagen) according to the manufacturer's instructions. Total RNA (1mg) was used for RT-PCR using a poly(T)-plus primer in a total volume of 20ml. The RT-PCR reaction was incubated with reverse transcriptase for 60 minutes at 42°C and the reaction was stopped by heating to 95°C for ten minutes. Twenty microliters of the cDNA was used as template for a subsequent PCR in a total volume of 50ml. PCR cycling conditions were as follows: Initial denaturation at 95°C for two minutes, 34 cycles of 95°C for 30 seconds, 57°C for 30 seconds and 72°C for one minute, followed by a final extension for ten minutes at 72°C. The PCR reactions were gel purified on a 2% agarose gel and excised. PCR product was then extracted from gel pieces using a Gel Purification Kit™ (Qiagen) according to the manufacturer's instructions. Optical densities (OD) of the products were taken in order to ensure a concentration of 30ng/ml was used in the sequencing reaction. Samples were submitted to the DNA Sequencing Core Laboratory for sequencing (Center for Mammalian Genetics, University of Florida, Gainesville, FL). Primer sequences used are listed in Appendix B.

Results

Mortality, Liver Injury and Apoptosis in rhTNFα and D-GalN Treated (NOD x B6) F1 mice.

To determine if resistance to rhTNFα and D-GalN treatment was a dominant or recessive trait, (NODXB6)F1 heterozygous mice were treated and mortality assessed. F1 mice were sensitive to D-GalN and rhTNFα, and their phenotype was more closely related to the B6 parental strain (figure 3-1). At our chosen dose of 8 mg D-GalN and 10 μg of rhTNFα, 100% of the parental C57BL/6 (55/55), 80% of the (NODxB6)F1 (24/30) and 0% of the parental NOD (0/55) mice died. Neither saline nor D-GalN administration was associated with any increase in caspase-3-like activity, whereas D-GalN when administered along with rhTNFα induced a significant response in both strains of mice (figure 3-2B). However, the increases in capase-3-like activity in response to D-GalN and rhTNFα were markedly less in NOD than in B6 mice (p<0.05). However, F1 mice most closely resembled their B6 parents and no significant differences were seen between B6 and F1 mice in liver caspase-3-like activity. (figure 3-2B)

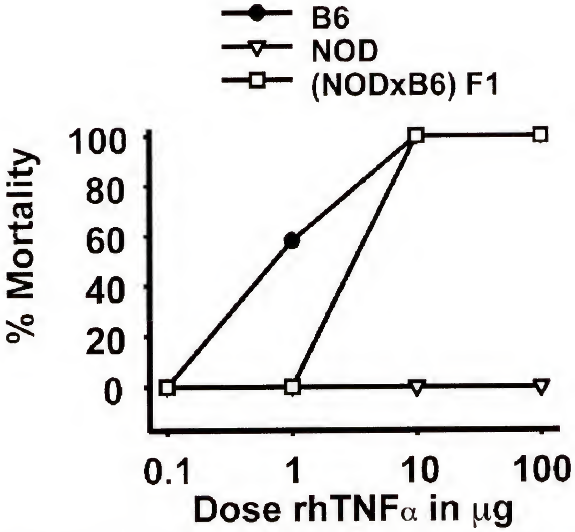

Figure 3-1. Survival Responses to Increasing Doses of rhTNF• in D-GalN-Sensitized B6, NOD and F1 Mice. Mice were challenged i.p. with 8 mg DGalN and increasing doses of rhTNF•. Survival was evaluated over the next 72 hours. Values represent the percent mortality of between 11 and 55 mice per dose of rhTNF• at 24 hours.

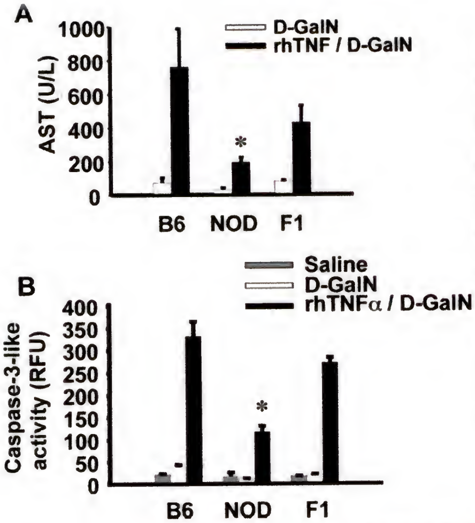

Figure 3-2. Liver Caspase-3-Like Activity and Serum AST in B6, NOD, and F1 Mice Challenged with Saline, D-GalN and/or rhTNF•. Animals were bled and sacrificed at five hours. Serum was evaluated for transaminase levels (AST)(A). Values represent the mean – SEM of six animals per strain for treated and four animals per strain for D-GalN controls. Livers were immediately processed for caspase-3-like activity. Values represent the mean – SEM of 26 animals per group.

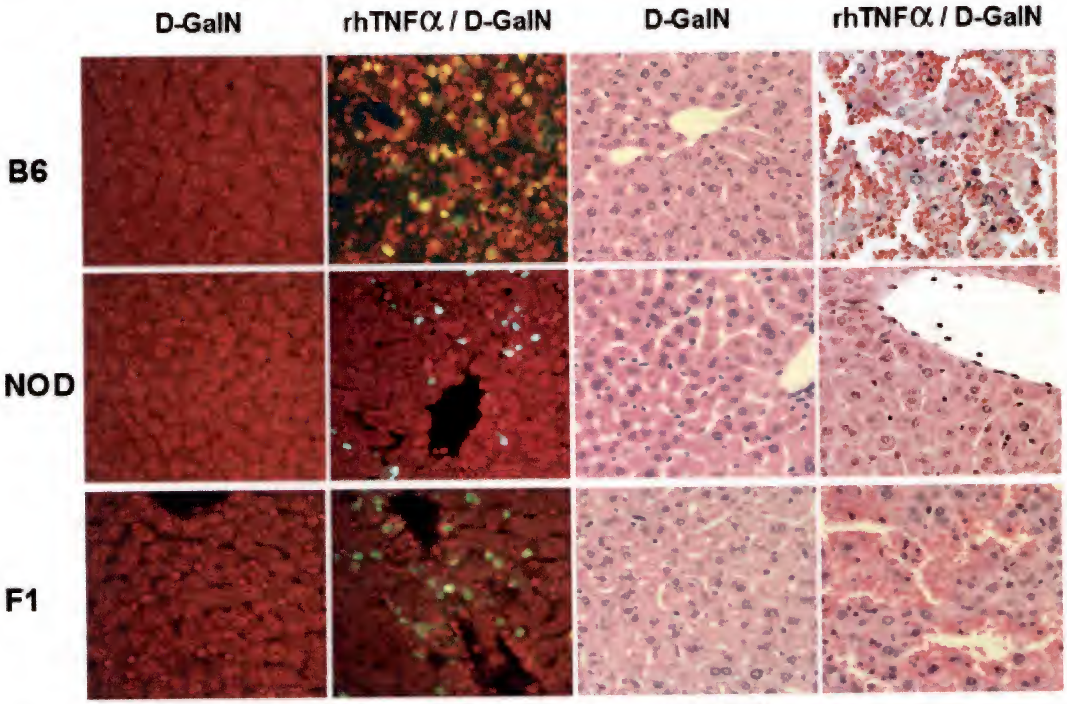

Figure 3-3. In situ TUNEL and Hematoxylin and Eosin (H&E) Staining Assay Results for Liver Tissue Sections from NOD, B6, and (NODxB6) F1 Mice. TUNEL results are depicted in the first two columns and H&E in the last two columns.

Additionally, serum AST levels (figure 3-2A) and TUNEL staining (figure 3-3) of F1 mouse livers were not significantly different from B6 mice. However, AST levels and TUNEL positive apoptotic cells were nearly always less in F1 mice than their B6 parentals. In contrast, serum AST levels and liver TUNEL staining of NOD mice were

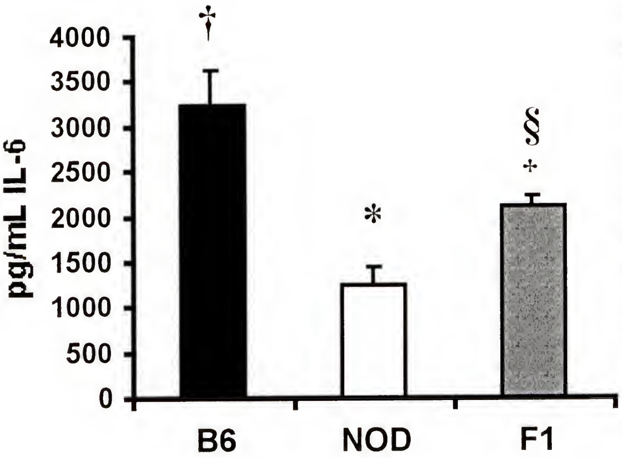

Figure 3-4. Serum IL-6 Levels from B6, NOD, and F1 Mice Treated with rhTNF• and DGalN. Mice were treated and bled at 5 hours for serum collection. ELISA for murine IL-6 levels was performed. Significantly higher levels of IL-6 was seen in serum from B6 and F1 mice compared to NOD (n=17 for all groups)
$* \ p < 0.001$ NOD vs. B6
§ $p = 0.004$ NOD vs. F1
† $p = 0.042$ B6 vs. F1

significantly lower than both B6 and F1 mice ($p<0.05$). These data suggest that F1 mice display an intermediate phenotype, which may also suggest that multiple genes are involved in the resistance of the NOD mouse.

IL-6 Response in NOD, B6 and F1 Mice after rhTNFα and D-GalN Treatment

An alternative explanation for the reduced apoptotic injury in hepatocytes from NOD mice treated with LPS or rhTNFα and D-GalN is that NF-κB activation is increased, resulting in greater expression of NF-κB dependent 'survival genes' (Schrum et al. 2000). Indirect evidence for a lack of increased NF-κB translocation is the serum IL-6 concentrations seen in NOD mice (figure 3-4). IL-6 is transcriptionally activated by the transcription factor NF-κB (Donnelly et al. 1993; Miyazawa et al. 1998); however, NOD mice treated with 10 mg rhTNFα and 8 mg D-GalN demonstrated significantly lower levels of IL-6 post-treatment when compared to both B6 an F1 mice ($p=0.001$ and $p=0.004$, respectively), which is not consistent with an increased NF-κB translocation.

rhTNFα and D-GalN -Induced Lethality in B6.NOD Congenic Mouse Strains

One of the strengths of these studies was the choice of the NOD mouse. Our intial studies revealed the SWR strain was also resistant to LPS and D-GalN-mediated lethality; however, for the many reasons outlined below, the NOD mouse was the strain chosen to perform these genome-wide analyses. Since its original development by Ohotori in

1966, the NOD mouse has been one of the most well studied strains to date, and the genetics of the NOD mouse has been well described (Leiter, E. and Atkinson 1998). Like many diseases, diabetes is a polygenic disease resulting from the complex interection of a multitude of genes. To date, congenic mapping of the NOD mouse has identified over twenty murine diabetogenic susceptibility loci (referred to as Idd loci) that have been mapped to several chromosomes in the mouse genome (Lyons and Wicker 1999; Hill et al. 2000; Lyons et al. 2000). While very few of the individual genes located within these diabetes susceptibility loci have been positively identified, studies using congenic mouse strains, in which genomic segments from the NOD mouse are introduced onto a control or diabetes resistant strain background, have provided researchers with valuable information regarding the involvement of these regions with various aspects of diabetes (Lyons et al. 2001).

The development of congenic strains of B6 mice at the University of Florida and The Jackson Laboratories provides a unique opportunity to rapidly assess known regions on the NOD and B6 genome for their ability to confer resistance or susceptibility in this model of rhTNFα-mediated hepatotoxicity. With congenic strains of mice obtained from the University of Florida Department of Pathology and the Jackson Laboratories, we have

Congenic Strain	**Idd locus**	**Size of Interval**	**% Mortality**
B6.NOD/c3	*Idd3, Idd10*	43	100
B6.NOD/c6	*Idd6*	24	100
B6.NOD/c11	*Idd4*	42	100
B6.NOD/c17	*Idd1*	19	100
B6.NOD/c1c	*Idd5*	44	100
B6.NOD/c1t	*Idd5*	47	100

Table 3-1. Results of TNFα and D-GalN-induced Mortality to in B6.NOD Congenic Mice.

evaluated lethality to D-GalN and rhTNFα treatment in six congenic B6 recipient strains of mice with NOD donor regions corresponding to known diabetes susceptibility loci (see (Yui et al. 1996) for congenic mouse chromosome maps)(see table 3-1).

All of the B6 congenic strains were sensitive to the lethal effects of D-GalN and rhTNFα, including the B6.NOD/c17 congenic mouse, which has regions of chromosome 17 from the NOD parental. This interval is especially interesting since it contains the NOD MHC loci, which is necessary, but not sufficient for expression of diabetes in the NOD mouse. This region also contains the TNF genes, thus these findings suggest that resistance to rhTNFα-mediated apoptosis in this model is not independently associated with any of the examined regions of the NOD genome previously shown to contribute to the development of diabetes. However, these loci in combination could still be involved in this rhTNFα resistance phenotype in the NOD mouse

Initial QTL Mapping of Mortality Trait

Recombinant progeny of a backcross between (NODxB6)F1 and NOD mice were treated with 10mg rhTNFα and 8 mg D-GalN and the phenotype of mortality was observed. Animals were monitored for 72 hours for mortality and tissues were then harvested for genotyping of the animals. Mortality studies of 149 female backcross progeny revealed an overall 46% mortality rate. Phenotypic and genotypic data from 149 recombinant progeny were analyzed for association using the Map Manager QTX™ software package.

QTL mapping methods include several levels of statistical analyses. The initial analyses are performed using marker regression or single-locus association where the significance of a trait association is determined for each marker individually. The major advantage of this method is its simplicity and also the marker loci do not have to be mapped relative to one another. This approach has several important weaknesses, however, including the lack of separate estimates of QTL location and effect (Broman

2001). In simple regression analysis, the only information derived about the potential location of a putative QTL is which markers give the greatest measure of association, thus, the ability to detect a QTL relies upon the choice of markers and whether those markers happen to be close enough to that QTL to give significant association values. Therefore, if the markers are widely spaced and density of coverage of the region is low, the QTL effect may be missed or radically underestimated in regression analysis. Another major disadvantage is that individuals with missing genotype data must be discarded (Broman 2001). Fortunately, there is another method of mapping developed by Lander and Botstein in 1989, referred to as interval mapping (Lander and Botstein 1989). This method posits each location, both at the marker loci and between adjacent markers, in the genome as the potential location of the QTL (Broman 2001). The advantages of interval mapping is that it produces data in the form of a curve that indicates the probability of a QTL at a location on the chromosome giving a better estimate of QTL location while providing improved estimates of QTL effect. In addition, Map Manager QTX™ also allows for composite interval mapping. When more than one QTL appears to be present, the marker nearest the QTL having the most significant association with the trait is set as a back-

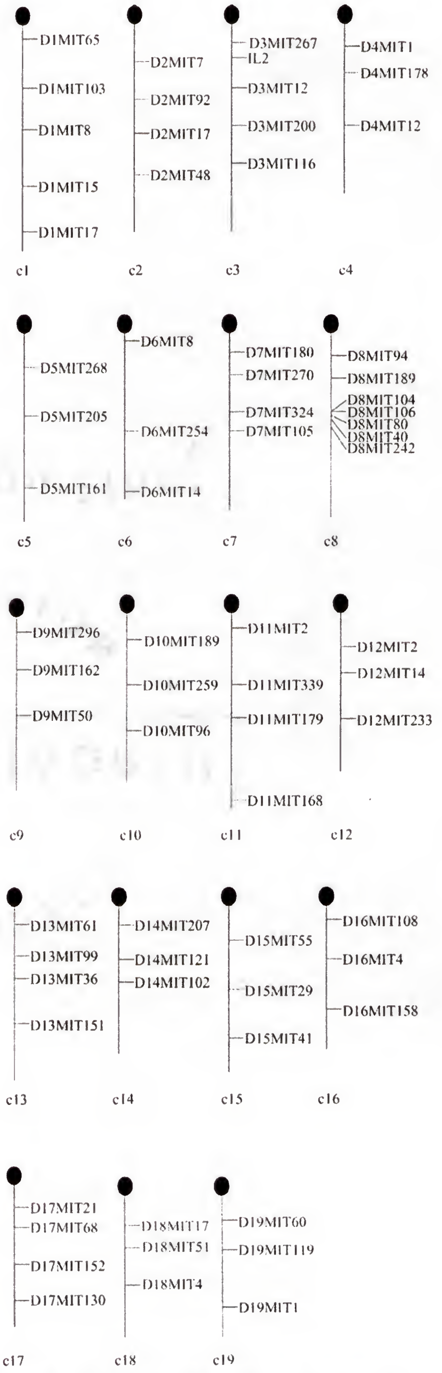
D1MIT65
D1MIT103
D1MIT8
D1MIT15
D1MIT17
c1
D2MIT7
D2MIT92
D2MIT17
D2MIT48
c2
D3MIT267
IL2
D3MIT12
D3MIT200
D3MIT116
c3
D4MIT1
D4MIT178
D4MIT12
c4
D5MIT268
D5MIT205
D5MIT161
c5
D6MIT8
D6MIT254
D6MIT14
c6
D7MIT180
D7MIT270
D7MIT324
D7MIT105
c7
D8MIT94
D8MIT189
D8MIT104
D8MIT106
D8MIT80
D8MIT40
D8MIT242
c8
D9MIT296
D9MIT162
D9MIT50
c9
D10MIT189
D10MIT259
D10MIT96
c10
D11MIT2
D11MIT339
D11MIT179
D11MIT168
c11
D12MIT2
D12MIT14
D12MIT233
c12
D13MIT61
D13MIT99
D13MIT36
D13MIT151
c13
D14MIT207
D14MIT121
D14MIT102
c14
D15MIT55
D15MIT29
D15MIT41
c15
D16MIT108
D16MIT4
D16MIT158
c16
D17MIT21
D17MIT68
D17MIT152
D17MIT130
c17
D18MIT17
D18MIT51
D18MIT4
c18
D19MIT60
D19MIT119
D19MIT1
c19

Figure 3-5. Polymorphic Markers used for Initial Mortality QTL Analysis

ground locus in order to control for the effect of that QTL upon other QTL in the analysis (Manly and Olson 1999; Manly et al. 2001). This allows for the evaluation of individual QTL without the effects of other nearby QTL thereby increasing the ability to detect discreet QTL on an individual chromosome. Background loci can also be used to control for unlinked QTL effects by selecting a single QTL having the highest LRS score from each chromosome except the one being mapped. This also allows for the evaluation of individual QTL without effects of other stronger QTL.

The significance of the trait association in both simple regression and interval mapping is tested using the likelihood ratio statistic (LRS) (Manly and Olson 1999). The LRS and the conventional LOD scores are essentially the same statistic differing only by a factor of 2ln(10) (Manly and Olson 1999). The LRS score is a reflection of the strength of evidence for the presence of a QTL at a given location.

Map Manager QTX™ uses the permutation test to establish levels of significance. This test calculates the maximum LRS across the entire genome given that there are no QTLs segregating by randomizing the phenotype data and keeping the genotype data intact (Broman 2001). Permutation test of the initial mortality data revealed that an LRS score of 6.1 was suggestive of linkage, an LRS score of 12.0 was significant, and an LRS score of 17.2 was highly significant. Map Manager QTX™ also calculates the percent of the trait variance that would be explained by a QTL at a particular locus. These values are calculated for markers in marker regression analysis and also for intervals between markers in the interval mapping analysis. Markers used for initial mortality analysis are outlined in figure 3-5.

Marker regression analysis revealed several suggestive loci on chromosomes 11, 13, and 8 (table 3-2). Subsequent simple interval mapping of chromosomes 8, 11, and 13 was performed and the data are shown in figure 3-6. The curves presented in all interval mapping figures correspond to the approximate distribution of the LRS for a given genomic position. The actual QT Links reports derived from Map Manager QTX™

marker regression analyses are presented in Appendix A along with the interval mapping reports for chromosomes 11, 13, and 8. Suggestive, significant, and highly significant values for each phenotype are indicated by the horizontal lines on the graphs in all interval mapping figures.

Marker regression analysis and simple interval mapping of chromosomes 8, 11, and 13 revealed similar marker associations with the mortality trait; however, interval mapping allows for the more precise localization of individual QTL. Marker regression analysis of chromosome 8 revealed a suggestive locus with a peak LRS of 6.1 at marker D8Mit80 that explained 3% of the total trait variance according to MapManager QTX™ and was associated with resistance to rhTNFα and D-GalN-mediated lethality (table 3-2). In addition, another suggestive locus on chromosome 11 with a peak LRS of 6.2 at marker D11Mit168, which explained 3% of the total trait variance, but was associated with susceptibility to rhTNFα and D-GalN-mediated lethality (table 3-2).

Table 3-2. Initial Mortality Marker Regression Analysis Results.

Locus	Position[1]	LRS[2]	p-value[3]	%[4]	Effect[5]
D8MIT104	38.3	6.1	0.01374	3	+
D8MIT106	39.3	5.1	0.02454	3	+
D8MIT80	41.5	5.4	0.02042	3	+
D11MIT2	4.4	4.4	0.03586	2	+
D11MIT168	75.4	6.2	0.01259	3	-
D13MIT61	7.7	5.9	0.01517	3	+

[1] Chromosome position in centimorgans (derived from MGI at www.informatics.jax.org).
[2] Likelihood ratio statistic for the association of the trait with this locus.
[3] p-value is the probability of an association this good happening by chance.
[4] Percent of the total trait variance which would be explained by a QTL at this location.
[5] Defined as +:resistance gene and -: susceptibility gene.

Subsequent interval mapping of chromosome 8 revealed a suggestive locus at marker D8Mit80 located at approximately 40cM associated with resistance to rhTNFα

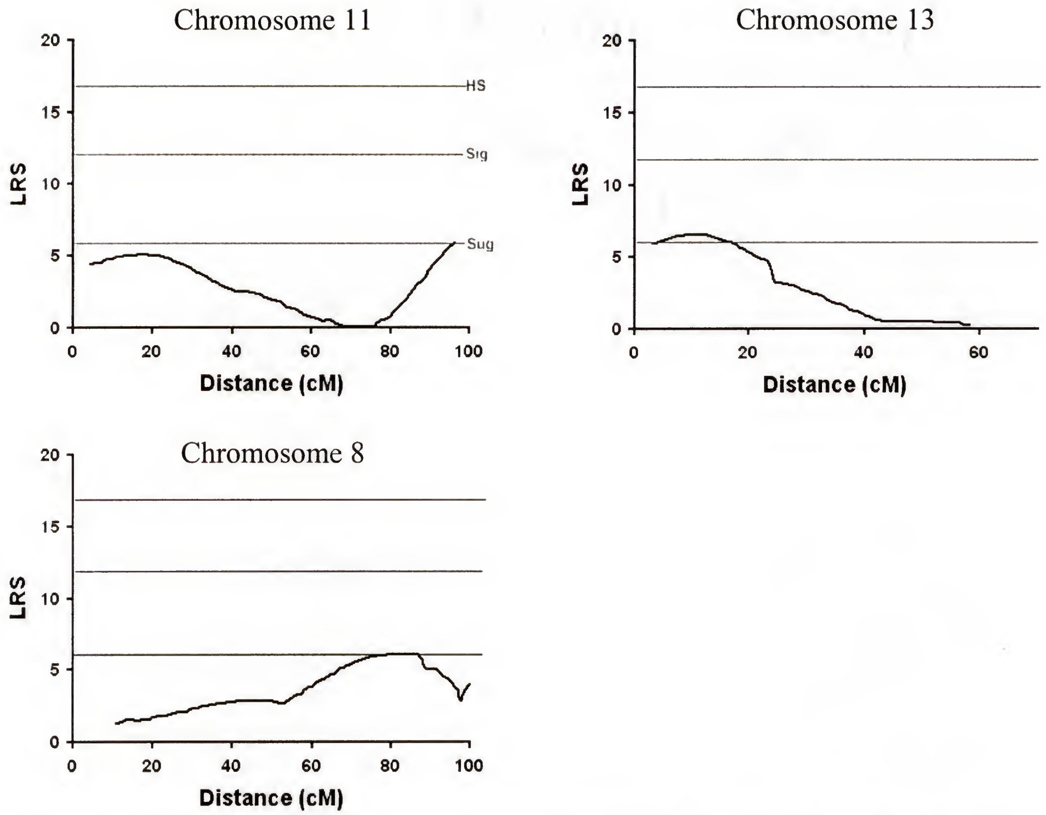

Figure 3-6. Interval Mapping figures of Chromosomes 8, 11, and 13 Using Initial Mortality Data from 149 Recombinant Progeny. Interval mapping of chromosomes 11, 13 and 8 revealed the following data with suggestive LRS scores (Sug) > 6.1, significant LRS scores (Sig) >12.0, and highly significant LRS scores (HS) >17.2 as depicted by the horizontal lines in the figures.

and D-GalN treatment with an LRS score of 6.1, which again explained 3% of the total trait variance (figure 3-6). Chromosome 13 also contained a suggestive locus associated with resistance to rhTNFα and D-GalN treatment (figure 3-6). The resistance locus was mapped to a region between markers D13Mit61 and D13 Mit99 at approximately 19cM with an LRS score of 6.5. This locus accounted for 4% of the total trait variance. In addition, chromosome 11 contained two separate interesting loci, one associated with resistance and the other locus associated with susceptibility to rhTNFα and D-GalN-induced mortality (figure 3-6). The first locus was mapped to a region between markers D11Mit2 and D11Mit339 at approximately 30cM and was associated with resistance giving an LRS score of 5.1 accounting for 3% of the total trait variance. The second locus mapped to the distal end of chromosome 11 at marker D11Mit168 giving an LRS score of 5.9 and was associated with susceptibility to rhTNFα and D-GalN-induced mortality. This locus also accounted for 3% of the total trait variance. In summary, resistance loci on chromosomes 8, 11, and 13 together explained 10% of the total trait variance.

Sequencing of the NOD and B6 TRADD Gene

Since the initial genome scan revealed a suggestive locus at marker D8Mit80 located at 38.3 cM on the distal portion of chromosome 8 and the distal region of this chromosome contains the TRADD candidate gene (location), which is a proximal mediator in the p55 TNF signaling pathway, we decided to proceed simultaneously with the sequencing of this gene, as well as with the second stage of the QTL analysis. The signal transduction of the p55 TNF receptor began to be elucidated with the discovery of a 34kDa protein, TRADD, from a yeast two-hybrid screen searching for proteins that interact with the intracellular portion of the p55 TNF receptor (Park and Baichwal 1996). In 1996, Pan et al. described the sequence and chromosomal location of the murine TRADD gene (Pan et al. 1995). The mouse and human TRADD genes share 75% amino acid homology indicating that this gene is highly conserved in structure and thus is likely to be conserved in function as well. The mTRADD gene contains 4 exons with the fourth exon containing the coding sequence for the entire death domain (amino acids 208-311). The 1.5 kb mTRADD mRNA is present in various tissues, but was found to be highly abundant in mouse liver, therefore, livers from B6 and NOD mice were used to prepare cDNA. Four sets of overlapping primer pairs were used to sequence mTRADD mRNA and the results are shown in Appendix B. Results include only partial B6 and NOD sequence alignment comparison as results for two of the primer sets were not achieved.

The difficulty in sequencing the remaining two regions was potentially due to their structure or function. The fourth exon encoding the death domain was not successfully sequenced using our specific approach nor was the 5'-most end of the sequence including the start codon. Therefore, results presented include only the regions spanning nucleotides 389 to 790 and nucleotides 1011 to 1350.

There were no apparent differences in reliable sequence between B6 and NOD mTRADD mRNA in the regions spanning nucleotides 389 to 790 and nucleotides 1011 to 1350. The slight differences detected occurred only in regions of unreliable sequence, such as at the ends of the amplified fragments, which need further confirmation by overlapping sequencing.

Final QTL Mapping of the Mortality Trait

The power to detect a QTL is the chance of getting a significant LRS at the location of a QTL and is dependent upon many experimental factors. Power depends upon how dense the typed markers are in the region of the QTL, the size of the QTL effect, the stringency of the significance level, the type of cross, and finally the number of mice (Broman 2001). Since our initial analysis failed to reveal significant loci and in an effort to increase our power to detect QTLs involved in the mortality trait, we increased the number of progeny analyzed and the density of markers to perform a second QTL analysis using only markers from chromosomes revealing suggestive LRS scores in the initial mortality analysis (markers used are outlined in figure 3-7). Results of a permutation test using the final mortality data revealed that an LRS score of 3.5 was suggestive of linkage, an LRS score of 9.3 was significant, and an LRS score of 12.2 was highly significant.

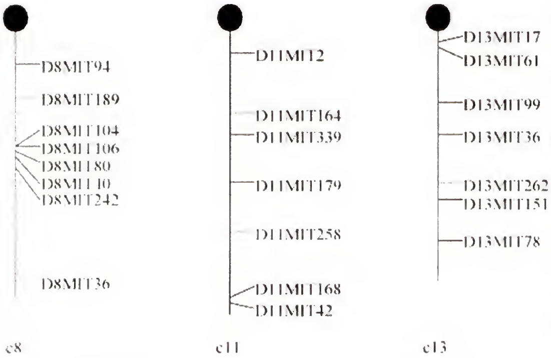
D8MIT94
D8MIT189
D8MIT104
D8MIT106
D8MIT80
D8MIT10
D8MIT242
D8MIT36
c8
D11MIT2
D11MIT164
D11MIT339
D11MIT179
D11MIT258
D11MIT168
D11MIT42
c11
D13MIT17
D13MIT61
D13MIT99
D13MIT36
D13MIT262
D13MIT151
D13MIT78
c13

Figure 3-7. Polymorphic Markers Used in Final Mortality QTL Analysis.

Mortality studies of 294 female backcross progeny revealed a 60% mortality rate in these mice. Final QTL analysis of the mortality phenotype using data from 294 recombinant mice and markers on chromosomes 13, 8, and 11 (loci implicated in the

Table 3-3 . Final Mortality Marker Regression Analysis Results

Locus	Position[1]	LRS[2]	p-value[3]	%[4]	Effect[5]
D8MIT104	38.3	6.4	0.01148	2	+
D8MIT106	39.3	6.8	0.00931	2	+
D8MIT80	41.5	6.5	0.01099	2	+
D11MIT2	4.4	3.5	0.05980	1	+
D11MIT168	75.4	4.8	0.02928	1	-
D13MIT61	7.7	9.4	0.00222	3	+
D13MIT99	25.1	7.6	0.00580	2	+

[1] Chromosome position in centimorgans (derived from MGI at www.informatics.jax.org).

[2] Likelihood ratio statistic for the association of the trait with this locus.

[3] p-value is the probability of an association this good happening by chance.

[4] Percent of the total trait variance which would be explained by a QTL at this location.

[5] Defined as +:resistance gene and -: susceptibility gene.

Table 3-3 . Final Mortality Marker Regression Analysis Results

initial analysis) revealed a resistance locus having significant association on chromosome 13 and suggestive loci on chromosomes 8 and 11. Marker regression analysis results are presented in table 3-3 and simple and composite interval mapping data are presented in figures 3-8 to 3-10. The actual QT Links reports derived from Map Manager QTX™ marker regression analyses are presented in Appendix A along with the interval mapping reports for chromosomes 11, 13, and 8.

Marker regression and subsequent interval mapping analysis using final mortality data revealed that chromosome 8 contained two suggestive loci, one associated with markers D8Mit80, D8Mit106, and D8Mit80 located at approximately 40cM and another associated with a region between markers D8Mit242 and D8Mit36 at approximately 55cM (figure 3-8). Both loci were associated with resistance to rhTNFα and D-GalN-induced mortality. The first locus associated with markers D8Mit104, D8Mit106, and D8Mit80 accounted for 2% of the total trait variance, as opposed to accounting for 3% in the initial mortality analysis. The second locus at approximately 50cM with a suggestive

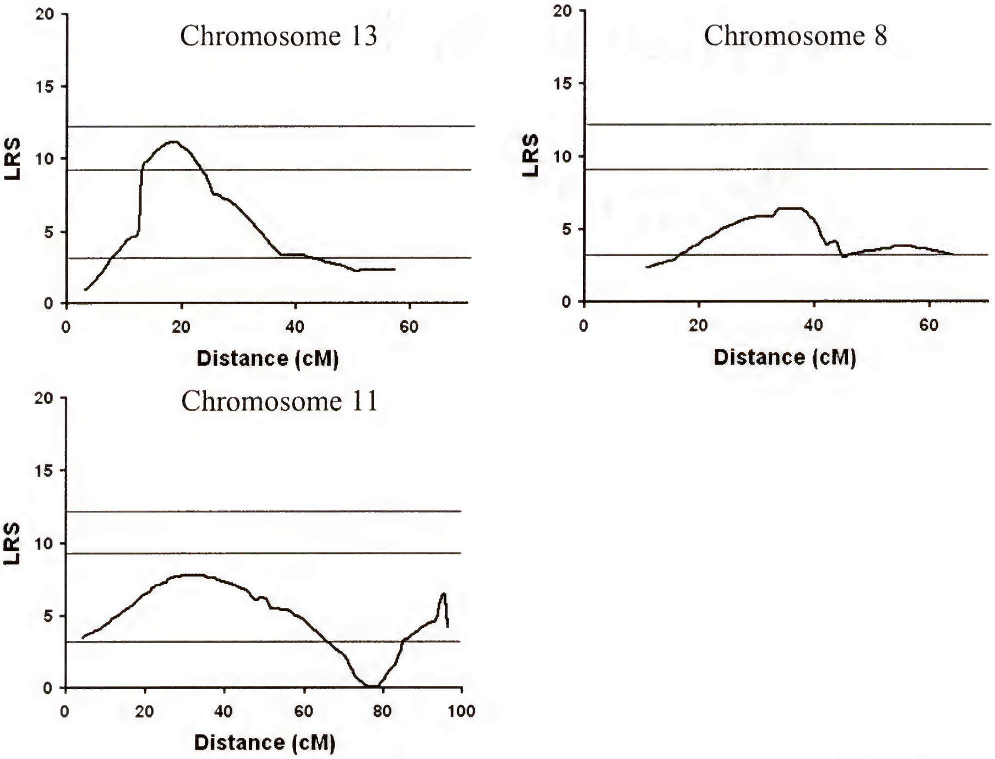

Figure 3-8. Results from Interval Mapping Analysis of Chromosomes 11,8, and 13 Using Final Mortality Data of 295 Recombinant Progeny. Permutation tests revealed suggestive LRS scores (Sug) > 3.5, significant LRS scores (Sig) >9.3, and highly significant LRS scores (HS) >12.2 as depicted by the horizontal lines.

LRS score of 3.8 accounted for only 1% of the total trait variance. Chromosome 13 contained a locus significantly associated with resistance to rhTNFα and D-GalN treatment. The resistance locus was mapped to a region between markers D13Mit61 and D13 Mit99 at approximately 19cM giving an LRS score of 11.1 accounting for 3% of the total trait variance(figure 3-8). In addition, chromosome 11 contained two separate suggestive loci, one associated with resistance and the other with susceptibility to rhTNFα and D-GalN treatment. The first locus was mapped to a region between markers D11Mit2 and D11Mit164 at approximately 30cM with an LRS of 7.8, which was associated with resistance explaining 2% of the total trait variance (figure 3-8). The other locus mapped to the distal end of chromosome 11 at marker D11Mit168 giving an LRS score of 6.5 and was associated with susceptibility accounting for 2% of the total trait variance (figure 3-8).

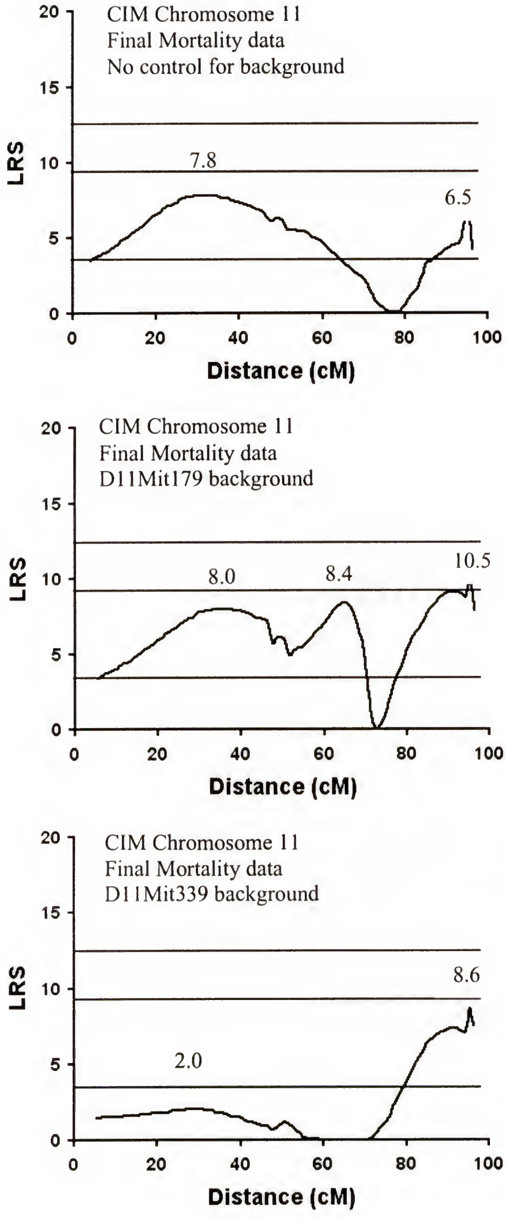

Figure 3-9. Composite Interval Mapping (CIM) of Chromosome 11 Using Final Mortality Data. CIM was performed using indicated background locus. Peak LRS scores are indicated above curves. Significance levels are indicated by the horizontal lines. Permutation test revealed an LRS of 3.5 was suggestive, an LRS of 9.3 was significant, and an LRS of 12.2 was highly significant.

Composite Interval Mapping of Chromosomes 11 and 13 Using Final Mortality Data

A trait can be affected by multiple QTL simultaneously, but these QTL can be either linked appearing on the same chromosome or unlinked to one another on different chromosomes. Therefore, QTL other than the one being mapped are often referred to as background loci, which have two possible effects on a mapped QTL. The first effect a background locus can have on another QTL is to behave like additional environmental effects when not linked to the QTL being mapped, thereby reducing the significance of association of the QTL with the trait. The second effect of background loci is that they may bias the estimated location of the QTL when linked to that QTL. Map Manager QTX™ allows the user to reduce the effects of background loci by including other markers in the regression analysis. In effect, it is possible to control for unlinked QTL by choosing a single marker significantly associated with the trait (highest LRS score) from each chromosome other than the one being mapped and subsequently, interval mapping each chromosome other than the one being mapped and subsequently, interval mapping analysis is then performed. The choice of background loci typically involves the use of as few loci as possible and only loci with the highest LRS. In order to control for linked QTL, a marker between the QTL being mapped and the region suspected of containing a second QTL on the same chromosome is selected as a background locus prior to interval mapping of that chromosome.

Since chromosome 11 appeared to have more than one QTL, composite interval mapping was performed by selecting a marker between the QTL being mapped and the region suspected of containing a second QTL. Results from these analyses are shown in figures 3-9 and 3-10. In the first analysis, to control for linked QTL on chromosome 11 marker D11Mit179 was included as a background locus and subsequent interval mapping was performed using mortality data from 294 F1xNOD progeny. Interval mapping analysis of chromosome 11 with the inclusion of D11Mit179 as a background locus (figure 3-9) revealed the potential presence of three loci with one being localized to a region between markers D11Mit2 and D11Mit164 with a peak LRS of 8.0 compared to 7.8 with simple interval mapping analysis. This locus explained 3% of the total trait variance. Another locus mapped between markers D11Mit339 and D11Mit179 with a peak LRS of 8.4 compared to no peak whatsoever with simple interval mapping analysis (figure 3-9). This trait explained 3% of the total trait variance. A third locus mapped near marker D11Mit168 at the distal end of the chromosome having a peak LRS of 10.5 compared to a peak LRS of 6.5 with simple interval mapping (figure 3-9) explaining 4% of the total trait variance.

In addition, composite interval mapping of chromosome 11 was performed using D11Mit339 as a background locus (figure 3-9). The marker D11Mit339 was also located between the original mapped loci and the suspected second locus; therefore the choice between D11Mit339 and D11Mit179 as background loci was arbitrary as both gave a peak LRS score of 1.0 or less with simple interval mapping analysis. It was expected that the data would not be affected by the choice of either marker as a background locus. Interestingly, inclusion of D11Mit339 yielded different results in that two of the loci disappeared leaving only the locus at the distal end of chromosome 11 near marker D11Mit168 with an LRS score of 8.6 (highly suggestive LRS score) compared to 10.5 (significant LRS score) with the inclusion of D11Mit179 as a background locus explaining 3% of the total trait variance (figure 3-9). These results are confounding and it is difficult to determine which of the two markers should be included as the background locus; however, both analysis methods revealed that a susceptibility locus near marker D11Mit168 may contain genes associated with increased mortality in response to rhTNFα and D-GalN mediated treatment.

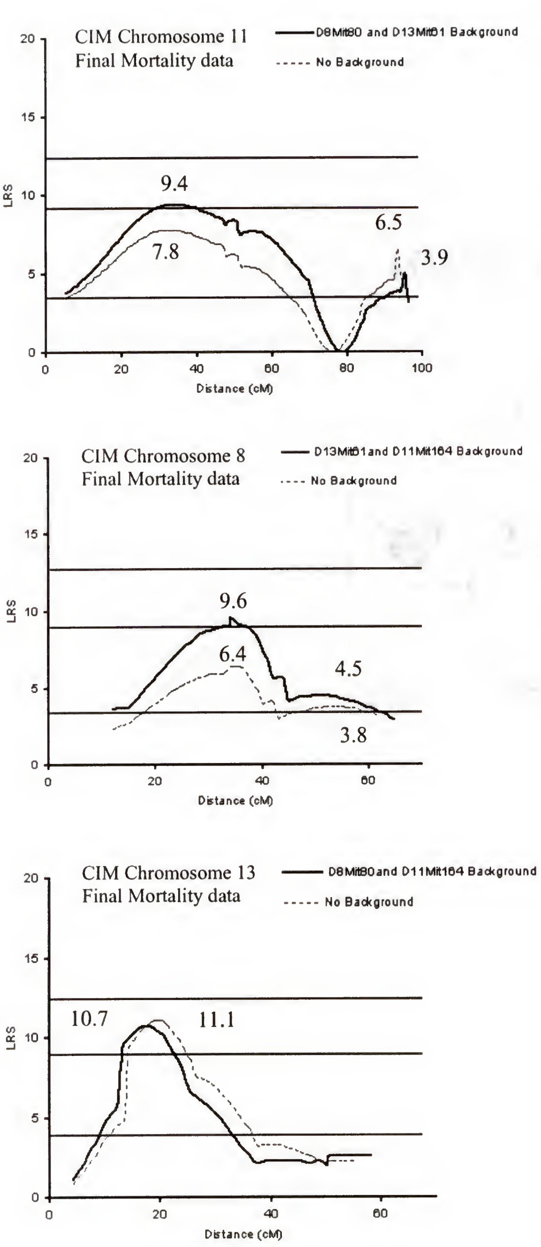

Figure 3-10. Composite Interval Mapping of Chromosomes 11, 13, and 8 Using Final Mortality Data. CIM was performed using indicated background loci and the resulting peak LRS scores indicated above the curves.

Additional composite interval mapping of chromosome 11 using markers D13Mit61 and D8Mit80 as background loci to control for the contribution of unlinked QTL revealed a increase in peak LRS from 7.8 to 9.4 between markers D11Mit2 and D11Mit164 with the inclusion of background loci (figure 3-10) accounting for 3% of the total trait variance. In addition, the LRS for the susceptibility locus near marker D11Mit168 decreased from 6.5 to 3.9 accounting for only 2% of the total trait variance. Also, composite interval mapping of chromosome 8 using markers D11Mit164 and D13Mit61 as background loci demonstrated an increase of LRS score from 6.4 with simple interval mapping to the significant LRS level of 9.4 with the inclusion of background loci (figure 3-10) explaining 3% of the total trait variance. These data indicate that the resistance locus near marker D8Mit80 was significantly associated with decreased mortality in response to rhTNFα and D-GalN mediated treatment. Finally, composite interval mapping of chromosome 13 using D11Mit164 and D8Mit80 as background loci revealed very modest changes in LRS score when compared to simple interval mapping (11.1 for simple and to 10.7 for composite interval mapping explaining 4 and 3% of the total trait variance, respectively.) (figure 3-10). These data were expected since this locus revealed the highest LRS score in initial simple interval mapping analysis and was unlikely to have been largely affected by other unlinked QTL having weaker LRS values.

QTL Mapping of Additional Traits

Recombinant progeny of a backcross between the (NODxB6)F1 and NOD mouse were treated with 10mg rhTNFα and 8mg D-GalN. Animals were then sacrificed and

Table 3-4. Permutation Test Results. Data presented are results from 1000 permutations of the indicated data.

Phenotype	Suggestive LRS	Significant LRS	Highly Significant LRS
AST	5.7	11.8	20.3
IL-6	4.4	8.3	17.0
Caspase-3 (DNA)	6.0	11.1	16.2
Caspase-3 (protein)	6.0	11.8	17.0

serum and liver tissue harvested for genotyping and phenotyping. The phenotypes used in this analysis were serum AST levels, serum IL-6 levels, and liver caspase-3-like

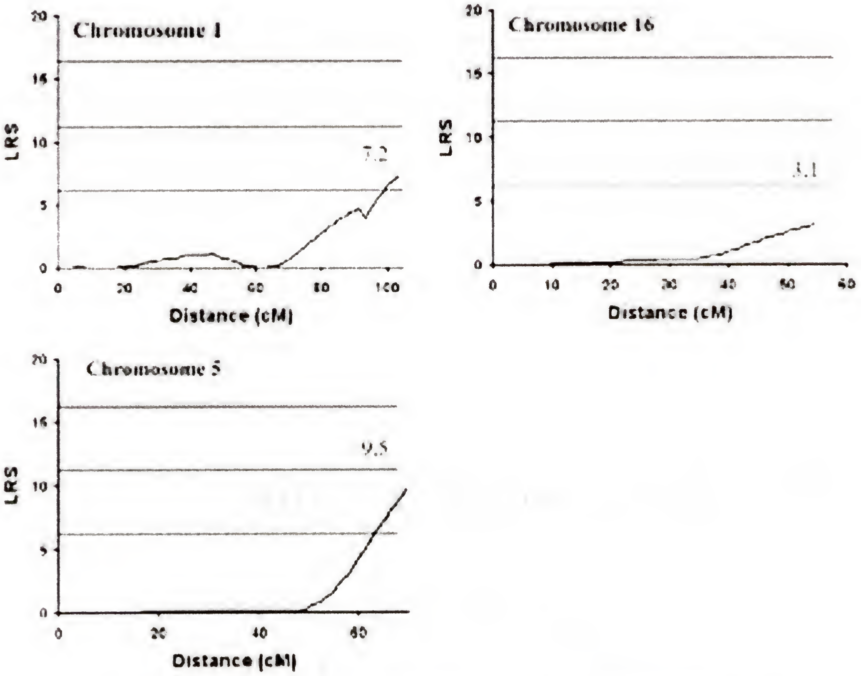

Figure 3-11. Results from Interval Mapping of Chromosomes 1, 5, and 16 from Analysis of DNA Normalized Caspase-3 Data Using 138 Recombinant Progeny. Interval mapping of chromosomes 1, 16, and 5 revealed the following data with suggestive LRS scores (Sug) >6.0, significant LRS scores (Sig) >11.1, and highly significant LRS scores (HS) >16.2 as depicted by the horizontal lines in the figures.

Table 3-5. Caspase-3 (DNA normalized) Marker Regression Analysis Results

Locus	Position[1]	LRS[2]	p-value[3]	%[4]	Effect[5]
D1MIT15	86.3	4.5	0.03385	3	-
D1MIT17	110.4	7.4	0.00648	5	-
D5MIT161	60.1	10.4	0.02042	7	+

[1] Chromosome position in centimorgans (derived from MGI at www.informatics.jax.org).

[2] Likelihood ratio statistic for the association of the trait with this locus.

[3] p-value is the probability of an association this good happening by chance.

[4] Percent of the total trait variance explained by a QTL at this location.

[5] Defined as +:resistance gene and -: susceptibility gene.

activity (DNA normalized or protein normalized). Phenotypic and genotypic data from 138 recombinant progeny were analyzed for association using the Map Manager QTX™ software package. Permutation tests using 1000 permutations were performed on the individual phenotypes and the results for all phenotypes are presented in table 3-4. Marker regression analysis results for all phenotypes are presented in tables 3-5 to 3-8, and simple and composite interval mapping data for chromosomes 1, 5, and 16 for all four phenotypes are presented in figures 3-11 to figure 3-16. In addition, actual QT Links and IM reports are presented in Appendix A.

Marker regression analysis revealed loci associated with caspase-3 (DNA normalized) on chromosomes 1 and 5 (table 3-5), with the locus on chromosome 5 approaching significance (see table 3-4 for significance levels). Subsequent interval mapping revealed no increase in LRS score at the chromosome 5 locus, since the score peaked with LRS of 10.4 at the marker D5Mit161 located at the distal end of the chromosome (60cM) and no predictions are made beyond that point in interval mapping analysis (figure 3-11). This locus on chromosome 5 accounted for 6% of the total trait variance. Chromosome 1 revealed a suggestive locus associated with decreased caspase-3-like activity levels at the distal end of the chromosome with a peak LRS of 7.2 at marker D1Mit17 (110cM) accounting for 5% of the total trait variance (figure 3-11).

Table 3-6. Caspase-3 (protein normalized) Marker Regression Analysis Results

Locus	Position[1]	LRS[2]	p-value[3]	%[4]	Effect[5]
D1MIT15	86.3	1.5	0.22751	0	-
D1MIT17	110.4	2.6	0.10406	1	-
D5MIT161	60.1	4.0	0.04500	2	+

[1] Chromosome position in centimorgans (derived from MGI at www.informatics.jax.org).

[2] Likelihood ratio statistic for the association of the trait with this locus.

[3] p-value is the probability of an association this good happening by chance.

[4] Percent of the total trait variance explained by a QTL at this location.

[5] Defined as +:resistance gene and -: susceptibility gene.

Comparison of caspase-3 data normalized by DNA quantitation (presented in figure 3-11 and table 3-5) and caspase-3 data normalized by protein (presented in figure 3-12 and table 3-6) revealed significant differences in LRS scores for chromosomes 1 and 5 (see table 3-4 for significance levels). Interval mapping of chromosome 1 using protein normalized caspase-3 data revealed an LRS score of only 2.5 associated with the distal end at marker D1Mit17 compared to an LRS score of 7.4 for DNA normalized caspase-3 data (figure 3-12). Also, the locus on the distal end of chromosome 5 that approached significance in the interval mapping analysis of DNA normalized caspase-3 (LRS=10.4) at marker D5Mit161 revealed an LRS of only 3.7 for protein normalized caspase-3 data

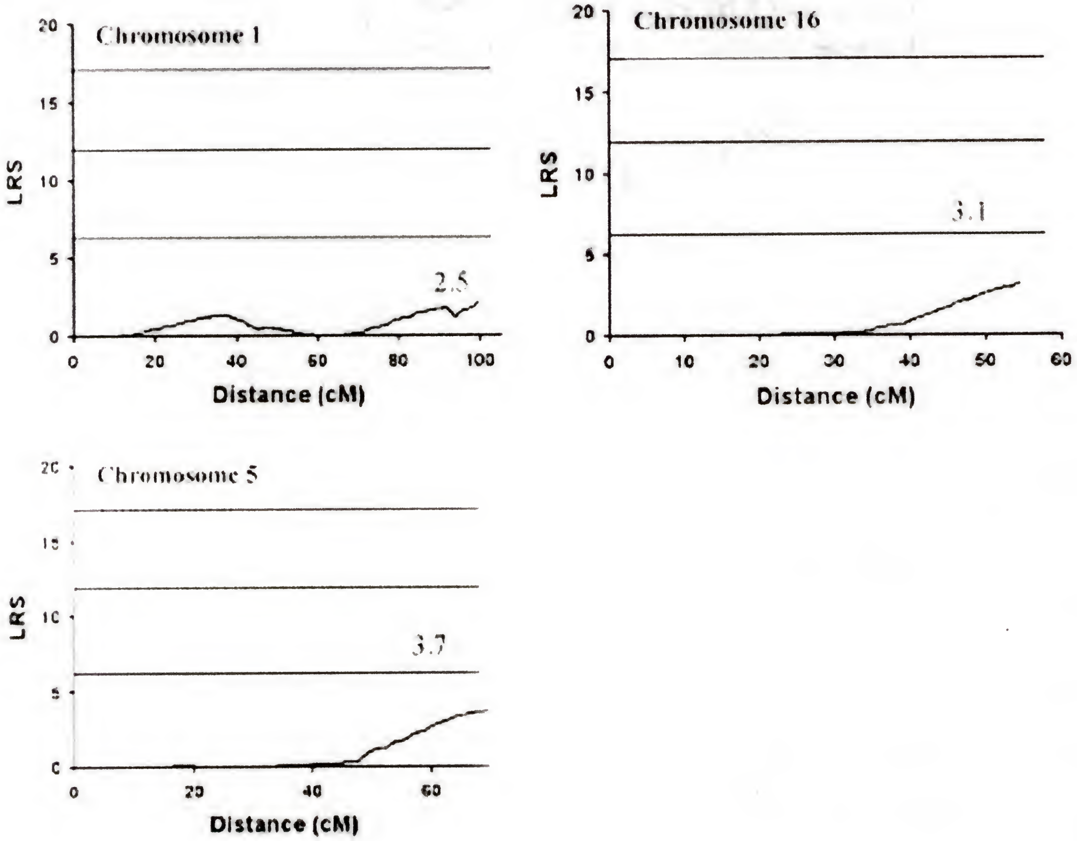

Figure 3-12. Results from Interval Mapping of Chromosomes 1, 5, and 16 from Analysis of Protein Normalized Caspase-3 Data Using 138 Recombinant Progeny. Interval mapping of chromosomes 1, 16, and 5 revealed the following data with suggestive LRS scores (Sug) >6.0, significant LRS scores (Sig) >11.8, and highly significant LRS scores (HS) >17.0 as depicted by the horizontal lines in the figures.

Table 3-7. AST Marker Regression Analysis Results.

Locus	Position[1]	LRS[2]	p-value[3]	%[4]	Effect[5]
D1MIT303	32.8	5.0	0.02469	3	+
D1MIT8	51.4	4.2	0.04106	2	+
D16MIT158	40.4	6.4	0.01161	4	+

[1] Chromosome position in centimorgans (derived from MGI at www.informatics.jax.org).
[2] Likelihood ratio statistic for the association of the trait with this locus.
[3] p-value is the probability of an association this good happening by chance.
[4] Percent of the total trait variance explained by a QTL at this location.
[5] Defined as +:resistance gene and -: susceptibility gene.

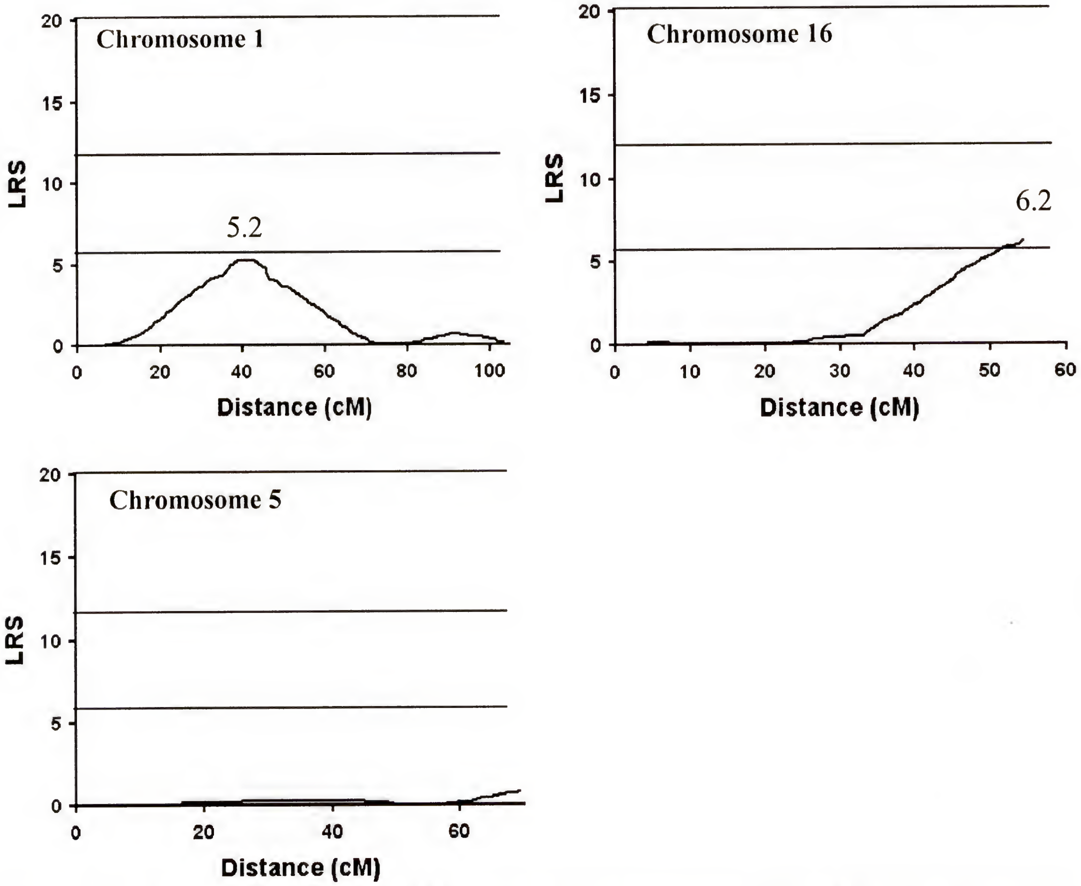

Figure 3-13. Results from Interval Mapping of Chromosomes 1, 5, and 16 from Analysis of AST Data Using 138 Recombinant Progeny. Interval mapping of chromosomes 1, 16, and 5 revealed the following data with suggestive LRS scores (Sug) >5.7, significant LRS scores (Sig) >11.8, and highly significant LRS scores (HS) >20.3 as depicted by the horizontal lines in the figures.

Table 3-8. IL-6 Marker Regression Analysis Results.

Locus	Position[1]	LRS[2]	p-value[3]	%[4]	Effect[5]
D1MIT303	32.8	3.2	0.07271	2	+
D1MIT8	51.4	3.5	0.05990	2	+

[1] Chromosome position in centimorgans (derived from MGI at www.informatics.jax.org).
[2] Likelihood ratio statistic for the association of the trait with this locus.
[3] p-value is the probability of an association this good happening by chance.
[4] Percent of the total trait variance explained by a QTL at this location.
[5] Defined as +:resistance gene and -: susceptibility gene.

(figure 3-12). These data suggest that the normalization of samples for DNA instead of protein content more accurately reflected the caspase-3 levels in liver tissues in this liver injury model. In contrast to AST data, chromosome 16 revealed no suggestive or significant associations with any of the typed markers with either caspase-3 phenotype (figure 3-11 and 12).

Marker regression analysis of the AST phenotype revealed suggestive or nearly suggestive loci on chromosomes 1 and 16 (table 3-7, also see table 3-4 for significance levels). Subsequent interval mapping analysis of chromosome 1 revealed a peak LRS of 5.2 between markers D1Mit303 and D1Mit8 (40cM) associated with decreased AST levels in response to rhTNFα and D-GalN treatment (figure 3-13) explaining 3% of the total trait variance. While the suggestive level was defined by an LRS score of 5.7 or higher, the loci on chromosome 1 remains interesting due to the 5.2 LRS score (see table 3-4 for significance levels). In addition, a suggestive LRS score of 6.2 on the distal end of chromosome 16 at marker D16Mit158 (40cM) was also associated with resistance accounting for 4% of the total trait variance (figure 3-13). In contrast to caspase-3 data, interval mapping of chromosome 5 revealed no suggestive associations with any of the typed markers (figure 3-13).

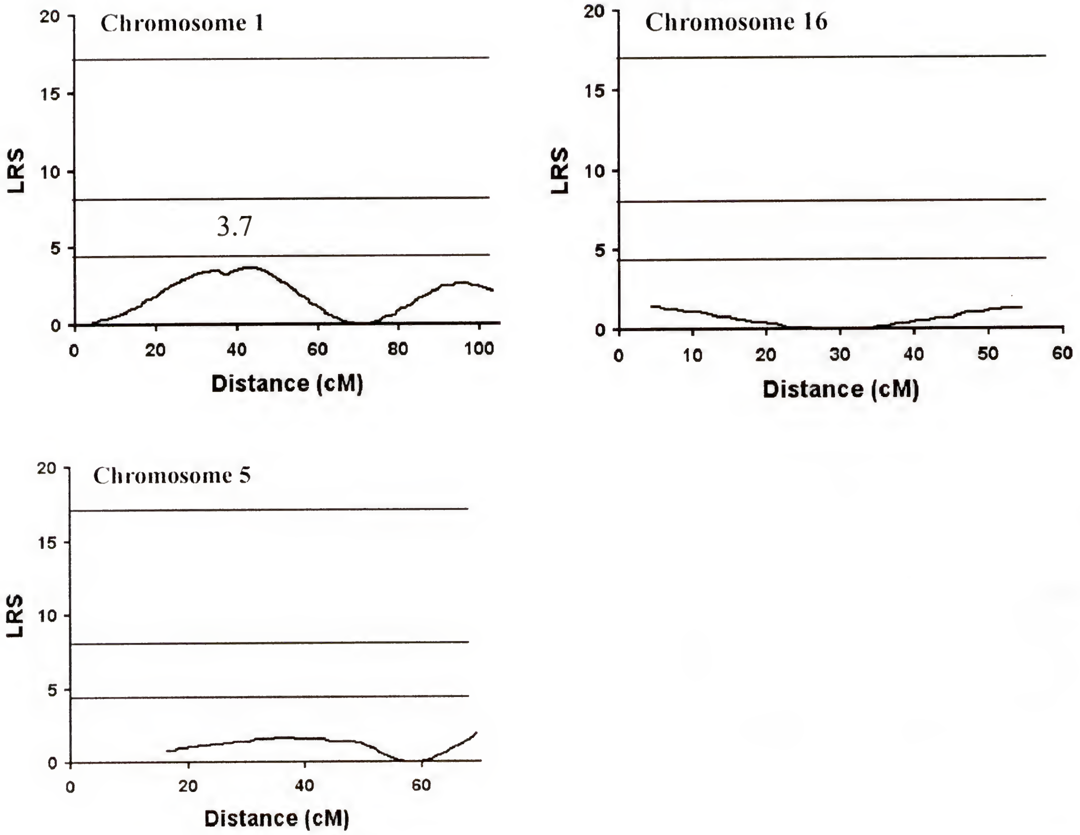

Figure 3-14. Results from Interval Mapping of Chromosomes 1, 5, and 16 from Analysis of IL-6 Data Using 149 Recombinant Progeny. Interval mapping of chromosomes 1, 16 and 5 revealed the following data with suggestive LRS scores (Sug) >4.4, significant LRS scores (Sig) >.8.3, and highly significant LRS scores (HS) >17.0 as depicted by the horizontal lines in the figures.

Marker regression analysis and interval mapping using the IL-6 phenotype revealed no suggestive or significant associations with any of the typed markers (see table 3-4 for significance levels). Marker regression data and interval mapping data for chromosomes 1, 5, and 16 are presented in table 3-8 and figure 3-14 for comparison with other phenotypes. Interval mapping of chromosome 1 revealed an LRS score of 3.7 for the interval between markers D1Mit303 and D1Mit8 at approximately 40cM, which approached the suggestive level determined to be 4.4 with these data (figure 3-14). Therefore, this locus on chromosome 1 may be potentially interesting given that it was found to be suggestive in interval mapping analysis of AST data (figure 3-13). In contrast to AST data, chromosome 16 revealed no suggestive or significant associations with any of the typed markers and all other identified loci were below the suggestive level for the IL-6 phenotype (figure 3-14).

Composite Interval Mapping of Chromosomes 1, 5, and 16 Using Additional Traits

Composite interval mapping using AST data

Simple interval mapping analysis of chromosomes 1, 5, and 16 using AST data revealed a suggestive locus on chromosome 16 associated with marker D16Mit158, and a nearly suggestive locus on chromosome 1 between markers D1Mit303 and D1Mit8 (figure 3-13). While further composite interval mapping analysis of chromosome 16

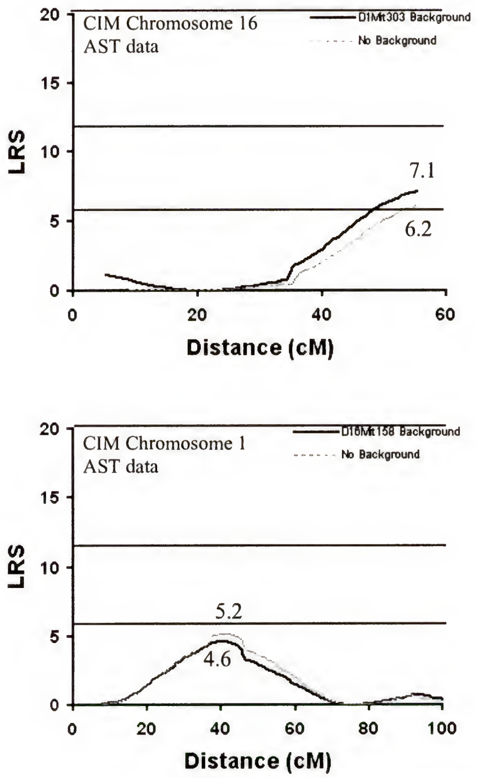

Figure 3-15. Composite Interval Mapping of Chromosomes 16 and 1 using AST Data.

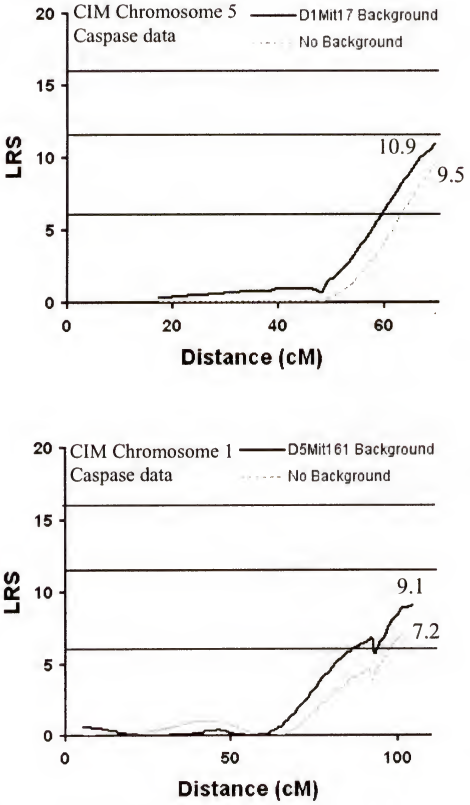

Figure 3-16. Composite Interval Mapping of Chromosomes 5 and 1 using DNA Normalized Caspase-3 Data.

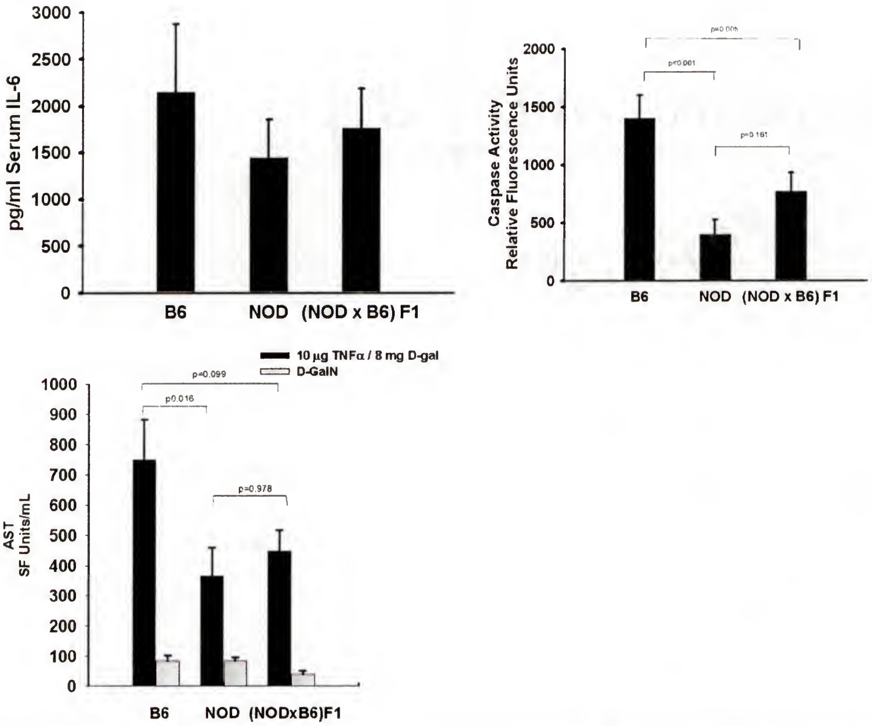

Figure 3-17. Data from Control Animals in Phenotypic Mapping Experiments. Each set of recombinant animals used for the phenotypic mapping (AST,Caspase-3, and IL-6) were phenotyped along with a set of control animals. These data are the results from analysis of control animals from these experiments. n=12 for all treatment groups. Statistics: ANOVA (Tukey)

using D1Mit303 as a background locus revealed an increase in peak LRS score from 6.2 to 7.1, both of these values remained just above the suggestive level (figure 3-15). In addition, composite interval mapping analysis of chromosome 1 using D16Mit158 as a background locus revealed only a modest decrease in peak LRS score from 5.2 to 4.6 thus remaining below the suggestive level (figure 3-15). Therefore, composite interval mapping data revealed no change in the overall conclusions regarding the possible association of the suggestive locus on chromosome 16 and the locus on chromosome 1 with decreased AST levels when compared to simple interval mapping.

<ins>Composite interval mapping using caspase-3 data</ins>

Simple interval mapping of chromosomes 1, 5, and 16 using caspase-3-like activity data (normalized for DNA content) revealed suggestive loci on chromosomes 1 and 5 (figure 3-11). Further composite interval mapping of chromosome 1 using D5Mit101 as a background locus revealed a modest increase in LRS score from 7.2 to 9.1 at marker D1Mit17 (figure 3-16). In addition, composite interval mapping of chromosome 5 using D1Mit17 as a background locus revealed a slight increase in LRS score from 9.5 to 10.9 (figure 3-16). Despite the increases in LRS scores for both loci with composite interval mapping, neither suggestive locus reached significance. However, the locus on chromosome 5 associated with D5Mit101 very closely approached the11.1 significance level with an LRS score of 10.9 indicating that this locus may contain genes contributing to decreased liver apoptosis in NOD mice with rhTNFα and D-GalN-mediated treatment (figure 3-16). Results from all mapping analyses are presented in Table 3-9 for simplicity.

Analysis of Control Animals from Individual Mapping Experiments

Each set of recombinant animals that were treated and serum and livers harvested were analyzed along with all three control strains (NOD, B6, and F1) to ensure consistency of data. Results of these data are presented in figure 3-17. Untreated controls were omitted from the IL-6 and caspase-3 graphs due to the fact that they were always below detectable limits of the assays.

Serum IL-6 data showed no significant difference between any of the control strains, unlike initial data from parental strains presented in figure 3-3. Also levels were significantly lower than expected indicating possible degradation of the serum samples occurred. Serum AST data revealed significant differences between B6 and NOD mice ($p=0.016$), however, no significant difference was observed between B6 and F1 ($p=0.099$) or NOD and F1 mice ($p=0.978$). Caspase-3 data normalized for DNA quantity revealed significant differences between NOD and B6 mice ($p<0.001$) and B6 and F1 mice ($p=0.005$; data presented in figure 3-17). In contrast, no significant differences between NOD and F1 mice were observed in liver caspase-3 levels ($p=0.161$).

Discussion and Comparison of Data from All Phenotypes

These data demonstrate that female (NODxB6)F1 mice are susceptible to rhTNFα and D-GalN treatment, thus the resistance in the NOD mouse is a recessive trait. Based on this information, the appropriate backcross between the F1 and NOD mouse was initiated. Interestingly, we also found SWR mice, an NOD related strain having a very similar genetic composition, were also resistant to rhTNFα and D-GalN treatment. Interestingly, the SWR strain does not develop diabetes and is actually a frequently used control strain for studies involving NOD mice. However, the availability of B6.NOD congenic strains provided unique opportunities to examine various genetic loci in isolation for their influence upon the resistance of NOD mice to rhTNFα and D-GalN-induced lethality and thus the decision was made to pursue this genetic analysis using the NOD mouse. Analysis of available B6 congenic mice with intervals from the NOD mouse indicated that the resistance to rhTNFα and D-GalN-induced liver injury, apoptosis, and lethality does not independently involve the NOD MHC loci or examined Idd regions on mouse chromosome 1, 3, 6, 11 or 17. These data do not exclude these intervals as potential resistance or susceptibility loci; however, none of these loci appear to be independently involved in the rhTNFα resistant phenotype in the NOD mouse.

In order to identify loci involved in the resistance of the NOD mouse, a QTL analysis was performed. Since our ultimate outcome was death in this model, but additional phenotypes increase the likelihood of success in QTL analysis, it was necessary to perform two independent studies using one group of backcross progeny for mortality determinations and another group for the analysis of apoptosis, liver injury, and cytokine production. Results from all interval mapping analyses are presented in table 3-9.

Marker regression analysis of mortality data derived from 149 recombinant (NODxB6) F1xNOD progeny revealed a suggestive locus on chromosome 13.

Further interval mapping analysis of chromosome 13 using an additional 146 animals for a total of 294 recombinant progeny, revealed this locus to be significantly

Table 3-9. Summary of Interval Mapping Data for All Phenotypes

Phenotype	Analysis	Chromosome	Locus	Background Loci	LRS Score	Results	Resistance or Susceptibility locus
Initial Mortality	SIM	8	D8Mit80		6.1	Suggestive	Resistance
	SIM	11	D11Mit2 to D11Mit339		5.1		Resistance
	SIM	11	D11Mit168		5.9		Susceptibility
	SIM	13	D13Mit61 to D13Mit99		6.1	Suggestive	Resistance
Final Mortality	SIM	8	D8Mit80		6.4	Suggestive	Resistance
	SIM	11	D11Mit2 to D11Mit339		7.8	Suggestive	Resistance
	SIM	11	D11Mit168		6.5	Suggestive	Susceptibility
	SIM	13	D13Mit61 to D13Mit99		11.1	**Significant**	Resistance
	CIM	8	D8Mit80	D11Mit168 and D13Mit61	9.6	**Significant**	Resistance
	CIM	11	D11Mit2 to D11Mit339	D8Mit80 and D13Mit61	9.4	**Significant**	Resistance
	CIM	11	D11Mit168	D8Mit80 and D13Mit62	3.9		Resistance
	CIM	11	D11Mit2 to D11Mit339	D11Mit179	8	Suggestive	Resistance
	CIM	11	D11Mit179 to D11Mit339	D11Mit179	8.4	Suggestive	Resistance
	CIM	11	D11Mit168	D11Mit179	10.5	**Significant**	Susceptibility
	CIM	11	D11Mit168	D11Mit339	8.6	Suggestive	Susceptibility
	CIM	13	D13Mit61 to D13Mit99	D11Mit168 and D8Mit80	10.7	**Significant**	Resistance
AST	SIM	1	D1Mit303 to D1Mit8		5.2		Resistance
	SIM	16	D16Mit158		6.2	Suggestive	Resistance
	CIM	1	D1Mit303 to D1Mit8	D16Mit158	4.6		Resistance
	CIM	16	D16Mit158	D1Mit303	7.1	Suggestive	Resistance
Caspase-3 (DNA)	SIM	1	D1Mit17		7.2	Suggestive	Susceptibility
	SIM	5	D5Mit161		9.5	Suggestive	Resistance
	CIM	1	D1Mit17	D5Mit161	9.1	Suggestive	Susceptibility
	CIM	5	D5Mit161	D1Mit17	10.9	Suggestive	Resistance

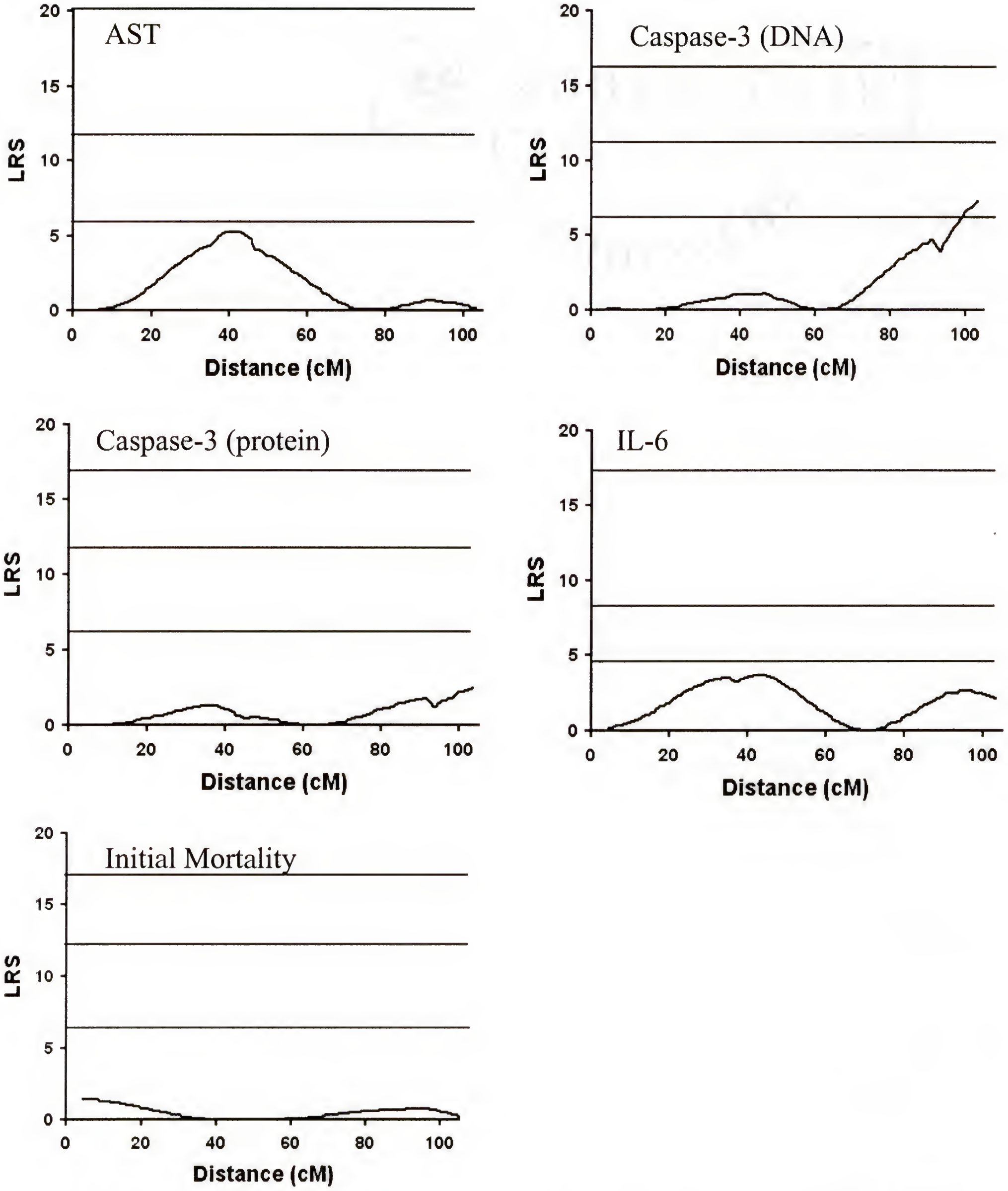

Figure 3-18. Comparison of Interval Mapping Data From Chromosome 1 Using All Phentoypes.

associated with the resistance of mice to rhTNFα and D-GalN treatment. Other interesting loci that were found to be suggestive in both analyses were localized to chromosomes 8 and 11. These loci were found to be significant upon further composite interval using background loci to control for unlinked QTL.

Marker regression and interval mapping of additional phenotypes (AST levels, IL-6 levels, and caspase-3-like activity) revealed only suggestive loci on chromosomes 1, 5, and 16. However, a locus on the distal portion of chromosome 5 at marker D5Mit161 (60cM) revealed in the DNA normalized caspase-3 interval mapping analysis

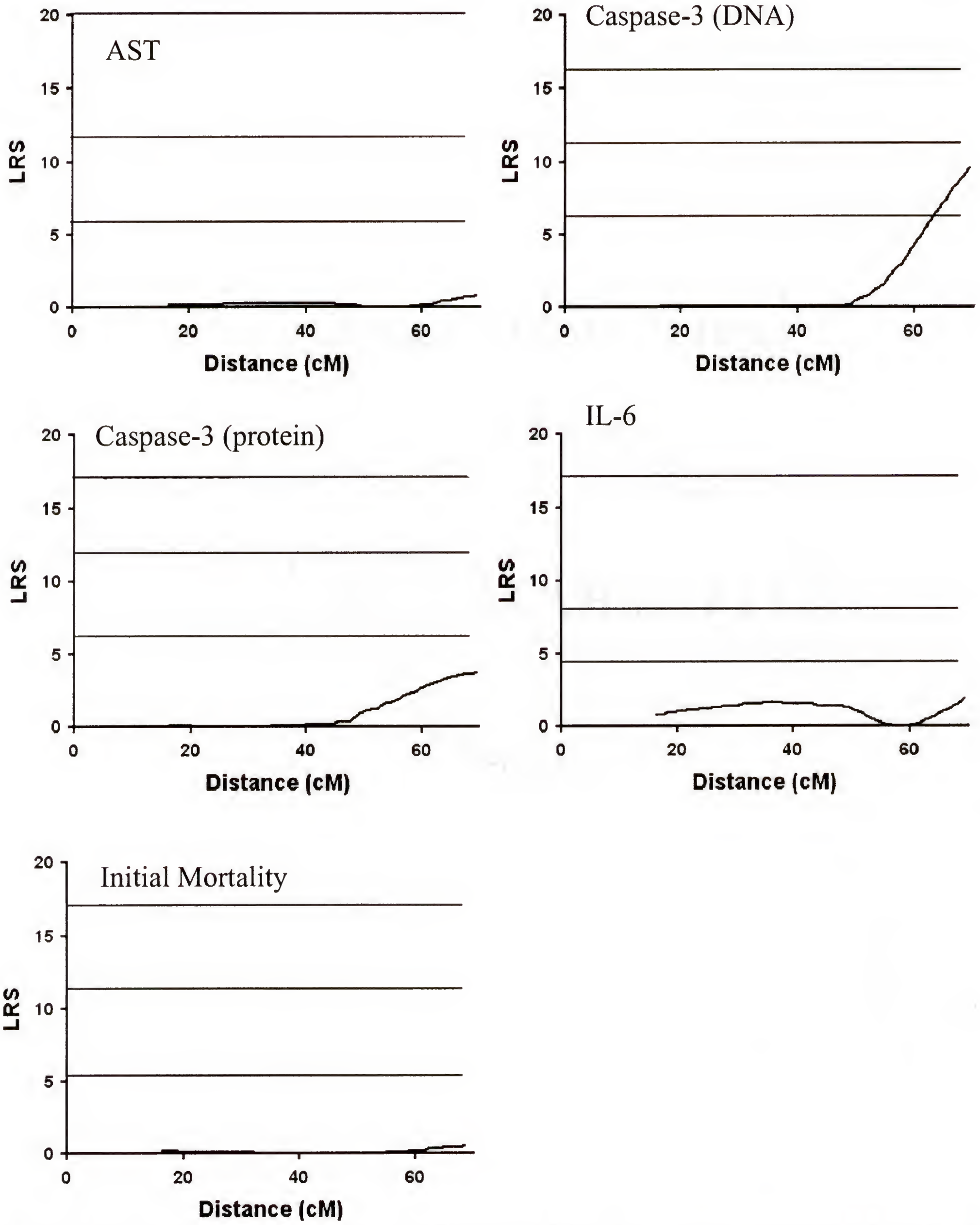

Figure 3-19. Comparison of Interval Mapping Data From Chromosome 5 Using All Phentoypes.

very closely approached significance with composite interval mapping, indicating a potentially interesting locus associated with decreased liver caspase-3-like activity.

In addition, interval mapping data for each chromosome containing loci associated with resistance or susceptibility to rhTNFα and D-GalN were compared for all phenotypes (figures 3-18 to 3-23) and it was noted that some of the identified loci were associated with more than a single phenotype. Figure 3-18 examined the similarities between LRS scores resulting from interval mapping of chromosome 1 for all phenotypes. Interestingly, LRS curves for all phenotypes showed a similar pattern. A susceptibility locus on the distal portion of chromosome 1 was suggestive of an association with increased liver caspase-3 (normalized for DNA content) and revealed increases in LRS curves of the IL-6 and AST phenotypes at this locus. Since markers from chromosome 1, 5, and 16 were not used in the final mortality analysis, only data for initial mortality was available. Although the LRS scores are very low for chromosome 1 with the initial mortality phenotype, the LRS curve does show a slight inflection at a similar locus. These data are encouraging and indicate that the LRS scores observed for all phenotypes are likely to reflect a true association of these loci with a given phenotype.

Similarly, interval mapping of an additional region on chromosome 1 located between markers D1Mit3030 and D1Mit8 (40cM) revealed increased LRS scores (though some were quite low) for all phenotypes examined. However, only peak LRS scores for IL-6 (peak of 3.7) and AST (peak o f 5.2) in this region on chromosome 1 approached suggestive levels indicating that the locus identified may be a common mediator of both IL-6 production and AST levels in response to rhTNFα and D-GalN treatment. Interval mapping analysis of chromosome 1with initial mortality data revealed no association with the identified loci and LRS scores peaked only near marker D1Mit65 at the proximal portion of the chromosome reaching a peak LRS of only 1.4.

Moreover, chromosome 5 revealed increased LRS scores for all phenotypes at the distal portion associated with marker D5Mit161 (figure 3-19). However, only increased caspase-3-like activity (normalized for DNA content) resulted in a suggestive LRS score (LRS=9.5) at this locus suggesting that it may contain genes specifically associated with liver caspase-3-like activity. Interval mapping of chromosome 1 using initial mortality data revealed no association with any locus on chromosome 5. In fact, LRS scores were below 0.5 at all intervals along the chromosome.

Also, the distal portion chromosome 16 revealed increased LRS scores for all phenotypes with interval mapping. A peak LRS score of 6.2 occurred at marker D16Mit158 and was associated with decreased AST levels. Interval mapping of chromosome 16 using the caspase-3 (DNA) phenotype revealed moderate increases in LRS scores at marker D16Mit168, which may indicate an association of this locus with both decreased serum AST levels and decreased liver caspase-3-like activity in response to rhTNFα and D-GalN treatment (figure 3-20). Interval mapping of initial mortality data also revealed an association of the mortality with D16Mit158 located at the distal end of chromosome 16 revealing a 4.8 LRS score, which more closely approached suggestive levels than LRS scores for caspase-3 (DNA) data. These data indicate that this locus may be associated with decreased AST levels, decreased caspase-3 levels and increased survival in response to rhTNFα and D-GalN treatment.

In addition, interval mapping data (using AST, IL-6, caspase-3 phenotypes) of chromosomes 8, 11, and 13, which revealed increased LRS scores in the initial and final mortality analyses, were examined for similarities in peak LRS scores (figures 3-21 to 3-23). Data from interval mapping of chromosome 8 using all phenotypes revealed that the locus associated with decreased mortality with a peak suggestive LRS score of 6.4 at markers D8Mit104, D8Mit106, and D8Mit80 revealed no similarities between the other phenotypes (figure 3-21). Instead, interval mapping of chromosome 8 using the IL-6 phenotype revealed a peak LRS of 3.1 at D8Mit189 with LRS scores decreasing toward the distal part of the chromosome including markers D8Mit104, D8Mit106, and D8Mit80. In contrast, interval mapping of chromosome 8 using AST data revealed increasing LRS

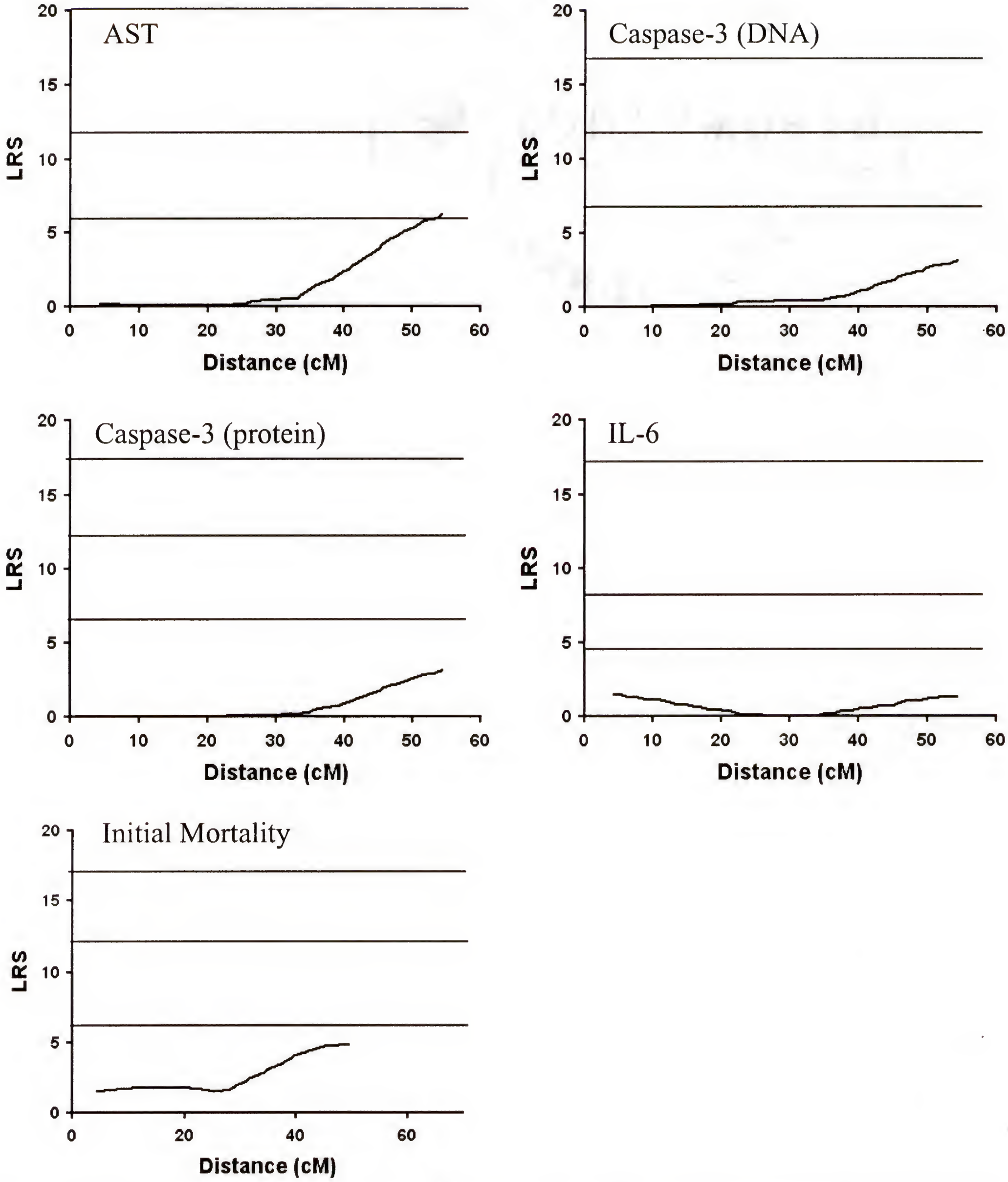

Figure 3-20. Comparison of Interval Mapping Data From Chromosome 16 Using All Phentoypes.

values near marker D8Mit80 as for the mortality data but with a peak LRS of only 1.4. However, there were also increases in LRS scores at marker D8Mit242 on chromosome 8 with interval mapping using the AST phenotype with a peak LRS of only 2.5. While the LRS values were very low at chromosome 8 for the AST phenotype, the trend in increasing LRS scores was similar at the D8Mit80 locus. Interval mapping analysis of

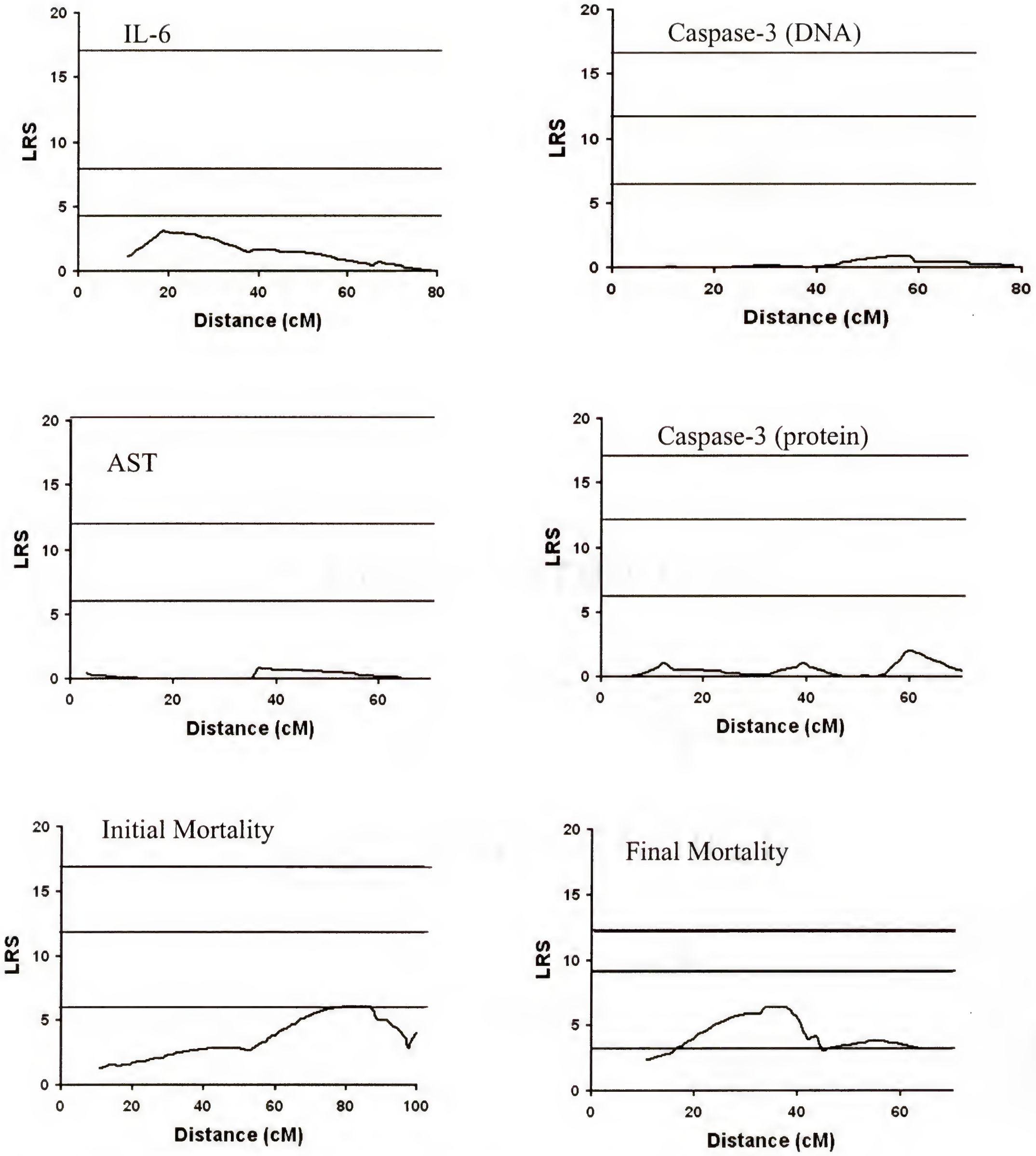

Figure 3-21. Comparison of Interval Mapping Data From Chromosome 8 Using All Phentoypes.

chromosome 8 using caspase-3-like activity data revealed very low LRS scores below 1.0 and thus no similarities were observed between this phenotype and the mortality analysis.

Interval mapping analysis of mortality data revealed a suggestive locus at the distal end of chromosome 11 at marker D11Mit179 associated with increased mortality

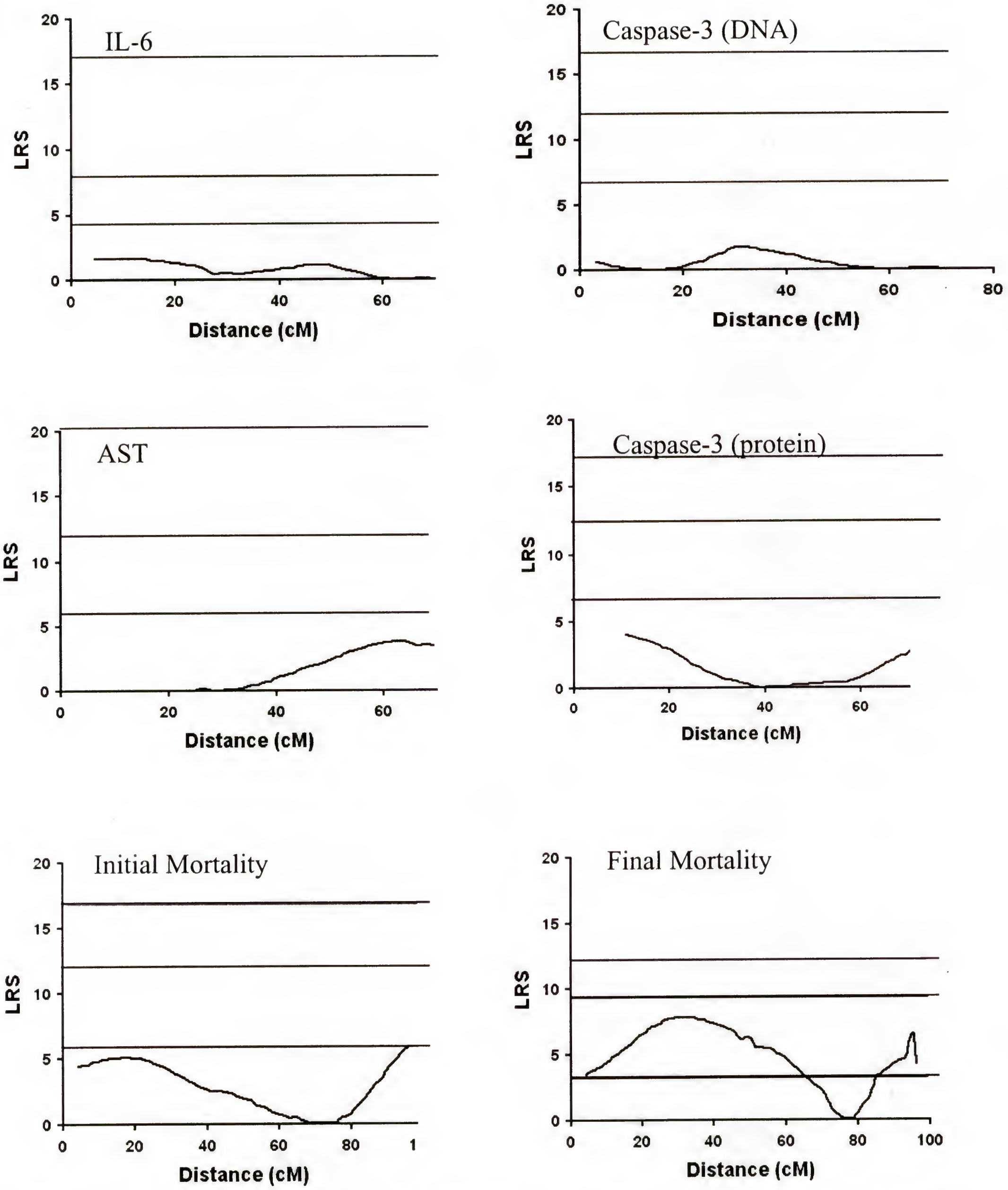

Figure 3-22. Comparison of Interval Mapping Data From Chromosome 11 Using All Phenotypes.

(susceptibility locus) (figure 3-22). In addition, a locus between markers D11Mit2 and D11Mit164 at the proximal end of the chromosome was associated with decreased mortality with a peak LRS of 7.8. Interval mapping of chromosome 11 using AST data revealed increased LRS scores between markers D11Mit179 and D11Mit258 (figure 3-22) associated with decreased AST levels. Interestingly, loci on the distal end of chromosome 11 identified in the interval mapping analysis of AST and mortality phenotypes were associated simultaneously with increased mortality and decreased AST levels indicating that the gene or genes mapped to this interval contributing to these two distinct traits may not be the same.

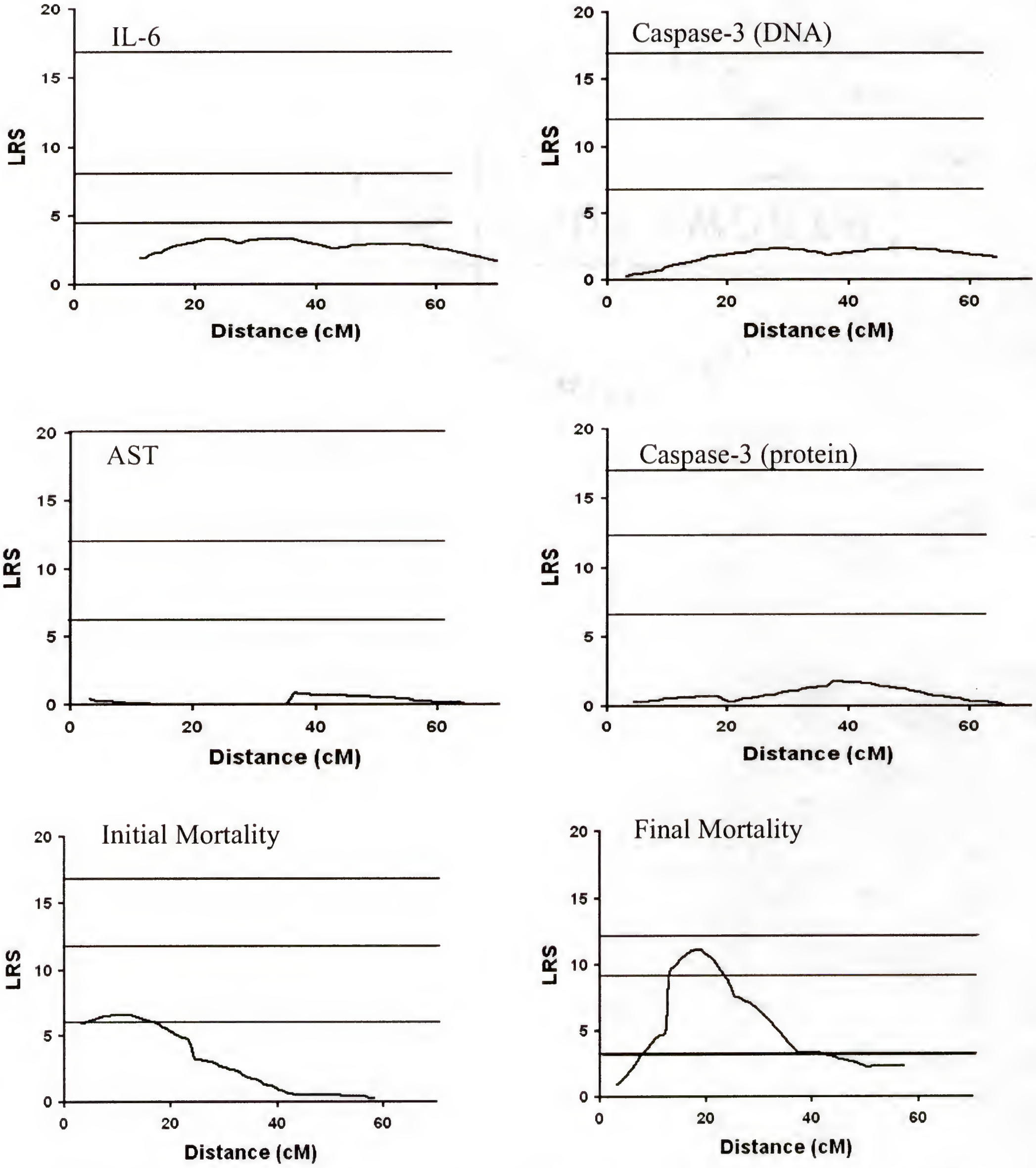

Figure 3-23. Comparison of Interval Mapping Data From Chromosome 13 Using All Phentoypes.

Interval mapping analysis of chromosome 11 using IL-6 data revealed only increases in LRS at D11Mit2 with a peak LRS of 1.6. Despite the very low LRS score (1.6), the trend toward increasing LRS scores was similar in chromosome 11 interval mapping of the IL-6 and mortality data (figure 3-22). In addition, caspase-3 (normalized for DNA content) data revealed a peak LRS of 1.7 between D11Mit164 and D11Mit339, unlike mortality data interval mapping analysis. Interestingly, caspase-3 (protein) data revealed different loci at D11Mit2 (peak LRS=4.0) and at the distal end of the chromosome associated with marker D11Mit168 (peak LRS=3.4) similar to interval mapping analysis of mortality data (figure 3-22).

Mortality data revealed that a locus between markers D13Mit61 and D13Mit99 was significantly associated with this trait with an LRS score of 11.1 (figure 3-23). Interval mapping analysis of chromosome 13 using IL-6 data revealed that LRS scores increased in the interval between markers D13Mit61 and D13Mit99 (peak LRS 3.3) and was associated with decreased IL-6 levels in response to rhTNFα and D-GalN. Though these LRS values were not suggestive or significant, the trend toward increasing LRS at this locus was similar to interval mapping of chromosome 13 using mortality as a phenotype. In addition, peak LRS score of 2.3 between markers D13Mit61 and D13Mit99 were also observed using the caspase-3 phenotype for interval mapping analysis of chromosome 13. The suggestive locus associated with mortality on chromosome 13 located between D13Mit61 was not strongly associated with the other phenotypes; however, a trend of higher LRS scores in this region was observed (figure 3-23).

Overall comparisons of interval mapping data using all phenotypes revealed that a susceptibility locus on distal chromosome 1 was associated primarily with increased liver apoptosis, but may also be associated with an increased proinflammatory response (as measured by serum IL-6 levels). In addition, another locus localized to the proximal region of chromosome 1 was associated predominantly with decreased liver injury (as measured by serum AST levels) but may also be associated with decreased proinflammatory response.

In contrast, a region on distal chromosome 5 was found to only associate with decreased apoptosis (as measured by caspase-3-like activity). Additionally, interval mapping data revealed that the resistance locus mapping to the proximal portion of chromosome 13 was primarily associated with decreased mortality in response to rhTNFα and D-GalN treatment with a significant LRS score of 11.1.

Interestingly, a locus on distal chromosome 11 was associated with increased mortality but decreased liver injury. Interval mapping of chromosome 11 using mortality and AST data revealed slightly different map locations. Using AST data, the region was mapped closer to marker D11Mit258 with an LRS of 3.8 while mortality data was localized to the more distal region of the chromosome associated with marker D11Mit168 with a suggestive LRS of 6.5. Another locus associated with decreased mortality having a peak LRS score of 7.8 was located between markers D11Mit2 and D11Mit164 and was also associated with decreased apoptosis, but only as measured by protein normalized and not DNA normalized caspase-3-like activity levels. The difference in location may also indicate that different genes are affecting these two phenotypes, but they happen to be located in similar regions of the chromosome.

Moreover, interval mapping of chromosome 16 revealed a suggestive association between a locus near marker D16Mit158 and decreased liver injury. In addition, increasing LRS scores were observed at this locus with interval mapping analysis using caspase-3 data as well as with the initial mortality data. Therefore, this locus is likely to be associated with decreased liver injury, decreased apoptosis, and increased survival in response to rhTNFα and D-GalN treatment. Finally, a locus on chromosome 8 was associated with decreased mortality, but was not associated with any other phenotype. Interestingly, another locus on chromosome 8 was revealed with interval mapping using

IL-6 data. With a peak LRS of 3.1 at marker D8Mit189, , this locus approached the suggestive level for these data (suggestive LRS=4.4).

Overall, marker regression analysis and interval mapping data suggested that the resistance of NOD mice to rhTNFα and D-GalN-mediated liver injury, apoptosis and death is likely to be a polygenic trait, with loci on multiple chromosomes (1, 5, 8, 11, 13, and 16) potentially contributing to various aspects of the overall phenotype. However, only the mortality phenotype revealed loci significantly associated with the trait. Both simple and composite interval mapping revealed a significant locus associated with decreased mortality located on chromosome 13 between markers D13Mit61 and D13Mit99. In addition, composite interval mapping of chromosome 8 revealed that marker D8Mit80 was significantly associated with resistance to death in response to rhTNFα and D-GalN treatment. Also, composite interval mapping of chromosome 11 revealed a significant locus at marker D11Mit168 associated with susceptibility to death in this model, as well as a locus between D11Mit2 and D11Mit339 associated with resistance to mortality.

Despite the lack of significant loci in the additional phenotypic analyses (AST, caspase-3, IL-6), further comparative analysis of mapping data for all phenotypes suggested that several loci may be associated with more than one phenotype indicating common pathways or mediators may be involved. Examination of candidate genes revealed that several Idd loci and various TNF-related signaling molecules were located in regions associated with increased LRS scores (see Table 4-1). Interestingly, chromosomes 1, 5, 11, and 13 contain Idd loci contributing to various aspects of diabetes in NOD mice and these, as well as other candidate genes/loci will be discussed extensively in the following chapter.

CHAPTER 4
SUMMARY AND CONCLUSIONS

Characterization of the Resistance of NOD Mice to Liver Injury and Lethality

This work primarily focused on the characterization of the differential responsiveness of NOD mice to rhTNFα and D-GalN-mediated liver injury and lethality as well as the underlying genetics of this resistance phenotype. While data from various laboratories have revealed that adult NOD mice are resistant to a variety of pathogens (Serreze and Leiter 2001), we have shown here that NOD mice are markedly less susceptible to both LPS or rhTNFα and D-GalN-mediated liver injury and death when compared to B6 mice. In contrast, no differences were observed in the responsiveness of NOD and B6 mice to the lethal hepatotoxic effects of the Fas agonist antibody, Jo-2. In fact, NOD mice appeared more sensitive to Jo-2 induced mortality than B6 mice though the differenes did not reach statistical significance. In addition, primary hepatocytes isolated from NOD mice and cultured in the presence of rhTNFα and D-GalN were also resistant to cell death and displayed less caspase-3 activity than hepatocytes from B6 mice. In contrast, Jo-2-induced cell death was equivalent in primary hepatocytes from both B6 and NOD mice treated in vitro. All of these data indicate that NOD mice are uniquely resistant to rhTNFα and D-GalN-mediated lethality and the intermediates involved in resistance are likely to be independent of signaling molecules common to the Fas death receptor signaling pathway. In addition, the resistance of NOD mice to rhTNFα-mediated lethality is likely due to differential responsiveness of NOD hepatocytes to rhTNFα and D-GalN treatment.

Moreover, (NODxB6) F1 heterozygotes were not resistant to rhTNFα and D-GalN-mediated lethality suggesting the differential responsiveness of NOD mice was a recessive trait. While lower serum AST levels, liver caspase-3-like activity, and TUNEL positive hepatocyte nuclei were always seen in F1 mice compared to the B6 parental strain, the differences were not statistically significant differences. In contrast, NOD mice displayed a significantly reduced increase in AST concentrations and liver caspase-3-like activity, as well as fewer TUNEL positive hepatocyte nuclei when compared to both B6 and F1 mice. The intermediate phenotype of the F1 progeny suggests that the resistance of NOD mice is a polygenic trait and genetic analysis of recombinant progeny should reveal loci associated with this resistance phenotype.

Summary of QTL Mapping Data

In order to identify loci involved in the resistance of the NOD mouse, a QTL analysis was performed. Since our ultimate outcome was death in this model, but additional phenotypes increase the likelihood of success in QTL analysis, it was necessary to perform two independent studies using one group of backcross progeny for mortality determinations and another group for the analysis of apoptosis, liver injury, and cytokine production. Genetic analysis of the progeny of a backcross between (NODxB6) F1 and NOD mice revealed several suggestive and significant loci associated with the resistance of NOD mice to rhTNFα-mediated lethality. Quantitative trait locus mapping using mortality, AST levels, IL-6 levels, and caspase-3-like activity as the phenotypes was performed. Initial interval mapping analysis of 149 recombinant progeny using the mortality phenotype revealed only suggestive loci on chromosomes 8, 11, and 13; however, further simple and composite interval mapping of a total of 294 recombinant progeny using mortality as the phenotype revealed similar loci on chromosomes 8, 11, and 13 with increased LRS scores above the significant level. Resistance loci on chromosomes 8, 11, and 13 together explained 13% of the total trait variance. Quantitative trait locus mapping using AST levels, IL-6 levels, and caspase-3-like activity as phenotypes was also performed. Data revealed no significant associations, however, a locus on chromosome 5 associated with decreased caspase-3-like activity levels approached the significant level. Table 3-9 summarizes the results from interval mapping analyses of chromosomes 1, 5, 8, 11, 13, and 16 using the various phenotypes.

Overall comparisons of interval mapping data using all phenotypes revealed that the resistance locus mapping to the proximal portion of chromosome 13 was significantly associated with decreased mortality in response to rhTNFα and D-GalN treatment. In addition, loci on chromosome 11 were significantly associated with increased mortality and also decreased liver injury. A locus on chromosome 11 identified using mortality data was localized to the more distal region of the chromosome associated with marker D11Mit168 with a suggestive LRS of 6.5. Another locus associated with decreased mortality was located between markers D11Mit2 and D11Mit164 and was also associated with decreased apoptosis. The difference in location may also indicate that different genes are affecting these two phenotypes, but they happen to be located in similar regions of the chromosome. Finally, a locus on chromosome 8 was significantly associated with decreased mortality, but was not associated with any other phenotype.

In addition, interval mapping data using all phenotypes revealed that a suggestive locus on distal chromosome 1 suggested an association primarily with increased liver apoptosis. In contrast, a suggestive region on distal chromosome 5 was found to only associate with decreased apoptosis (as measured by caspase-3-like activity). Moreover, interval mapping of chromosome 16 revealed a suggestive association between a locus near marker D16Mit158 and decreased liver injury.

Diabetes Susceptibility (*Idd*) Loci and Candidate Genes

Examination of candidate genes in the identified QTL regions revealed that several diabetes susceptibility or *Idd* loci and various TNF-related signaling molecules were located in regions associated with increased LRS scores (Table 4-1). Chromosomes

1, 5, 11, and 13 have been shown to contain *Idd* loci contributing to various aspects of diabetes in NOD mice.

The most significant QTL identified in our studies was the interval between markers D13Mit61 (7.7cM) and D13Mit99 (25.1cM) on chromosome 13 mapping to 19cM. Interestingly, studies by McAleer et al. (1995) involving crosses of NOD mice with the related NON strain revealed that analysis of F2 progeny identified a new *Idd* locus (referred to as *Idd*14) linked to marker D13Mit61 with strong effects on diabetes susceptibility when homozygous for NOD alleles at this marker locus. Interestingly, our studies revealed that an interval involving the D13Mit61 marker was significantly associated with decreased mortality in response to rhTNFα and D-GalN treatment indicating that the diabetes susceptibility locus may contain genes contributing to both diabetes and the resistance phenotype observed in NOD mice. However, there has been no further mapping of the *Idd*14 diabetes susceptibility locus to date and no specific genes have been identified in this interval to be associated with diabetes in NOD mice.

Another significant region identified by interval mapping of chromosome 11 and found to be associated with the resistance of NOD mice to mortality in response to rhTNFα and D-GalN was mapped to a region between markers D11Mit2 and D11Mit164 at approximately 30cM. Studies by Grattan et al. (2002) demonstrate that genetic control of the unresponsiveness of T-cell to proliferative stimuli in NOD mice is linked to a locus on chromosome 11 referred to as *Idd*4. Congenic mapping of NOD.B6/Idd4 diabetes-resistant mouse strains have shown that *Idd*4 is confined to a 5.2-cM interval of chromosome 11 (Grattan et al. 2002). This region was mapped between markers D11Nds1 (43.8 cM) and to an interval between markers D11Mit38 and D11Mit325 (49.0 cM), which dramatically reduces the development of both insulitis and type 1 diabetes.

As with the *Idd*5 locus discussed later in this chapter, data suggest that diabetes resistance conferred by *Idd*4 is mediated by two loci. *Idd*4.1 has been associated with the marker D11Nds1 and this interval influences the incidence of both diabetes and insulitis

Table 4-1. Candidate Genes For Chromosomes 1, 5, 8, 11, 13, and16.

Chromosome	cM Position	Name
1	30.1	*CD152*
1	30.1	*CD28*
1	30.1	*cflar* , FADD-like apoptosis regulator
1	30.1	*cas8* , Caspase-8
1	40	*idd5* , insulin dependent diabetes susceptibility 5
5	syntenic	*idd15,* insulin dependent diabetes susceptibility 15
5	65	*nos1,* nitric oxide sythase,1
8	26	*tradd* , TNF receptor associated protein with death domain
8	33.6	*ap1* , activator protein 1
8	51	*cas3* , caspase-3
11	44	*Idd4* , insulin dependent diabetes susceptibility 4
11	55	*galgt2* , UDP-N-acetyl-alpha-D-galactosamine
11	75	*grb2* , growth factor receptor bound protein 2
13	syntenic	*Idd14* , insulin dependent diabetes susceptibility 14
13	16	*ripk1,* receptor (TNFRSF)-interacting serine-threonine kinase
13	26	*edn1* , endothelin 1
16	26.9	*CD86*
16	28	*CD80*

(Grattan et al. 2002). Additionally, *Idd*4.2 was localized between markers D11Mit38 and D11Mit325 and primarily plays a role in diabetes incidence and appears to restore T-cell proliferative responsiveness (Grattan et al. 2002). Interestingly, a QTL analysis for experimental allergic encephalomyelitis (EAE), the primary animal model of the human autoimmune disease multiple sclerosis, was localized to the same region on chromosome 11, and is referred to as the *eae*7 locus (Butterfield et al. 1998).

The genes influencing diabetes and EAE in the Idd4 susceptibility locus have yet to be elucidated; however the *Idd*4 region contains three potential candidate genes coding for platelet activating factor acetylhydrolase Ib1, nitric oxide synthase-2, and CC chemokine genes, which are localized in the 5.2-cM interval (Grattan et al. 2002). While our region was mapped closer to the proximal end of the chromosome closer to 30cM, the imprecise nature of interval mapping in locating the position of QTL on a chromosome makes the genes contained within the *Idd4* locus remain interesting candidates for the resistance of NOD mice to rhTNFα-mediated liver injury and lethality.

One of our identified QTL regions having only a suggestive association with decreased apoptosis and liver injury in our model mapped to chromosome 1 between markers D1Mit103 and D1Mit8 mapping to approximately 40cM associated with decreased liver injury (AST levels) and decreased proinflammatory response (IL-6 levels) is a region that has been found to contain a diabetes susceptibility locus, *Idd5*. *Idd5* has been localized to chromosome 1 and has been recently shown to contain two loci, *Idd5*.1 and *Idd5*.2. *Idd5*.1 is the candidate homolog for the human *IDDM*12 locus and this region has been reduced in the mouse to an interval spanning only 5cM (Lamhamedi-Cherradi et al. 2001). This interval does not include Cas8 and Cflar candidate genes, but does include *Cd28* and *Ctla4*. Interestingly, NOD mice express lower levels of *Ctla4*; however, *Ctla4* NOD congenic mice having the *Idd5*.1 region from C57BL/6 mice retained this low level of expression indicating that this locus does not independently control the defective *Ctla4* expression in NOD mice (Lamhamedi-Cherradi et al. 2001).

These congenic mice also reveal that the *Idd5*.1 locus does not prevent infiltration of inflammatory cells into islets of Langerhans even though it did prevent diabetes in these animals (Lamhamedi-Cherradi et al. 2001). Also, prediabetic splenocytes from NOD and *Idd5*.1 congenic mice were both capable of inducing diabetes in immunodeficient NOD.scid/scid mice (Lamhamedi-Cherradi et al. 2001). These data indicate that this locus may control late events of the development of diabetes, subsequent to insulitis and possibly involve events that transpire in the islets of Langerhans. The identity and role of genes in the *Idd5* region in diabetes have yet to be determined, however, this region continues to be extensively examined and will eventually reveal genes involved in this disease.

Moreover, the role of *Idd4* and *Idd5* loci in the resistance of NOD mice was examined in our studies using the B6.NOD/c11 (Idd4), B6.NOD/c1t and B6.NOD/c1c

(*Idd5*) mice (see ((Yui et al. 1996) for chromosome maps for congenic mice). The B6.NOD/c1t and B6.NOD/c1c mice carrying overlapping NOD derived chromosome 1 intervals (Yui et al. 1996) including the Idd5 locus (as well as our identified QTL located at approximately 30cM) on a B6 background allowing for the specific examination of the independent involvement of this chromosome 1 interval with disease. Interestingly, despite the identification of this locus in our QTL mapping analysis our studies found no difference in responsiveness to rhTNFα and D-GalN-mediated lethality between B6.NOD/c1t or B6.NOD/c1c mice and B6 controls indicating little involvement of this locus in the overall mortality phenotype in this setting.

Similarly, the B6.NOD/c11 mouse carrying the Idd4 locus from the NOD mouse on a mostly B6 background was no different that the B6 parental strain in the mortality phenotype. However, it is important to note that these congenic mice carried NOD intervals on a B6 background indicating that perhaps the influence of this locus is contingent upon the extent of NOD background genes (such is the case for our recombinant mice derived from F1xNOD cross giving a pool of 75% NOD alleles in the BC1 progeny). Therefore, analysis of this locus using reciprocal congenic mouse carrying chromosome 1 and 11 intervals containing the Idd5 and Idd4 loci, respectively, on a mostly NOD background or progeny from an F2 cross allowing for increased presence of background homozygous NOD alleles may reveal a more pronounced role for this locus in the resistance phenotoype of the NOD mouse.

Another nearly significant locus associated with decreased caspase-3-like activity was associated with marker D5Mit161. Again, McAleer et al. (1995) identified a locus referred to as *Idd*15 associated with marker D5Mit48 located on chromosome 5 from analysis of the progeny of an F2 cross between NOD and the related NON mouse. This locus was found to associate with diabetes susceptibility, however, the data was only suggestive and did not reach the level of significant. Similarly, this was also the level of association (highly suggestive) seen in our studies as well indicating that this locus may be below the level of detectability with standard mapping techniques and our experimental design. The similarities between these data suggest, however, that this locus may be involved in both diabetes susceptibility and the resistance of NOD to rhTNFα and D-GalN mediated lethality despite the lack of statistical significance.

The question remains as to whether or not the chromosomes containing *Idd* loci identified in our mapping analyses contain genes common to both diabetes and resistance in our model of liver injury and death. It is apparent that the putative location of QTLs identified in our studies do not exactly coincide with the location of the previously mapped *Idd* loci. Traditionally the position where the maximum LOD score is detected is posited as the position of the QTL and the interval where the LOD score is within one LOD unit of the maximum is taken as a 96.8% confidence interval (Lander, E. S. and Botstein 1989). In general, this method of QTL region localization gives accurate predictions only for very strong QTLs, since the LOD scores for weaker QTLs does not follow a c2 distribution (Manly and Olson 1999). The strength of the QTL being mapped is critical to establishing an accurate location and thus weaker QTLs can typically only be associated with a particular chromosome and not mapped with any more exactness (Darvasi et al. 1993; Visscher et al. 1996). In fact, weak QTLs, which account for a few percent of the trait variance, may require up to several hundred progeny for a 50%chance of detection (Darvasi,1998). Even strong QTLs can only be resolved in a large backcross or intercross analysis to regions of about 11cM according to Darvasi et al. (1993). Given these data it is apparent that the identification of the actual location of a QTL using interval mapping techniques is imprecise enough to implicate nearby *Idd* loci as potentially interesting candidates.

QTL mapping is also often imperfect in its ability to locate linked QTL. In fact, further analysis of congenic mice have revealed that the *Idd*4 and *Idd*5 loci actually contain multiple QTL within the mapped interval (Grattan et al. 2002, (Lamhamedi-Cherradi et al. 2001). Since interval mapping essentially estimates the intervals between markers with the assumption that there is only one QTL segregating it cannot separate any linked QTL unless they are of opposite sign (have opposite effects). For example, in our studies a locus on distal chromosome 11 linked to marker D11Mit168 was associated with increased susceptibility to mortality in our mapping analysis. In addition, a locus between markers D11Mit2 and D11Mit164 was associated with decreased mortality in our mapping studies. Interestingly, the interval between the two loci found was found to possibly contain a third locus with data derived from composite interval mapping of chromosome 11 using D11Mit179 (a marker between the two identified loci of opposite sign) as a background locus. While QTL mapping does not allow for the resolution of these two loci given that they are both resistance loci in adjacent intervals, these data introduce the possibility of the existence of multiple loci and thus must await further confirmation using congenic mice.

Since studies examining the genetics of diabetes in the NOD mouse using congenic mice have suggested that the overall genomic background of the animal influences the contributions of susceptibility loci, further analysis of congenic strains having mostly NOD background genes (NOD.B6 congenics) would likely determine if the loci on chromosomes 1, 5, 11 and 13 are involved in the resistance or susceptibility of NOD mice to rhTNFα and D-GalN-mediated liver injury, liver apoptosis, and lethality.

In addition to the Idd loci, various candidate genes have been identified in the regions suspected of contributing to the resistance of the NOD mouse to rhTNFα and D-GalN treatment (see table 4-1). Since this model is dependent upon TNF signaling through the type 1 TNF receptor, the most interesting genes may be those related to TNF-mediated signaling. For example, chromosome 1 contains the *cflar* gene coding for the FADD-like apoptosis regulator or FLIP (flice-like inhibitory protein). This protein has been shown to be involved in the inhibition of the proximal caspase, caspase-8, in the TNF-mediated apoptotic cascade (see figure 1-2). However, this gene is also involved in Fas-mediated apoptosis and thus may not be involved in our phenotype due to the senesitivity of NOD mice to the Fas-agonist, Jo-2. In addition, the gene encoding the caspase-8 protein is also located on chromosome1 and thus remains an interesting candidate.

Candidate genes on chromosome 8 coding for the proteins *TRADD*, *AP-1* and *caspase-8* are particularly interesting since they are all important signaling molecules in the TNF receptor pathway. All of these proteins are involved in TNF-mediated signaling and thus further examination of these genes and their involvement in the resistance of NOD mice is warranted. Candidate genes on chromosomes 13 included *ripk1* (receptor (TNFRSF)-interacting serine-threonine kinase and *edn1* (endothelin 1), while candidates on chromosome 16 included *CD80* and *CD86*, respectively. There are scores of genes located on the identified chromosomes that could be posited as the gene influencing resistance in the NOD mouse; however, without more precise localization of the putative QTL, it is difficult to speculate on the identity of the contributing genes.

In addition, the putative gene may involve the anti-apoptotic pathways induced by TNFα signaling. The role of NF-κB in cell survival and the proinflammatory response makes this protein complex a good candidate for study. NF-κB activation prevents apoptosis in our liver injury model; , therefore, aberrant or enhanced activation of this pathway would be consistant with the resistance phenotype of the NOD mouse. Interestingly, recent studies suggest that NOD mice have a defect in proteosome function leading to an impaired proteosome-mediated degredation of the NF-κB inhibitor IκBa as well as processing of the p105 and p100 precursor molecules which result in the production of the active p50 or p52 subunits (Hayashi and Faustman 1999; 2000). These subunits are components of the active NF-κB heterodimer which can be composed of either p50, p52, or p65 (RelA) subunits.

The proteosome is a multiprotein complex catalyzing the degradation or processing of intracellular proteins such as the NF-κB subunits. Data from studies in NOD mice suggest that defective expression of a key subunit of the proteosome LMP2, which is involved in the selective degradation of self-proteins for presentation in the binding groove of MHC molecules, may lead to a deranged production of self-peptides by the proteosome (Hayashi and Faustman 1999; 2000). In contrast to our studies, Hayashi et al. found that T cells from NOD mice were susceptible to TNFα -mediated apoptosis and concluded that this sensitivity was due to defective production of NF-κB dependent survival genes (Hayashi and Faustman 1999; 2000). Despite the fact that the data suggest that defective LMP2 expression paralleled disease progression, these data regarding the defect in NF-κB activation in NOD mice are conflicting. Data from other groups have shown that the LMP2 subunit may not be necessary for the production of the mature p50 protein in T cells (Hayashi and Faustman 1999; 2000). Also, data suggest that the Balb/c control mouse used in the previous studies in comparison with NOD mice expresses higher levels of LMP2 than other control strains, particularly the B6 mouse, indicating that the conclusions drawn from these studies may be inappropriate (Hayashi and Faustman 1999; 2000). Nevertheless, the role of NF-κB in prevention of apoptosis and the fact that D-GalN does not fully inhibit transcription in our liver injury model makes this an attractive candidate for the resistance in the NOD mouse.

While we can speculate on the likely role of immune and TNF-related candidate genes located in the genomic intervals implicated by our mapping analyses, it cannot be assumed that the resistance genes involved must be genes involved in immunity. While this is likely to be the case for some, this may not be true for all loci. In addition, since most Idd loci have been found to contain multiple genes contributing to diabetes, the fact that our linkage analysis reveals similar associations does not necessarily imply that common genes are involved in our phenotype. Therefore, in order to speculate on the actual genes involved in this resistance of NOD mice to rhTNFα and D-GalN-mediated treatment, it is necessary to first narrow the intervals to a manageable distance in order to further determine the role of specific candidate genes.

Lessons from QTL Mapping Studies in Other Mouse Models

Similar studies investigating the resistance of DBA/2 mice to a high dose TNFα model of lethal shock have revealed loci involved in this phenotype using BxD recombinant inbred mice. Unlike the NOD mouse, the resistance of DBA/2 mice was dominant since (C57BL/6 x DBA/2)F1 mice were also resistant. The resistance to TNFα mapped to loci including candidate genes for corticosteroid-binding globulin (*Cbg*), alpha1-protease inhibitor *(Spi1)*, contrapsin (*Spi2*) and the contrapsin-regulating gene *Spi2r* that form a gene cluster on chromosome 12 (Libert et al. 1999). These studies, unlike ours, uses a model that is more complex and thus loci implicated in the disease phenotype are likely to be very different from the loci identified in our studies. This model uses murine TNFα and thus involves signaling via both TNF receptors (Brouckaert et al. 1989; Brouckaert et al. 1992). Data suggests that the physiological and molecular mechanisms involved in the high dose TNF and LPS models are very different from that involved in the lethality induced by the D-GalN models indicating that genetic studies involving these separate models are not comparable (Mignon et al. 1999)..

Addiitional studies describe the hyporesponsiveness of SPRET/Ei mice to lethal shock induced by TNFα. An interspecific backcross experiment using B6 and SPRET/Ei mice revealed that the TNF resistance is linked to intervals on chromosomes 2, 6, and 11 (Staelens et al. 2002). Since chromosome 11 was also identified as containing potential resistance loci in our studies as well as in diabetes, this locus may contain similar genes involved in both resistance phenotypes. As stated previously, however, the size of the intervals identified via QTL analysis are quite large and estimates of location are flawed. Therefore the identification of similar chromosome associations with any two given phenotypes can occur by chance.

Other experimental approaches that would likely reveal mediators involved in the resistance of NOD mice involve the examination of the responsiveness of NOD mice to other TNFα -mediated models of disease. For instance, injection of the superantigen staphylococcal enterotoxin B (SEB) and D-GalN produces a similar hepatic injury in mice (Nagaki et al. 1994). Furhermore, injection of anti-TNFα neutralizing monoclonal antibodies protected animals from injury indicating that this model is dependent upon TNFα signaling (Nagaki et al. 1994). Another well-described model of hepatitis in mice involves the injection of concanavalin A (ConA) which produces a phenotype similar to both the SEB and rhTNFα with D-GalN models. However, an important difference between our model and both the ConA and SEB models is that these models depend upon the presence of T cells (Nagaki et al. 1994; Aroeira and Martinez 1999). Nevertheless, the requirement for TNFα signaling in all of these models allows for the further characterization of possible defects in the TNFα signaling pathway in the NOD mouse.

Conclusions

In the past two years, significant efforts have been taken to identify genetic susceptibilities to human diseases, and considerable research interest has been focused on TNFα polymorphisms and their role in various disease processes. These studies have indeed revealed that hospitalized patients with TNFα polymorphisms have varying susceptibility to a variety of inflammatory diseases and autoimmune diseases, including multiple sclerosis, type 1 immune hepatitis, primary sclerosing cholanitis, and systemic lupus erythematosis (Kaijzel et al. 1998; Mycko et al. 1998; Bernal et al. 1999; Czaja et al. 1999; Komata et al. 1999; Li Kam Wa et al. 1999; Mira et al. 1999). These clinical studies in particular have attracted a great deal of attention with both the scientific and lay-press, but they too are often limited to confirming the importance of previously identified mediators and pathways. Additionally, these types of polymorphisms often account for disease in only a limited portion of the patient population. There has been, at present, very little investigation into genetic polymorphisms in TNFα signaling pathway molecules and their relationship to human disease; however these polymorphisms surely exist and may contribute to susceptibility or resistance to TNFα-mediated diseases.

Moreover, genetic approaches using knockout and transgenic mice have been frequently used to identify the contribution of individual gene products and specific signal transduction pathways in TNFα-mediated injury. While effective, these techniques are inherently limited because they identify only the contribution of known genes involved in previously described TNFα-dependent pathways.

Though much progress in the past decade, present knowledge of pathways and mediators involved in TNFα-mediated apoptosis is incomplete. In fact, data suggests that TNFα signaling occurs in a cell-specific manner and thus generalized functions cannot be easily assigned to the various signaling molecules . Therefore, it is clear that considerable work will be required before TNFα signal transduction in hepatocytes and other cell populations is fully understood.

Although a wealth of information exists regarding TNFα signal transduction pathways, the majority of this data was derived from in vitro studies with various cell lines. Few studies have examined TNFα signaling in great detail in primary hepatocytes, therefore, the aberrant TNFα response seen in the NOD mouse also provides an ideal dys-regulated system for analysis of hepatocyte-specific TNFα signaling pathways. Detailed analysis of the functions of known TNF receptor-associated signaling proteins in NOD and B6 mice may reveal previously unidentified defects in intracellular signaling and provide new avenues of research in the study of human autoimmune diabetes and TNFα-mediated apoptosis. It is clear that in order to consider specific pathways in TNFα signaling as possible therapeutic targets, considerable research must be performed to create a better understanding of these pathways and their significance in acute inflammation. All of this information eventually may provide the basis for a rational pharmacological approach aimed at abrogating the undesirable effects of TNFα, while leaving other more beneficial aspects of TNF signaling unaffected. In addition, these studies will provide novel information about TNFα signaling defects in the NOD mouse and may give insight into the role of these defects in diabetes.

Furthermore, target genes identified from these studies can be probed mechanistically for their function and applied simultaneously to the analyses of human populations for their contribution to related clinical syndromes. Our approach aimed to ultimately identify resistance or susceptibility loci in the NOD mouse conferring survival to TNFα and D-GalN-induced liver injury and mortality. The identification of potential resistance or susceptibility loci and ultimately individual resistance or susceptibility genes, provides the opportunity to examine human populations for similar polymorphisms. These data could provide for better diagnosis and treatment of patients by providing the opportunity to administer patient-specific therapy based on the presence or absence of particular genetic polymorphisms. In addition, the identification of these genes may provide novel therapeutic targets for treatment of TNFα-mediated diseases.

Additionally, since the NOD mouse is a murine model of human diabetes and TNFα has been suggested to play a role in this disease, the information obtained from these studies may be useful in elucidating the associated mechanism of autoimmunity. One of the major limitations in the identification of susceptibility loci in diabetes has been the incomplete knowledge of the complex molecular events involved in the initiation and progression of diabetes in NOD mice. While much progress has been made concerning the immune defects present in the NOD mouse, it is unclear as to how to determine the contributions of the many susceptibility loci due to the difficulty in the phenotypic analysis of this complex disease trait. Importantly, given that some of the loci identified in our studies were common to diabetes,. our findings could assist in the elucidation of candidate genes located in various Idd loci, since a clearer phenotypic analysis may be possible with the TNFα and D-GalN model system. If indeed loci such as Idd4, 5, 14, or 15 were examined in more detail using this model, it may allow for dissection of diabetes-related genes with more precision given the more quantitative and well-defined nature of our liver injury model.

While the genes accounting for the predisposition to disease in an animal model may not be identical to the loci involved in the human disease, understanding the mechanisms involved in disease susceptibility in animals may provide information about similar disease processes in humans. In addition, gaining an understanding of the many intracellular signaling molecules involved in various signaling pathways allow s for the regulation of these proteins by the manipulation of their intracellular concentrations the inhibition or promotion of their actions. These approaches aimed at regulation of particular portions of TNF receptor signal transduction pathways allow for the fine-tuning of TNFα-mediated cellular responses. The failure of many anti-TNFα therapies may have resulted from inhibition of the favorable proinflammatory response and thus signaling complexes may be a more attractive target for therapy, ultimately shifting the balance from one outcome to another resulting in a more beneficial response overall.

Recently, the targeted inhibition of intracellular signaling molecules has been proposed as a new therapeutic approach to the treatment of various diseases and disorders thought to arise from hypercytokinemia or aberrant proinflammatory responses, such as sepsis (Seino et al. 2001). Studies investigating the protective effect of a FADD dominant negative (DN) mutant using an adenoviral vector expressed in the livers of mice treated with Jo-2 or TNFα and D-GalN revealed that expression of the FADD (DN) mutant inhibited apoptosis while having no effect on NFkB activity (Seino et al. 2001). In addition, the FADD(DN) mutant ameliorated the T-cell-mediated liver injury seen with another TNFα-dependent model involving concanavalin A treatment of mice (Seino et al. 2001). Effectively, these studies suggest that this is a viable therapeutic approach provided the identity and function of key signaling molecules involved in chronic inflammatory diseases and liver injury are known.

As with studies of diabetes in the NOD mouse, the combination of further genetic mapping, identification and investigation of identified susceptibility or resistance loci using congenic strains and subsequent gene identification followed by sequencing data will ultimately lead to the understanding of the signaling pathways involved in the resistance of NOD mice to rhTNFα and D-GalN-mediated lethality and might possibly provide new intracellular targets for therapies.

APPENDIX A

MAP MANAGER QTX LINKS, SIMPLE INTERVAL MAPPING (SIM) AND COMPOSITE INTERVAL MAPPING (CIM) REPORTS

```
QT Links Report for Initial Mortality Analysis of 149
Recombinant Mice
QT Links report for set QT Links Report Initial QTL
mortality.TEXT(test)
Using quantitative trait mortality1
Chi Square Stats, P = 0.05
Additive regression model
With no control for other QTLs.

Significance determined by 1000 permutations
SUGGESTIVE:  6.1
SIGNIFICANT: 12
HIGHLY SIG : 17


140  to  149  informative progeny  from Progeny Order
Internal
 Chr            Locus        Stat  %     P      Add
chrom2       :: D2MIT92      0.2   0  0.64082    0.04
chrom2       :: D2MIT7       1.6   0  0.21167   -0.10
chrom2       :: D2MIT17      0.0   0  0.93902   -0.01
chrom2       :: D2MIT48      0.5   0  0.49724   -0.05
chrom3       :: D3MIT267     0.3   0  0.61516    0.04
chrom3       :: IL2          0.0   0  0.91344    0.01
chrom3       :: D3MIT12      0.5   0  0.46357    0.06
chrom3       :: D3MIT200     0.2   0  0.67848    0.03
chrom3       :: D3MIT116     0.2   0  0.62541    0.04
chrom4       :: D4MIT1       3.8   2  0.05026    0.16
chrom4       :: D4MIT178     0.9   0  0.34594    0.08
chrom4       :: D4MIT12      1.3   0  0.25314    0.09
chrom5       :: D5MIT268     0.2   0  0.68394    0.03
chrom5       :: D5MIT205     0.0   0  0.95945   -0.00
chrom5       :: D5MIT161     0.5   0  0.47235   -0.06
chrom6       :: D6MIT8       1.6   0  0.21242    0.10
```

```
chrom6        :: D6MIT254     3.5   2  0.05960     0.15
chrom6        :: D6MIT14      1.8   1  0.18063     0.11
chrom7        :: D7MIT180     0.3   0  0.59514    -0.04
chrom7        :: D7MIT270     0.4   0  0.54950    -0.05
chrom7        :: D7MIT324     0.0   0  0.86490    -0.01
chrom7        :: D7MIT105     0.1   0  0.78974     0.02
chrom9        :: D9MIT296     1.8   1  0.18063     0.11
chrom9        :: D9MIT162     0.2   0  0.64082     0.04
chrom9        :: D9MIT50      0.4   0  0.54395     0.05
chrom10       :: D10MIT189    0.6   0  0.43997     0.06
chrom10       :: D10MIT96     0.5   0  0.46882     0.06
chrom10       :: D10MIT259    0.5   0  0.46167     0.06
chrom11       :: D11MIT2      4.4   2  0.03586     0.17
chrom11       :: D11MIT339    2.5   1  0.11423     0.13
chrom11       :: D11MIT179    0.4   0  0.54766     0.05
chrom11       :: D11MIT168    6.2   3  0.01259    -0.20
chrom12       :: D12MIT2      4.7   2  0.02975     0.17
chrom12       :: D12MIT233    0.0   0  0.87658     0.01
chrom12       :: D12MIT14     3.3   2  0.06858     0.15
chrom13       :: D13MIT61     5.9   3  0.01517     0.20
chrom13       :: D13MIT99     3.3   2  0.06961     0.15
chrom13       :: D13MIT36     0.6   0  0.43785     0.06
chrom13       :: D13MIT151    0.3   0  0.59315     0.04
chrom14       :: D14MIT207    0.5   0  0.49045     0.06
chrom14       :: D14MIT121    0.0   0  0.95030    -0.01
chrom14       :: D14MIT102    0.1   0  0.72617     0.03
chrom14       :: D14MIT95     3.4   2  0.06667     0.15
chrom15       :: D15MIT55     0.6   0  0.42228     0.06
chrom15       :: D15MIT41     0.0   0  0.95153     0.01
chrom15       :: D15MIT29     1.0   0  0.31623     0.08
chrom16       :: D16MIT108    1.5   0  0.22733     0.10
chrom16       :: D16MIT4      1.4   0  0.23768     0.10
chrom16       :: D16MIT158    4.7   2  0.02938     0.18
chrom17       :: D17MIT27     1.9   1  0.16568    -0.11
chrom17       :: D17MIT152    2.0   1  0.15906    -0.11
chrom17       :: D17MIT130    0.7   0  0.40730    -0.07
chrom17       :: D17MIT68     2.4   1  0.12239    -0.12
chrom18       :: D18MIT17     0.6   0  0.44948     0.06
chrom18       :: D18MIT51     0.2   0  0.67087    -0.03
chrom18       :: D18MIT4      0.7   0  0.39159    -0.07
chrom19       :: D19MIT119    0.0   0  0.92246     0.01
chrom19       :: D19MIT60     0.0   0  0.83611    -0.02
chrom19       :: D19MIT1      0.1   0  0.74401     0.03
chrom1        :: D1MIT65      1.4   0  0.22866    -0.10
chrom1        :: D1MIT303     0.0   0  0.99682    -0.00
```

```
chrom1        :: D1MIT8      0.0   0  0.90114     0.01
chrom1        :: D1MIT15     0.8   0  0.37949     0.07
chrom1        :: D1MIT17     0.0   0  0.99682     0.00
chrom8        :: D8MIT94     1.3   0  0.25619     0.09
chrom8        :: D8MIT189    1.5   0  0.22238     0.10
chrom8        :: D8MIT261    2.7   1  0.09951     0.16
chrom8        :: D8MIT104    6.1   3  0.01374     0.20
chrom8        :: D8MIT106    5.1   3  0.02454     0.18
chrom8        :: D8MIT80     5.4   3  0.02042     0.19
chrom8        :: D8MIT40     2.9   1  0.09125     0.14
chrom8        :: D8MIT242    4.5   2  0.03430     0.18
```

SIM Reports for Chromosomes 8, 11, and 13 from Initial Mortality Analysis

```
SIMCHROMOSOME 8
Interval  mapping  for  Dataset:  initial mortality
analysis(test)
constrained additive regression,140  to  149  informative
progeny  from Progeny Order  Internal
mapping  QTL  mortality1   on  chr  chrom8
using  Kosambi  mapping  function
With no control for other QTLs.
                map        Stat        %      Add
D8MIT94         0.00       1.3         0      0.09
                0.01       1.4         0      0.10
                0.02       1.5         0      0.10
                0.03       1.6         0      0.10
D8MIT189        0.05       1.5         0      0.10
                0.06       1.5         0      0.10
                0.07       1.6         0      0.10
                0.08       1.6         0      0.11
                0.09       1.7         0      0.11
                0.10       1.7         0      0.12
                0.11       1.8         1      0.12
                0.12       1.8         1      0.12
                0.13       1.9         1      0.13
                0.14       2.0         1      0.13
                0.15       2.0         1      0.14
                0.16       2.1         1      0.14
                0.17       2.1         1      0.14
                0.18       2.2         1      0.15
                0.19       2.3         1      0.15
                0.20       2.3         1      0.16
                0.21       2.4         1      0.16
                0.22       2.5         1      0.17
```

	0.23	2.5	1	0.17
	0.24	2.6	1	0.17
	0.25	2.6	1	0.17
	0.26	2.7	1	0.18
	0.27	2.7	1	0.18
	0.28	2.8	1	0.18
	0.29	2.8	1	0.18
	0.30	2.8	1	0.18
	0.31	2.9	1	0.18
	0.32	2.9	1	0.18
	0.33	2.9	1	0.18
	0.34	2.9	1	0.18
	0.35	2.9	1	0.18
	0.36	2.9	1	0.18
	0.37	2.9	1	0.18
	0.38	2.9	1	0.17
	0.39	2.9	1	0.17
	0.40	2.8	1	0.17
D8MIT261	0.42	2.7	1	0.16
	0.43	2.9	1	0.17
	0.44	3.0	1	0.17
	0.45	3.2	1	0.18
	0.46	3.3	2	0.18
	0.47	3.5	2	0.19
	0.48	3.7	2	0.20
	0.49	3.8	2	0.20
	0.50	4.0	2	0.21
	0.51	4.2	2	0.21
	0.52	4.3	2	0.22
	0.53	4.5	2	0.22
	0.54	4.7	2	0.23
	0.55	4.8	3	0.23
	0.56	5.0	3	0.23
	0.57	5.1	3	0.24
	0.58	5.3	3	0.24
	0.59	5.4	3	0.24
	0.60	5.5	3	0.24
	0.61	5.6	3	0.24
	0.62	5.7	3	0.24
	0.63	5.8	3	0.24
	0.64	5.9	3	0.24
	0.65	5.9	3	0.24
	0.66	6.0	3	0.23
	0.67	6.0	3	0.23
	0.68	6.0	3	0.23

```
                0.69      6.1        3     0.23
                0.70      6.1        3     0.22
                0.71      6.1        3     0.22
                0.72      6.1        3     0.22
                0.73      6.1        3     0.21
                0.74      6.1        3     0.21
                0.75      6.1        3     0.20
D8MIT104        0.76      6.1        3     0.20
                0.77      5.7        3     0.20
D8MIT106        0.78      5.1        3     0.18
D8MIT80         0.80      5.0        3     0.18
                0.81      4.9        3     0.18
                0.82      4.7        2     0.18
                0.83      4.5        2     0.18
                0.84      4.2        2     0.17
                0.85      3.9        2     0.17
                0.86      3.6        2     0.16
D8MIT40         0.87      2.9        1     0.14
                0.88      3.5        2     0.16
                0.89      4.0        2     0.17
D8MIT36

SIM CHROMOSOME 11
Interval  mapping  for  Dataset:  QT Links Report Initial
QTL mortality.TEXT(test)
constrained additive regression,144  to  149  informative
progeny  from Progeny Order  Internal
mapping  QTL  mortality1   on  chr  chrom11
using  Kosambi  mapping  function
With no control for other QTLs.
                 map       Stat        %      Add
D11MIT2         0.00      4.4        2     0.17
                0.01      4.5        2     0.18
                0.02      4.5        2     0.18
                0.03      4.6        2     0.19
                0.04      4.7        3     0.19
                0.05      4.7        3     0.20
                0.06      4.8        3     0.20
                0.07      4.9        3     0.21
                0.08      4.9        3     0.21
                0.09      5.0        3     0.21
                0.10      5.0        3     0.22
                0.11      5.0        3     0.22
                0.12      5.1        3     0.23
                0.13      5.1        3     0.23
```

	0.14	5.1	3	0.23
	0.15	5.0	3	0.23
	0.16	5.0	3	0.23
	0.17	5.0	3	0.24
	0.18	4.9	3	0.23
	0.19	4.8	3	0.23
	0.20	4.7	3	0.23
	0.21	4.6	2	0.23
	0.22	4.5	2	0.22
	0.23	4.4	2	0.22
	0.24	4.3	2	0.21
	0.25	4.1	2	0.21
	0.26	4.0	2	0.20
	0.27	3.8	2	0.20
	0.28	3.7	2	0.19
	0.29	3.5	2	0.18
	0.30	3.4	2	0.18
	0.31	3.2	2	0.17
	0.32	3.1	1	0.16
	0.33	2.9	1	0.16
	0.34	2.8	1	0.15
	0.35	2.7	1	0.14
	0.36	2.6	1	0.14
	0.37	2.5	1	0.13
D11MIT339	0.39	2.5	1	0.13
	0.40	2.4	1	0.13
	0.41	2.4	1	0.13
	0.42	2.3	1	0.13
	0.43	2.2	1	0.13
	0.44	2.1	1	0.13
	0.45	2.0	1	0.13
	0.46	1.9	1	0.12
	0.47	1.8	1	0.12
	0.48	1.7	0	0.12
	0.49	1.5	0	0.11
	0.50	1.4	0	0.11
	0.51	1.3	0	0.10
	0.52	1.2	0	0.10
	0.53	1.0	0	0.09
	0.54	0.9	0	0.08
	0.55	0.8	0	0.08
	0.56	0.7	0	0.07
	0.57	0.6	0	0.07
	0.58	0.5	0	0.06
	0.59	0.4	0	0.05

```
D11MIT179       0.60      0.5        0      0.06
                0.61      0.4        0      0.05
                0.62      0.3        0      0.05
                0.63      0.2        0      0.04
                0.64      0.1        0      0.03
                0.65      0.1        0      0.03
                0.66      0.0        0      0.02
                0.67      0.0        0      0.01
                0.68      0.0        0     -0.00
                0.69      0.0        0     -0.01
                0.70      0.1        0     -0.02
                0.71      0.1        0     -0.03
                0.72      0.2        0     -0.05
                0.73      0.4        0     -0.06
                0.74      0.5        0     -0.07
                0.75      0.7        0     -0.08
                0.76      0.9        0     -0.10
                0.77      1.2        0     -0.11
                0.78      1.5        0     -0.12
                0.79      1.8        1     -0.13
                0.80      2.1        1     -0.14
                0.81      2.4        1     -0.15
                0.82      2.8        1     -0.16
                0.83      3.1        1     -0.17
                0.84      3.4        2     -0.18
                0.85      3.8        2     -0.18
                0.86      4.1        2     -0.19
                0.87      4.5        2     -0.19
                0.88      4.8        3     -0.19
                0.89      5.1        3     -0.20
                0.90      5.4        3     -0.20
                0.91      5.7        3     -0.20
                0.92      5.9        3     -0.20
D11MIT168

SIM CHROMOSOME 13
Interval  mapping  for  Dataset:  QT Links Report Initial
QTL mortality.TEXT(test)
constrained additive regression,146  to  149  informative
progeny  from Progeny Order  Internal
mapping  QTL  mortality1   on  chr  chrom13
using  Kosambi  mapping  function
With no control for other QTLs.
                map       Stat       %      Add
D13MIT61        0.00      5.9        3      0.20
```

	0.01	6.0	3	0.20
	0.02	6.2	3	0.21
	0.03	6.3	4	0.21
	0.04	6.4	4	0.22
	0.05	6.4	4	0.22
	0.06	6.5	4	0.23
	0.07	6.5	4	0.23
	0.08	6.5	4	0.23
	0.09	6.5	4	0.23
	0.10	6.4	4	0.23
	0.11	6.3	4	0.23
	0.12	6.2	3	0.23
	0.13	6.0	3	0.22
	0.14	5.9	3	0.22
	0.15	5.7	3	0.21
	0.16	5.5	3	0.21
	0.17	5.2	3	0.20
	0.18	5.0	3	0.19
	0.19	4.8	3	0.18
	0.20	4.6	2	0.18
D13MIT99	0.21	3.3	2	0.15
	0.22	3.2	1	0.15
	0.23	3.1	1	0.15
	0.24	3.0	1	0.15
	0.25	2.9	1	0.15
	0.26	2.7	1	0.14
	0.27	2.6	1	0.14
	0.28	2.4	1	0.14
	0.29	2.3	1	0.13
	0.30	2.1	1	0.13
	0.31	1.9	1	0.12
	0.32	1.7	0	0.12
	0.33	1.6	0	0.11
	0.34	1.4	0	0.10
	0.35	1.2	0	0.10
	0.36	1.1	0	0.09
	0.37	0.9	0	0.08
	0.38	0.8	0	0.07
D13MIT36	0.40	0.5	0	0.06
	0.41	0.5	0	0.06
	0.42	0.5	0	0.06
	0.43	0.5	0	0.06
	0.44	0.5	0	0.06
	0.45	0.5	0	0.06
	0.46	0.5	0	0.06

```
                0.47      0.5         0     0.06
                0.48      0.5         0     0.06
                0.49      0.4         0     0.06
                0.50      0.4         0     0.06
                0.51      0.4         0     0.06
                0.52      0.4         0     0.05
                0.53      0.4         0     0.05
                0.54      0.3         0     0.05
                0.55      0.3         0     0.05
D13MIT151

QT Links Report for Final Mortality Analysis of 294
Recombinant Mice
QT Links report for set SECONDWNEWPRSIMERS(SECOND)
Using quantitative trait MORTALITY
Chi Square Stats, P = 0.05
Additive regression model
With no control for other QTLs.

Significance determined by 1000 permutations
SUGGESTIVE:  3.5
SIGNIFICANT: 9.3
HIGHLY SIG : 12

261  to  294  informative progeny  from Progeny Order
Internal
 Chr             Locus          Stat  %      P         Add
CHROM11      :: D11MIT2         3.5   1  0.05980     0.11
CHROM11      :: D11MIT164       6.1   2  0.01372     0.14
CHROM11      :: D11MIT339       5.5   2  0.01859     0.14
CHROM11      :: D11MIT179       2.5   1  0.11502     0.09
CHROM11      :: D11MIT258       3.3   1  0.07059    -0.11
CHROM11      :: D11MIT168       4.8   1  0.02928    -0.13
CHROM11      :: D11MIT42        1.5   0  0.21995    -0.07
CHROM13      :: D13MIT17        0.9   0  0.33148     0.06
CHROM13      :: D13MIT61        9.4   3  0.00222     0.18
CHROM13      :: D13MIT99        7.6   2  0.00580     0.16
CHROM13      :: D13MIT36        3.3   1  0.06932     0.11
CHROM13      :: D13MIT262       2.4   0  0.12217     0.09
CHROM13      :: D13MIT151       2.0   0  0.15650     0.08
CHROM13      :: D13MIT78        2.2   0  0.13436     0.09
CHROM8       :: D8MIT94         2.4   0  0.12151     0.09
CHROM8       :: D8MIT189        2.8   1  0.09459     0.10
CHROM8       :: D8MIT104        6.4   2  0.01148     0.15
CHROM8       :: D8MIT106        6.8   2  0.00931     0.15
```

```
CHROM8        :: D8MIT80     6.5   2  0.01099    0.15
CHROM8        :: D8MIT40     4.0   1  0.04464    0.12
CHROM8        :: D8MIT242    4.0   1  0.04442    0.12
CHROM8        :: D8MIT36     3.0   1  0.08243    0.10
```

SIM Reports for Chromosomes 8, 11, and 13 for Final
Mortality Analysis
SIM CHROMOSOME 8

```
Interval  mapping  for  Dataset:  SECONDWNEWPRSIMERS(SECOND)
constrained additive regression,285  to  294  informative
progeny  from Progeny Order  Internal
mapping  QTL  MORTALITY   on  chr  CHROM8
using  Kosambi  mapping  function
With no control for other QTLs.
                 map       Stat       %      Add
D8MIT94          0.00      2.4        0      0.09
                 0.01      2.5        1      0.09
                 0.02      2.6        1      0.10
D8MIT189         0.04      2.8        1      0.10
                 0.05      3.0        1      0.10
                 0.06      3.3        1      0.11
                 0.07      3.5        1      0.12
                 0.08      3.8        1      0.12
                 0.09      4.0        1      0.13
                 0.10      4.3        1      0.13
                 0.11      4.5        1      0.14
                 0.12      4.8        1      0.14
                 0.13      5.0        1      0.15
                 0.14      5.2        1      0.15
                 0.15      5.4        1      0.15
                 0.16      5.5        2      0.15
                 0.17      5.7        2      0.15
                 0.18      5.8        2      0.15
                 0.19      5.9        2      0.15
                 0.20      5.9        2      0.15
                 0.21      5.9        2      0.15
                 0.22      6.0        2      0.15
D8MIT104         0.23      6.4        2      0.15
D8MIT106         0.25      6.4        2      0.15
D8MIT80          0.27      6.4        2      0.15
                 0.28      6.0        2      0.14
                 0.29      5.5        2      0.14
                 0.30      4.9        1      0.13
D8MIT40          0.31      4.0        1      0.12
```

```
                0.32      4.1       1     0.12
                0.33      4.1       1     0.12
D8MIT242        0.34      3.1       1     0.10
                0.35      3.2       1     0.11
                0.36      3.3       1     0.11
                0.37      3.4       1     0.11
                0.38      3.5       1     0.12
                0.39      3.5       1     0.12
                0.40      3.6       1     0.12
                0.41      3.7       1     0.13
                0.42      3.7       1     0.13
                0.43      3.8       1     0.13
                0.44      3.8       1     0.13
                0.45      3.8       1     0.13
                0.46      3.8       1     0.13
                0.47      3.7       1     0.13
                0.48      3.7       1     0.13
                0.49      3.6       1     0.12
                0.50      3.5       1     0.12
                0.51      3.4       1     0.12
                0.52      3.3       1     0.11
                0.53      3.2       1     0.11
D8MIT36

SIM CHROMOSOME 11
Interval  mapping  for  Dataset:  SECONDWNEWPRSIMERS(SECOND)
constrained additive regression,272  to  294  informative
progeny  from Progeny Order  Internal
mapping  QTL  MORTALITY   on  chr  CHROM11
using  Kosambi  mapping  function
With no control for other QTLs.
                map       Stat      %     Add
D11MIT2         0.00      3.5       1     0.11
                0.01      3.7       1     0.12
                0.02      3.8       1     0.12
                0.03      4.0       1     0.13
                0.04      4.1       1     0.13
                0.05      4.3       1     0.14
                0.06      4.5       1     0.14
                0.07      4.7       1     0.15
                0.08      4.9       1     0.15
                0.09      5.1       1     0.16
                0.10      5.3       2     0.17
                0.11      5.5       2     0.17
                0.12      5.7       2     0.18
```

	0.13	5.9	2	0.18
	0.14	6.2	2	0.19
	0.15	6.4	2	0.20
	0.16	6.6	2	0.20
	0.17	6.8	2	0.21
	0.18	7.0	2	0.21
	0.19	7.1	2	0.21
	0.20	7.3	2	0.22
	0.21	7.4	2	0.22
	0.22	7.6	2	0.22
	0.23	7.7	2	0.22
	0.24	7.7	2	0.22
	0.25	7.8	2	0.22
	0.26	7.8	2	0.22
	0.27	7.8	2	0.22
	0.28	7.8	2	0.22
	0.29	7.8	2	0.21
	0.30	7.8	2	0.21
	0.31	7.7	2	0.21
	0.32	7.6	2	0.20
	0.33	7.6	2	0.20
	0.34	7.5	2	0.19
	0.35	7.4	2	0.19
	0.36	7.3	2	0.18
	0.37	7.2	2	0.18
	0.38	7.1	2	0.18
	0.39	7.0	2	0.17
	0.40	6.9	2	0.17
	0.41	6.8	2	0.16
D11MIT164	0.43	6.1	2	0.14
	0.44	6.2	2	0.15
	0.45	6.3	2	0.15
	0.46	6.2	2	0.15
D11MIT339	0.47	5.5	2	0.14
	0.48	5.5	2	0.14
	0.49	5.5	2	0.14
	0.50	5.4	1	0.14
	0.51	5.4	1	0.14
	0.52	5.3	1	0.14
	0.53	5.1	1	0.14
	0.54	5.0	1	0.14
	0.55	4.8	1	0.14
	0.56	4.6	1	0.14
	0.57	4.3	1	0.13
	0.58	4.1	1	0.13

```
                0.59      3.8       1     0.12
                0.60      3.6       1     0.12
                0.61      3.3       1     0.11
                0.62      3.1       1     0.11
                0.63      2.8       1     0.10
D11MIT179       0.65      2.5       1     0.09
                0.66      2.0       0     0.08
                0.67      1.5       0     0.08
                0.68      1.1       0     0.06
                0.69      0.7       0     0.05
                0.70      0.4       0     0.04
                0.71      0.2       0     0.03
                0.72      0.0       0     0.01
                0.73      0.0       0    -0.00
                0.74      0.1       0    -0.02
                0.75      0.3       0    -0.04
                0.76      0.6       0    -0.05
                0.77      1.0       0    -0.06
                0.78      1.4       0    -0.08
                0.79      1.9       0    -0.09
                0.80      2.5       1    -0.10
D11MIT258       0.81      3.3       1    -0.11
                0.82      3.5       1    -0.11
                0.83      3.7       1    -0.12
                0.84      3.9       1    -0.12
                0.85      4.1       1    -0.12
                0.86      4.3       1    -0.13
                0.87      4.5       1    -0.13
                0.88      4.6       1    -0.13
                0.89      4.7       1    -0.13
D11MIT168       0.91      6.5       2    -0.15
                0.92      4.2       1    -0.13
D11MIT42

SIM CHROMOSOME 13
Interval  mapping  for  Dataset:  SECONDWNEWPRSIMERS(SECOND)
constrained additive regression,261  to  294  informative
progeny  from Progeny Order  Internal
mapping  QTL  MORTALITY   on  chr  CHROM13
using  Kosambi  mapping  function
With no control for other QTLs.
                map       Stat      %     Add
D13MIT17        0.00      0.9       0     0.06
                0.01      1.3       0     0.07
                0.02      1.7       0     0.09
```

	0.03	2.2	0	0.10
	0.04	2.7	1	0.12
	0.05	3.3	1	0.13
	0.06	3.8	1	0.14
	0.07	4.2	1	0.14
	0.08	4.6	1	0.14
	0.09	4.8	1	0.14
D13MIT61	0.10	9.4	3	0.18
	0.11	9.9	3	0.19
	0.12	10.4	3	0.20
	0.13	10.7	3	0.21
	0.14	11.0	3	0.21
	0.15	11.1	3	0.22
	0.16	11.1	3	0.22
	0.17	10.8	3	0.21
	0.18	10.4	3	0.21
	0.19	9.9	3	0.20
	0.20	9.3	3	0.19
	0.21	8.7	3	0.18
D13MIT99	0.22	7.6	2	0.16
	0.23	7.5	2	0.16
	0.24	7.3	2	0.16
	0.25	7.1	2	0.16
	0.26	6.8	2	0.16
	0.27	6.4	2	0.16
	0.28	6.0	2	0.16
	0.29	5.6	2	0.15
	0.30	5.1	1	0.14
	0.31	4.6	1	0.14
	0.32	4.2	1	0.13
D13MIT36	0.34	3.3	1	0.11
	0.35	3.3	1	0.11
	0.36	3.3	1	0.11
	0.37	3.3	1	0.11
	0.38	3.3	1	0.11
	0.39	3.2	1	0.11
	0.40	3.1	1	0.11
	0.41	3.0	1	0.11
	0.42	2.8	1	0.10
	0.43	2.7	1	0.10
D13MIT262	0.45	2.6	1	0.09
	0.46	2.4	0	0.09
D13MIT151	0.47	2.2	0	0.09
	0.48	2.3	0	0.09
	0.49	2.3	0	0.09

```
                0.50       2.3        0      0.09
                0.51       2.3        0      0.09
                0.52       2.3        0      0.09
                0.53       2.3        0      0.09
                0.54       2.3        0      0.09
D13MIT78
```

CIM Reports for Chromosomes 8, 11, and 13 Using Final Mortality Data

```
CIM CHROMOSOME 11 WITH D11MIT339 BACKGROUND
Interval  mapping  for  Dataset:  final mortality
data(SECOND)constrained  additive  regression,  272  to  294
informative progeny  from Progeny Order  Internalmapping
QTL  MORTALITY  on  chr  CHROM11using  Kosambi map
function;  Evaluating interval QTL only
Using  D11Mit 179 Background  to  control for  other  QTLs.
                map       Stat        %      Add
D11MIT2         0.00       3.3        1      0.11
                0.01       3.4        1      0.11
                0.02       3.6        1      0.12
                0.03       3.7        1      0.12
                0.04       3.8        1      0.13
                0.05       4.0        1      0.13
                0.06       4.1        1      0.14
                0.07       4.3        2      0.14
                0.08       4.4        2      0.15
                0.09       4.6        2      0.16
                0.10       4.8        2      0.16
                0.11       5.0        2      0.17
                0.12       5.2        2      0.18
                0.13       5.4        2      0.18
                0.14       5.6        2      0.19
                0.15       5.8        2      0.20
                0.16       6.0        2      0.20
                0.17       6.2        2      0.21
                0.18       6.4        2      0.22
                0.19       6.6        2      0.22
                0.20       6.8        2      0.23
                0.21       7.0        2      0.24
                0.22       7.2        3      0.24
                0.23       7.4        3      0.25
                0.24       7.5        3      0.25
                0.25       7.7        3      0.25
                0.26       7.8        3      0.25
                0.27       7.9        3      0.26
```

	0.28	7.9	3	0.26
	0.29	8.0	3	0.26
	0.30	8.0	3	0.26
	0.31	8.0	3	0.25
	0.32	8.0	3	0.25
	0.33	8.0	3	0.25
	0.34	7.9	3	0.24
	0.35	7.9	3	0.24
	0.36	7.8	3	0.24
	0.37	7.7	3	0.23
	0.38	7.6	3	0.23
	0.39	7.5	3	0.22
	0.40	7.4	3	0.22
	0.41	7.3	3	0.21
	0.42	7.2	3	0.21
D11MIT164	0.43	5.7	2	0.18
	0.44	6.0	2	0.19
	0.45	6.1	2	0.19
	0.46	6.0	2	0.19
D11MIT339	0.47	4.9	2	0.17
	0.48	5.1	2	0.18
	0.49	5.3	2	0.19
	0.50	5.4	2	0.21
	0.51	5.7	2	0.22
	0.52	5.9	2	0.24
	0.53	6.2	2	0.27
	0.54	6.5	2	0.29
	0.55	6.8	2	0.33
	0.56	7.1	2	0.36
	0.57	7.5	3	0.40
	0.58	7.9	3	0.45
	0.59	8.2	3	0.50
	0.60	8.4	3	0.55
	0.61	8.4	3	0.59
	0.62	8.1	3	0.62
	0.63	7.4	2	0.61
	0.64	6.4	2	0.58
D11MIT179	0.65	5.8	2	0.55
	0.66	2.8	1	0.38
	0.67	0.9	0	0.21
	0.68	0.1	0	0.06
	0.69	0.1	0	-0.06
	0.70	0.7	0	-0.14
	0.71	1.5	0	-0.19
	0.72	2.3	1	-0.21

```
                0.73       3.2          1    -0.23
                0.74       4.0          1    -0.23
                0.75       4.7          2    -0.23
                0.76       5.4          2    -0.23
                0.77       6.0          2    -0.22
                0.78       6.5          2    -0.22
                0.79       6.9          2    -0.21
                0.80       7.3          2    -0.20
D11MIT258       0.81       7.8          3    -0.19
                0.82       8.2          3    -0.20
                0.83       8.5          3    -0.21
                0.84       8.8          3    -0.21
                0.85       9.0          3    -0.21
                0.86       9.1          3    -0.21
                0.87       9.1          3    -0.21
                0.88       9.1          3    -0.21
                0.89       9.0          3    -0.20
                0.90       8.8          3    -0.20
D11MIT168       0.91      10.5          4    -0.21
                0.92       7.9          3    -0.20
D11MIT42

CIM CHROMOSOME 11 WITH D11MIT339 BACKGROUND
Interval  mapping  for  Dataset:  final mortality
data(SECOND)constrained  additive  regression,  272  to
294  informative progeny  from Progeny Order  Internal-
mapping  QTL  MORTALITY   on  chr  CHROM11using
Kosambi map function;  Evaluating interval QTL onlyUsing
Background  to  control  for  other  QTLs.
                Map       Stat          %     Add
D11MIT2         0.00       1.4          0     0.07
                0.01       1.4          0     0.08
                0.02       1.4          1     0.08
                0.03       1.5          1     0.08
                0.04       1.5          1     0.08
                0.05       1.5          1     0.09
                0.06       1.5          1     0.09
                0.07       1.5          1     0.09
                0.08       1.6          1     0.10
                0.09       1.6          1     0.10
                0.10       1.6          1     0.10
                0.11       1.6          1     0.11
                0.12       1.7          1     0.11
                0.13       1.7          1     0.12
                0.14       1.7          1     0.12
```

	0.15	1.8	1	0.13
	0.16	1.8	1	0.13
	0.17	1.8	1	0.14
	0.18	1.8	1	0.15
	0.19	1.9	1	0.15
	0.20	1.9	1	0.16
	0.21	1.9	1	0.16
	0.22	1.9	1	0.17
	0.23	2.0	1	0.18
	0.24	2.0	1	0.18
	0.25	2.0	1	0.19
	0.26	2.0	1	0.19
	0.27	1.9	1	0.19
	0.28	1.9	1	0.20
	0.29	1.9	1	0.20
	0.30	1.8	1	0.20
	0.31	1.8	1	0.20
	0.32	1.7	1	0.19
	0.33	1.6	1	0.19
	0.34	1.5	1	0.18
	0.35	1.5	1	0.18
	0.36	1.4	0	0.17
	0.37	1.3	0	0.16
	0.38	1.2	0	0.16
	0.39	1.1	0	0.15
	0.40	1.0	0	0.14
	0.41	0.9	0	0.13
	0.42	0.9	0	0.12
D11MIT164	0.43	0.7	0	0.11
	0.44	0.8	0	0.15
	0.45	1.0	0	0.22
	0.46	1.2	0	0.38
D11MIT339	0.47	1.1	0	0.62
	0.48	0.9	0	0.57
	0.49	0.6	0	0.39
	0.50	0.4	0	0.24
	0.51	0.2	0	0.15
	0.52	0.1	0	0.10
	0.53	0.1	0	0.07
	0.54	0.1	0	0.05
	0.55	0.0	0	0.04
	0.56	0.0	0	0.03
	0.57	0.0	0	0.02
	0.58	0.0	0	0.02
	0.59	0.0	0	0.01

```
                0.60      0.0        0     0.01
                0.61      0.0        0     0.01
                0.62      0.0        0     0.01
                0.63      0.0        0     0.01
                0.64      0.0        0     0.01
D11MIT179       0.65      0.0        0     0.01
                0.66      0.0        0    -0.01
                0.67      0.1        0    -0.03
                0.68      0.3        0    -0.04
                0.69      0.6        0    -0.06
                0.70      0.9        0    -0.08
                0.71      1.3        0    -0.09
                0.72      1.8        1    -0.11
                0.73      2.4        1    -0.12
                0.74      2.9        1    -0.13
                0.75      3.5        1    -0.14
                0.76      4.0        1    -0.14
                0.77      4.5        2    -0.15
                0.78      5.0        2    -0.15
                0.79      5.5        2    -0.15
                0.80      5.9        2    -0.15
D11MIT258       0.81      6.4        2    -0.15
                0.82      6.7        2    -0.16
                0.83      6.9        2    -0.16
                0.84      7.1        2    -0.16
                0.85      7.2        2    -0.17
                0.86      7.3        2    -0.17
                0.87      7.3        2    -0.17
                0.88      7.3        2    -0.16
                0.89      7.2        2    -0.16
                0.90      7.1        2    -0.16
D11MIT168       0.91      8.6        3    -0.18
                0.92      7.5        3    -0.18
D11MIT42


CIM CHROMOSOME 11 WITH D13MIT61 AND D8MIT80 BACKGROUND
Interval  mapping  for  Dataset:  (SECOND)constrained  addi-
tive  regression,  271  to  293  informative progeny  from
Progeny Order  Internalmapping  QTL  MORTALITY   on  chr
CHROM11using  Kosambi map function;  Evaluating interval
QTL onlyUsing  Background  to  control  for  other  QTLs.
                map      Stat        %     Add
D11MIT2         0.00      3.6        1     0.11
```

	0.01	3.8	1	0.11
	0.02	4.0	1	0.12
	0.03	4.2	1	0.12
	0.04	4.3	1	0.13
	0.05	4.6	2	0.14
	0.06	4.8	2	0.14
	0.07	5.0	2	0.15
	0.08	5.2	2	0.15
	0.09	5.5	2	0.16
	0.10	5.7	2	0.17
	0.11	6.0	2	0.17
	0.12	6.3	2	0.18
	0.13	6.6	2	0.19
	0.14	6.9	2	0.19
	0.15	7.1	2	0.20
	0.16	7.4	2	0.21
	0.17	7.7	3	0.21
	0.18	7.9	3	0.22
	0.19	8.2	3	0.22
	0.20	8.4	3	0.22
	0.21	8.6	3	0.23
	0.22	8.8	3	0.23
	0.23	9.0	3	0.23
	0.24	9.1	3	0.23
	0.25	9.2	3	0.23
	0.26	9.3	3	0.23
	0.27	9.4	3	0.23
	0.28	9.4	3	0.23
	0.29	9.4	3	0.23
	0.30	9.4	3	0.22
	0.31	9.4	3	0.22
	0.32	9.4	3	0.22
	0.33	9.3	3	0.21
	0.34	9.2	3	0.21
	0.35	9.2	3	0.20
	0.36	9.1	3	0.20
	0.37	9.0	3	0.19
	0.38	8.9	3	0.19
	0.39	8.8	3	0.18
	0.40	8.7	3	0.18
	0.41	8.6	3	0.18
	0.42	8.5	3	0.17
D11MIT164	0.43	8.1	3	0.16
	0.44	8.3	3	0.17
	0.45	8.4	3	0.17

	0.46	8.3	3	0.17
D11MIT339	0.47	7.5	2	0.15
	0.48	7.6	2	0.16
	0.49	7.6	2	0.16
	0.50	7.7	2	0.16
	0.51	7.7	2	0.17
	0.52	7.6	2	0.17
	0.53	7.6	2	0.17
	0.54	7.4	2	0.17
	0.55	7.3	2	0.17
	0.56	7.1	2	0.17
	0.57	6.9	2	0.16
	0.58	6.6	2	0.16
	0.59	6.3	2	0.15
	0.60	6.0	2	0.15
	0.61	5.7	2	0.14
	0.62	5.4	2	0.14
	0.63	5.1	2	0.13
	0.64	4.8	2	0.12
D11MIT179	0.65	4.6	1	0.12
	0.66	3.9	1	0.11
	0.67	3.1	1	0.11
	0.68	2.4	1	0.10
	0.69	1.8	1	0.08
	0.70	1.2	0	0.07
	0.71	0.7	0	0.05
	0.72	0.4	0	0.04
	0.73	0.1	0	0.02
	0.74	0.0	0	0.00
	0.75	0.0	0	-0.01
	0.76	0.2	0	-0.03
	0.77	0.5	0	-0.04
	0.78	0.9	0	-0.06
	0.79	1.4	0	-0.07
	0.80	1.9	1	-0.08
D11MIT258	0.81	2.7	1	-0.09
	0.82	2.9	1	-0.10
	0.83	3.1	1	-0.10
	0.84	3.3	1	-0.11
	0.85	3.4	1	-0.11
	0.86	3.6	1	-0.11
	0.87	3.7	1	-0.11
	0.88	3.8	1	-0.11
	0.89	3.9	1	-0.11
	0.90	3.9	1	-0.11

```
D11MIT168       0.91      5.0        2    -0.13
                0.92      3.2        1    -0.11
D11MIT42

CIM CHROMOSOME 8 WITH D13MIT61 AND D11MIT164 BACKGROUND
Interval  mapping  for  Dataset:  (SECOND)constrained
additive  regression,  283  to  292  informative progeny
from Progeny Order  Internalmapping  QTL  MORTALITY   on
chr  CHROM8using  Kosambi map function;  Evaluating interval
QTL onlyUsing  Background  to  control  for  other  QTLs.
                map      Stat        %      Add
D8MIT94         0.00      3.4        1      0.11
                0.01      3.6        1      0.11
                0.02      3.7        1      0.11
                0.03      3.7        1      0.11
D8MIT189        0.04      3.7        1      0.11
                0.05      4.0        1      0.12
                0.06      4.4        1      0.12
                0.07      4.8        2      0.13
                0.08      5.2        2      0.14
                0.09      5.6        2      0.15
                0.10      6.0        2      0.15
                0.11      6.4        2      0.16
                0.12      6.8        2      0.17
                0.13      7.2        2      0.17
                0.14      7.5        2      0.18
                0.15      7.8        3      0.18
                0.16      8.1        3      0.18
                0.17      8.4        3      0.18
                0.18      8.6        3      0.18
                0.19      8.7        3      0.18
                0.20      8.8        3      0.18
                0.21      8.9        3      0.18
                0.22      9.0        3      0.18
                0.23      9.0        3      0.17
D8MIT104        0.23      9.6        3      0.18
D8MIT106        0.25      9.1        3      0.17
                0.26      9.0        3      0.17
D8MIT80         0.27      8.8        3      0.17
                0.28      8.3        3      0.17
                0.29      7.6        2      0.16
                0.30      6.8        2      0.15
D8MIT40         0.31      5.7        2      0.14
                0.32      5.7        2      0.14
                0.33      5.6        2      0.14
```

```
D8MIT242        0.34      4.2          1      0.12
                0.35      4.3          1      0.12
                0.36      4.4          1      0.12
                0.37      4.4          1      0.13
                0.38      4.4          1      0.13
                0.39      4.5          1      0.13
                0.40      4.5          1      0.13
                0.41      4.5          1      0.14
                0.42      4.4          1      0.14
                0.43      4.4          1      0.14
                0.44      4.3          1      0.13
                0.45      4.2          1      0.13
                0.46      4.1          1      0.13
                0.47      4.0          1      0.13
                0.48      3.9          1      0.13
                0.49      3.7          1      0.12
                0.50      3.6          1      0.12
                0.51      3.4          1      0.11
                0.52      3.3          1      0.11
                0.53      3.1          1      0.11
                0.54      2.9          1      0.10
D8MIT36

CIM CHROMOSOME 13 WITH D8MIT80 AND D11MIT164 BACKGROUND
Interval  mapping  for  Dataset:  (SECOND)constrained  addi-
tive  regression,  261  to  293  informative progeny  from
Progeny Order  Internalmapping  QTL  MORTALITY  on  chr
CHROM13using  Kosambi map function;  Evaluating interval
QTL onlyUsing  Background  to  control  for  other  QTLs.
                map       Stat         %       Add
D13MIT17        0.00       0.7         0      0.05
                0.01       1.1         0      0.06
                0.02       1.6         1      0.08
                0.03       2.1         1      0.10
                0.04       2.8         1      0.11
                0.05       3.4         1      0.13
                0.06       4.1         1      0.14
                0.07       4.7         2      0.14
                0.08       5.3         2      0.15
                0.09       5.7         2      0.15
D13MIT61        0.10       9.5         3      0.17
                0.11       9.9         3      0.18
                0.12      10.3         3      0.19
                0.13      10.6         3      0.20
                0.14      10.7         3      0.20
```

	0.15	10.7	3	0.21
	0.16	10.5	3	0.21
	0.17	10.2	3	0.20
	0.18	9.7	3	0.19
	0.19	9.1	3	0.19
	0.20	8.5	3	0.17
	0.21	7.8	2	0.16
D13MIT99	0.22	6.6	2	0.15
	0.23	6.4	2	0.15
	0.24	6.1	2	0.15
	0.25	5.8	2	0.15
	0.26	5.5	2	0.14
	0.27	5.1	2	0.14
	0.28	4.7	1	0.13
	0.29	4.2	1	0.13
	0.30	3.8	1	0.12
	0.31	3.3	1	0.11
	0.32	2.9	1	0.10
	0.33	2.5	1	0.09
D13MIT36	0.34	2.1	1	0.09
	0.35	2.2	1	0.09
	0.36	2.3	1	0.09
	0.37	2.3	1	0.09
	0.38	2.3	1	0.09
	0.39	2.3	1	0.09
	0.40	2.3	1	0.09
	0.41	2.3	1	0.09
	0.42	2.3	1	0.09
	0.43	2.2	1	0.09
	0.44	2.1	1	0.08
D13MIT262	0.45	2.3	1	0.09
	0.46	2.2	1	0.09
	0.47	2.0	1	0.08
D13MIT151	0.47	2.5	1	0.09
	0.48	2.6	1	0.09
	0.49	2.6	1	0.09
	0.50	2.6	1	0.09
	0.51	2.6	1	0.09
	0.52	2.6	1	0.09
	0.53	2.6	1	0.09
	0.54	2.6	1	0.09
	0.55	2.6	1	0.09
D13MIT78				

QT Links Reports for AST, IL-6, Caspase-3 (DNA), and

```
Caspase-3 (Protein) Data Analyses
QT LINKS AST
QT Links report for set
nonmortalitywith80casun(nonmortality)
Using quantitative trait AST
Chi Square Stats, P = 0.05
Additive regression model
With no control for other QTLs.
61  to  136  informative progeny  from Progeny Order
Internal
 Chr             Locus        Stat  %      P       Add
chrom1        :: D1MIT65      0.0   0   0.93473    -8.73
chrom1        :: D1MIT303     5.0   3   0.02469  -223.36
chrom1        :: D1MIT8       4.2   2   0.04106  -215.02
chrom1        :: D1MIT15      0.7   0   0.39723    84.35
chrom1        :: D1MIT17      0.1   0   0.70981    37.27
chrom2        :: D2MIT7       0.0   0   0.90580   -11.73
chrom2        :: D2MIT92      1.2   0   0.27325  -110.89
chrom2        :: D2MIT17      0.2   0   0.63825   -41.62
chrom3        :: D3MIT267     0.1   0   0.78951    30.17
chrom3        :: D3MIT12      0.8   0   0.36057   -93.54
chrom3        :: D3MIT200     0.9   0   0.35581   -94.84
chrom3        :: D3MIT116     2.7   1   0.10047  -166.51
chrom4        :: D4MIT1       0.4   0   0.50473   -68.50
chrom4        :: D4MIT178     2.9   1   0.08880  -179.82
chrom4        :: D4MIT12      0.0   0   0.82735    21.99
chrom5        :: D5MIT268     0.2   0   0.67130    43.74
chrom5        :: D5MIT205     0.1   0   0.78716    26.73
chrom5        :: D5MIT161     1.0   0   0.31841   -98.41
chrom6        :: D6MIT8       1.6   0   0.20691   127.52
chrom6        :: D6MIT254     1.4   0   0.23557   115.12
chrom6        :: D6MIT14      3.0   2   0.08095   172.02
chrom7        :: D7MIT270     0.5   0   0.46485   -74.10
chrom7        :: D7MIT63      2.9   1   0.08606  -175.84
chrom7        :: D7MIT105     4.2   5   0.04038  -340.28
chrom8        :: D8MIT94      0.0   0   0.83709    23.10
chrom8        :: D8MIT189     1.5   0   0.22700  -123.75
chrom8        :: D8MIT106     0.6   0   0.44526   -75.83
chrom8        :: D8MIT80      0.1   0   0.75003   -31.55
chrom8        :: D8MIT40      0.0   0   0.99306     0.80
chrom8        :: D8MIT242     1.7   0   0.19379  -127.26
chrom8        :: D8MIT36      0.4   0   0.51478   -63.04
chrom13       :: D13MIT17     0.4   0   0.54363    59.95
chrom13       :: D13MIT61     0.0   0   0.95345     5.78
chrom13       :: D13MIT99     0.0   0   0.98939     1.19
```

```
chrom13      :: D13MIT151    0.1   0  0.73157   -33.21
chrom19      :: D19MIT60     0.2   0  0.67465   -42.02
chrom19      :: D19MIT119    1.5   0  0.21708  -117.87
chrom19      :: D19MIT1      0.3   0  0.59536   -50.05
chrom18      :: D18MIT17     0.9   0  0.33418    96.00
chrom18      :: D18MIT51     0.7   0  0.39144    85.28
chrom18      :: D18MIT4      0.2   0  0.68499   -40.18
chrom17      :: D17MIT21     0.1   0  0.78079    27.27
chrom17      :: D17MIT68     0.1   0  0.81574    22.72
chrom17      :: D17MIT152    0.2   0  0.62111    48.20
chrom17      :: D17MIT130    0.5   0  0.48931    75.31
chrom16      :: D16MIT108    0.2   0  0.64076    46.84
chrom16      :: D16MIT4      0.7   0  0.38803   -84.51
chrom16      :: D16MIT158    6.4   4  0.01161  -246.25
chrom15      :: D15MIT55     2.1   1  0.14394  -147.76
chrom15      :: D15MIT29     0.2   0  0.66117   -44.02
chrom15      :: D15MIT41     0.0   0  0.95946    -5.46
chrom14      :: D14MIT207    2.3   2  0.12559   146.16
chrom14      :: D14MIT121    0.0   0  0.87044    16.04
chrom14      :: D14MIT102    0.0   0  0.88515   -14.33
chrom14      :: D14MIT95     0.9   0  0.35229   -97.02
chrom12      :: D12MIT2      0.0   0  0.86036   -17.52
chrom12      :: D12MIT14     1.3   0  0.25820   112.59
chrom11      :: D11MIT2      0.0   0  0.89071    12.87
chrom11      :: D11MIT164    0.2   0  0.63573    54.51
chrom11      :: D11MIT339    0.1   0  0.76207   -30.49
chrom11      :: D11MIT179    2.3   1  0.12580  -153.48
chrom11      :: D11MIT258    3.8   2  0.05248  -189.44
chrom11      :: D11MIT168    3.3   2  0.07083  -186.90
chrom10      :: D10MIT124    1.3   0  0.26049    87.43
chrom10      :: D10MIT189    0.0   0  0.91487   -10.38
chrom10      :: D10MIT259    1.2   0  0.26937  -106.06
chrom10      :: D10MIT96     0.0   0  0.91894     9.77
chrom9       :: D9MIT296     0.8   0  0.36294   -93.21
chrom9       :: D9MIT162     0.1   0  0.70839   -37.51
chrom9       :: D9MIT50      0.1   0  0.76121    31.16

QTLINKS IL-6
QT Links report for set
nonmortalitywith80casun(nonmortality)
Using quantitative trait IL6
Chi Square Stats, P = 0.05
Additive regression model
With no control for other QTLs.
39  to  112  informative progeny  from Progeny Order
```

```
Internal
 Chr             Locus         Stat  %      P        Add
chrom1       :: D1MIT65        0.2   0   0.66846   -38.70
chrom1       :: D1MIT303       3.2   2   0.07271 -150.46
chrom1       :: D1MIT8         3.5   2   0.05990 -164.09
chrom1       :: D1MIT15        2.7   2   0.10050  137.59
chrom1       :: D1MIT17        1.9   1   0.17234  115.29
chrom2       :: D2MIT7         0.7   0   0.39526   70.72
chrom2       :: D2MIT92        0.0   0   0.86505   14.42
chrom2       :: D2MIT17        0.7   0   0.40861   68.78
chrom3       :: D3MIT267       0.7   0   0.41079  -77.69
chrom3       :: D3MIT12        0.4   0   0.52547  -53.65
chrom3       :: D3MIT200       1.4   0   0.23607 -100.20
chrom3       :: D3MIT116       0.7   0   0.40321  -72.13
chrom4       :: D4MIT1         0.6   0   0.43091  -69.16
chrom4       :: D4MIT178       1.6   1   0.20012 -117.48
chrom4       :: D4MIT12        1.5   0   0.22027 -104.02
chrom5       :: D5MIT268       0.8   0   0.36888   76.87
chrom5       :: D5MIT205       1.3   0   0.25611   94.63
chrom5       :: D5MIT161       2.2   1   0.13584 -123.57
chrom6       :: D6MIT8         0.7   0   0.41380   69.99
chrom6       :: D6MIT254       1.2   0   0.26861   90.04
chrom6       :: D6MIT14        1.2   0   0.26846   92.28
chrom7       :: D7MIT270       0.0   0   0.86474  -14.74
chrom7       :: D7MIT63        0.5   0   0.49244   58.84
chrom7       :: D7MIT105       0.3   0   0.55598   56.51
chrom8       :: D8MIT94        1.1   0   0.29547  -99.59
chrom8       :: D8MIT189       2.9   2   0.08789 -144.41
chrom8       :: D8MIT106       1.5   0   0.22107 -101.95
chrom8       :: D8MIT80        1.5   0   0.22692 -100.15
chrom8       :: D8MIT40        0.9   0   0.33290  -81.18
chrom8       :: D8MIT242       0.4   0   0.54614  -49.59
chrom8       :: D8MIT36        0.1   0   0.80630   19.95
chrom13      :: D13MIT17       1.9   1   0.17157 -113.61
chrom13      :: D13MIT61       3.0   2   0.08086 -143.75
chrom13      :: D13MIT99       2.5   1   0.11697 -128.41
chrom13      :: D13MIT151      1.4   0   0.23961 -102.86
chrom19      :: D19MIT60       0.8   0   0.36356   77.05
chrom19      :: D19MIT119      0.4   0   0.53818   28.14
chrom19      :: D19MIT1        0.0   0   0.85372    8.76
chrom18      :: D18MIT17       1.7   1   0.19031  108.35
chrom18      :: D18MIT51       1.6   1   0.21025  104.68
chrom18      :: D18MIT4        1.0   0   0.32469   46.26
chrom17      :: D17MIT21       2.0   1   0.16025  115.02
chrom17      :: D17MIT68       1.7   1   0.19364  105.67
```

```
chrom17        :: D17MIT152     2.1   1  0.14842  117.64
chrom17        :: D17MIT130     0.7   0  0.40484   80.35
chrom16        :: D16MIT108     1.4   0  0.23263  102.22
chrom16        :: D16MIT4       0.1   0  0.77164  -24.42
chrom16        :: D16MIT158     1.4   0  0.23862 -102.93
chrom15        :: D15MIT55      1.8   1  0.17486 -115.34
chrom15        :: D15MIT29      0.0   0  0.83622  -17.54
chrom15        :: D15MIT41      1.2   0  0.27437  -98.39
chrom14        :: D14MIT207     0.2   0  0.69096  -19.34
chrom14        :: D14MIT121     0.0   0  0.92989    3.97
chrom14        :: D14MIT102     1.5   0  0.22430 -100.54
chrom14        :: D14MIT95      0.5   0  0.46528   63.78
chrom12        :: D12MIT2       0.5   0  0.48015   58.93
chrom12        :: D12MIT14      3.7   2  0.05557  158.39
chrom11        :: D11MIT2       1.6   1  0.20797 -119.71
chrom11        :: D11MIT164     0.4   0  0.51102  -66.07
chrom11        :: D11MIT339     0.4   0  0.50702  -55.92
chrom11        :: D11MIT179     1.1   0  0.29642  -88.47
chrom11        :: D11MIT258     0.1   0  0.81581   19.24
chrom11        :: D11MIT168     0.0   0  0.95243    5.17
chrom10        :: D10MIT124     3.1   2  0.07840   72.01
chrom10        :: D10MIT189     0.8   0  0.36243   40.89
chrom10        :: D10MIT259     3.5   2  0.06289 -154.28
chrom10        :: D10MIT96      0.1   0  0.73290  -16.39
chrom9         :: D9MIT296      0.0   0  0.99183    0.81
chrom9         :: D9MIT162      0.0   0  0.96541   -3.62
chrom9         :: D9MIT50       0.9   0  0.33726   85.53

QT LINKS CASPASE-3 (DNA)
QT Links report for set
nonmortalitywith80casun(nonmortality)
Using quantitative trait CASPASE-3
Chi Square Stats, P = 0.05
Additive regression model
With no control for other QTLs.
61  to  136  informative progeny  from Progeny Order
Internal
 Chr              Locus         Stat  %     P       Add
chrom1         :: D1MIT65       0.1   0  0.73841   32.07
chrom1         :: D1MIT303      0.9   0  0.33494  -87.95
chrom1         :: D1MIT8        0.9   0  0.33483  -92.77
chrom1         :: D1MIT15       4.5   3  0.03385  191.02
chrom1         :: D1MIT17       7.4   5  0.00648  243.29
chrom2         :: D2MIT7        0.1   0  0.76417  -26.99
chrom2         :: D2MIT92       0.2   0  0.65418  -41.19
```

```
chrom2          :: D2MIT17      0.0   0  0.98652    1.42
chrom3          :: D3MIT267     0.0   0  0.83408  -21.26
chrom3          :: D3MIT12      0.3   0  0.61584  -46.47
chrom3          :: D3MIT200     0.8   0  0.36685  -83.87
chrom3          :: D3MIT116     0.0   0  0.84559   17.65
chrom4          :: D4MIT1       0.1   0  0.79150   24.79
chrom4          :: D4MIT178     1.1   0  0.28513 -103.41
chrom4          :: D4MIT12      2.1   1  0.15098 -128.40
chrom5          :: D5MIT268     0.0   0  0.97602    2.87
chrom5          :: D5MIT205     0.3   0  0.58422  -49.23
chrom5          :: D5MIT161    10.4   7  0.00127 -284.50
chrom6          :: D6MIT8       1.5   0  0.21345  113.61
chrom6          :: D6MIT254     0.9   0  0.34451   83.61
chrom6          :: D6MIT14      1.3   0  0.25406  102.18
chrom7          :: D7MIT270     0.6   0  0.43616  -71.98
chrom7          :: D7MIT63      0.0   0  1.00000   -0.07
chrom7          :: D7MIT105     0.2   0  0.68431   68.47
chrom8          :: D8MIT94      0.0   0  0.90217   12.21
chrom8          :: D8MIT189     0.0   0  0.83357  -19.67
chrom8          :: D8MIT106     0.2   0  0.64476   41.78
chrom8          :: D8MIT80      0.0   0  0.83208   19.15
chrom8          :: D8MIT40      0.7   0  0.40167   76.65
chrom8          :: D8MIT242     0.9   0  0.34806   83.89
chrom8          :: D8MIT36      0.2   0  0.66736   38.39
chrom13         :: D13MIT17     0.3   0  0.58634  -47.58
chrom13         :: D13MIT61     1.8   1  0.17532 -122.02
chrom13         :: D13MIT99     2.0   1  0.16060 -124.81
chrom13         :: D13MIT151    1.5   0  0.21597 -115.70
chrom19         :: D19MIT60     0.8   0  0.36851   81.73
chrom19         :: D19MIT119    0.3   0  0.57347  -53.43
chrom19         :: D19MIT1      0.0   0  0.96669   -4.04
chrom18         :: D18MIT17     1.4   0  0.24332 -104.86
chrom18         :: D18MIT51     0.2   0  0.64694  -41.50
chrom18         :: D18MIT4      0.5   0  0.46698  -72.45
chrom17         :: D17MIT21     1.2   0  0.27021   98.15
chrom17         :: D17MIT68     0.7   0  0.40776   73.37
chrom17         :: D17MIT152    0.0   0  0.90898  -10.17
chrom17         :: D17MIT130    0.3   0  0.56559  -56.36
chrom16         :: D16MIT108    0.0   0  0.90985  -10.36
chrom16         :: D16MIT4      0.2   0  0.64499  -41.16
chrom16         :: D16MIT158    3.2   2  0.07209 -161.02
chrom15         :: D15MIT55     0.9   0  0.35253   83.94
chrom15         :: D15MIT29     1.4   0  0.23056  109.04
chrom15         :: D15MIT41     0.2   0  0.66488   41.15
chrom14         :: D14MIT207    0.6   0  0.42907   69.40
```

```
chrom14       :: D14MIT121    0.1   0  0.75061   28.62
chrom14       :: D14MIT102    0.2   0  0.67711  -37.64
chrom14       :: D14MIT95     1.7   1  0.19235 -122.36
chrom12       :: D12MIT2      0.0   0  0.84265   18.29
chrom12       :: D12MIT14     2.4   1  0.12429  137.83
chrom11       :: D11MIT2      0.6   0  0.45102  -68.43
chrom11       :: D11MIT164    1.1   0  0.28428  112.76
chrom11       :: D11MIT339    1.7   0  0.19425  118.83
chrom11       :: D11MIT179    0.3   0  0.56010   53.45
chrom11       :: D11MIT258    0.1   0  0.73841  -29.94
chrom11       :: D11MIT168    0.1   0  0.80820  -23.22
chrom10       :: D10MIT124    0.1   0  0.73427   26.05
chrom10       :: D10MIT189    0.0   0  0.86892  -15.55
chrom10       :: D10MIT259    0.4   0  0.50494  -60.85
chrom10       :: D10MIT96     0.4   0  0.52136   57.25
chrom9        :: D9MIT296     1.7   1  0.19578 -120.31
chrom9        :: D9MIT162     0.0   0  0.97344   -2.93
chrom9        :: D9MIT50      1.5   0  0.22130  115.18

QT LINKS CASPASE-3 (PROTEIN)
QT Links report for set
nonmortalitywith80casun(nonmortality)
Using quantitative trait Caspase-3un
Chi Square Stats, P = 0.05
Additive regression model
With no control for other QTLs.
61  to  136  informative progeny  from Progeny Order
Internal
 Chr             Locus          Stat  %      P       Add
chrom1        :: D1MIT65      0.0   0  0.96532    4.66
chrom1        :: D1MIT303     1.3   0  0.25944 -117.53
chrom1        :: D1MIT8       0.4   0  0.52638  -69.87
chrom1        :: D1MIT15      1.5   0  0.22751  125.17
chrom1        :: D1MIT17      2.6   1  0.10406  168.24
chrom2        :: D2MIT7       1.1   0  0.28965 -106.94
chrom2        :: D2MIT92      0.1   0  0.80397   26.17
chrom2        :: D2MIT17      0.0   0  0.86779  -16.88
chrom3        :: D3MIT267     0.0   0  0.84596  -22.89
chrom3        :: D3MIT12      0.4   0  0.54561  -64.12
chrom3        :: D3MIT200     0.0   0  0.93160    9.14
chrom3        :: D3MIT116     0.4   0  0.52685  -63.64
chrom4        :: D4MIT1       0.0   0  0.85455  -19.75
chrom4        :: D4MIT178     2.0   1  0.15593 -157.57
chrom4        :: D4MIT12      0.4   0  0.50328  -69.79
chrom5        :: D5MIT268     0.1   0  0.76926   30.75
```

```
chrom5         :: D5MIT205      0.9   0  0.33358   -99.54
chrom5         :: D5MIT161      4.0   2  0.04500  -205.24
chrom6         :: D6MIT8        0.7   0  0.39907    84.66
chrom6         :: D6MIT254      1.0   0  0.31609   101.49
chrom6         :: D6MIT14       2.6   1  0.10410   161.91
chrom7         :: D7MIT270      0.1   0  0.74570   -33.75
chrom7         :: D7MIT63       1.0   0  0.31520  -107.56
chrom7         :: D7MIT105      0.5   0  0.47314  -134.73
chrom8         :: D8MIT94       0.0   0  0.93997     8.74
chrom8         :: D8MIT189      0.5   0  0.47386    76.75
chrom8         :: D8MIT106      0.2   0  0.68845    41.63
chrom8         :: D8MIT80       1.0   0  0.32117   102.44
chrom8         :: D8MIT40       0.1   0  0.77927   -29.38
chrom8         :: D8MIT242      2.4   1  0.12210   157.91
chrom8         :: D8MIT36       0.1   0  0.71696   -37.62
chrom13        :: D13MIT17      0.3   0  0.60160   -50.41
chrom13        :: D13MIT61      0.3   0  0.56108   -60.12
chrom13        :: D13MIT99      1.5   0  0.22673  -123.31
chrom13        :: D13MIT151     0.1   0  0.74405   -34.42
chrom19        :: D19MIT60      3.3   2  0.06801   189.26
chrom19        :: D19MIT119     0.0   0  0.93916     8.62
chrom19        :: D19MIT1       0.4   0  0.54004    70.22
chrom18        :: D18MIT17      0.1   0  0.70507    39.08
chrom18        :: D18MIT51      1.8   1  0.18443   137.32
chrom18        :: D18MIT4       2.2   1  0.14231   171.36
chrom17        :: D17MIT21      0.5   0  0.50028   -68.78
chrom17        :: D17MIT68      1.1   0  0.29370  -106.45
chrom17        :: D17MIT152     2.2   1  0.14086  -149.15
chrom17        :: D17MIT130     1.5   0  0.22311  -109.35
chrom16        :: D16MIT108     0.0   0  0.83978    21.26
chrom16        :: D16MIT4       0.1   0  0.74753   -32.95
chrom16        :: D16MIT158     3.3   2  0.06997  -174.78
chrom15        :: D15MIT55      3.9   2  0.04697   207.23
chrom15        :: D15MIT29      1.5   0  0.22470   126.86
chrom15        :: D15MIT41      0.0   0  0.84455   -21.29
chrom14        :: D14MIT207     0.5   0  0.46666    88.84
chrom14        :: D14MIT121     0.4   0  0.50546    71.18
chrom14        :: D14MIT102     0.1   0  0.80427    25.66
chrom14        :: D14MIT95      1.1   0  0.30522  -108.31
chrom12        :: D12MIT2       0.0   0  0.92942    -9.47
chrom12        :: D12MIT14      0.4   0  0.54116    63.69
chrom11        :: D11MIT2       4.0   3  0.04600  -227.11
chrom11        :: D11MIT164     0.4   0  0.50522   -79.81
chrom11        :: D11MIT339     0.0   0  0.85228   -19.58
chrom11        :: D11MIT179     0.5   0  0.49372   -71.90
```

```
chrom11       :: D11MIT258    3.2   2  0.07509 -181.79
chrom11       :: D11MIT168    3.3   2  0.06749 -195.70
chrom10       :: D10MIT124    0.2   0  0.68350   46.64
chrom10       :: D10MIT189    0.1   0  0.75676   35.30
chrom10       :: D10MIT259    0.3   0  0.57075   60.24
chrom10       :: D10MIT96     0.0   0  0.84936   22.58
chrom9        :: D9MIT296     0.2   0  0.64603  -48.98
chrom9        :: D9MIT162     0.3   0  0.56671   59.62
chrom9        :: D9MIT50      0.1   0  0.79738   27.49
```

SIM Reports for Chromosome 5 for AST, IL-6, Caspase-3 (DNA) and Caspase-3 (Protein)

```
SIM CHROMOSOME 5 FOR AST
Interval  mapping  for  Dataset:
nonmortalitywith80casun(nonmortality)
constrained additive regression,128  to  133  informative
progeny  from Progeny Order  Internal
mapping  QTL  AST   on  chr  chrom5
using  Kosambi  mapping  function
With no control for other QTLs.
                map        Stat        %     Add
D5MIT268        0.00       0.2         0    43.74
                0.01       0.2         0    45.45
                0.02       0.2         0    47.22
                0.03       0.2         0    49.02
                0.04       0.2         0    50.85
                0.05       0.2         0    52.69
                0.06       0.2         0    54.53
                0.07       0.2         0    56.34
                0.08       0.2         0    58.10
                0.09       0.2         0    59.79
                0.10       0.3         0    61.37
                0.11       0.3         0    62.82
                0.12       0.3         0    64.11
                0.13       0.3         0    65.22
                0.14       0.3         0    66.12
                0.15       0.3         0    66.79
                0.16       0.3         0    67.22
                0.17       0.3         0    67.40
                0.18       0.3         0    67.33
                0.19       0.3         0    67.01
                0.20       0.3         0    66.46
                0.21       0.3         0    65.70
                0.22       0.3         0    64.73
                0.23       0.3         0    63.60
                0.24      0.3        0    62.32
                0.25      0.3        0    60.92
                0.26      0.3        0    59.43
                0.27      0.3        0    57.87
                0.28      0.3        0    56.26
                0.29      0.2        0    54.63
                0.30      0.2        0    53.00
                0.31      0.2        0    51.37
D5MIT205        0.33      0.1        0    26.73
                0.34      0.0        0    22.08
                0.35      0.0        0    16.94
                0.36      0.0        0    11.31
                0.37      0.0        0     5.22
                0.38      0.0        0    -1.31
                0.39      0.0        0    -8.21
                0.40      0.0        0   -15.42
                0.41      0.0        0   -22.83
                0.42      0.1        0   -30.35
                0.43      0.1        0   -37.86
                0.44      0.2        0   -45.24
                0.45      0.2        0   -52.38
                0.46      0.3        0   -59.16
                0.47      0.4        0   -65.50
                0.48      0.4        0   -71.32
                0.49      0.5        0   -76.57
                0.50      0.6        0   -81.21
                0.51      0.7        0   -85.23
                0.52      0.7        0   -88.65
                0.53      0.8        0   -91.47
D5MIT161

SIM CHROMOSOME 5 FOR IL-6
Interval  mapping  for  Dataset:
nonmortalitywith80casun(nonmortality)
constrained additive regression,107  to  110  informative
progeny  from Progeny Order  Internal
mapping  QTL  IL6   on  chr  chrom5
using  Kosambi  mapping  function
With no control for other QTLs.
                map       Stat       %     Add
D5MIT268        0.00      0.8        0    76.87
                0.01      0.8        0    80.40
                0.02      0.9        0    84.08
                0.03      0.9        0    87.89
                0.04      1.0        0    91.81
```

	0.05	1.0	0	95.82
	0.06	1.1	0	99.87
	0.07	1.1	0	103.94
	0.08	1.2	0	107.96
	0.09	1.2	0	111.89
	0.10	1.3	0	115.66
	0.11	1.3	0	119.21
	0.12	1.4	0	122.47
	0.13	1.4	0	125.37
	0.14	1.4	0	127.85
	0.15	1.5	0	129.87
	0.16	1.5	0	131.37
	0.17	1.5	0	132.34
	0.18	1.5	0	132.75
	0.19	1.6	0	132.61
	0.20	1.6	1	131.94
	0.21	1.6	1	130.78
	0.22	1.5	0	129.15
	0.23	1.5	0	127.13
	0.24	1.5	0	124.76
	0.25	1.5	0	122.11
	0.26	1.5	0	119.23
	0.27	1.5	0	116.19
	0.28	1.4	0	113.03
	0.29	1.4	0	109.80
	0.30	1.4	0	106.54
	0.31	1.4	0	103.30
D5MIT205	0.33	1.3	0	94.63
	0.34	1.1	0	88.19
	0.35	0.9	0	80.75
	0.36	0.7	0	72.29
	0.37	0.5	0	62.81
	0.38	0.3	0	52.32
	0.39	0.2	0	40.91
	0.40	0.1	0	28.68
	0.41	0.0	0	15.79
	0.42	0.0	0	2.42
	0.43	0.0	0	-11.21
	0.44	0.1	0	-24.86
	0.45	0.2	0	-38.30
	0.46	0.3	0	-51.29
	0.47	0.5	0	-63.63
	0.48	0.7	0	-75.16
	0.49	0.9	0	-85.73
	0.50	1.1	0	-95.27

```
                0.51       1.4          0  -103.73
                0.52       1.6          1  -111.10
                0.53       1.9          1  -117.41
D5MIT161

SIM CHROMOSOME 5 FOR CASPASE-3 (DNA)
Interval  mapping  for  Dataset:
nonmortalitywith80casun(nonmortality)
constrained additive regression,128  to  133  informative
progeny  from Progeny Order  Internal
mapping  QTL  CASPASE  on  chr  chrom5
using  Kosambi  mapping  function
With no control for other QTLs.
                map        Stat         %     Add
D5MIT268        0.00       0.0          0     2.87
                0.01       0.0          0     2.17
                0.02       0.0          0     1.39
                0.03       0.0          0     0.54
                0.04      -0.0          0    -0.40
                0.05       0.0          0    -1.41
                0.06       0.0          0    -2.51
                0.07       0.0          0    -3.69
                0.08       0.0          0    -4.94
                0.09       0.0          0    -6.27
                0.10       0.0          0    -7.65
                0.11       0.0          0    -9.07
                0.12       0.0          0   -10.53
                0.13       0.0          0   -12.01
                0.14       0.0          0   -13.49
                0.15       0.0          0   -14.94
                0.16       0.0          0   -16.36
                0.17       0.0          0   -17.71
                0.18       0.0          0   -18.99
                0.19       0.0          0   -20.18
                0.20       0.0          0   -21.27
                0.21       0.0          0   -22.24
                0.22       0.0          0   -23.09
                0.23       0.0          0   -23.82
                0.24       0.1          0   -24.43
                0.25       0.1          0   -24.93
                0.26       0.1          0   -25.31
                0.27       0.1          0   -25.59
                0.28       0.1          0   -25.77
                0.29       0.1          0   -25.87
                0.30       0.1          0   -25.89
                0.31      0.1        0    -25.84
D5MIT205        0.33      0.3        0    -49.23
                0.34      0.5        0    -61.86
                0.35      0.7        0    -75.36
                0.36      0.9        0    -89.66
                0.37      1.2        0   -104.65
                0.38      1.5        0   -120.19
                0.39      1.9        1   -136.09
                0.40      2.3        1   -152.15
                0.41      2.8        1   -168.12
                0.42      3.3        2   -183.74
                0.43      3.9        2   -198.77
                0.44      4.5        3   -212.94
                0.45      5.1        3   -226.05
                0.46      5.7        3   -237.88
                0.47      6.3        4   -248.32
                0.48      6.9        4   -257.26
                0.49      7.4        5   -264.66
                0.50      8.0        5   -270.53
                0.51      8.5        6   -274.93
                0.52      9.0        6   -277.94
                0.53      9.5        6   -279.67
D5MIT161

SIM CHROMOSOME 5 FOR CASPASE-3 (PROTEIN)
Interval  mapping  for  Dataset:
nonmortalitywith80casun(nonmortality)
constrained additive regression,128  to  133  informative
progeny  from Progeny Order  Internal
mapping  QTL  caspaseun   on  chr  chrom5
using  Kosambi  mapping  function
With no control for other QTLs.
                map       Stat       %      Add
D5MIT268        0.00      0.1        0     30.75
                0.01      0.1        0     29.26
                0.02      0.1        0     27.56
                0.03      0.1        0     25.62
                0.04      0.0        0     23.44
                0.05      0.0        0     21.00
                0.06      0.0        0     18.30
                0.07      0.0        0     15.33
                0.08      0.0        0     12.10
                0.09      0.0        0      8.61
                0.10      0.0        0      4.88
```

	0.11	0.0	0	0.93
	0.12	0.0	0	-3.20
	0.13	0.0	0	-7.47
	0.14	0.0	0	-11.83
	0.15	0.0	0	-16.24
	0.16	0.0	0	-20.64
	0.17	0.0	0	-24.96
	0.18	0.1	0	-29.16
	0.19	0.1	0	-33.19
	0.20	0.1	0	-37.00
	0.21	0.1	0	-40.55
	0.22	0.1	0	-43.82
	0.23	0.1	0	-46.78
	0.24	0.2	0	-49.42
	0.25	0.2	0	-51.75
	0.26	0.2	0	-53.76
	0.27	0.2	0	-55.47
	0.28	0.2	0	-56.90
	0.29	0.3	0	-58.05
	0.30	0.3	0	-58.96
	0.31	0.3	0	-59.65
D5MIT205	0.33	0.9	0	-99.54
	0.34	1.1	0	-107.90
	0.35	1.2	0	-116.57
	0.36	1.3	0	-125.48
	0.37	1.5	0	-134.53
	0.38	1.6	0	-143.60
	0.39	1.8	1	-152.55
	0.40	2.0	1	-161.24
	0.41	2.2	1	-169.51
	0.42	2.3	1	-177.21
	0.43	2.5	1	-184.19
	0.44	2.7	1	-190.33
	0.45	2.9	1	-195.54
	0.46	3.0	1	-199.75
	0.47	3.2	2	-202.91
	0.48	3.3	2	-205.04
	0.49	3.4	2	-206.16
	0.50	3.5	2	-206.34
	0.51	3.6	2	-205.64
	0.52	3.6	2	-204.18
	0.53	3.7	2	-202.04
D5MIT161				

```
SIM Reports for Chromosome 1 for AST, IL-6, Caspase-3 (DNA)
and Caspase-3 (Protein)
SIM CHROMOSOME 1 FOR AST
Interval  mapping  for  Dataset:
nonmortalitywith80casun(nonmortality)
constrained additive regression,125  to  133  informative
progeny  from Progeny Order  Internal
mapping  QTL  AST   on  chr  chrom1
using  Kosambi  mapping  function
With no control for other QTLs.
                map        Stat        %      Add
D1MIT65         0.00       0.0         0      -8.73
                0.01       0.0         0     -15.18
                0.02       0.0         0     -22.22
                0.03       0.1         0     -29.88
                0.04       0.1         0     -38.17
                0.05       0.2         0     -47.10
                0.06       0.2         0     -56.65
                0.07       0.3         0     -66.80
                0.08       0.4         0     -77.49
                0.09       0.5         0     -88.67
                0.10       0.6         0    -100.23
                0.11       0.8         0    -112.07
                0.12       0.9         0    -124.05
                0.13       1.1         0    -136.04
                0.14       1.3         0    -147.86
                0.15       1.5         0    -159.36
                0.16       1.7         1    -170.38
                0.17       1.9         1    -180.76
                0.18       2.1         1    -190.37
                0.19       2.3         1    -199.10
                0.20       2.6         1    -206.85
                0.21       2.8         1    -213.58
                0.22       3.0         2    -219.26
                0.23       3.2         2    -223.89
                0.24       3.4         2    -227.49
                0.25       3.6         2    -230.13
                0.26       3.7         2    -231.86
                0.27       3.9         2    -232.75
                0.28       4.1         2    -232.90
                0.29       4.2         3    -232.39
                0.30       4.3         3    -231.31
                0.31       4.4         3    -229.73
D1MIT303        0.33       5.0         3    -223.43
                0.34       5.1         3    -229.73
```

	0.35	5.2	3	-235.00
	0.36	5.2	3	-239.00
	0.37	5.2	3	-241.52
	0.38	5.2	3	-242.39
	0.39	5.1	3	-241.52
	0.40	5.0	3	-238.88
	0.41	4.8	3	-234.54
D1MIT8	0.42	4.1	2	-214.32
	0.43	4.0	2	-215.44
	0.44	3.9	2	-216.32
	0.45	3.7	2	-216.89
	0.46	3.6	2	-217.11
	0.47	3.5	2	-216.94
	0.48	3.3	2	-216.29
	0.49	3.2	2	-215.12
	0.50	3.0	1	-213.37
	0.51	2.8	1	-210.96
	0.52	2.6	1	-207.83
	0.53	2.5	1	-203.93
	0.54	2.3	1	-199.18
	0.55	2.1	1	-193.56
	0.56	1.9	1	-187.01
	0.57	1.7	1	-179.53
	0.58	1.5	0	-171.11
	0.59	1.3	0	-161.76
	0.60	1.1	0	-151.54
	0.61	1.0	0	-140.50
	0.62	0.8	0	-128.75
	0.63	0.7	0	-116.39
	0.64	0.5	0	-103.55
	0.65	0.4	0	-90.39
	0.66	0.3	0	-77.05
	0.67	0.2	0	-63.69
	0.68	0.1	0	-50.47
	0.69	0.1	0	-37.52
	0.70	0.0	0	-24.98
	0.71	0.0	0	-12.96
	0.72	0.0	0	-1.55
	0.73	0.0	0	9.19
	0.74	0.0	0	19.21
	0.75	0.0	0	28.47
	0.76	0.1	0	36.96
	0.77	0.1	0	44.70
	0.78	0.2	0	51.69
	0.79	0.2	0	57.97

```
                0.80      0.3       0    63.57
                0.81      0.3       0    68.53
                0.82      0.4       0    72.89
                0.83      0.5       0    76.70
                0.84      0.5       0    80.00
                0.85      0.6       0    82.83
                0.86      0.7       0    85.25
                0.87      0.7       0    87.28
D1MIT15         0.89      0.6       0    78.82
                0.90      0.6       0    78.03
                0.91      0.5       0    76.66
                0.92      0.5       0    74.67
                0.93      0.5       0    72.07
                0.94      0.4       0    68.87
                0.95      0.4       0    65.12
                0.96      0.3       0    60.92
                0.97      0.3       0    56.35
                0.98      0.2       0    51.54
                0.99      0.2       0    46.59
D1MIT17

SIM CHROMOSOME 1 FOR IL-6
Interval  mapping  for  Dataset:
nonmortalitywith80casun(nonmortality)
constrained additive regression,102  to  110  informative
progeny  from Progeny Order  Internal
mapping  QTL  IL6   on  chr  chrom1
using  Kosambi  mapping  function
With no control for other QTLs.
                map       Stat      %      Add
D1MIT65         0.00      0.2       0   -38.70
                0.01      0.2       0   -43.97
                0.02      0.3       0   -49.68
                0.03      0.3       0   -55.86
                0.04      0.4       0   -62.50
                0.05      0.5       0   -69.60
                0.06      0.6       0   -77.15
                0.07      0.7       0   -85.11
                0.08      0.8       0   -93.43
                0.09      0.9       0  -102.04
                0.10      1.0       0  -110.86
                0.11      1.2       0  -119.77
                0.12      1.3       0  -128.66
                0.13      1.5       0  -137.38
```

	0.14	1.6	1	-145.79
	0.15	1.8	1	-153.74
	0.16	1.9	1	-161.09
	0.17	2.1	1	-167.73
	0.18	2.3	1	-173.55
	0.19	2.4	1	-178.46
	0.20	2.6	2	-182.44
	0.21	2.7	2	-185.47
	0.22	2.9	2	-187.56
	0.23	3.0	2	-188.75
	0.24	3.1	2	-189.11
	0.25	3.2	2	-188.71
	0.26	3.3	2	-187.65
	0.27	3.3	2	-186.01
	0.28	3.4	2	-183.88
	0.29	3.4	2	-181.35
	0.30	3.5	2	-178.51
	0.31	3.5	2	-175.42
D1MIT303	0.33	3.2	2	-150.58
	0.34	3.4	2	-156.83
	0.35	3.5	2	-162.36
	0.36	3.6	2	-166.95
	0.37	3.6	2	-170.37
	0.38	3.7	2	-172.46
	0.39	3.7	2	-173.10
	0.40	3.7	2	-172.26
	0.41	3.6	2	-169.98
D1MIT8	0.42	3.5	2	-164.93
	0.43	3.4	2	-164.71
	0.44	3.2	2	-164.18
	0.45	3.1	2	-163.29
	0.46	2.9	2	-162.00
	0.47	2.7	2	-160.27
	0.48	2.6	1	-158.04
	0.49	2.4	1	-155.26
	0.50	2.2	1	-151.87
	0.51	2.0	1	-147.83
	0.52	1.8	1	-143.09
	0.53	1.6	1	-137.60
	0.54	1.4	0	-131.34
	0.55	1.3	0	-124.26
	0.56	1.1	0	-116.37
	0.57	0.9	0	-107.66
	0.58	0.7	0	-98.15
	0.59	0.6	0	-87.88

```
                 0.60      0.4        0   -76.91
                 0.61      0.3        0   -65.33
                 0.62      0.2        0   -53.23
                 0.63      0.1        0   -40.73
                 0.64      0.1        0   -27.96
                 0.65      0.0        0   -15.07
                 0.66      0.0        0    -2.19
                 0.67      0.0        0    10.52
                 0.68      0.0        0    22.94
                 0.69      0.1        0    34.94
                 0.70      0.2        0    46.42
                 0.71      0.2        0    57.27
                 0.72      0.4        0    67.43
                 0.73      0.5        0    76.86
                 0.74      0.6        0    85.52
                 0.75      0.7        0    93.39
                 0.76      0.9        0   100.48
                 0.77      1.0        0   106.81
                 0.78      1.2        0   112.41
                 0.79      1.3        0   117.30
                 0.80      1.5        0   121.54
                 0.81      1.7        1   125.16
                 0.82      1.8        1   128.23
                 0.83      2.0        1   130.77
                 0.84      2.1        1   132.85
                 0.85      2.2        1   134.50
                 0.86      2.4        1   135.78
                 0.87      2.5        1   136.72
D1MIT15          0.89      2.5        1   135.63
                 0.90      2.6        1   139.30
                 0.91      2.6        1   142.19
                 0.92      2.6        1   144.14
                 0.93      2.6        1   145.01
                 0.94      2.5        1   144.72
                 0.95      2.5        1   143.23
                 0.96      2.4        1   140.59
                 0.97      2.3        1   136.87
                 0.98      2.2        1   132.23
                 0.99      2.1        1   126.83
D1MIT17
```

SIM CHROMOSOME 1 FOR CASPASE-3 (DNA)
Interval mapping for Dataset:
nonmortalitywith80casun(nonmortality)

```
constrained additive regression,125  to  133  informative
progeny  from Progeny Order  Internal
mapping  QTL  CASPASE   on  chr  chrom1
using  Kosambi  mapping  function
With no control for other QTLs.
                map        Stat       %     Add
D1MIT65         0.00       0.1        0     32.07
                0.01       0.1        0     29.81
                0.02       0.1        0     27.26
                0.03       0.1        0     24.39
                0.04       0.0        0     21.18
                0.05       0.0        0     17.62
                0.06       0.0        0     13.69
                0.07       0.0        0      9.41
                0.08       0.0        0      4.76
                0.09       0.0        0     -0.22
                0.10       0.0        0     -5.52
                0.11       0.0        0    -11.10
                0.12       0.0        0    -16.90
                0.13       0.0        0    -22.87
                0.14       0.1        0    -28.93
                0.15       0.1        0    -35.01
                0.16       0.1        0    -41.03
                0.17       0.2        0    -46.90
                0.18       0.2        0    -52.56
                0.19       0.2        0    -57.92
                0.20       0.3        0    -62.94
                0.21       0.3        0    -67.56
                0.22       0.4        0    -71.74
                0.23       0.4        0    -75.47
                0.24       0.5        0    -78.73
                0.25       0.5        0    -81.53
                0.26       0.6        0    -83.89
                0.27       0.6        0    -85.83
                0.28       0.7        0    -87.37
                0.29       0.7        0    -88.54
                0.30       0.8        0    -89.38
                0.31       0.8        0    -89.92
D1MIT303        0.33       0.9        0    -87.64
                0.34       1.0        0    -90.91
                0.35       1.0        0    -93.82
                0.36       1.0        0    -96.27
                0.37       1.0        0    -98.15
                0.38       1.0        0    -99.39
```

	0.39	1.0	0	-99.93
	0.40	1.0	0	-99.74
	0.41	1.0	0	-98.83
D1MIT8	0.42	1.1	0	-101.25
	0.43	1.0	0	-99.12
	0.44	0.9	0	-96.58
	0.45	0.8	0	-93.59
	0.46	0.7	0	-90.10
	0.47	0.7	0	-86.06
	0.48	0.6	0	-81.42
	0.49	0.5	0	-76.14
	0.50	0.4	0	-70.18
	0.51	0.3	0	-63.49
	0.52	0.2	0	-56.05
	0.53	0.2	0	-47.83
	0.54	0.1	0	-38.82
	0.55	0.1	0	-29.02
	0.56	0.0	0	-18.45
	0.57	0.0	0	-7.15
	0.58	0.0	0	4.82
	0.59	0.0	0	17.37
	0.60	0.1	0	30.39
	0.61	0.1	0	43.77
	0.62	0.2	0	57.37
	0.63	0.3	0	71.02
	0.64	0.4	0	84.57
	0.65	0.6	0	97.85
	0.66	0.7	0	110.71
	0.67	0.9	0	123.01
	0.68	1.1	0	134.61
	0.69	1.3	0	145.42
	0.70	1.5	0	155.34
	0.71	1.7	1	164.33
	0.72	2.0	1	172.34
	0.73	2.2	1	179.39
	0.74	2.4	1	185.47
	0.75	2.6	1	190.61
	0.76	2.8	1	194.87
	0.77	3.0	2	198.29
	0.78	3.3	2	200.93
	0.79	3.4	2	202.87
	0.80	3.6	2	204.17
	0.81	3.8	2	204.89
	0.82	4.0	2	205.11

```
                0.83      4.1         2   204.88
                0.84      4.3         2   204.27
                0.85      4.4         3   203.32
                0.86      4.5         3   202.09
                0.87      4.7         3   200.62
D1MIT15         0.89      3.9         2   179.11
                0.90      4.3         2   191.19
                0.91      4.7         3   202.82
                0.92      5.1         3   213.69
                0.93      5.5         3   223.48
                0.94      5.9         4   231.92
                0.95      6.2         4   238.77
                0.96      6.6         4   243.85
                0.97      6.8         4   247.10
                0.98      7.0         5   248.50
                0.99      7.2         5   248.15
D1MIT17

SIM CHROMOSOME 1 FOR CASPASE-3 (PROTEIN)
Interval  mapping  for  Dataset:
nonmortalitywith80casun(nonmortality)
constrained additive regression,125  to  133  informative
progeny  from Progeny Order  Internal
mapping  QTL  caspaseun   on  chr  chrom1
using  Kosambi  mapping  function
With no control for other QTLs.

      map       Stat      %      Add
D1MIT65         0.00      0.0         0     4.66
                0.01      0.0         0     1.20
                0.02      0.0         0    -2.60
                0.03      0.0         0    -6.75
                0.04      0.0         0   -11.28
                0.05      0.0         0   -16.18
                0.06      0.0         0   -21.45
                0.07      0.0         0   -27.08
                0.08      0.1         0   -33.04
                0.09      0.1         0   -39.30
                0.10      0.1         0   -45.81
                0.11      0.2         0   -52.52
                0.12      0.2         0   -59.34
                0.13      0.3         0   -66.21
                0.14      0.3         0   -73.03
                0.15      0.4         0   -79.71
                0.16      0.4         0   -86.16
```

	0.17	0.5	0	-92.28
	0.18	0.6	0	-98.00
	0.19	0.6	0	-103.25
	0.20	0.7	0	-107.98
	0.21	0.8	0	-112.15
	0.22	0.8	0	-115.74
	0.23	0.9	0	-118.74
	0.24	0.9	0	-121.17
	0.25	1.0	0	-123.05
	0.26	1.1	0	-124.41
	0.27	1.1	0	-125.29
	0.28	1.2	0	-125.73
	0.29	1.2	0	-125.79
	0.30	1.3	0	-125.51
	0.31	1.3	0	-124.93
D1MIT303	0.33	1.3	0	-117.51
	0.34	1.2	0	-115.33
	0.35	1.1	0	-112.18
	0.36	1.0	0	-108.01
	0.37	0.9	0	-102.81
	0.38	0.7	0	-96.65
	0.39	0.6	0	-89.62
	0.40	0.5	0	-81.86
	0.41	0.4	0	-73.56
D1MIT8	0.42	0.5	0	-81.19
	0.43	0.5	0	-79.76
	0.44	0.5	0	-78.03
	0.45	0.4	0	-75.98
	0.46	0.4	0	-73.55
	0.47	0.3	0	-70.73
	0.48	0.3	0	-67.47
	0.49	0.3	0	-63.75
	0.50	0.2	0	-59.52
	0.51	0.2	0	-54.76
	0.52	0.1	0	-49.44
	0.53	0.1	0	-43.54
	0.54	0.1	0	-37.05
	0.55	0.0	0	-29.98
	0.56	0.0	0	-22.33
	0.57	0.0	0	-14.13
	0.58	0.0	0	-5.42
	0.59	0.0	0	3.73
	0.60	0.0	0	13.26
	0.61	0.0	0	23.07

```
                 0.62       0.0         0     33.06
                 0.63       0.1         0     43.13
                 0.64       0.1         0     53.14
                 0.65       0.2         0     62.98
                 0.66       0.2         0     72.54
                 0.67       0.3         0     81.70
                 0.68       0.4         0     90.38
                 0.69       0.5         0     98.49
                 0.70       0.5         0    105.97
                 0.71       0.6         0    112.78
                 0.72       0.7         0    118.88
                 0.73       0.8         0    124.28
                 0.74       0.9         0    128.97
                 0.75       1.0         0    132.98
                 0.76       1.1         0    136.33
                 0.77       1.1         0    139.07
                 0.78       1.2         0    141.24
                 0.79       1.3         0    142.87
                 0.80       1.4         0    144.04
                 0.81       1.4         0    144.77
                 0.82       1.5         0    145.13
                 0.83       1.6         0    145.15
                 0.84       1.6         0    144.87
                 0.85       1.7         0    144.34
                 0.86       1.7         1    143.60
                 0.87       1.8         1    142.67
D1MIT15          0.89       1.2         0    113.56
                 0.90       1.3         0    122.49
                 0.91       1.5         0    131.21
                 0.92       1.6         0    139.51
                 0.93       1.8         1    147.17
                 0.94       1.9         1    153.95
                 0.95       2.1         1    159.68
                 0.96       2.2         1    164.22
                 0.97       2.3         1    167.47
                 0.98       2.4         1    169.42
                 0.99       2.5         1    170.09
D1MIT17
```

SIM Reports for Chromosome 16 for AST, IL-6, Caspase-3 (DNA) and Caspase-3 (Protein)

```
SIM CHROMOSOME 16 FOR AST
Interval  mapping  for  Dataset:
nonmortalitywith80casun(nonmortality)
constrained additive regression,129  to  130  informative
```

```
progeny  from Progeny Order  Internal
mapping  QTL  AST  on  chr  chrom16
using  Kosambi  mapping  function
With no control for other QTLs.
                map        Stat        %      Add
D16MIT108       0.00       0.2         0     46.84
                0.01       0.2         0     44.77
                0.02       0.2         0     42.37
                0.03       0.1         0     39.63
                0.04       0.1         0     36.52
                0.05       0.1         0     33.02
                0.06       0.1         0     29.13
                0.07       0.0         0     24.83
                0.08       0.0         0     20.13
                0.09       0.0         0     15.05
                0.10       0.0         0      9.61
                0.11       0.0         0      3.86
                0.12       0.0         0     -2.17
                0.13       0.0         0     -8.39
                0.14       0.0         0    -14.75
                0.15       0.0         0    -21.15
                0.16       0.0         0    -27.52
                0.17       0.1         0    -33.77
                0.18       0.1         0    -39.81
                0.19       0.1         0    -45.58
                0.20       0.2         0    -51.02
                0.21       0.2         0    -56.06
                0.22       0.3         0    -60.68
                0.23       0.3         0    -64.85
                0.24       0.4         0    -68.55
                0.25       0.4         0    -71.80
                0.26       0.4         0    -74.59
                0.27       0.5         0    -76.96
                0.28       0.5         0    -78.92
                0.29       0.6         0    -80.51
D16MIT4         0.31       1.3         0   -112.49
                0.32       1.5         0   -123.42
                0.33       1.7         1   -134.77
                0.34       1.9         1   -146.44
                0.35       2.2         1   -158.29
                0.36       2.5         1   -170.16
                0.37       2.8         1   -181.87
                0.38       3.1         2   -193.22
                0.39       3.4         2   -204.01
                0.40      3.7        2  -214.04
                0.41      4.0        2  -223.13
                0.42      4.4        3  -231.12
                0.43      4.7        3  -237.91
                0.44      4.9        3  -243.41
                0.45      5.2        3  -247.59
                0.46      5.4        3  -250.47
                0.47      5.7        4  -252.10
                0.48      5.9        4  -252.55
                0.49      6.0        4  -251.94
                0.50      6.2        4  -250.39
D16MIT158

SIM CHROMOSOME 16 FOR IL-6
Interval  mapping  for  Dataset:
nonmortalitywith80casun(nonmortality)
constrained additive regression,105  to  106  informative
progeny  from Progeny Order  Internal
mapping  QTL  IL6   on  chr  chrom16
using  Kosambi  mapping  function
With no control for other QTLs.
                map       Stat       %      Add
D16MIT108       0.00      1.4        0    102.22
                0.01      1.4        0    102.32
                0.02      1.3        0    102.19
                0.03      1.3        0    101.77
                0.04      1.2        0    101.04
                0.05      1.1        0     99.96
                0.06      1.1        0     98.49
                0.07      1.0        0     96.60
                0.08      0.9        0     94.26
                0.09      0.8        0     91.45
                0.10      0.8        0     88.15
                0.11      0.7        0     84.37
                0.12      0.6        0     80.11
                0.13      0.5        0     75.41
                0.14      0.4        0     70.28
                0.15      0.4        0     64.80
                0.16      0.3        0     59.01
                0.17      0.3        0     52.99
                0.18      0.2        0     46.81
                0.19      0.1        0     40.57
                0.20      0.1        0     34.33
                0.21      0.1        0     28.18
                0.22      0.0         0     22.17
                0.23      0.0         0     16.38
                0.24      0.0         0     10.86
                0.25      0.0         0      5.63
                0.26      0.0         0      0.73
                0.27      0.0         0     -3.83
                0.28      0.0         0     -8.04
                0.29      0.0         0    -11.89
D16MIT4         0.31      0.2         0    -39.75
                0.32      0.2         0    -44.58
                0.33      0.3         0    -49.64
                0.34      0.3         0    -54.91
                0.35      0.4         0    -60.32
                0.36      0.5         0    -65.80
                0.37      0.5         0    -71.25
                0.38      0.6         0    -76.58
                0.39      0.7         0    -81.70
                0.40      0.7         0    -86.49
                0.41      0.8         0    -90.87
                0.42      0.9         0    -94.74
                0.43      1.0         0    -98.06
                0.44      1.0         0   -100.77
                0.45      1.1         0   -102.85
                0.46      1.2         0   -104.32
                0.47      1.2         0   -105.19
                0.48      1.3         0   -105.51
                0.49      1.3         0   -105.32
                0.50      1.3         0   -104.70
D16MIT158

SIM CHROMOSOME 16 FOR CASPASE-3 (DNA)
Interval  mapping  for  Dataset:
nonmortalitywith80casun(nonmortality)
constrained additive regression,129  to  130  informative
progeny  from Progeny Order  Internal
mapping  QTL  CASPASE   on  chr  chrom16
using  Kosambi  mapping  function
With no control for other QTLs.
                map       Stat        %      Add
D16MIT108       0.00      0.0         0    -10.36
                0.01      0.0         0    -12.18
                0.02      0.0         0    -14.15
                0.03      0.0         0    -16.27
                0.04      0.0         0    -18.55
```

	0.05	0.0	0	-20.97
	0.06	0.1	0	-23.54
	0.07	0.1	0	-26.23
	0.08	0.1	0	-29.04
	0.09	0.1	0	-31.93
	0.10	0.1	0	-34.89
	0.11	0.1	0	-37.87
	0.12	0.1	0	-40.84
	0.13	0.2	0	-43.77
	0.14	0.2	0	-46.60
	0.15	0.2	0	-49.30
	0.16	0.2	0	-51.84
	0.17	0.2	0	-54.17
	0.18	0.3	0	-56.26
	0.19	0.3	0	-58.11
	0.20	0.3	0	-59.68
	0.21	0.3	0	-60.98
	0.22	0.3	0	-62.01
	0.23	0.3	0	-62.77
	0.24	0.4	0	-63.28
	0.25	0.4	0	-63.56
	0.26	0.4	0	-63.62
	0.27	0.4	0	-63.49
	0.28	0.4	0	-63.19
	0.29	0.4	0	-62.75
D16MIT4	0.31	0.5	0	-64.49
	0.32	0.6	0	-71.73
	0.33	0.7	0	-79.29
	0.34	0.8	0	-87.10
	0.35	0.9	0	-95.09
	0.36	1.1	0	-103.14
	0.37	1.2	0	-111.15
	0.38	1.4	0	-118.97
	0.39	1.6	0	-126.48
	0.40	1.7	1	-133.54
	0.41	1.9	1	-140.02
	0.42	2.1	1	-145.82
	0.43	2.2	1	-150.84
	0.44	2.4	1	-155.04
	0.45	2.5	1	-158.38
	0.46	2.7	1	-160.86
	0.47	2.8	1	-162.51
	0.48	2.9	1	-163.37
	0.49	3.0	2	-163.51

```
                0.50      3.1         2  -162.99
D16MIT158

SIM CHROMOSOME 16 FOR CASPASE-3 (PROTEIN)
Interval  mapping  for  Dataset:
nonmortalitywith80casun(nonmortality)
constrained additive regression,129  to  130  informative
progeny  from Progeny Order  Internal
mapping  QTL  caspaseun  on  chr  chrom16
using  Kosambi  mapping  function
With no control for other QTLs.
                map       Stat        %     Add
D16MIT108       0.00      0.0         0     21.26
                0.01      0.0         0     20.01
                0.02      0.0         0     18.58
                0.03      0.0         0     16.97
                0.04      0.0         0     15.15
                0.05      0.0         0     13.13
                0.06      0.0         0     10.90
                0.07      0.0         0      8.45
                0.08      0.0         0      5.80
                0.09      0.0         0      2.96
                0.10      0.0         0     -0.07
                0.11      0.0         0     -3.26
                0.12      0.0         0     -6.57
                0.13      0.0         0     -9.97
                0.14      0.0         0    -13.42
                0.15      0.0         0    -16.88
                0.16      0.0         0    -20.30
                0.17      0.0         0    -23.63
                0.18      0.0         0    -26.82
                0.19      0.1         0    -29.86
                0.20      0.1         0    -32.69
                0.21      0.1         0    -35.30
                0.22      0.1         0    -37.66
                0.23      0.1         0    -39.77
                0.24      0.1         0    -41.62
                0.25      0.1         0    -43.22
                0.26      0.1         0    -44.57
                0.27      0.2         0    -45.69
                0.28      0.2         0    -46.59
                0.29      0.2         0    -47.30
D16MIT4         0.31      0.4         0    -60.20
                0.32      0.5         0    -68.19
                0.33      0.6         0    -76.58
                0.34      0.7        0    -85.31
                0.35      0.8        0    -94.27
                0.36      0.9        0   -103.37
                0.37      1.1        0   -112.46
                0.38      1.3        0   -121.42
                0.39      1.4        0   -130.07
                0.40      1.6        0   -138.29
                0.41      1.8        1   -145.91
                0.42      2.0        1   -152.82
                0.43      2.1        1   -158.91
                0.44      2.3        1   -164.11
                0.45      2.5        1   -168.37
                0.46      2.6        1   -171.68
                0.47      2.8        1   -174.07
                0.48      2.9        1   -175.57
                0.49      3.0        2   -176.25
                0.50      3.1        2   -176.20
D16MIT158


SIM CHROMOSOME 8 FOR AST
Interval  mapping  for  Dataset:
nonmortalitywith80casun(nonmortality)
constrained additive regression,116  to  136  informative
progeny  from Progeny Order  Internal
mapping  QTL  AST   on  chr  chrom8
using  Kosambi  mapping  function
With no control for other QTLs.
                map       Stat       %      Add
D8MIT94         0.00      0.0        0     23.10
                0.01      0.0        0     11.54
                0.02      0.0        0     -1.12
                0.03      0.0        0    -14.65
                0.04      0.1        0    -28.76
                0.05      0.1        0    -43.05
                0.06      0.2        0    -57.12
                0.07      0.3        0    -70.55
                0.08      0.5        0    -82.98
D8MIT189        0.10      1.4        0   -122.82
                0.11      1.4        0   -124.64
                0.12      1.4        0   -125.99
                0.13      1.4        0   -126.78
                0.14      1.4        0   -126.93
                0.15      1.3        0   -126.38
```

	0.16	1.3	0	-125.09
	0.17	1.2	0	-123.04
	0.18	1.2	0	-120.26
	0.19	1.1	0	-116.79
	0.20	1.0	0	-112.69
	0.21	1.0	0	-108.07
	0.22	0.9	0	-103.03
	0.23	0.8	0	-97.69
	0.24	0.8	0	-92.17
	0.25	0.7	0	-86.57
D8MIT106	0.27	0.6	0	-75.83
	0.28	0.5	0	-72.98
	0.29	0.5	0	-69.24
	0.30	0.4	0	-64.64
	0.31	0.3	0	-59.28
	0.32	0.3	0	-53.31
	0.33	0.2	0	-46.94
	0.34	0.2	0	-40.35
D8MIT80	0.35	0.1	0	-31.55
	0.36	0.1	0	-29.99
	0.37	0.1	0	-28.14
	0.38	0.1	0	-26.01
	0.39	0.1	0	-23.60
	0.40	0.0	0	-20.94
	0.41	0.0	0	-18.09
	0.42	0.0	0	-15.09
	0.43	0.0	0	-12.00
	0.44	0.0	0	-8.91
	0.45	0.0	0	-5.86
	0.46	0.0	0	-2.91
D8MIT40	0.47	0.0	0	0.80
	0.48	0.0	0	-14.38
	0.49	0.1	0	-30.31
	0.50	0.2	0	-46.57
	0.51	0.4	0	-62.70
	0.52	0.6	0	-78.24
	0.53	0.8	0	-92.73
	0.54	1.1	0	-105.83
	0.55	1.4	0	-117.27
D8MIT242	0.56	2.5	1	-152.14
	0.57	2.4	1	-153.61
	0.58	2.4	1	-154.58
	0.59	2.3	1	-154.97
	0.60	2.2	1	-154.70

```
                0.61      2.1        1  -153.71
                0.62      2.0        1  -151.94
                0.63      1.9        1  -149.36
                0.64      1.8        1  -145.96
                0.65      1.7        1  -141.74
                0.66      1.6        0  -136.77
                0.67      1.5        0  -131.10
                0.68      1.3        0  -124.82
                0.69      1.2        0  -118.06
                0.70      1.1        0  -110.94
                0.71      1.0        0  -103.57
                0.72      0.8        0   -96.10
                0.73      0.7        0   -88.63
                0.74      0.6        0   -81.27
                0.75      0.6        0   -74.10
D8MIT36

SIM CHROMOSOME 8 FOR IL-6
Interval  mapping  for  Dataset:
nonmortalitywith80casun(nonmortality)
constrained additive regression,95  to  112  informative
progeny  from Progeny Order  Internal
mapping  QTL  IL6   on  chr  chrom8
using  Kosambi  mapping  function
With no control for other QTLs.
                map       Stat       %     Add
D8MIT94         0.00      1.1        0   -99.59
                0.01      1.3        0  -111.57
                0.02      1.6        1  -123.57
                0.03      1.8        1  -135.24
                0.04      2.1        1  -146.15
                0.05      2.3        1  -155.91
                0.06      2.6        2  -164.16
                0.07      2.8        2  -170.64
                0.08      3.1        2  -175.20
D8MIT189        0.10      2.9        2  -142.90
                0.11      2.9        2  -145.52
                0.12      2.9        2  -147.67
                0.13      2.8        2  -149.26
                0.14      2.8        2  -150.21
                0.15      2.8        2  -150.44
                0.16      2.7        2  -149.89
                0.17      2.6        1  -148.54
                0.18      2.6        1  -146.37
```

	0.19	2.5	1	-143.43
	0.20	2.4	1	-139.75
	0.21	2.2	1	-135.42
	0.22	2.1	1	-130.55
	0.23	2.0	1	-125.23
	0.24	1.9	1	-119.60
	0.25	1.7	1	-113.76
D8MIT106	0.27	1.5	0	-101.95
	0.28	1.6	0	-106.10
	0.29	1.6	1	-109.28
	0.30	1.6	1	-111.28
	0.31	1.6	1	-111.96
	0.32	1.6	1	-111.25
	0.33	1.6	1	-109.20
	0.34	1.5	0	-105.97
D8MIT80	0.35	1.5	0	-100.15
	0.36	1.5	0	-102.83
	0.37	1.5	0	-104.95
	0.38	1.5	0	-106.38
	0.39	1.5	0	-107.01
	0.40	1.4	0	-106.76
	0.41	1.4	0	-105.59
	0.42	1.3	0	-103.52
	0.43	1.3	0	-100.60
	0.44	1.2	0	-96.94
	0.45	1.1	0	-92.67
	0.46	1.0	0	-87.95
D8MIT40	0.47	0.9	0	-81.18
	0.48	0.9	0	-80.88
	0.49	0.8	0	-79.67
	0.50	0.8	0	-77.50
	0.51	0.7	0	-74.41
	0.52	0.6	0	-70.48
	0.53	0.6	0	-65.86
	0.54	0.5	0	-60.74
	0.55	0.4	0	-55.32
D8MIT242	0.56	0.7	0	-66.51
	0.57	0.6	0	-64.72
	0.58	0.5	0	-62.53
	0.59	0.5	0	-59.93
	0.60	0.4	0	-56.90
	0.61	0.4	0	-53.43
	0.62	0.3	0	-49.54
	0.63	0.3	0	-45.26

```
                 0.64      0.2         0   -40.61
                 0.65      0.2         0   -35.67
                 0.66      0.1         0   -30.50
                 0.67      0.1         0   -25.16
                 0.68      0.0         0   -19.75
                 0.69      0.0         0   -14.34
                 0.70      0.0         0    -9.02
                 0.71      0.0         0    -3.86
                 0.72      0.0         0     1.09
                 0.73      0.0         0     5.76
                 0.74      0.0         0    10.12
                 0.75      0.0         0    14.15
D8MIT36

SIM CHROMOSOME 8 FOR CASPASE-3 (DNA)
Interval  mapping  for  Dataset:
nonmortalitywith80casun(nonmortality)
constrained additive regression,116  to  136  informative
progeny  from Progeny Order  Internal
mapping  QTL  CASPASE   on  chr  chrom8
using  Kosambi  mapping  function
With no control for other QTLs.
      map        Stat        %     Add
D8MIT94          0.00      0.0         0    12.21
                 0.01      0.0         0    13.92
                 0.02      0.0         0    15.64
                 0.03      0.0         0    17.34
                 0.04      0.0         0    18.96
                 0.05      0.0         0    20.46
                 0.06      0.0         0    21.78
                 0.07      0.0         0    22.88
                 0.08      0.1         0    23.75
D8MIT189         0.10      0.0         0   -19.08
                 0.11      0.0         0   -15.94
                 0.12      0.0         0   -12.48
                 0.13      0.0         0    -8.73
                 0.14      0.0         0    -4.72
                 0.15      0.0         0    -0.51
                 0.16      0.0         0     3.84
                 0.17      0.0         0     8.26
                 0.18      0.0         0    12.68
                 0.19      0.0         0    17.00
                 0.20      0.0         0    21.16
                 0.21      0.1         0    25.08
                 0.22      0.1         0    28.72
```

	0.23	0.1	0	32.02
	0.24	0.1	0	34.97
	0.25	0.2	0	37.55
D8MIT106	0.27	0.2	0	41.78
	0.28	0.2	0	40.40
	0.29	0.2	0	38.54
	0.30	0.1	0	36.21
	0.31	0.1	0	33.48
	0.32	0.1	0	30.41
	0.33	0.1	0	27.12
	0.34	0.1	0	23.71
D8MIT80	0.35	0.0	0	19.15
	0.36	0.1	0	24.41
	0.37	0.1	0	29.96
	0.38	0.1	0	35.71
	0.39	0.2	0	41.55
	0.40	0.2	0	47.33
	0.41	0.3	0	52.93
	0.42	0.4	0	58.19
	0.43	0.4	0	62.99
	0.44	0.5	0	67.23
	0.45	0.6	0	70.83
	0.46	0.6	0	73.77
D8MIT40	0.47	0.7	0	76.65
	0.48	0.7	0	80.18
	0.49	0.8	0	83.22
	0.50	0.8	0	85.62
	0.51	0.9	0	87.28
	0.52	0.9	0	88.15
	0.53	0.9	0	88.20
	0.54	0.9	0	87.47
	0.55	0.9	0	86.03
D8MIT242	0.56	0.4	0	58.05
	0.57	0.4	0	59.20
	0.58	0.4	0	60.22
	0.59	0.4	0	61.08
	0.60	0.4	0	61.75
	0.61	0.4	0	62.19
	0.62	0.4	0	62.37
	0.63	0.4	0	62.28
	0.64	0.4	0	61.89
	0.65	0.4	0	61.20
	0.66	0.4	0	60.20
	0.67	0.3	0	58.92
	0.68	0.3	0	57.38

```
                0.69      0.3        0    55.59
                0.70      0.3        0    53.61
                0.71      0.3        0    51.47
                0.72      0.3        0    49.21
                0.73      0.2        0    46.88
                0.74      0.2        0    44.52
                0.75      0.2        0    42.15
D8MIT36

SIM CHROMOSOME 8 FOR CASPASE-3 (PROTEIN)
Interval  mapping  for  Dataset:
nonmortalitywith80casun(nonmortality)
constrained additive regression,116  to  136  informative
progeny  from Progeny Order  Internal
mapping  QTL  caspaseun   on  chr  chrom8
using  Kosambi  mapping  function
With no control for other QTLs.
                map       Stat       %     Add
D8MIT94         0.00      0.0        0     8.74
                0.01      0.0        0    21.86
                0.02      0.1        0    35.92
                0.03      0.2        0    50.63
                0.04      0.3        0    65.64
                0.05      0.4        0    80.51
                0.06      0.6        0    94.81
                0.07      0.8        0   108.11
                0.08      1.0        0   120.08
D8MIT189        0.10      0.5        0    76.63
                0.11      0.5        0    77.59
                0.12      0.5        0    78.19
                0.13      0.5        0    78.36
                0.14      0.5        0    78.09
                0.15      0.5        0    77.32
                0.16      0.4        0    76.05
                0.17      0.4        0    74.27
                0.18      0.4        0    72.03
                0.19      0.4        0    69.35
                0.20      0.3        0    66.31
                0.21      0.3        0    62.97
                0.22      0.3        0    59.42
                0.23      0.2        0    55.73
                0.24      0.2        0    52.00
                0.25      0.2        0    48.28
D8MIT106        0.27      0.2        0    41.63
```

	0.28	0.2	0	50.64
	0.29	0.3	0	59.73
	0.30	0.4	0	68.62
	0.31	0.5	0	77.02
	0.32	0.6	0	84.66
	0.33	0.7	0	91.33
	0.34	0.8	0	96.88
D8MIT80	0.35	1.0	0	102.44
	0.36	0.8	0	95.43
	0.37	0.7	0	87.25
	0.38	0.5	0	77.93
	0.39	0.4	0	67.57
	0.40	0.3	0	56.33
	0.41	0.2	0	44.43
	0.42	0.1	0	32.13
	0.43	0.0	0	19.69
	0.44	0.0	0	7.42
	0.45	0.0	0	-4.43
	0.46	0.0	0	-15.64
D8MIT40	0.47	0.1	0	-29.38
	0.48	0.0	0	-8.28
	0.49	0.0	0	14.12
	0.50	0.1	0	37.28
	0.51	0.3	0	60.55
	0.52	0.6	0	83.27
	0.53	1.0	0	104.78
	0.54	1.4	0	124.55
	0.55	1.9	1	142.15
D8MIT242	0.56	2.0	1	147.03
	0.57	1.8	1	143.49
	0.58	1.7	0	139.08
	0.59	1.5	0	133.75
	0.60	1.3	0	127.45
	0.61	1.1	0	120.18
	0.62	1.0	0	111.95
	0.63	0.8	0	102.83
	0.64	0.6	0	92.90
	0.65	0.5	0	82.27
	0.66	0.4	0	71.11
	0.67	0.3	0	59.57
	0.68	0.2	0	47.86
	0.69	0.1	0	36.15
	0.70	0.0	0	24.64
	0.71	0.0	0	13.47
	0.72	0.0	0	2.81

```
                0.73      0.0         0    -7.25
                0.74      0.0         0   -16.62
                0.75      0.1         0   -25.24
D8MIT36

SIM CHROMOSOME 11 FOR AST
Interval  mapping  for  Dataset:
nonmortalitywith80casun(nonmortality)
constrained additive regression,114  to  136  informative
progeny  from Progeny Order  Internal
mapping  QTL  AST   on  chr  chrom11
using  Kosambi  mapping  function
With no control for other QTLs.
                map       Stat        %      Add
D11MIT2         0.00      0.0         0     12.87
                0.01      0.0         0     12.47
                0.02      0.0         0     12.02
                0.03      0.0         0     11.52
                0.04      0.0         0     10.97
                0.05      0.0         0     10.36
                0.06      0.0         0      9.68
                0.07      0.0         0      8.94
                0.08      0.0         0      8.13
                0.09      0.0         0      7.26
                0.10      0.0         0      6.33
                0.11      0.0         0      5.35
                0.12      0.0         0      4.34
                0.13      0.0         0      3.29
                0.14      0.0         0      2.24
                0.15      0.0         0      1.20
                0.16      0.0         0      0.18
                0.17      0.0         0     -0.81
                0.18      0.0         0     -1.76
                0.19      0.0         0     -2.65
                0.20      0.0         0     -3.48
                0.21      0.0         0     -4.24
D11MIT164       0.23      0.2         0     51.13
                0.24      0.1         0     32.04
                0.25      0.0         0     13.00
                0.26      0.0         0     -5.47
D11MIT339       0.28      0.1         0    -30.43
                0.29      0.1         0    -38.15
                0.30      0.2         0    -46.42
                0.31      0.3         0    -55.15
                0.32      0.4       0    -64.28
                0.33      0.4       0    -73.68
                0.34      0.6       0    -83.20
                0.35      0.7       0    -92.67
                0.36      0.8       0   -101.91
                0.37      1.0       0   -110.74
                0.38      1.1       0   -118.98
                0.39      1.3       0   -126.48
                0.40      1.4       0   -133.12
                0.41      1.6       0   -138.81
                0.42      1.7       1   -143.52
                0.43      1.9       1   -147.25
                0.44      2.0       1   -150.04
                0.45      2.1       1   -151.95
D11MIT179       0.46      2.2       1   -150.14
                0.47      2.4       1   -157.99
                0.48      2.6       1   -165.69
                0.49      2.7       1   -173.08
                0.50      2.9       1   -180.00
                0.51      3.0       1   -186.30
                0.52      3.2       2   -191.83
                0.53      3.3       2   -196.46
                0.54      3.4       2   -200.07
                0.55      3.5       2   -202.61
                0.56      3.6       2   -204.04
                0.57      3.7       2   -204.37
                0.58      3.7       2   -203.66
                0.59      3.8       2   -201.97
                0.60      3.8       2   -199.43
                0.61      3.8       2   -196.14
D11MIT258       0.63      3.4       2   -190.09
                0.64      3.5       2   -195.03
                0.65      3.5       2   -196.75
                0.66      3.4       2   -195.03
D11MIT168

SIM CHROMOSOME 11 FOR IL-6
Interval  mapping  for  Dataset:
nonmortalitywith80casun(nonmortality)
constrained additive regression,94  to  112  informative
progeny  from Progeny Order  Internal
mapping  QTL  IL6   on  chr  chrom11
using  Kosambi  mapping  function
With no control for other QTLs.
```

	map	Stat	%	Add
D11MIT2	0.00	1.6	1	-119.71
	0.01	1.6	1	-122.82
	0.02	1.6	1	-125.98
	0.03	1.6	1	-129.13
	0.04	1.6	1	-132.20
	0.05	1.6	1	-135.11
	0.06	1.6	1	-137.77
	0.07	1.6	1	-140.07
	0.08	1.6	1	-141.91
	0.09	1.6	1	-143.17
	0.10	1.6	1	-143.76
	0.11	1.5	1	-143.59
	0.12	1.5	1	-142.63
	0.13	1.5	0	-140.84
	0.14	1.4	0	-138.25
	0.15	1.3	0	-134.91
	0.16	1.3	0	-130.91
	0.17	1.2	0	-126.37
	0.18	1.1	0	-121.40
	0.19	1.1	0	-116.13
	0.20	1.0	0	-110.69
	0.21	0.9	0	-105.20
D11MIT164	0.23	0.4	0	-65.94
	0.24	0.5	0	-68.24
	0.25	0.5	0	-69.75
	0.26	0.5	0	-70.46
D11MIT339	0.28	0.4	0	-55.84
	0.29	0.5	0	-59.91
	0.30	0.5	0	-64.13
	0.31	0.6	0	-68.42
	0.32	0.6	0	-72.73
	0.33	0.7	0	-76.95
	0.34	0.7	0	-80.99
	0.35	0.8	0	-84.75
	0.36	0.9	0	-88.11
	0.37	0.9	0	-90.98
	0.38	0.9	0	-93.28
	0.39	1.0	0	-94.97
	0.40	1.0	0	-96.00
	0.41	1.1	0	-96.40
	0.42	1.1	0	-96.18
	0.43	1.1	0	-95.40
	0.44	1.1	0	-94.12

```
                0.45      1.1        0    -92.43
D11MIT179       0.46      1.0        0    -86.19
                0.47      0.9        0    -82.48
                0.48      0.8        0    -78.12
                0.49      0.7        0    -73.12
                0.50      0.6        0    -67.49
                0.51      0.5        0    -61.29
                0.52      0.4        0    -54.59
                0.53      0.3        0    -47.49
                0.54      0.2        0    -40.08
                0.55      0.1        0    -32.50
                0.56      0.1        0    -24.87
                0.57      0.0        0    -17.32
                0.58      0.0        0     -9.97
                0.59      0.0        0     -2.91
                0.60      0.0        0      3.76
                0.61      0.0        0     10.00
D11MIT258       0.63      0.1        0     26.96
                0.64      0.1        0     22.69
                0.65      0.0        0     17.86
                0.66      0.0        0     12.68
D11MIT168

SIM CHROMOSOME 11 FOR CASPASE-3 (DNA)
Interval  mapping  for  Dataset:
nonmortalitywith80casun(nonmortality)
constrained additive regression,114  to  136  informative
progeny  from Progeny Order  Internal
mapping  QTL  CASPASE   on  chr  chrom11
using  Kosambi  mapping  function
With no control for other QTLs.
                map       Stat       %      Add
D11MIT2         0.00      0.6        0    -68.43
                0.01      0.5        0    -65.12
                0.02      0.4        0    -61.25
                0.03      0.3        0    -56.76
                0.04      0.3        0    -51.61
                0.05      0.2        0    -45.76
                0.06      0.1        0    -39.19
                0.07      0.1        0    -31.91
                0.08      0.1        0    -23.94
                0.09      0.0        0    -15.34
                0.10      0.0        0     -6.21
                0.11      0.0        0      3.31
                0.12      0.0        0     13.08
```

	0.13	0.0	0	22.92
	0.14	0.1	0	32.65
	0.15	0.1	0	42.10
	0.16	0.2	0	51.11
	0.17	0.3	0	59.53
	0.18	0.4	0	67.29
	0.19	0.5	0	74.30
	0.20	0.6	0	80.55
	0.21	0.7	0	86.02
D11MIT164	0.23	1.1	0	109.32
	0.24	1.2	0	117.11
	0.25	1.4	0	123.67
	0.26	1.6	0	128.88
D11MIT339	0.28	1.7	0	118.90
	0.29	1.7	0	120.43
	0.30	1.6	0	121.50
	0.31	1.6	0	122.03
	0.32	1.5	0	121.93
	0.33	1.5	0	121.12
	0.34	1.4	0	119.56
	0.35	1.3	0	117.22
	0.36	1.2	0	114.09
	0.37	1.1	0	110.21
	0.38	1.1	0	105.64
	0.39	1.0	0	100.49
	0.40	0.9	0	94.85
	0.41	0.8	0	88.88
	0.42	0.7	0	82.69
	0.43	0.6	0	76.44
	0.44	0.5	0	70.22
	0.45	0.5	0	64.15
D11MIT179	0.46	0.4	0	56.29
	0.47	0.3	0	52.90
	0.48	0.3	0	49.00
	0.49	0.2	0	44.59
	0.50	0.2	0	39.70
	0.51	0.1	0	34.38
	0.52	0.1	0	28.69
	0.53	0.1	0	22.71
	0.54	0.0	0	16.56
	0.55	0.0	0	10.33
	0.56	0.0	0	4.14
	0.57	0.0	0	-1.91
	0.58	0.0	0	-7.73

```
                0.59      0.0        0   -13.23
                0.60      0.0        0   -18.35
                0.61      0.1        0   -23.06
D11MIT258       0.63      0.1        0   -26.02
                0.64      0.1        0   -26.14
                0.65      0.1        0   -25.81
                0.66      0.1        0   -25.03
D11MIT168

SIM CHROMOSOME 11 FOR CASPASE-3 (PROTEIN)
Interval  mapping  for  Dataset:
nonmortalitywith80casun(nonmortality)
constrained additive regression,114  to  136  informative
progeny  from Progeny Order  Internal
mapping  QTL  caspaseun   on  chr  chrom11
using  Kosambi  mapping  function
With no control for other QTLs.
                map       Stat       %      Add
D11MIT2         0.00      4.0        3  -227.11
                0.01      3.9        3  -230.08
                0.02      3.8        2  -232.65
                0.03      3.7        2  -234.70
                0.04      3.6        2  -236.09
                0.05      3.5        2  -236.68
                0.06      3.4        2  -236.31
                0.07      3.2        2  -234.83
                0.08      3.0        2  -232.11
                0.09      2.9        2  -228.07
                0.10      2.7        1  -222.62
                0.11      2.5        1  -215.77
                0.12      2.3        1  -207.56
                0.13      2.0        1  -198.10
                0.14      1.8        1  -187.57
                0.15      1.6        1  -176.17
                0.16      1.4        0  -164.13
                0.17      1.2        0  -151.72
                0.18      1.1        0  -139.18
                0.19      0.9        0  -126.73
                0.20      0.8        0  -114.57
                0.21      0.6        0  -102.85
D11MIT164       0.23      0.5        0   -83.30
                0.24      0.4        0   -73.52
                0.25      0.3        0   -63.28
                0.26      0.2        0   -52.89
```

```
D11MIT339       0.28       0.0         0   -19.41
                0.29       0.0         0   -22.72
                0.30       0.1         0   -26.29
                0.31       0.1         0   -30.11
                0.32       0.1         0   -34.13
                0.33       0.1         0   -38.28
                0.34       0.1         0   -42.50
                0.35       0.2         0   -46.71
                0.36       0.2         0   -50.82
                0.37       0.2         0   -54.74
                0.38       0.2         0   -58.37
                0.39       0.3         0   -61.64
                0.40       0.3         0   -64.50
                0.41       0.3         0   -66.90
                0.42       0.4         0   -68.82
                0.43       0.4         0   -70.26
                0.44       0.4         0   -71.24
                0.45       0.4         0   -71.79
D11MIT179       0.46       0.4         0   -67.67
                0.47       0.5         0   -77.28
                0.48       0.6         0   -87.26
                0.49       0.8         0   -97.46
                0.50       0.9         0  -107.74
                0.51       1.1         0  -117.93
                0.52       1.3         0  -127.84
                0.53       1.5         0  -137.27
                0.54       1.7         0  -146.06
                0.55       1.9         1  -154.05
                0.56       2.1         1  -161.11
                0.57       2.3         1  -167.14
                0.58       2.4         1  -172.11
                0.59       2.6         1  -175.99
                0.60       2.8         1  -178.82
                0.61       2.9         1  -180.66
D11MIT258       0.63       3.2         2  -191.81
                0.64       3.3         2  -198.44
                0.65       3.4         2  -201.86
                0.66       3.4         2  -201.77
D11MIT168

SIM CHROMOSOME 13 FOR AST
Interval  mapping  for  Dataset:
nonmortalitywith80casun(nonmortality)
constrained additive regression,123  to  136  informative
```

```
progeny  from Progeny Order  Internal
mapping  QTL  AST   on  chr  chrom13
using  Kosambi  mapping  function
With no control for other QTLs.
                map        Stat         %      Add
D13MIT17        0.00       0.4          0     59.95
                0.01       0.3          0     57.96
                0.02       0.3          0     55.51
                0.03       0.3          0     52.60
                0.04       0.2          0     49.20
                0.05       0.2          0     45.35
                0.06       0.1          0     41.07
                0.07       0.1          0     36.42
                0.08       0.1          0     31.48
                0.09       0.1          0     26.33
                0.10       0.0          0     21.08
                0.11       0.0          0     15.81
                0.12       0.0          0     10.64
                0.13       0.0          0      5.65
                0.14       0.0          0      0.90
D13MIT61        0.16       0.0          0      5.78
                0.17       0.0          0      5.65
                0.18       0.0          0      5.51
                0.19       0.0          0      5.33
                0.20       0.0          0      5.14
                0.21       0.0          0      4.91
                0.22       0.0          0      4.66
                0.23       0.0          0      4.39
                0.24       0.0          0      4.09
                0.25       0.0          0      3.78
                0.26       0.0          0      3.46
                0.27       0.0          0      3.13
                0.28       0.0          0      2.80
                0.29       0.0          0      2.47
                0.30       0.0          0      2.14
                0.31       0.0          0      1.83
                0.32       0.0          0      1.53
D13MIT99        0.33       0.8          0    -85.31
                0.34       0.8          0    -86.66
                0.35       0.8          0    -87.91
                0.36       0.7          0    -89.02
                0.37       0.7          0    -89.95
                0.38       0.7          0    -90.69
                0.39       0.7          0    -91.19
                0.40       0.7        0    -91.42
                0.41       0.7        0    -91.35
                0.42       0.6        0    -90.96
                0.43       0.6        0    -90.21
                0.44       0.6        0    -89.10
                0.45       0.6        0    -87.61
                0.46       0.5        0    -85.76
                0.47       0.5        0    -83.55
                0.48       0.5        0    -81.01
                0.49       0.5        0    -78.17
                0.50       0.4        0    -75.08
                0.51       0.4        0    -71.77
                0.52       0.4        0    -68.31
                0.53       0.3        0    -64.74
                0.54       0.3        0    -61.10
                0.55       0.3        0    -57.47
                0.56       0.2        0    -53.86
                0.57       0.2        0    -50.32
                0.58       0.2        0    -46.89
                0.59       0.2        0    -43.58
                0.60       0.2        0    -40.41
                0.61       0.1        0    -37.41
D13MIT151

SIM CHROMOSOME 13 FOR IL-6
Interval  mapping  for  Dataset:
nonmortalitywith80casun(nonmortality)
constrained additive regression,103  to  112  informative
progeny  from Progeny Order  Internal
mapping  QTL  IL6   on  chr  chrom13
using  Kosambi  mapping  function
With no control for other QTLs.
                map        Stat       %      Add
D13MIT17        0.00       1.9        1   -113.61
                0.01       2.0        1   -120.77
                0.02       2.2        1   -127.90
                0.03       2.3        1   -134.85
                0.04       2.5        1   -141.46
                0.05       2.7        1   -147.55
                0.06       2.8        2   -152.94
                0.07       2.9        2   -157.47
                0.08       3.0        2   -161.01
                0.09       3.1        2   -163.46
                0.10       3.2        2   -164.77
```

	0.11	3.3	2	-164.95
	0.12	3.3	2	-164.05
	0.13	3.3	2	-162.16
	0.14	3.3	2	-159.40
D13MIT61	0.16	3.0	2	-143.75
	0.17	3.1	2	-148.27
	0.18	3.2	2	-152.43
	0.19	3.2	2	-156.12
	0.20	3.3	2	-159.23
	0.21	3.3	2	-161.65
	0.22	3.3	2	-163.28
	0.23	3.3	2	-164.05
	0.24	3.3	2	-163.92
	0.25	3.3	2	-162.87
	0.26	3.2	2	-160.92
	0.27	3.1	2	-158.13
	0.28	3.0	2	-154.58
	0.29	2.9	2	-150.37
	0.30	2.8	2	-145.63
	0.31	2.7	2	-140.47
	0.32	2.6	1	-135.02
D13MIT99	0.33	2.7	2	-144.19
	0.34	2.7	2	-148.25
	0.35	2.8	2	-152.27
	0.36	2.8	2	-156.21
	0.37	2.8	2	-160.01
	0.38	2.9	2	-163.61
	0.39	2.9	2	-166.93
	0.40	2.9	2	-169.91
	0.41	2.9	2	-172.46
	0.42	2.9	2	-174.52
	0.43	2.9	2	-176.01
	0.44	2.9	2	-176.88
	0.45	2.8	2	-177.07
	0.46	2.8	2	-176.55
	0.47	2.8	2	-175.31
	0.48	2.7	2	-173.35
	0.49	2.6	2	-170.70
	0.50	2.5	1	-167.40
	0.51	2.5	1	-163.52
	0.52	2.4	1	-159.13
	0.53	2.3	1	-154.32
	0.54	2.2	1	-149.17
	0.55	2.1	1	-143.78

```
                0.56       2.0          1  -138.22
                0.57       1.9          1  -132.59
                0.58       1.8          1  -126.95
                0.59       1.7          1  -121.36
                0.60       1.6          1  -115.87
                0.61       1.5          0  -110.53
D13MIT151

SIM CHROMOSOME 13 FOR CASPASE-3 (DNA)
Interval  mapping  for  Dataset:
nonmortalitywith80casun(nonmortality)
constrained additive regression,123  to  136  informative
progeny  from Progeny Order  Internal
mapping  QTL  CASPASE   on  chr  chrom13
using  Kosambi  mapping  function
With no control for other QTLs.
                map        Stat         %     Add
D13MIT17        0.00       0.3          0    -47.58
                0.01       0.4          0    -53.94
                0.02       0.4          0    -60.58
                0.03       0.5          0    -67.40
                0.04       0.6          0    -74.31
                0.05       0.7          0    -81.17
                0.06       0.8          0    -87.87
                0.07       1.0          0    -94.25
                0.08       1.1          0   -100.19
                0.09       1.2          0   -105.55
                0.10       1.3          0   -110.24
                0.11       1.4          0   -114.19
                0.12       1.5          0   -117.35
                0.13       1.6          0   -119.71
                0.14       1.7          1   -121.30
D13MIT61        0.16       1.8          1   -122.02
                0.17       1.9          1   -126.71
                0.18       2.0          1   -131.16
                0.19       2.0          1   -135.29
                0.20       2.1          1   -138.98
                0.21       2.2          1   -142.13
                0.22       2.2          1   -144.63
                0.23       2.2          1   -146.43
                0.24       2.3          1   -147.45
                0.25       2.3          1   -147.67
                0.26       2.3          1   -147.08
                0.27       2.2          1   -145.72
                0.28      2.2         1  -143.64
                0.29      2.2         1  -140.92
                0.30      2.1         1  -137.66
                0.31      2.1         1  -133.94
                0.32      2.0         1  -129.88
D13MIT99        0.33      1.8         1  -128.08
                0.34      1.9         1  -132.22
                0.35      1.9         1  -136.39
                0.36      2.0         1  -140.55
                0.37      2.0         1  -144.65
                0.38      2.1         1  -148.63
                0.39      2.1         1  -152.44
                0.40      2.2         1  -156.01
                0.41      2.2         1  -159.27
                0.42      2.2         1  -162.16
                0.43      2.2         1  -164.59
                0.44      2.3         1  -166.52
                0.45      2.3         1  -167.89
                0.46      2.3         1  -168.64
                0.47      2.3         1  -168.77
                0.48      2.2         1  -168.25
                0.49      2.2         1  -167.10
                0.50      2.2         1  -165.33
                0.51      2.2         1  -163.00
                0.52      2.1         1  -160.14
                0.53      2.1         1  -156.82
                0.54      2.0         1  -153.12
                0.55      2.0         1  -149.11
                0.56      1.9         1  -144.86
                0.57      1.8         1  -140.44
                0.58      1.8         1  -135.91
                0.59      1.7         1  -131.35
                0.60      1.7         1  -126.79
                0.61      1.6         0  -122.29
D13MIT151

SIM CHROMOSOME 13 FOR CASPASE-3 (PROTEIN)
Interval  mapping  for  Dataset:
nonmortalitywith80casun(nonmortality)
constrained additive regression,123  to  136  informative
progeny  from Progeny Order  Internal
mapping  QTL  caspaseun   on  chr  chrom13
using  Kosambi  mapping  function
With no control for other QTLs.
```

	map	Stat	%	Add
D13MIT17	0.00	0.3	0	-50.41
	0.01	0.3	0	-54.50
	0.02	0.3	0	-58.65
	0.03	0.4	0	-62.80
	0.04	0.4	0	-66.87
	0.05	0.5	0	-70.78
	0.06	0.5	0	-74.45
	0.07	0.5	0	-77.78
	0.08	0.6	0	-80.70
	0.09	0.6	0	-83.15
	0.10	0.6	0	-85.08
	0.11	0.7	0	-86.47
	0.12	0.7	0	-87.31
	0.13	0.7	0	-87.62
	0.14	0.7	0	-87.44
D13MIT61	0.16	0.3	0	-60.12
	0.17	0.4	0	-66.19
	0.18	0.5	0	-72.42
	0.19	0.5	0	-78.73
	0.20	0.6	0	-85.01
	0.21	0.7	0	-91.16
	0.22	0.8	0	-97.07
	0.23	0.8	0	-102.60
	0.24	0.9	0	-107.66
	0.25	1.0	0	-112.14
	0.26	1.1	0	-115.97
	0.27	1.1	0	-119.10
	0.28	1.2	0	-121.50
	0.29	1.3	0	-123.18
	0.30	1.3	0	-124.17
	0.31	1.4	0	-124.50
	0.32	1.4	0	-124.25
D13MIT99	0.33	1.8	1	-142.52
	0.34	1.8	1	-144.14
	0.35	1.7	1	-145.52
	0.36	1.7	1	-146.61
	0.37	1.7	1	-147.35
	0.38	1.6	0	-147.69
	0.39	1.6	0	-147.57
	0.40	1.5	0	-146.95
	0.41	1.4	0	-145.78
	0.42	1.4	0	-144.02
	0.43	1.3	0	-141.64

```
                 0.44      1.2        0  -138.64
                 0.45      1.2        0  -135.01
                 0.46      1.1        0  -130.78
                 0.47      1.0        0  -125.98
                 0.48      0.9        0  -120.67
                 0.49      0.8        0  -114.93
                 0.50      0.7        0  -108.82
                 0.51      0.7        0  -102.44
                 0.52      0.6        0   -95.88
                 0.53      0.5        0   -89.24
                 0.54      0.5        0   -82.59
                 0.55      0.4        0   -76.03
                 0.56      0.3        0   -69.61
                 0.57      0.3        0   -63.39
                 0.58      0.3        0   -57.43
                 0.59      0.2        0   -51.76
                 0.60      0.2        0   -46.40
                 0.61      0.1        0   -41.36
D13MIT151
```

CIM Reports for Chromosomes 1, 5, and 16 Using AST Data

```
CIM CHROMOSOME 1 WITH D16MIT158 BACKGROUND
Interval  mapping  for  Dataset:
Nonmortality(nonmortality)constrained  additive  regression,
118  to  126  informative progeny  from Progeny
Order  Internalmapping  QTL  AST   on  chr
chrom1using  Kosambi map function;  Evaluating interval QTL
onlyUsing  Background  to  control  for  other  QTLs.
                 map      STAT        %     Add
D1MIT65          0.00      0.0        0    -0.97
                 0.01      0.0        0    -7.08
                 0.02      0.0        0   -13.80
                 0.03      0.0        0   -21.14
                 0.04      0.1        0   -29.12
                 0.05      0.1        0   -37.75
                 0.06      0.2        0   -47.02
                 0.07      0.2        0   -56.92
                 0.08      0.3        0   -67.40
                 0.09      0.4        0   -78.40
                 0.10      0.5        0   -89.84
                 0.11      0.6        0  -101.61
                 0.12      0.8        1  -113.59
                 0.13      0.9        1  -125.63
```

	0.14	1.1	1	-137.57
	0.15	1.3	1	-149.25
	0.16	1.5	1	-160.49
	0.17	1.7	1	-171.15
	0.18	1.9	1	-181.07
	0.19	2.1	2	-190.14
	0.20	2.3	2	-198.26
	0.21	2.5	2	-205.36
	0.22	2.7	2	-211.41
	0.23	2.9	2	-216.41
	0.24	3.1	2	-220.37
	0.25	3.3	3	-223.35
	0.26	3.5	3	-225.40
	0.27	3.6	3	-226.59
	0.28	3.8	3	-227.02
	0.29	3.9	3	-226.77
	0.30	4.1	3	-225.93
	0.31	4.2	3	-224.57
	0.32	4.3	3	-222.78
D1MIT303	0.33	4.5	3	-212.83
	0.34	4.5	3	-218.60
	0.35	4.6	3	-223.27
	0.36	4.6	3	-226.61
	0.37	4.6	3	-228.41
	0.38	4.5	3	-228.52
	0.39	4.4	3	-226.89
	0.40	4.3	3	-223.51
	0.41	4.1	3	-218.49
D1MIT8	0.42	3.3	2	-192.55
	0.43	3.2	2	-193.54
	0.44	3.1	2	-194.30
	0.45	3.0	2	-194.79
	0.46	2.9	2	-194.96
	0.47	2.8	2	-194.76
	0.48	2.6	2	-194.14
	0.49	2.5	2	-193.05
	0.50	2.4	2	-191.41
	0.51	2.2	2	-189.18
	0.52	2.1	2	-186.28
	0.53	2.0	1	-182.68
	0.54	1.8	1	-178.30
	0.55	1.6	1	-173.11
	0.56	1.5	1	-167.07
	0.57	1.3	1	-160.16

	0.58	1.2	1	-152.38
	0.59	1.0	1	-143.75
	0.60	0.9	1	-134.30
	0.61	0.7	1	-124.11
	0.62	0.6	0	-113.25
	0.63	0.5	0	-101.82
	0.64	0.4	0	-89.97
	0.65	0.3	0	-77.81
	0.66	0.2	0	-65.50
	0.67	0.1	0	-53.18
	0.68	0.1	0	-41.00
	0.69	0.0	0	-29.09
	0.70	0.0	0	-17.57
	0.71	0.0	0	-6.54
	0.72	0.0	0	3.91
	0.73	0.0	0	13.71
	0.74	0.0	0	22.84
	0.75	0.1	0	31.25
	0.76	0.1	0	38.94
	0.77	0.1	0	45.93
	0.78	0.2	0	52.22
	0.79	0.2	0	57.85
	0.80	0.3	0	62.85
	0.81	0.3	0	67.25
	0.82	0.4	0	71.10
	0.83	0.4	0	74.44
	0.84	0.5	0	77.32
	0.85	0.5	0	79.77
	0.86	0.6	0	81.84
	0.87	0.6	0	83.57
	0.88	0.7	1	84.99
D1MIT15	0.89	0.7	1	84.00
	0.90	0.7	0	83.37
	0.91	0.6	0	82.22
	0.92	0.6	0	80.53
	0.93	0.5	0	78.30
	0.94	0.5	0	75.55
	0.95	0.5	0	72.31
	0.96	0.4	0	68.67
	0.97	0.4	0	64.69
	0.98	0.3	0	60.46
	0.99	0.3	0	56.08
	1.00	0.3	0	51.63
D1MIT17				

```
CIM CHROMOSOME 16 WITH D1MIT303 BACKGROUND
Interval  mapping  for  Dataset:
Nonmortality(nonmortality)constrained  additive  regression,
126  to  127  informative progeny  from Progeny
Order  Internalmapping  QTL  AST   on  chr
chrom16using  Kosambi map function;  Evaluating interval
QTL onlyUsing  Background  to  control  for  other  QTLs.
                map        Stat        %    Add
D16MIT108       0.00       1.1         1   109.11
                0.01       1.1         1   106.78
                0.02       1.0         1   103.95
                0.03       0.9         1   100.60
                0.04       0.8         1    96.66
                0.05       0.7         1    92.12
                0.06       0.6         0    86.94
                0.07       0.5         0    81.10
                0.08       0.4         0    74.61
                0.09       0.3         0    67.47
                0.10       0.3         0    59.71
                0.11       0.2         0    51.38
                0.12       0.1         0    42.54
                0.13       0.1         0    33.27
                0.14       0.0         0    23.67
                0.15       0.0         0    13.86
                0.16       0.0         0     3.95
                0.17       0.0         0    -5.92
                0.18       0.0         0   -15.65
                0.19       0.0         0   -25.11
                0.20       0.1         0   -34.20
                0.21       0.1         0   -42.83
                0.22       0.2         0   -50.93
                0.23       0.3         0   -58.45
                0.24       0.3         0   -65.35
                0.25       0.4         0   -71.62
                0.26       0.5         0   -77.25
                0.27       0.6         0   -82.26
                0.28       0.6         0   -86.66
                0.29       0.7         1   -90.50
                0.30       0.8         1   -93.79
D16MIT4         0.31       1.7         1  -131.06
                0.32       1.9         1  -142.70
                0.33       2.2         2  -154.75
                0.34       2.5         2  -167.10
                0.35       2.8         2   -179.60
                0.36       3.1         2   -192.06
                0.37       3.5         3   -204.27
                0.38       3.8         3   -216.02
                0.39       4.2         3   -227.08
                0.40       4.5         3   -237.24
                0.41       4.8         4   -246.30
                0.42       5.2         4   -254.10
                0.43       5.5         4   -260.53
                0.44       5.8         4   -265.52
                0.45       6.1         5   -269.05
                0.46       6.3         5   -271.14
                0.47       6.5         5   -271.89
                0.48       6.7         5   -271.38
                0.49       6.9         5   -269.76
                0.50       7.0         5   -267.16
                0.51       7.1         5   -263.74
D16MIT158
```

CIM Reports for Chromosomes 1, 5, and 16 Using Caspase-3 Data

```
CIM CHROMOSOME 1 WITH D5MIT161 BACKGROUND
Interval  mapping  for  Dataset:
Nonmortality(nonmortality)constrained  additive  regression,
124  to  132  informative progeny  from Progeny
Order  Internalmapping  QTL  CASPASE   on  chr
chrom1using  Kosambi map function;  Evaluating interval QTL
onlyUsing  Background  to  control  for  other  QTLs.
                map        Stat        %      Add
D1MIT65         0.00       0.7         0     77.16
                0.01       0.6         0     76.98
                0.02       0.6         0     76.58
                0.03       0.6         0     75.92
                0.04       0.5         0     74.98
                0.05       0.5         0     73.71
                0.06       0.5         0     72.09
                0.07       0.4         0     70.09
                0.08       0.4         0     67.69
                0.09       0.3         0     64.86
                0.10       0.3         0     61.60
                0.11       0.3         0     57.91
                0.12       0.2         0     53.80
                0.13       0.2         0     49.30
                0.14       0.1         0     44.44
```

	0.15	0.1	0	39.29
	0.16	0.1	0	33.90
	0.17	0.1	0	28.34
	0.18	0.0	0	22.69
	0.19	0.0	0	17.04
	0.20	0.0	0	11.45
	0.21	0.0	0	6.01
	0.22	0.0	0	0.76
	0.23	0.0	0	-4.22
	0.24	0.0	0	-8.92
	0.25	0.0	0	-13.28
	0.26	0.0	0	-17.30
	0.27	0.0	0	-20.97
	0.28	0.1	0	-24.29
	0.29	0.1	0	-27.26
	0.30	0.1	0	-29.91
	0.31	0.1	0	-32.24
	0.32	0.1	0	-34.28
D1MIT303	0.33	0.1	0	-31.92
	0.34	0.1	0	-35.40
	0.35	0.2	0	-38.91
	0.36	0.2	0	-42.34
	0.37	0.2	0	-45.63
	0.38	0.3	0	-48.70
	0.39	0.3	0	-51.45
	0.40	0.3	0	-53.83
	0.41	0.3	0	-55.79
D1MIT8	0.42	0.4	0	-59.82
	0.43	0.3	0	-56.53
	0.44	0.3	0	-52.78
	0.45	0.2	0	-48.52
	0.46	0.2	0	-43.71
	0.47	0.1	0	-38.31
	0.48	0.1	0	-32.28
	0.49	0.1	0	-25.57
	0.50	0.0	0	-18.16
	0.51	0.0	0	-10.00
	0.52	0.0	0	-1.08
	0.53	0.0	0	8.61
	0.54	0.0	0	19.06
	0.55	0.1	0	30.25
	0.56	0.1	0	42.15
	0.57	0.2	0	54.67
	0.58	0.3	0	67.75

	0.59	0.4	0	81.27
	0.60	0.6	0	95.10
	0.61	0.7	1	109.09
	0.62	0.9	1	123.08
	0.63	1.1	1	136.90
	0.64	1.4	1	150.38
	0.65	1.6	1	163.34
	0.66	1.9	1	175.64
	0.67	2.2	2	187.14
	0.68	2.4	2	197.73
	0.69	2.7	2	207.32
	0.70	3.0	2	215.84
	0.71	3.3	2	223.28
	0.72	3.6	3	229.63
	0.73	3.9	3	234.90
	0.74	4.2	3	239.14
	0.75	4.4	3	242.41
	0.76	4.7	3	244.77
	0.77	4.9	3	246.30
	0.78	5.2	4	247.07
	0.79	5.4	4	247.17
	0.80	5.6	4	246.68
	0.81	5.8	4	245.68
	0.82	5.9	4	244.23
	0.83	6.1	4	242.40
	0.84	6.2	4	240.26
	0.85	6.4	4	237.86
	0.86	6.5	4	235.25
	0.87	6.6	5	232.47
	0.88	6.7	5	229.57
D1MIT15	0.89	5.7	4	210.29
	0.90	6.1	4	222.46
	0.91	6.6	5	233.94
	0.92	7.0	5	244.41
	0.93	7.5	5	253.54
	0.94	7.9	5	261.04
	0.95	8.2	6	266.70
	0.96	8.5	6	270.37
	0.97	8.8	6	272.01
	0.98	8.9	6	271.68
	0.99	9.0	6	269.50
	1.00	9.1	6	265.67
D1MIT17				

```
CIM CHROMOSOME 5 WITH D1MIT17 BACKGROUND
Interval  mapping  for  Dataset:
Nonmortality(nonmortality)constrained  additive  regression,
125  to  130  informative progeny  from Progeny
Order  Internalmapping  QTL  CASPASE   on  chr
chrom5using  Kosambi map function;  Evaluating interval QTL
onlyUsing  Background  to  control  for  other  QTLs.
                  map      Stat        %    Add
D5MIT268          0.00      0.3        0   -49.29
                  0.01      0.3        0   -52.13
                  0.02      0.3        0   -55.12
                  0.03      0.3        0   -58.25
                  0.04      0.4        0   -61.50
                  0.05      0.4        0   -64.88
                  0.06      0.4        0   -68.34
                  0.07      0.5        0   -71.87
                  0.08      0.5        0   -75.44
                  0.09      0.5        0   -78.99
                  0.10      0.5        0   -82.49
                  0.11      0.6        0   -85.89
                  0.12      0.6        0   -89.13
                  0.13      0.6        0   -92.17
                  0.14      0.7        1   -94.94
                  0.15      0.7        1   -97.40
                  0.16      0.7        1   -99.51
                  0.17      0.8        1  -101.24
                  0.18      0.8        1  -102.56
                  0.19      0.8        1  -103.45
                  0.20      0.8        1  -103.93
                  0.21      0.8        1  -104.01
                  0.22      0.8        1  -103.69
                  0.23      0.9        1  -103.02
                  0.24      0.9        1  -102.03
                  0.25      0.9        1  -100.76
                  0.26      0.9        1   -99.24
                  0.27      0.9        1   -97.53
                  0.28      0.9        1   -95.66
                  0.29      0.9        1   -93.66
                  0.30      0.9        1   -91.58
                  0.31      0.8        1   -89.45
                  0.32      0.8        1   -87.28
D5MIT205          0.33      1.4        1  -106.82
                  0.34      1.7        1  -119.88
                  0.35        2.0           1   -133.54
                  0.36        2.4           2   -147.69
                  0.37        2.8           2   -162.19
                  0.38        3.3           2   -176.86
                  0.39        3.8           3   -191.50
                  0.40        4.3           3   -205.88
                  0.41        4.8           3   -219.79
                  0.42        5.4           4   -232.99
                  0.43        6.0           4   -245.26
                  0.44        6.6           5   -256.40
                  0.45        7.2           5   -266.26
                  0.46        7.7           5   -274.71
                  0.47        8.3           6   -281.70
                  0.48        8.8           6   -287.19
                  0.49        9.3           7   -291.21
                  0.50        9.8           7   -293.82
                  0.51       10.2           7   -295.12
                  0.52       10.5           7   -295.23
                  0.53       10.9           8   -294.27
D5MIT161
```

APPENDIX B
TRADD SEQUENCING DATA

```
                              Bold = extra 5'UTR
                        ........... = Forward/reverse primers

mtradd        (    1) gagccgcgcgcagcaaagccaggcgagtgtgcggcggccaggaggcaagatggcagccgg
B6            (    1) ------------------------------------------------------------
NOD           (    1) ------------------------------------------------------------


mtradd        (   61) tcagaatggccacgaggagtgggtgggcagtgcatacctgtttttggagtctgcggtaga
B6            (     ) ------------------------------------------------------------
NOD           (     ) ------------------------------------------------------------


mtradd        (  121) caaggtgatcctgtctgaagcctacacggatcccaagaagaaggtggcaatatacaaggc
B6            (     ) ------------------------------------------------------------
NOD           (     ) ------------------------------------------------------------


mtradd        (  181) tctgcagactgcactgtcagagagtggggacagctctgacgtactgcagatactcaagat
B6            (     ) ------------------------------------------------------------
NOD           (     ) ------------------------------------------------------------


mtradd        (  241) ccactgcagcgaccctcagctcatcgtccagttgcggttctgcgggcgcgtgctgtgcgg
B6            (     ) ------------------------------------------------------------
NOD           (     ) ------------------------------------------------------------


mtradd        (  301) ccgcttcctccaagcctaccgcgagggggcgctgcgcaccgcgctgcagaggtgcatggc
B6            (     ) ------------------------------------------------------------
NOD           (    ) ------------------------------------------------------------

                                 Forward2
                                                   _______+++++++++_++++++++++++++
mtradd        (  361) cccggcgcttgcccaggaagcgctgcggtTGCAGCTGGAGTTGCGTGCAGGTGCGGAGCA
B6            (    1) ------------------------------------GGAGTTGCGNGCAGGTGCGGAGCA
NOD           (    1) -----------------------------TGCAGCTGGAGTTGCGTGCAGGTGCGGAGCA

                                    Reverse1
                      ++++++++++++++++++++++++++++++++++++++++++++++++++++++++++++
mtradd        (  421) GCTGGACAGTTGGCTGACTGATGAAGAGCGCTGTTTGAATTACATCTTAGCCCAGAAGCC
B6            (   25) GCTGGACAGTTGGCTGACTGATGAAGAGCGCTGTTTGAATTACATCTTAGCCCAGAAGCC
NOD           (   32) GCTGGACAGTTGGCTGACTGATGAAGAGCGCTGTTTGAATTACATCTTAGCCCAGAAGCC
```

```
                     ++++++++++++++++++++++++++++++++++++++++++++++++++++++++++++
mtradd      (   481) CGACCGGCTCAGGGACGAGGAACTCGCGGAGCTGGAGGATGAGCTCTGCAAACTGACGTG
B6          (    85) CGACCGGCTCAGGGACGAGGAACTCGCGGAGCTGGAGGATGAGCTCTGCAAACTGACGTG
NOD         (    92) CGACCGGCTCAGGGACGAGGAACTCGCGGAGCTGGAGGATGAGCTCTGCAAACTGACGTG


                     ++++++++++++++++++++++++++++++++++++++++++++++++++++++++++++
mtradd      (   541) TGACTGCACTGGCCAGGGTGGAGCCATACAGGTAGCTTCTGCAGGTTCGAAGTTCCCGGT
B6          (   145) TGACTGCACTGGCCAGGGTGGAGCCATACAGGTAGCTTCTGCAGGTTCGAAGTTCCCGGT
NOD         (   152) TGACTGCACTGGCCAGGGTGGAGCCATACAGGTAGCTTCTGCAGGTTCGAAGTTCCCGGT


                     ++++++++++++++++++++++++++++++++++++++++++++++++++++++++++++
mtradd      (   601) TTCCTCTCCGACCGAGGAGAAACCACTGCCGGCCGCCTGCCAGACTTTTCTGTTCCACGG
B6          (   205) TTCCTCTCCGACCGAGGAGAAACCACTGCCGGCCGCCTGCCAGACTTTTCTGTTCCACGG
NOD         (   212) TTCCTCTCCGACCGAGGAGAAACCACTGCCGGCCGCCTGCCAGACTTTTCTGTTCCACGG

                                                 Forward3
                     ++++++++++++++++++++++++++++++++++++++++++++++++++++++++++++
mtradd      (   661) GCAGCTCGTAGTGAACCGGCCACTGACTCTTCAAGACCAGCAGACGTTTGCGCGCTCGGT
B6          (   265) GCAGCTCGTAGTGAACCGGCCACTGACTCTTCAAGACCAGCAGACGTTTGCGCGCTCGGT
NOD         (   272) GCAGCTCGTAGTGAACCGGCCACTGACTCTTCAAGACCAGCAGACGTTTGCGCGCTCGGT

                                                                           Reverse2
                     ++++++++++++++++++++++++++++++++++++++++++++++++++++++++++++
mtradd      (   721) GGGTCTCAAGTGGCGCAGGGTGGGGCGCTCGCTGCAGCGTAACTGTCGGGCACTGAGAGA
B6          (   325) GGGTCTCAAGTGGCGCAGGGTGGGGCGCTCGCTGCAGCGTAACTGTCGGGCACTGAGAGA
NOD         (   332) GGGTCTCAAGTGGCGCAGGGTGGGGCGCTCGCTGCAGCGTAACTGTCGGGCACTGAGAGA


                     ++++++++++
mtradd      (   781) TCCTGCCCTCGACTCGCTggCCTACgagtatgagcgtgatgggctatacgagcaggcctt
B6          (   385) TCCTGCCCTC--------------------------------------------------
NOD         (   392) TCCTGCCCTC--------------------------------------------------


mtradd      (   841) ccagctgctgcgccgtttcatgcaagccgagggccgccgtgccacactgcagcgcctggt
B6          (      ) ------------------------------------------------------------
NOD         (      ) ------------------------------------------------------------


mtradd      (   901) ggaggcgctggaggagaacgaactcactagtctagcaggagggatcttgttgggccaggc
B6          (      ) ------------------------------------------------------------
NOD         (      ) ------------------------------------------------------------

                                                                        Forward4
                                                                       +_++++++++
mtradd      (   961) ggagccggatggcggcctggcctaagtctagtactgtggggaagggcggcCAACCAGCAG
B6          (    1 ) --------------------------------------------------CCACCAGCAG
NOD         (    1 ) --------------------------------------------------CAACCAGCAG

                                                                      Reverse3
                     ++++++++++++++++++++++++++++++++++++++++++++++++++++++++++++
mtradd      (  1021) TTCAGTGTTTGAAACCCACGGGTGGCTGTTGGGGTATATTTTTACCGCTGATGTTGCTAC
B6          (    11) TTCAGTGTTTGAAACCCACGGGTGGCTGTTGGGGTATTTTTTTACCGCTGATGTTGCTAC
NOD         (    11) TTCAGTGTTTGAAACCCACGGGTGGCTGTTGGGGTATTTTTTTACCGCTGATGTTGCTAC


                     ++++++++++++++++++++++++++++++++++++++++++++++++++++++++++++
mtradd      (  1081) TGCTGACCACTTTCCATCTACTGGACTTGGAGAGCATACGCACGCCCCACCTAGCTGAGC
B6          (    71) TGCTGACCACTTTCCATCTACTGGACTTGGAGAGCATACGCACGCCCCACCTAGCTGAGC
NOD         (    71) TGCTGACCACTTTCCATCTACTGGACTTGGAGAGCATACGCACGCCCCACCTAGCTGAGC
```

```
                      ++++++++++++++++++++++++++++++++++++++++++++++++++++++++++++
mtradd       (  1141) TGCTGGAGTGCAACTAACTGCCCCTCCCCCCGCCCCCCAGGAGTCAGGCAAGCAGCGCAG
B6           (   131) TGCTGGAGTGCAACTAACTGCCCCTCCCCCCGCCCCCCAGGAGCCAGGCAAGCAGCGCAG
NOD          (   131) TGCTGGAGTGCAACTAACTGCCCCTCCCCCCGCCCCCCAGGAGCCAGGCAAGCAGCGCAG

                      ++++++++++++++++++++++++++++++++++++++++++++++++++++++++++++
mtradd       (  1201) GGGTAAATCACTGATGATCATACAAAAAGAGGACTTGCTGCAAAGACCCTCTAAGTACCC
B6           (   191) GGGTAAATCACTGATGATCATACAAAAAGAGGACTTGCTGCAAAGACCCTCTAAGTACCC
NOD          (   191) GGGTAAATCACTGATGATCATACAAAAAGAGGACTTGCTGCAAAGACCCTCTAAGTACCC

                      ++++++++++++++++++++++++++++++++++++++++++++++++++++++++++++
mtradd       (  1261) GGACCTTCTGAAACCTAGCTCAAGGTGCTACAAAAACTGTCGGGAGCAGGATGCACGATT
B6           (   251) GGACCTTCTGAAACCTAGCTCAAGGTGCTACAAAAACTGTCGGGAGCAGGATGCACGATT
NOD          (   251) GGACCTTCTGAAACCTAGCTCAAGGTGCTACAAAAACTGTCGGGAGCAGGATGCACGATT

                                                          Reverse4
                      _+___+++++_+++++++__+++_+++_++__+__
mtradd       (  1321) TTCCCCGCCCTTGGCATATACTCATCGTGGGACCGaagcaccttgtctgcagcgataata
B6           (   311) NTNTGCGCCCTTGGCATA:GCTCGTCGAGGG-----------------------------
NOD          (   311) TTCCCCGCCC:TGGCATATACTCATCGGGGATCAA-------------------------


mtradd       (  1381) aaatgtaactcttttacagaaaaaaaaaaaaaaaaaaaaaaaaaaaaaaaaaaaaaaaaaa
B6           (      ) ------------------------------------------------------------
NOD          (      ) ------------------------------------------------------------


mtradd       (  1441) aaaaaaaaaaaaaaaaaaaaaaaaaaaaaa
B6           (      ) ------------------------------
NOD          (      ) ------------------------------
```

Primers sequences used:

f1#1	gagccgcgcgcagcaaag
f1#2	gagtgtgcggcggccagg
f2	cttgcccaggaagcgctg
f3#1	acgggcagctcgtagtg
f3#2	gccggccgcctgccagac
f4	gccaaccagcagttcagtgt
r1#1	gccggtcgggcttctggg
r1#2	tccctgagccggtcgggc
r2	gagggcaggatctctcagtg
r3#1	gtgcgtatgctctccaa
r3#2	ccccaacagccacccgtg
r4	tgcagacaaggtgcttcggt

LIST OF REFERENCES

Abraham, E., R. Wunderink, H. Silverman, T. M. Perl, S. Nasraway, H. Levy, R. Bone, R. P. Wenzel, R. Balk and R. Allred (1995). "Efficacy and safety of monoclonal antibody to human tumor necrosis factor alpha in patients with sepsis syndrome. A randomized, controlled, double-blind, multicenter clinical trial. TNF-alpha MAb Sepsis Study Group." JAMA 273(12): 934-941.

Alexander-Miller, M. A., M. A. Derby, A. Sarin, P. A. Henkart and J. A. Berzofsky (1998). "Supraoptimal peptide-major histocompatibility complex causes a decrease in bcl-2 levels and allows tumor necrosis factor alpha receptor II- mediated apoptosis of cytotoxic T lymphocytes." J Exp Med 188(8): 1391-9.

Alleva, D. G., R. P. Pavlovich, C. Grant, S. B. Kaser and D. I. Beller (2000). "Aberrant macrophage cytokine production is a conserved feature among autoimmune-prone mouse strains: elevated interleukin (IL)-12 and an imbalance in tumor necrosis factor-alpha and IL-10 define a unique cytokine profile in macrophages from young nonobese diabetic mice." Diabetes 49(7): 1106-15.

Aroeira, L. S. and A. C. Martinez (1999). "The role of IL-4 in the staphylococcal enterotoxin B-triggered immune response: increased susceptibility to shock and deletion of CD8Vbeta8+ T cells in IL-4 knockout mice." Eur J Immunol 29(4): 1397-405.

Bahjat, F. R., V. R. Dharnidharka, K. Fukuzuka, L. Morel, J. M. Crawford, M. J. Clare-Salzler and L. L. Moldawer (2000). "Reduced susceptibility of nonobese diabetic mice to TNF-alpha and D- galactosamine-mediated hepatocellular apoptosis and lethality." J Immunol 165(11): 6559-67.

Baker, S. J. and E. P. Reddy (1996). "Transducers of life and death: TNF receptor superfamily and associated proteins."Oncogene 12: 1-9.

Bazzoni, F. and B. Beutler (1995). "Comparative expression of TNF-alpha alleles from normal and autoimmune- prone MHC haplotypes." J Inflamm 45(2): 106-14.

Bernal, W., M. Moloney, J. Underhill and P. T. Donaldson (1999). "Association of tumor necrosis factor polymorphism with primary sclerosing cholangitis." J Hepatol 30(2): 237-41.

Bjornberg, F., M. Lantz and U. Gullberg (1995). "Metalloproteases and serineproteases are involved in the cleavage of the two tumour necrosis factor (TNF) receptors to soluble forms in the myeloid cell lines U-937 and THP-1."Scand.J.Immunol. 42: 418-424.

Bohlinger, I., M. Leist, F. Gantner, S. Angermuller, G. Tiegs and A. Wendel (1996). "DNA fragmentation in mouse organs during endotoxic shock." Am.J.Pathol. 149(4): 1381-1393.

Bradham, C. A., J. Plumpe, M. P. Manns, D. A. Brenner and C. Trautwein (1998). "Mechanisms of hepatic toxicity. I. TNF-induced liver injury." Am J Physiol 275(3 Pt 1): G387-92.

Broman, K. W. (2001). "Review of statistical methods for QTL mapping in experimental crosses." Lab Anim (NY) 30(7): 44-52.

Brouckaert, P., C. Libert, B. Everaerdt and W. Fiers (1992). "Selective species specificity of tumor necrosis factor for toxicity in the mouse." Lymphokine Cytokine Res 11(4): 193-6.

Brouckaert, P. G., B. Everaerdt, C. Libert, N. Takahashi and W. Fiers (1989). "Species specificity and involvement of other cytokines in endotoxic shock action of recombinant tumour necrosis factor in mice." Agents Actions 26: 196-198.

Brynskov, J., O. H. Nielson, I. Ahnfelt-Ronne and K. Bendtzen (1994). "Cytokines (immunoinflammatory hormones) and their natural regulation in inflammatory bowel disease (Crohn's disease and ulcerative colitis): a review." Dig.Disease 12: 290.

Butterfield, R. J., J. D. Sudweeks, E. P. Blankenhorn, R. Korngold, J. C. Marini, J. A. Todd, R. J. Roper and C. Teuscher (1998). "New genetic loci that control susceptibility and symptoms of experimental allergic encephalomyelitis in inbred mice." J Immunol 161(4): 1860-7.

Carswell, E. A., L. J. Old, R. L. Kassel, S. Green, N. Fiore and B. Williamson (1975). "An endotoxin-induced serum factor that causes necrosis of tumors." Proc.Natl.Acad.Sci.U.S.A. 72: 3666-3670.

Cavaillon, J. M. and N. Haeffner Cavaillon (1993). "[Cytokines and inflammation]." Rev.Prat. 43: 547-552.

Chosich, N., E. Rockett and L. C. Harrison (1994). "Endogenous TNF production differs between high and low diabetes incidence non-obese diabetic (NOD) mice." Autoimmunity 18(3): 163-8.

Chu, Z. L., T. A. McKinsey, L. Liu, J. J. Gentry, M. H. Malim and D. W. Ballard (1997). "Suppression of tumor necrosis factor-induced cell death by inhibitor of apoptosis c-IAP2 is under NF-kappaB control [In Process Citation]." Proc.Natl Acad.Sci.U.S.A. 94(19): 10057-10062.

Czaja, A. J., S. Cookson, P. K. Constantini, M. Clare, J. A. Underhill and P. T. Donaldson (1999). "Cytokine polymorphisms associated with clinical features and treatment outcome in type 1 autoimmune hepatitis." Gastroenterology 117(3): 645-52.

Darvasi, A., A. Weinreb, V. Minke, J. I. Weller and M. Soller (1993). "Detecting marker-QTL linkage and estimating QTL gene effect and map location using a saturated genetic map." Genetics 134(3): 943-51.

Denekamp, J. (1993). "Review article: angiogenesis, neovascular proliferation and vascular pathophysiology as targets for cancer therapy." Br.J.Radiol. 66(783): 181-196.

Doerge, R. W. and G. A. Churchill (1996). "Permutation tests for multiple loci affecting a quantitative character." Genetics 142(1): 285-94.

Donnelly, R. P., L. J. Crofford, S. L. Freeman, J. Buras, E. Remmers, R. L. Wilder and M. J. Fenton (1993). "Tissue-specific regulation of IL-6 production by IL-4. Differential effects of IL-4 on nuclear factor-kappa B activity in monocytes and fibroblasts."J.Immunol. 151: 5603-5612.

Elliott, M. J. and R. N. Maini (1994). "New directions for biological therapy in rheumatoid arthritis." Int.Arch.Allergy Immunol. 104: 112-125.

Elliott, M. J., R. N. Maini, M. Feldmann, J. R. Kalden, C. Antoni, J. S. Smolen, B. Leeb, F. C. Breedveld, J. D. Macfarlane and H. Bijl (1994a). "Randomised double-blind comparison of chimeric monoclonal antibody to tumour necrosis factor alpha (cA2) versus placebo in rheumatoid arthritis." Lancet 344(8930): 1105-1110.

Elliott, M. J., R. N. Maini, M. Feldmann, A. Long-Fox, P. Charles, H. Bijl and J. N. Woody (1994b). "Repeated therapy with monoclonal antibody to tumour necrosis factor alpha (cA2) in patients with rheumatoid arthritis." Lancet 344(8930): 1125-1127.

Enari, M., H. Hug, M. Hayakawa, F. Ito, Y. Nishimura and S. Nagata (1996). "Different apoptotic pathways mediated by Fas and the tumor-necrosis- factor receptor. Cytosolic phospholipase A2 is not involved in Fas- mediated apoptosis." Eur.J.Biochem. 236(2): 533-538.

Enari, M., H. Hug and S. Nagata (1995). "Involvement of an ICE-like protease in FAS-mediated apoptosis." Nature 375: 78-81.

Faubion, W. A. and G. J. Gores (1999). "Death receptors in liver biology and pathobiology." Hepatology 29(1): 1-4.

Feldmann, M., F. M. Brennan and R. N. Maini (1996). “Role of cytokines in rheumatoid arthritis.” Annu.Rev.Immunol. 14:397-440: 397-440.

Fisher, C. J., Jr., S. M. Opal, J. F. Dhainaut, S. Stephens, J. L. Zimmerman, P. Nightingale, S. J. Harris, R. M. Schein, E. A. Panacek, J. L. Vincent and et al (1993). “Influence of an anti-tumor necrosis factor monoclonal antibody on cytokine levels in patients with sepsis. The CB0006 Sepsis Syndrome Study Group [see comments].” Crit.Care Med. 21: 318-327.

Fisler, J. S. and C. H. Warden (1997). “Mapping of mouse obesity genes: A generic approach to a complex trait.” J Nutr 127(9): 1909S-1916S.

Freudenberg, M. A., D. Keppler and C. Galanos (1986). “Requirement for lipopolysaccharide-responsive macrophages in galactosamine-Induced sensitization to endotoxin.” Infection and Immunity 51, No. 3: 891-895.

Fukuda, R., S. Satoh, X. T. Nguyen, Y. Uchida, N. Kohge, S. Akagi, S. Ikeda, M. Watanabe and S. Fukumoto (1995). “Expression rate of cytokine mRNA in the liver of chronic hepatitis C: comparison with chronic hepatitis B.” J Gastroenterol 30(1): 41-7.

Fukuzuka, K., J. J. Rosenberg, G. C. Gaines, C. K. d. Edwards, M. Clare-Salzler, E. M. d. Copeland, L. L. Moldawer and D. W. Mozingo (1999). “Caspase-3 dependent organ apoptosis early after burn injury.” Ann Surg 229(6): 851-858.

Galanos, C. and M. A. Freudenberg (1993). “Mechanisms of endotoxin shock and endotoxin hypersensitivity.” Immunobiology 187: 346-356.

Galanos, C., M. A. Freudenberg and W. Reutter (1979). “Galactosamine-induced sensitization to the lethal effects of endotoxin.” Proc.Natl.Acad.Sci.U.S.A. 76(11): 5939-5943.

Gehr, G., R. Gentz, M. Brockhaus, H. Loetscher and W. Lesslauer (1992). “Both tumor necrosis factor receptor types mediate proliferative signals in human mononuclear cell activation.” J.Immunol. 149: 911-917.

Ghosh, S., M. J. May and E. B. Kopp (1998). “NF-kappa B and Rel proteins: evolutionarily conserved mediators of immune responses.” Annu Rev Immunol 16: 225-60.

Gonzalez-Amaro, R., C. Garcia-Monzon, L. Garcia-Buey, R. Moreno-Otero, J. L. Alonso, E. Yague, J. P. Pivel, M. Lopez-Cabrera, E. Fernandez-Ruiz and F. Sanchez-Madrid (1994). “Induction of tumor necrosis factor alpha production by human hepatocytes in chronic viral hepatitis.” J Exp Med 179(3): 841-8.

Graff, R. J., W. H. Hildemann and G. D. Snell (1966). “Histocompatibility genes of mice. VI. Allografts in mice congenic at various non-H-2 histocompatibility loci.” Transplantation 4(4): 425-37.

Grattan, M., Q. S. Mi, C. Meagher and T. L. Delovitch (2002). "Congenic mapping of the diabetogenic locus Idd4 to a 5.2-cM region of chromosome 11 in NOD mice: identification of two potential candidate subloci." Diabetes 51(1): 215-23.

Green, E. A., E. E. Eynon and R. A. Flavell (1998). "Local expression of TNFalpha in neonatal NOD mice promotes diabetes by enhancing presentation of islet antigens." Immunity 9(5): 733-43.

Grell, M., F. M. Becke, H. Wajant, D. N. Mannel and P. Scheurich (1998). "TNF receptor type 2 mediates thymocyte proliferation independently of TNF receptor type 1." Eur.J.Immunol. 28(1): 257-263.

Grewal, I. S., K. D. Grewal, F. S. Wong, D. E. Picarella, C. A. Janeway, Jr. and R. A. Flavell (1996). "Local expression of transgene encoded TNF alpha in islets prevents autoimmune diabetes in nonobese diabetic (NOD) mice by preventing the development of auto-reactive islet-specific T cells." J Exp Med 184(5): 1963-74.

Griffiths, M. M., J. A. Encinas, E. F. Remmers, V. K. Kuchroo and R. L. Wilder (1999). "Mapping autoimmunity genes." Curr Opin Immunol 11(6): 689-700.

Hale, K. K., C. G. Smith, S. L. Baker, R. W. Vanderslice, C. H. Squires, T. M. Gleason, K. K. Tucker, T. Kohno and D. A. Russell (1995). "Multifunctional regulation of the biological effects of TNF-alpha by the soluble type I and type II TNF receptors." Cytokine. 7(1): 26-38.

Hatano, E., C. A. Bradham, A. Stark, Y. Iimuro, J. J. Lemasters and D. A. Brenner (2000). "The mitochondrial permeability transition augments Fas-induced apoptosis in mouse hepatocytes." J Biol Chem 275(16): 11814-23.

Hayashi, T. and D. Faustman (1999). "NOD mice are defective in proteasome production and activation of NF- kappaB." Mol Cell Biol 19(12): 8646-59.

Hayashi, T. and D. Faustman (2000). "The role of the proteasome in autoimmunity." Diabetes Metab Res Rev 16(5): 325-37.

Held, W., H. R. MacDonald, I. L. Weissman, M. W. Hess and C. Mueller (1990). "Genes encoding tumor necrosis factor alpha and granzyme A are expressed during development of autoimmune diabetes." Proc Natl Acad Sci U S A 87(6): 2239-43.

Herbein, G., U. Mahlknecht, F. Batliwalla, P. Gregersen, T. Pappas, J. Butler, W. A. O'Brien and E. Verdin (1998). "Apoptosis of CD8+ T cells is mediated by macrophages through interaction of HIV gp120 with chemokine receptor CXCR4." Nature 395(6698): 189-94.

Hill, N. J., P. A. Lyons, N. Armitage, J. A. Todd, L. S. Wicker and L. B. Peterson (2000). "NOD Idd5 locus controls insulitis and diabetes and overlaps the orthologous CTLA4/IDDM12 and NRAMP1 loci in humans." Diabetes 49(10): 1744-7.

Hsu, H., H. B. Shu, M. G. Pan and D. V. Goeddel (1996). "TRADD-TRAF2 and TRADD-FADD interactions define two distinct TNF receptor 1 signal transduction pathways." Cell 84: 299-308.

Hu, S., C. Vincenz, J. Ni, R. Gentz and V. M. Dixit (1997). "I-FLICE, a novel inhibitor of tumor necrosis factor receptor-1- and CD- 95-induced apoptosis." J Biol Chem 272(28): 17255-7.

Iimuro, Y., T. Nishiura, C. Hellerbrand, K. E. Behrns, R. Schoonhoven, J. W. Grisham and D. A. Brenner (1998). "NFkappaB prevents apoptosis and liver dysfunction during liver regeneration." J Clin Invest 101(4): 802-11.

Jacob, C. O., S. K. Lee and G. Strassmann (1996). "Mutational analysis of TNF-alpha gene reveals a regulatory role for the 3'-untranslated region in the genetic predisposition to lupus-like autoimmune disease." J Immunol 156(8): 3043-50.

Jaeschke, H., M. A. Fisher, J. A. Lawson, C. A. Simmons, A. Farhood and D. A. Jones (1998). "Activation of caspase 3 (CPP32)-like proteases is essential for TNF- alpha-induced hepatic parenchymal cell apoptosis and neutrophil- mediated necrosis in a murine endotoxin shock model." J Immunol 160(7): 3480-6.

Josephs, M., F. R. Bahjat, K. Fukuzuka, R. Ksontini, C. C. Solorzano, C. K. Edwards III and L. L. Moldawer (2000). "Lipopolysaccharide and D-galactosamine-induced hepatic injury is mediated by TNF-alpha and not by Fas ligand." Am J Physiol Regul Integr Comp Physiol 278(5): R1196-201.

Kagi, D., A. Ho, B. Odermatt, A. Zakarian, P. S. Ohashi and T. W. Mak (1999). "TNF receptor 1-dependent beta cell toxicity as an effector pathway in autoimmune diabetes." J Immunol 162(8): 4598-605.

Kaijzel, E. L., M. V. van Krugten, B. M. Brinkman, T. W. Huizinga, T. van der Straaten, J. M. Hazes, H. W. Ziegler-Heitbrock, S. A. Nedospasov, F. C. Breedveld and C. L. Verweij (1998). "Functional analysis of a human tumor necrosis factor alpha (TNF-alpha) promoter polymorphism related to joint damage in rheumatoid arthritis." Mol Med 4(11): 724-33.

Komata, T., N. Tsuchiya, M. Matsushita, K. Hagiwara and K. Tokunaga (1999). "Association of tumor necrosis factor receptor 2 (TNFR2) polymorphism with susceptibility to systemic lupus erythematosus." Tissue Antigens 53(6): 527-33.

Kondo, T., T. Suda, H. Fukuyama, M. Adachi and S. Nagata (1997). "Essential roles of the Fas ligand in the development of hepatitis." Nat Med 3(4): 409-13.

Kowdley, K. V. (1999). "TNF-alpha in chronic hepatitis C: the smoking gun?" Am J Lamhamedi-Cherradi, S. E., O. Boulard, C. Gonzalez, N. Kassis, D. Damotte, L. Eloy, G. Fluteau, M. Levi-Strauss and H. J. Garchon (2001). "Further mapping of the Idd5.1 locus for autoimmune diabetes in NOD mice." Diabetes 50(12): 2874-8.

Lander, E. and L. Kruglyak (1995). “Genetic dissection of complex traits: guidelines for interpreting and reporting linkage results.” Nat Genet 11(3): 241-7.

Lander, E. S. and D. Botstein (1989). “Mapping mendelian factors underlying quantitative traits using RFLP linkage maps.” Genetics 121(1): 185-99.

Larrea, E., N. Garcia, C. Qian, M. P. Civeira and J. Prieto (1996). “Tumor necrosis factor alpha gene expression and the response to interferon in chronic hepatitis C.” Hepatology 23(2): 210-7.

Lau, K. S., O. Nakashima, G. R. Aalund, L. Hogarth, K. Ujiie, J. Yuen and R. A. Star (1995). “TNF-à and IFN-gamma induce expression of nitric oxide synthase in cultured rat medullary interstitial cells.” Am.J.Physiol.Renal,Fluid Electrolyte Physiol. 269: F212-F217.

Lawson, J. A., M. A. Fisher, C. A. Simmons, A. Farhood and H. Jaeschke (1999). “Inhibition of Fas receptor (CD95)-induced hepatic caspase activation and apoptosis by acetaminophen in mice.” Toxicol Appl Pharmacol 156(3): 179-86.

Leist, M., F. Gantner, I. Bohlinger, P. G. Germann, G. Tiegs and A. Wendel (1994). “Murine hepatocyte apoptosis induced in vitro and in vivo by TNF-à requires transcriptional arrest.” J.Immunol. 153: 1778-1788.

Leist, M., F. Gantner, S. Jilg and A. Wendel (1995). “Activation of the 55 kDa TNF receptor is necessary and sufficient for TNF-induced liver failure, hepatocyte apoptosis, and nitrite release.” J.Immunol. 154: 1307-1316.

Leiter, E. and M. Atkinson (1998). NOD Mice and Related Strains: Research Applications in Diabetes, AIDS, Cancer and Other Diseases. Austin, TX, R. G. Landes Co.

Leiter, E. H. and D. V. Serreze (1992). “Antigen presenting cells and the immunogenetics of autoimmune diabetes in NOD mice.” Reg Immunol 4(5): 263-73.

Lesslauer, W., H. Tabuchi, R. Gentz, M. Brockhaus, E. J. Schlaeger, G. Grau, P. F. Piguet, P. Pointaire, P. Vassalli and H. Loetscher (1991). “Recombinant soluble tumor necrosis factor receptor proteins protect mice from lipopolysaccharide-induced lethality.” Eur.J.Immunol. 21: 2883-2886.

Li Kam Wa, T. C., A. H. Mansur, J. Britton, G. Williams, I. Pavord, K. Richards, D. A. Campbell, N. Morton, S. T. Holgate and J. F. Morrison (1999). “Association between - 308 tumour necrosis factor promoter polymorphism and bronchial hyperreactivity in asthma.” Clin Exp Allergy 29(9): 1204-8.

Libert, C., B. Wielockx, G. L. Hammond, P. Brouckaert, W. Fiers and R. W. Elliott (1999). “Identification of a locus on distal mouse chromosome 12 that controls resistance to tumor necrosis factor-induced lethal shock.” Genomics 55(3): 284-9.

Luo, X., I. Budihardjo, H. Zou, C. Slaughter and X. Wang (1998). “Bid, a Bcl2 interacting protein, mediates cytochrome c release from mitochondria in response to activation of cell surface death receptors.” Cell 94(4): 481-90.

Lynn, W. A. and D. T. Golenbock (1992). “Lipopolysaccharide antagonists.” Immunol Today 13(7): 271-6.

Lyons, P. A., N. Armitage, C. J. Lord, M. S. Phillips, J. A. Todd, L. B. Peterson and L. S. Wicker (2001). “Mapping by genetic interaction: high-resolution congenic mapping of the type 1 diabetes loci Idd10 and Idd18 in the NOD mouse.” Diabetes 50(11): 2633-7.

Lyons, P. A., W. W. Hancock, P. Denny, C. J. Lord, N. J. Hill, N. Armitage, T. Siegmund, J. A. Todd, M. S. Phillips, J. F. Hess, S. L. Chen, P. A. Fischer, L. B. Peterson and L. S. Wicker (2000). “The NOD Idd9 genetic interval influences the pathogenicity of insulitis and contains molecular variants of Cd30, Tnfr2, and Cd137.” Immunity 13(1): 107-15.

Lyons, P. A. and L. S. Wicker (1999). “Localising quantitative trait loci in the NOD mouse model of type 1 diabetes.” Curr Dir Autoimmun 1: 208-25.

Mahler, M., I. J. Bristol, E. H. Leiter, A. E. Workman, E. H. Birkenmeier, C. O. Elson and J. P. Sundberg (1998). “Differential susceptibility of inbred mouse strains to dextran sulfate sodium-induced colitis.” Am J Physiol 274(3 Pt 1): G544-51.

Manly, K. F., R. H. Cudmore, Jr. and J. M. Meer (2001). “Map Manager QTX, cross-platform software for genetic mapping.” Mamm Genome 12(12): 930-2.

Manly, K. F. and J. M. Olson (1999). “Overview of QTL mapping software and introduction to map manager QT.” Mamm Genome 10(4): 327-34.

McDevitt, H. O. (1998). “The role of MHC class II molecules in susceptibility and resistance to autoimmunity.” Curr Opin Immunol 10(6): 677-81.

McIndoe, R. A., B. Bohlman, E. Chi, E. Schuster, M. Lindhardt and L. Hood (1999). “Localization of non-Mhc collagen-induced arthritis susceptibility loci in DBA/1j mice.” Proc Natl Acad Sci U S A 96(5): 2210-4.

Medvedev, A. E., A. Sundan and T. Espevik (1994). “Involvement of the tumor necrosis factor receptor p75 in mediating cytotoxicity and gene regulating activities.”Eur.J.Immunol. 24: 2842-2849.

Miethke, T., C. Wahl, K. Heeg, B. Echtenacher, P. H. Krammer and H. Wagner (1992). “T cell-mediated lethal shock triggered in mice by the superantigen staphylococcal enterotoxin B: critical role of tumor necrosis factor.” J.Exp.Med. 175: 91-98.

Mignon, A., N. Rouquet, M. Fabre, S. Martin, J. C. Pages, J. F. Dhainaut, A. Kahn, P. Briand and V. Joulin (1999). "LPS challenge in D-galactosamine-sensitized mice accounts for caspase- dependent fulminant hepatitis, not for septic shock." Am.J.Respir.Crit.Care Med. 159(4 Pt 1): 1308-1315.

Mira, J. P., A. Cariou, F. Grall, C. Delclaux, M. R. Losser, F. Heshmati, C. Cheval, M. Monchi, J. L. Teboul, F. Riche, G. Leleu, L. Arbibe, A. Mignon, M. Delpech and J. F. Dhainaut (1999). "Association of TNF2, a TNF-alpha promoter polymorphism, with septic shock susceptibility and mortality: a multicenter study." Jama 282(6): 561-8.

Miyazawa, K., A. Mori, K. Yamamoto and H. Okudaira (1998). "Constitutive transcription of the human interleukin-6 gene by rheumatoid synoviocytes: spontaneous activation of NF-kappaB and CBF1 [see comments]." Am.J.Pathol. 152(3): 793-803.

Morikawa, A., T. Sugiyama, Y. Kato, N. Koide, G. Z. Jiang, K. Takahashi, Y. Tamada and T. Yokochi (1996). "Apoptotic cell death in the response of D-galactosamine-sensitized mice to lipopolysaccharide as an experimental endotoxic shock model." Infect.Immun. 64(3): 734-738.

Mycko, M., W. Kowalski, M. Kwinkowski, A. C. Buenafe, B. Szymanska, E. Tronczynska, A. Plucienniczak and K. Selmaj (1998). "Multiple sclerosis: the frequency of allelic forms of tumor necrosis factor and lymphotoxin-alpha." J Neuroimmunol 84(2): 198-206.

Nagaki, M., Y. Muto, H. Ohnishi, S. Yasuda, K. Sano, T. Naito, T. Maeda, T. Yamada and H. Moriwaki (1994). "Hepatic injury and lethal shock in galactosamine-sensitized mice induced by the superantigen staphylococcal enterotoxin B." Gastroenterology 106: 450-458.

Nowak, M., G. C. Gaines, J. J. Rosenberg, R. M. Minter, F. R. Bahjat, J. Rectenwald, S. L. D. MacKay and C. K. Edwards III (2000). "Lipopolysaccharide-induced liver injury in D-galactosamine sensitized mice requires secreted TNF alpha and the TNF p55 receptor." Am J Physiol Regul Integr Comp Physiol 278(5): R1202-9.

Ogasawara, J., R. Watanabe-Fukunaga, M. Adachi, A. Matsuzawa, T. Kasugai, Y. Kitamura, N. Itoh, T. Suda and S. Nagata (1993). "Lethal effect of the anti-Fas antibody in mice." Nature 364: 806-809.

Osawa, Y., M. Nagaki, Y. Banno, Y. Yamada, M. Imose, Y. Nozawa, H. Moriwaki and S. Nakashima (2001). "Possible involvement of reactive oxygen species in D-galactosamine- induced sensitization against tumor necrosis factor-alpha-induced hepatocyte apoptosis." J Cell Physiol 187(3): 374-85.

Pakala, S. V., M. Chivetta, C. B. Kelly and J. D. Katz (1999). “In autoimmune diabetes the transition from benign to pernicious insulitis requires an islet cell response to tumor necrosis factor alpha.” J Exp Med 189(7): 1053-62.

Pan, M. G., J. Xiong, N. G. Copeland, D. J. Gilbert, N. A. Jenkins and D. V. Goeddel (1995). “Sequence, genomic organization, and chromosome localization of the mouse TRADD gene.” J Inflamm 46(3): 168-75.

Park, A. and V. R. Baichwal (1996). “Systematic mutational analysis of the death domain of the tumor necrosis factor receptor 1-associated protein TRADD.” J Biol Chem 271(16): 9858-62.

Pimentel-Muinos, F. X. and B. Seed (1999). “Regulated commitment of TNF receptor signaling: a molecular switch for death or activation.” Immunity 11(6): 783-93.

Ponton, A., M. V. Clement and I. Stamenkovic (1996). “The CD95 (APO-1/Fas) receptor activates NF-kappaB independently of its cytotoxic function.” J Biol Chem 271(15): 8991-5.

Quartey-Papafio, R., T. Lund, P. Chandler, J. Picard, P. Ozegbe, S. Day, P. R. Hutchings, L. O’Reilly, D. Kioussis, E. Simpson and et al. (1995). “Aspartate at position 57 of nonobese diabetic I-Ag7 beta-chain diminishes the spontaneous incidence of insulin-dependent diabetes mellitus.” J Immunol 154(10): 5567-75.

Raine, C. S. (1995). “Multiple sclerosis: TNF revisited, with promise.” Nature Med. 1: 211-214.

Rensing Ehl, A., S. Hess, H. W. Ziegler Heitbrock, G. Riethmuller and H. Engelmann (1995). “Fas/Apo-1 activates nuclear factor kappa B and induces interleukin-6 production.”J.Inflamm. 45: 161-174.

Rodriguez, I., K. Matsura, C. Ody, S. Nagata and P. Vassalli (1996). “Systemic injection of a tripeptide inhibits the intracellular activaton of CPP32-like proteases in vivo and fully protects mice against Fas-mediated fuliminant liver destruction and death.” J.Exp.Med. 184: 2067-2072.

Rothe, J., W. Lesslauer, H. Lotscher, Y. Lang, P. Koebel, F. Kontgen, A. Althage, R. Zinkernagel, M. Steinmetz and H. Bluethmann (1993). “Mice lacking the tumour necrosis factor receptor 1 are resistant to TNF-mediated toxicity but highly susceptible to infection by Listeria monocytogenes.” Nature 364: 798-802.

Sass, G., K. Koerber, R. Bang, H. Guehring and G. Tiegs (2001). “Inducible nitric oxide synthase is critical for immune-mediated liver injury in mice.” J Clin Invest 107(4): 439-47.

Schrum, L. W., D. Black, Y. Iimuro, R. A. Rippe, D. A. Brenner and K. E. Behrns (2000). "c-Jun does not mediate hepatocyte apoptosis following NFkappaB inhibition and partial hepatectomy." J Surg Res 88(2): 142-9.

Seino, K., Y. Setoguchi, T. Ogino, N. Kayagaki, H. Akiba, H. Nakano, H. Taniguchi, Y. Takada, K. Yuzawa, T. Todoroki, Y. Fukuchi, H. Yagita, K. Okumura and K. Fukao (2001). "Protection against Fas-mediated and tumor necrosis factor receptor 1- mediated liver injury by blockade of FADD without loss of nuclear factor-kappaB activation." Ann Surg 234(5): 681-8.

Serreze, D. V. (1993). "Autoimmune diabetes results from genetic defects manifest by antigen presenting cells." Faseb J 7(11): 1092-6.

Serreze, D. V., J. W. Gaedeke and E. H. Leiter (1993a). "Hematopoietic stem-cell defects underlying abnormal macrophage development and maturation in NOD/Lt mice: defective regulation of cytokine receptors and protein kinase C." Proc Natl Acad Sci U S A 90(20): 9625-9.

Serreze, D. V., H. R. Gaskins and E. H. Leiter (1993b). "Defects in the differentiation and function of antigen presenting cells in NOD/Lt mice." J Immunol 150(6): 2534-43.

Serreze, D. V. and E. H. Leiter (1994). "Genetic and pathogenic basis of autoimmune diabetes in NOD mice." Curr Opin Immunol 6(6): 900-6.

Serreze, D. V. and E. H. Leiter (2001). "Genes and cellular requirements for autoimmune diabetes susceptibility in nonobese diabetic mice." Curr Dir Autoimmun 4: 31-67.

Setoguchi, J., K. Hashiramoto, K. Nakano, Y. Kitagawa, N. Nakamura, T. Kanatsuna, M. Kondo and K. Uno (1992). "Prediction of insulin dependent diabetes mellitus in non-obese diabetic mice by the endogeneous tumor necrosis factor-alpha level." Diabetes Res 19(2): 63-7.

Siegel, R. M. and T. A. Fleisher (1999). "The role of Fas and related death receptors in autoimmune and other disease states." J Allergy Clin Immunol 103(5 Pt 1): 729-38.

Smith, R. A., M. Kirstein, W. Fiers and C. Baglioni (1986). "Species specificity of human and murine tumor necrosis factor. A comparative study of tumor necrosis factor receptors." J Biol Chem 261(32): 14871-4.

Solorzano, C. C., R. Ksontini, J. H. Pruitt, P. J. Hess, P. D. Edwards, A. Kaibara, A. Abouhamze, T. Auffenberg, R. E. Galardy, J. N. Vauthey, E. M. Copeland, C. K. Edwards, G. Y. Lauwers, M. Clare-Salzler, S. L. MacKay, L. L. Moldawer and D. D. Lazarus (1997). "Involvement of 26-kDa cell-associated TNF-alpha in experimental hepatitis and exacerbation of liver injury with a matrix metalloproteinase inhibitor." J.Immunol. 158(1): 414-419.

Staelens, J., B. Wielockx, L. Puimege, F. Van Roy, J. L. Guenet and C. Libert (2002). "Hyporesponsiveness of SPRET/Ei mice to lethal shock induced by tumor necrosis factor and implications for a TNF-based antitumor therapy." Proc Natl Acad Sci U S A 27: 27.

Tartaglia, L. A., D. V. Goeddel, C. Reynolds, I. S. Figari, R. F. Weber, B. M. Fendly and M. A. J. Palladino (1993). "Stimulation of human T-cell proliferation by specific activation of the 75-kDa tumor necrosis factor receptor." J.Immunol. 151: 4637-4641.

Taub, R. (1996). "Liver regeneration 4: transcriptional control of liver regeneration." Faseb J 10(4): 413-27.

Tiegs, G., M. Wolter and A. Wendel (1989). "Tumor necrosis factor is a terminal mediator in galactosamine/endotoxin- induced hepatitis in mice." Biochem Pharmacol 38(4): 627-31.

Todd, J. A. (1999). "From genome to aetiology in a multifactorial disease, type 1 diabetes." Bioessays 21(2): 164-74.

Ulich, T. R., S. Yin, D. G. Remick, D. Russell, S. P. Eisenberg and T. Kohno (1993). "Intratracheal administration of endotoxin and cytokines. IV. The soluble tumor necrosis factor receptor type I inhibits acute inflammation." Am.J.Pathol. 142: 1335-1338.

Van Zee, K. J., T. Kohno, E. Fischer, C. S. Rock, L. L. Moldawer and S. F. Lowry (1992). "Tumor necrosis factor soluble receptors circulate during experimental and clinical inflammation and can protect against excessive tumor necrosis factor alpha in vitro and in vivo."Proc.Natl.Acad.Sci.U.S.A. 89: 4845-4849.

Visscher, P. M., R. Thompson and C. S. Haley (1996). "Confidence intervals in QTL mapping by bootstrapping." Genetics 143(2): 1013-20.

Wakeland, E., L. Morel, K. Achey, M. Yui and J. Longmate (1997). "Speed congenics: a classic technique in the fast lane (relatively speaking)." Immunol Today 18(10): 472-7.

Wallach, D., M. Boldin, T. Goncharov, Y. Goltsev, I. Mett, N. Malinin, R. Adar, A. Kovalenko and E. Varfolomeev (1996). "Exploring cell death mechanisms by analyzing signaling cascades of the TNF/NGF receptor family." Behring.Inst.Mitt.(97): 144-155.

Wallach, D., E. E. Varfolomeev, N. L. Malinin, Y. V. Goltsev, A. V. Kovalenko and M. P. Boldin (1999). "Tumor necrosis factor receptor and Fas signaling mechanisms." Annu Rev Immunol 17: 331-67.

Ware, C. F., P. D. Crowe, T. L. Vanarsdale, J. L. Andrews, M. H. Grayson, R. Jerzy, C. A. Smith and R. G. Goodwin (1991). "Tumor necrosis factor (TNF) receptor expression in T lymphocytes. Differential regulation of the type I TNF receptor during activation of resting and effector T cells." J Immunol 147(12): 4229-38.

Wong, G. H. and D. V. Goeddel (1994). "Fas antigen and p55 TNF receptor signal apoptosis through distinct pathways."J.Immunol. 152: 1751-1755.

Xu, Y., S. Bialik, B. E. Jones, Y. Iimuro, R. N. Kitsis, A. Srinivasan, D. A. Brenner and M. J. Czaja (1998). "NF-kappaB inactivation converts a hepatocyte cell line TNF-alpha response from proliferation to apoptosis." Am J Physiol 275(4 Pt 1): C1058-66.

Yang, X. D., R. Tisch, S. M. Singer, Z. A. Cao, R. S. Liblau, R. D. Schreiber and H. O. McDevitt (1994). "Effect of tumor necrosis factor alpha on insulin-dependent diabetes mellitus in NOD mice. I. The early development of autoimmunity and the diabetogenic process." J Exp Med 180(3): 995-1004.

Yokota, S., T. D. Geppert and P. E. Lipsky (1988). "Enhancement of antigen- and mitogen-induced human T lymphocyte proliferation by tumor necrosis factor-alpha." J Immunol 140(2): 531-6.

Yui, M. A., K. Muralidharan, B. Moreno-Altamirano, G. Perrin, K. Chestnut and E. K. Wakeland (1996). "Production of congenic mouse strains carrying NOD-derived diabetogenic genetic intervals: an approach for the genetic dissection of complex traits." Mamm Genome 7(5): 331-4.

Zhao, Y., S. Li, E. E. Childs, D. K. Kuharsky and X. M. Yin (2001). "Activation of pro-death Bcl-2 family proteins and mitochondria apoptosis pathway in tumor necrosis factor-alpha-induced liver injury." J Biol Chem 276(29): 27432-40.

Zheng, L., G. Fisher, R. E. Miller, J. Peschon, D. H. Lynch and M. J. Lenardo (1995). "Induction of apoptosis in mature T cells by tumour necrosis factor."Nature 377: 348-351.

BIOGRAPHICAL SKETCH

Frances Rena Castoe-Bahjat was born in Tulsa, Oklahoma on May 11, 1973. She grew up with her parents and brother in Oologah, Oklahoma. She graduated from Oologah-Talala High School in 1990 and attended Oklahoma State University where she met her husband, Keith Bahjat. Rena finished her bachelors in science at Benedictine University in 1997 and decided to pursue a doctorate in biomedical sciences. She began her graduate work at the University of Florida in the Interdisciplinary Program in Biomedical Sciences in 1998, and subsequently began her doctoral work one year later under the supervision of Dr. Mike Clare-Salzler, M.D. and Lyle L. Moldawer, Ph.D. in the departments of Immunology and Surgery, respectively. After receiving her doctorate, Rena plans to pursue a post-doctoral position and continue research in the field of immunology.

I certify that I have read this study and that in my opinion it conforms to acceptable standards of scholarly presentation and is fully adequate, in scope and quality, as a dissertation for the degree of Doctor of Philosophy.

Michael J. Clare-Salzler, Chair
Associate Professor of Immunology,
Pathology and Laboratory Medicine

I certify that I have read this study and that in my opinion it conforms to acceptable standards of scholarly presentation and is fully adequate, in scope and quality, as a dissertation for the degree of Doctor of Philosophy.

James Crawford
Associate Professor of Immunology,
Pathology and Laboratory Medicine

I certify that I have read this study and that in my opinion it conforms to acceptable standards of scholarly presentation and is fully adequate, in scope and quality, as a dissertation for the degree of Doctor of Philosophy.

Laurence Morel
Assistant Professor of Immunology,
Pathology and Laboratory Medicine

I certify that I have read this study and that in my opinion it conforms to acceptable standards of scholarly presentation and is fully adequate, in scope and quality, as a dissertation for the degree of Doctor of Philosophy.

Margaret Wallace

Margaret Wallace
Associate Professor of Molecular
Genetics and Microbiology

This dissertation was submitted to the Graduate Faculty of the College of Medicine and to the Graduate School and was accepted as partial fulfillment of the requirements for the degree of Doctor of Philosophy.

August 2002

Wayne T McCormack

Dean, College of Medicine

Winfred M Phillips

Dean, Graduate School